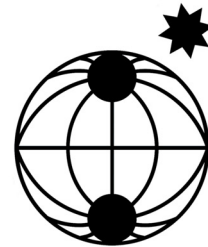


Berichte

**zur Polar-
und Meeresforschung**

**617
2010**

**Reports
on Polar and Marine Research**



**The Expedition of the Research Vessel "Polarstern"
to the Amundsen Sea, Antarctica, in 2010 (ANT-XXVI/3)**

**Edited by
Karsten Gohl
with contributions of the participants**



ALFRED-WEGENER-INSTITUT FÜR
POLAR- UND MEERESFORSCHUNG
In der Helmholtz-Gemeinschaft
D-27570 BREMERHAVEN
Bundesrepublik Deutschland

ISSN 1866-3192

Hinweis

Die Berichte zur Polar- und Meeresforschung werden vom Alfred-Wegener-Institut für Polar- und Meeresforschung in Bremerhaven* in unregelmäßiger Abfolge herausgegeben.

Sie enthalten Beschreibungen und Ergebnisse der vom Institut (AWI) oder mit seiner Unterstützung durchgeführten Forschungsarbeiten in den Polargebieten und in den Meeren.

Es werden veröffentlicht:

- Expeditionsberichte (inkl. Stationslisten und Routenkarten)
- Expeditionsergebnisse (inkl. Dissertationen)
- wissenschaftliche Ergebnisse der Antarktis-Stationen und anderer Forschungs-Stationen des AWI
- Berichte wissenschaftlicher Tagungen

Die Beiträge geben nicht notwendigerweise die Auffassung des Instituts wieder.

Notice

The Reports on Polar and Marine Research are issued by the Alfred Wegener Institute for Polar and Marine Research in Bremerhaven*, Federal Republic of Germany. They appear in irregular intervals.

They contain descriptions and results of investigations in polar regions and in the seas either conducted by the Institute (AWI) or with its support.

The following items are published:

- expedition reports (incl. station lists and route maps)
- expedition results (incl. Ph.D. theses)
- scientific results of the Antarctic stations and of other AWI research stations
- reports on scientific meetings

The papers contained in the Reports do not necessarily reflect the opinion of the Institute.

The „Berichte zur Polar- und Meeresforschung“
continue the former „Berichte zur Polarforschung“

* Anschrift / Address

Alfred-Wegener-Institut
Für Polar- und Meeresforschung
D-27570 Bremerhaven
Germany
www.awi.de

Editor in charge:
Dr. Horst Bornemann

Assistant editor:
Birgit Chiaventone

Die "Berichte zur Polar- und Meeresforschung" (ISSN 1866-3192) werden ab 2008 ausschließlich als Open-Access-Publikation herausgegeben (URL: <http://epic.awi.de>).

Since 2008 the "Reports on Polar and Marine Research" (ISSN 1866-3192) are only available as web based open-access-publications (URL: <http://epic.awi.de>)

**The Expedition of the Research Vessel "Polarstern"
to the Amundsen Sea, Antarctica, in 2010 (ANT-XXVI/3)**

**Edited by
Karsten Gohl
with contributions of the participants**

**Please cite or link this item using the identifier
hdl: 10013/epic.35668 or <http://hdl.handle.net/10013/epic.35668>
ISSN 1866-3192**

ANT-XXVI/3

29 January - 5 April 2010

Wellington – Punta Arenas

**Chief scientist
Karsten Gohl**

**Coordinator
Eberhard Fahrbach**

CONTENTS

1. Zusammenfassung und Fahrtverlauf	4
Summary and Itinerary	6
2. Weather conditions	8
3. Bathymetry	12
4. Geophysics: Tectonic, sedimentary and glacial processes of the continental margin of the Amundsen Sea, West Antarctica	17
4.1 Seismics	19
4.2 Magnetics and gravimetry	30
4.3 Geothermal heat-flow measurements	40
5. Marine-sedimentary Geology: West Antarctic continental margin sediments as recorded of variability of the West Antarctic ice sheet and palaeoclimatic changes during the Quaternary	44
6. Oceanography	65
7. Land geology: Exhumation and deglaciation history of coastal Marie Byrd Land and Ellsworth Land	88
8. GPS observations in West Antarctica for the determination of vertical and horizontal deformations of the Earth's crust and for the investigation of the tidal dynamics of ice shelves	102
9. Climate induced changes and biodiversity of Antarctic phytoplankton	107
10. Methane in-situ production in surface water during the phytoplankton bloom in the Amundsen Sea	111
11. Marine mammals and seabirds	114
12. MAPS: Marine mammal perimeter surveillance	118

APPENDIX	125
A.1 Teilnehmende Institute / participating institutions	126
A.2 Fahrtteilnehmer / cruise participants	128
A.3 Schiffsbesatzung / ship's crew	130
A.4 Stationsliste / station list PS 75/106-75/263	131

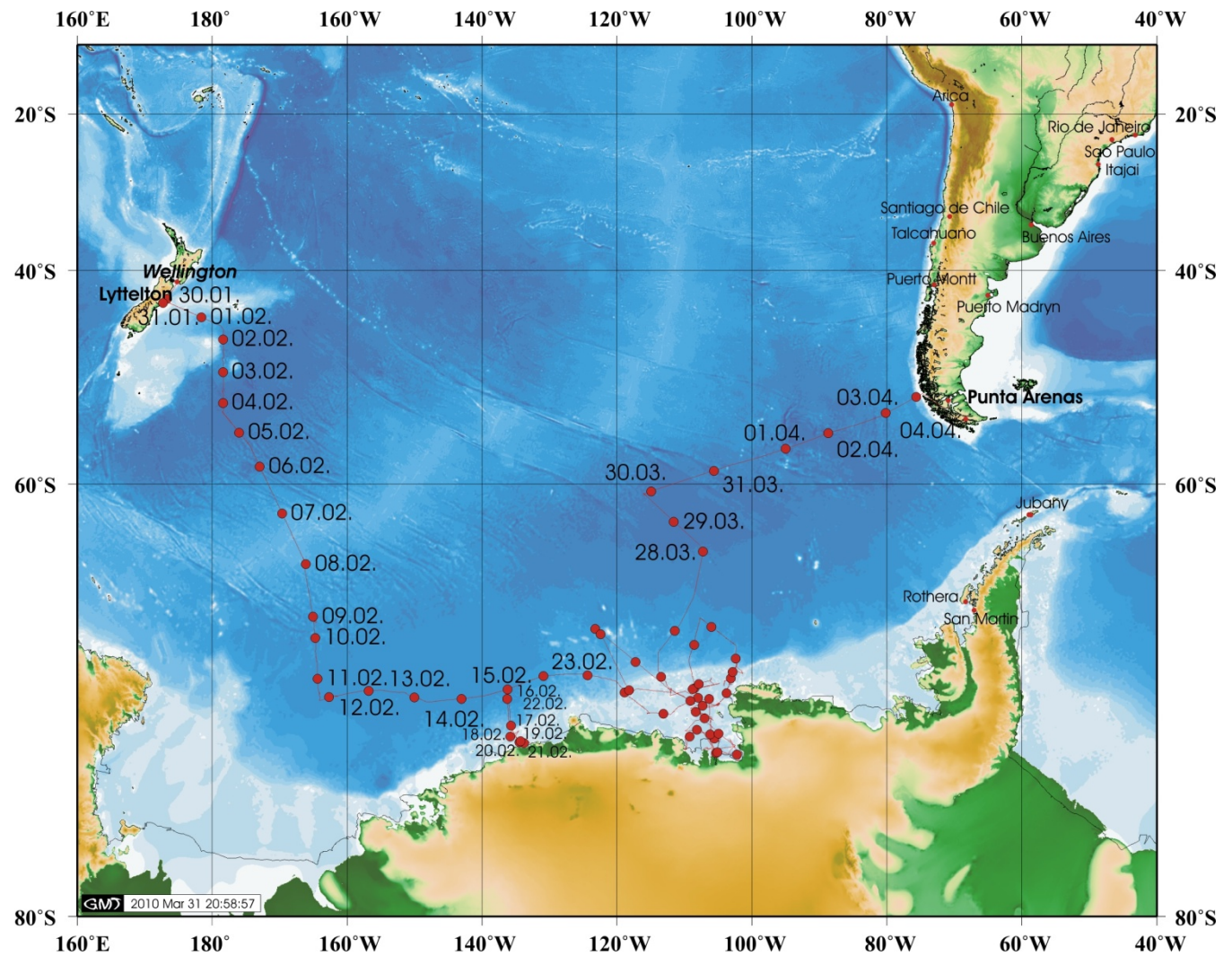


Abb. 1.1: Kurskarte der Polarstern Reise ANT-XXVI/3 mit jeweiligem Datum
 Fig. 1.1: Cruise track of Polarstern during the expedition ANT-XXVI/3 with dates

1. ZUSAMMENFASSUNG UND FAHRTVERLAUF

Seit dem letzten glazialen Maximum erfuhr der westantarktische Eisschild (WAIS) dramatische Volumenänderungen innerhalb kurzer Zeiträume. Der WAIS hat das Potenzial, den globalen Meeresspiegel um 3 - 5 m ansteigen zu lassen. Untersuchungen, die diese Variationen mit denen in der geologischen Vergangenheit vergleichen und somit Parameter für Vorhersagemodelle ableiten lassen, sind daher dringend erforderlich. Mit dieser vordringlichen Fragestellung vor Augen begann der FS *Polarstern*-Fahrtabschnitt ANT-XXVI/3 am 29. Januar 2010 in Wellington (Neuseeland) und endete am 5. April 2010 in Punta Arenas (Chile). Die Expedition hatte primär geophysikalische und geologische Forschungsziele, die die vorglaziale und glaziale Entwicklung der Westantarktis entschlüsseln helfen sollen. Des Weiteren wurden ozeanographische, geodätische, biogeochemische und plankton-biologische Projekte sowie ein Programm zur Beobachtung von Meeressäugern und Vögeln durchgeführt.

Das geowissenschaftliche Programm begann mit seismischen Voruntersuchungen an vorgeschlagenen IODP-Bohrlokalisationen entlang der Transitstrecke von Neuseeland zum nordöstlichen Rossmeer. Seismische Profile wurden vom östlichen Rossmeer auf dem Kontinentalfuß entlang des Kontinentalrandes von Marie-Byrd-Land aufgenommen, um das existierende seismische Profilnetz des Rossmeeres mit den Profilen im Amundsenmeer für eine überregionale Stratigraphie zur Rekonstruktion einer zirkum-antarktischen Paläobathymetrie zu verbinden. Die seismischen Daten werden in Verbindung mit helikopter-magnetischen Messflugdaten auch für Untersuchungen des kontinentalen Aufbruchs zwischen Neuseeland und Marie-Byrd-Land in der Spätkreide genutzt. Günstige Eisbedingungen ermöglichen seismische und bathymetrische Vermessungen, geologische Beprobungen und ozeanographische Einsätze im westlichen Wrigley-Golf vor der Hobbs-Küste. Mit Erreichen des Hauptarbeitsgebietes im Amundsen Sea Embayment wurden die seismischen, sedimentechographischen, bathymetrischen und helikopter-magnetischen Messungen fortgesetzt. Die ungewöhnlich eisfreien Verhältnisse in der Pine Island Bay in dieser Saison erlaubten wesentlich ausgiebigere Untersuchungen in diesem Gebiet als ursprünglich geplant. Kenntnisse über die Beschaffenheit und Eigenschaften der Sedimente und des Basements ergeben wichtige Parameter für die Rekonstruktion der tektonischen Entwicklung sowie der glazial-interglazialen Zyklizität von der frühesten Vereisung bis zum letzten glazialen Maximum. Im Amundsen Sea Embayment sind Sedimentkerne zur Datierung und Rekonstruktion vergangener Eisschildrückzüge gezogen worden. Auch fand eine erfolgreiche Beprobung der erst kürzlich an den Marie-Byrd-Seamounts entdeckten Tiefseekorallen statt. Aufgeschlossene Gesteinsformationen wurden entlang der Küste von Marie-Byrd-Land, auf den Hudson Mountains und Thurston Island

1. Zusammenfassung und Fahrtverlauf

aufgesucht, um Proben für die Analyse kosmogener Nuklide für die Datierung des Eisschildrückzuges zu sammeln. Weitere Gesteinsproben dienen der Rekonstruktion der Denudations- und Hebungsgeschichte von Marie-Byrd-Land mit Hilfe von Spaltspurenanalysen. Geodätische GPS-Messpunkte auf Felsformationen konnten nach vier Jahren wiederholt eingemessen werden und liefern Daten zur Bestimmung der horizontalen und vertikalen Bewegungskomponenten der Erdkruste.

Primäre Ursachen für die z.Z. beobachteten beschleunigten Gletscherrückzüge in der Pine Island Bay werden in ozeanographischen Prozessen vermutet. Das ozeanographische Messprogramm mit CTD-Messungen, aber auch die Messungen mit der geothermischen Wärmelanze, lieferten neue und wichtige Daten zur Verteilung des Zirkumpolaren Tiefenwassers und der ozeanographischen Dynamik auf den Schelfen des Amundsen Sea Embayment und des Wrigley-Golfs.

Die Methanproduktion während der Phytoplanktonblüte ist ein Prozess, der für den Südozean unzureichend verstanden ist. Zahlreiche Wasserproben wurden für Methangasanalysen gesammelt. Weiterhin wurden Proben von antarktischem Phytoplankton genutzt, um die klimainduzierten Änderungen und die Biodiversität zu untersuchen.

Die Beobachtung von Meeressäugern und Vögeln fand während des gesamten Fahrtabschnitts statt. Weiterhin ist das schiffseigene thermographische System zur automatischen Detektion von Walen getestet worden.

Dokumentiert wurde die Expedition von einem Filmteam im Auftrag von Arte für eine Filmproduktion über aktuelle polare Klima- und Paläoklimaforschung.

SUMMARY AND ITINERARY

Since the last glacial maximum, the West Antarctic Ice-Sheet (WAIS) has experienced dramatic volume changes within short periods of time. The WAIS has the potential to increase the global sea-level by 3 - 5 m. Hence, studies are urgently required to show if these short-term variations can be compared to volume changes in the older and younger geological past which will provide parameters for prediction models. With this high-priority objective in mind, we began the cruise leg ANT-XXVI/3 of *Polarstern* in Wellington (New Zealand) on 29 January 2010 and arrived in Punta Arenas (Chile) on 5 April 2010. The expedition had primarily geophysical and geological objectives with the goal to decipher the pre-glacial and glacial development of West Antarctica. Oceanographic, geodetic, biogeochemistry and plankton-biological projects as well as a programme of marine mammal and bird observations were also conducted.

The geoscientific programme began with seismic pre-site surveys on proposed IODP drill sites along the transit from New Zealand to the northeastern Ross Sea. Continued seismic profiling on the continental rise from the eastern Ross Sea along the continental margin off Marie Byrd Land connected the existing seismic grid of the Ross Sea to the profiles in the Amundsen Sea Embayment in order to correlate the stratigraphy for reconstructing a circum-Antarctic paleobathymetry. The seismic data are also used with the addition of helicopter-magnetic surveying for studies on the Late Cretaceous continental break-up between New Zealand and Marie Byrd Land. Favourable sea-ice conditions enabled seismic and bathymetric surveying, geological sampling and oceanographic measurements in the western Wrigley Gulf near Hobbs Coast. Arriving in the main working area, the Amundsen Sea Embayment, seismic and Parasound profiling, bathymetric surveying and helicopter-magnetic surveying continued. The unusual ice-free conditions in Pine Island Bay this season allowed more extended investigations in this area than previously planned. The knowledge of the composition and properties of sediments and basement provides important parameters for the reconstruction of the tectonic evolution as well as the glacial-interglacial cyclicity from early glaciation until the last glacial maximum. Cores of Quaternary sediments were collected from the Amundsen Sea Embayment for analyses aimed to date past ice-shelf retreats. Recently discovered deep-sea corals were sampled from the Marie Byrd Seamounts. Hard-rock outcrops along the Marie Byrd Land coast, the Hudson Mts and Thurston Island were visited for sampling rocks for cosmogenic nuclide analysis aimed at dating the ice-sheet retreat history and to reconstruct the denudation and uplift history of Marie Byrd Land via fission-track analysis. GPS data from on rock outcrop sites measured four years after the initial measurements will be used to derive horizontal and vertical crustal motion.

Oceanographic processes have been proposed as likely causes for the presently occurring accelerated glacier retreats in Pine Island Bay. The oceanographic programme with CTD casts, but also the data from the geothermal heat-flux sensor, provided new and important data for studying the distribution of Circumpolar Deep Water and the oceanographic dynamics on the continental shelves of the Amundsen Sea Embayment and Wrigley Gulf.

Methane production during the phytoplankton bloom is a process not well understood in the Southern Ocean. Numerous water samples were collected for methane gas analyses. Samples of Antarctic phytoplankton were collected to study their climate induced changes and biodiversity.

Observations of marine mammals and birds took place during the entire cruise leg. The ship-borne thermographic system for the automatic detection of whales was also thoroughly tested.

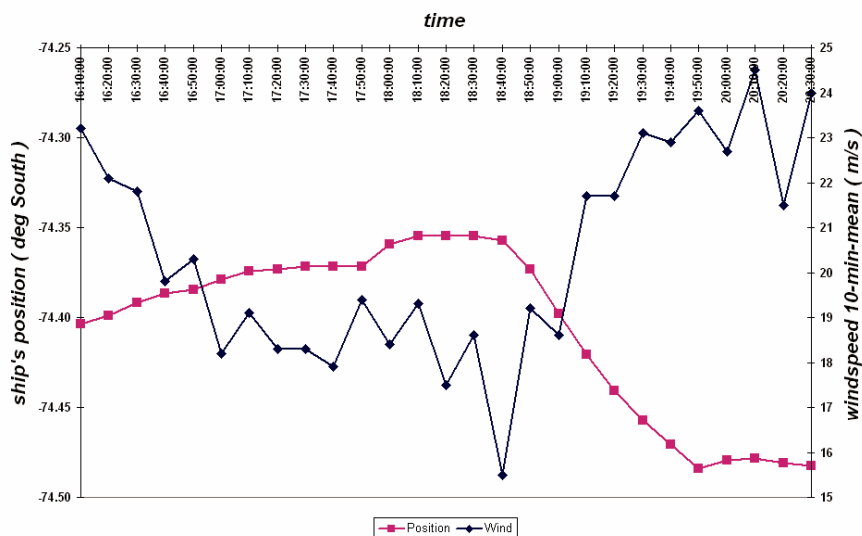
A film team documented the expedition for an *Arte* film production on polar climate and paleo-climate research.

2. WEATHER CONDITIONS

Max Miller, Hartmut Sonnabend
Deutscher Wetterdienst

In the afternoon of 29 January *Polarstern* left Wellington. The first destination was Lyttelton on the South Island of New Zealand to bunker fuel. Finally in the early morning hours of 1 February *Polarstern* started its expedition to Antarctica. First we cruised under high pressure influence with weak easterly winds. Shortly afterwards a strong low was forecasted to hamper the first measurements. As a result of this the chief scientist decided to cancel this way points and *Polarstern* headed directly (more westerly) to the south. Therefore the wind from southwest reached Bft 8, with short periods of Bft 9 and the waves grew up to 8 meters. Along the original route there would have been a minimum of Bft 10 and waves exceeding 10 meters and it would have been impossible to carry out the planned work. After this strong cyclone had moved away, first station work was possible on 5 February at a wind force of Bft 6. A new storm on 6 Feb. with short periods of Bft 9 caused no considerable difficulties, because *Polarstern* was on transit.

Fig. 2.1: Jet at the ice shelf



During the whole stay in the Ross Sea and Amundsen Sea *Polarstern* was located south of the frontal zone. Although a few strong lows affected us and the wind increased, there were no problems concerning the work on the vessel, because the waves were either damped by ice or couldn't grow in the inner part of bays. Obviously the edge of the ice shelf and mountains beyond functioned as a jet. On 18 Feb., as *Polarstern* got a little bit closer to the edge of the ice shelf in Wrigley Gulf,

wind force increased from Bft 9 up to 10, but decreased again, when the vessel turned to north (Fig. 2.1).

One of the scientific priorities of the journey was based on helicopter flights: on the one hand magnetic measurements, which covered a circle of about 100 sea miles around the vessel; on the other hand teams were flown to land, to sample rocks or to lower GPS-instruments. Such a GPS-instrument was fixed on 17 Feb., while *Polarstern* came closer to the Wrigley Golf. During the next days conditions were too bad to catch the GPS-instrument. A last attempt (*Polarstern* headed further to the east) was made on 20 Feb., but had to be stopped at the ice shelf because of poor visibility.

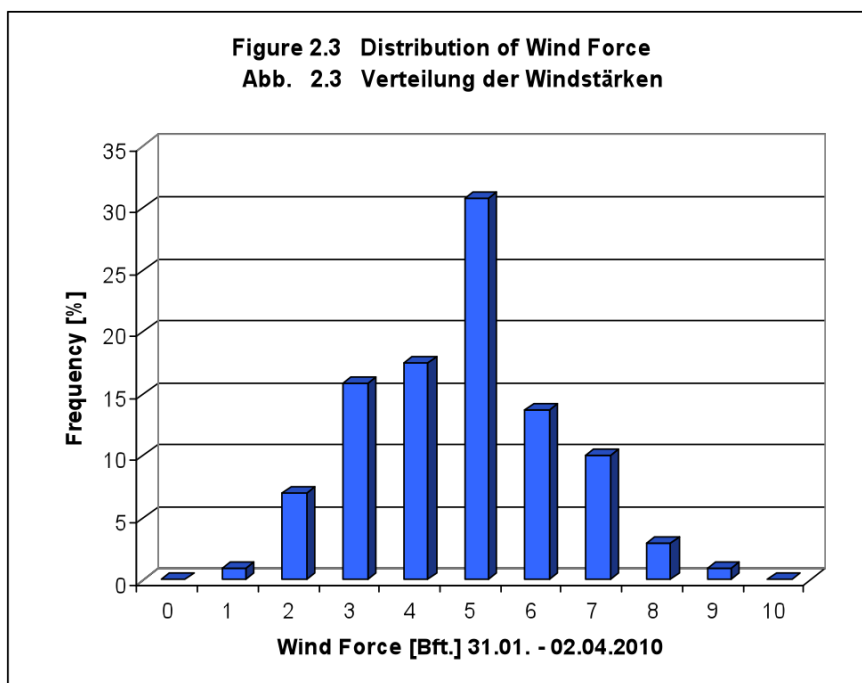
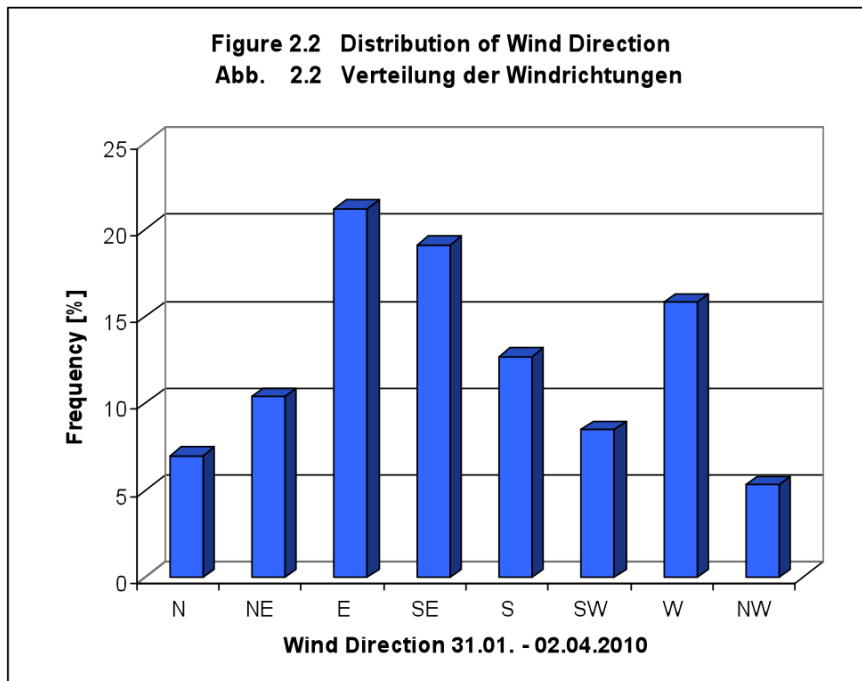
On 27 Feb. *Polarstern* was in sight to the Swedish research vessel *Oden*. At good flight conditions the helicopters of *Polarstern* transported scientists to visit each other. Good conditions for flights to Mt. Murphy were predicted for 4 March and all activities on land could be done well. Only the last helicopter shortened its stay on land, because more clouds approached.

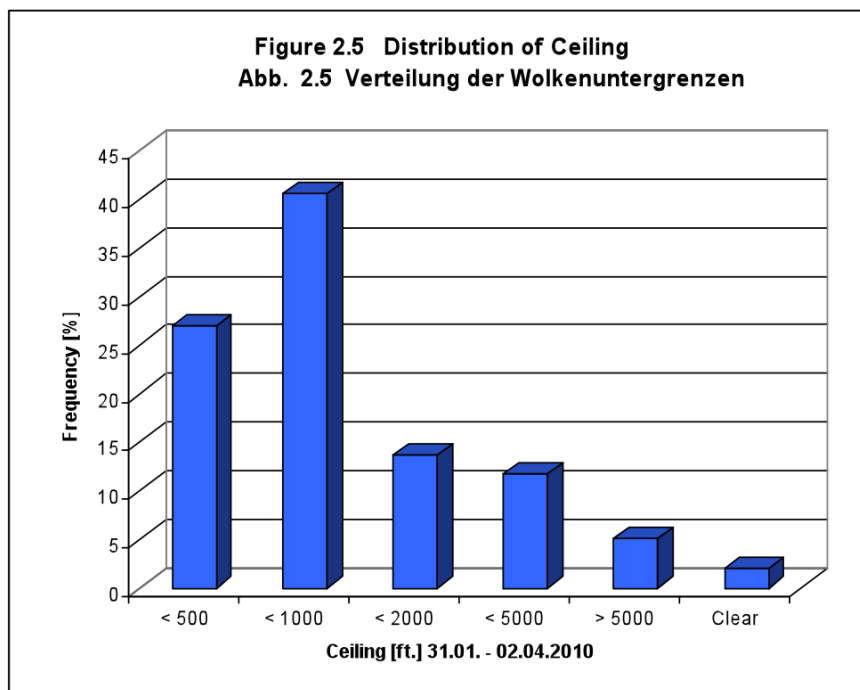
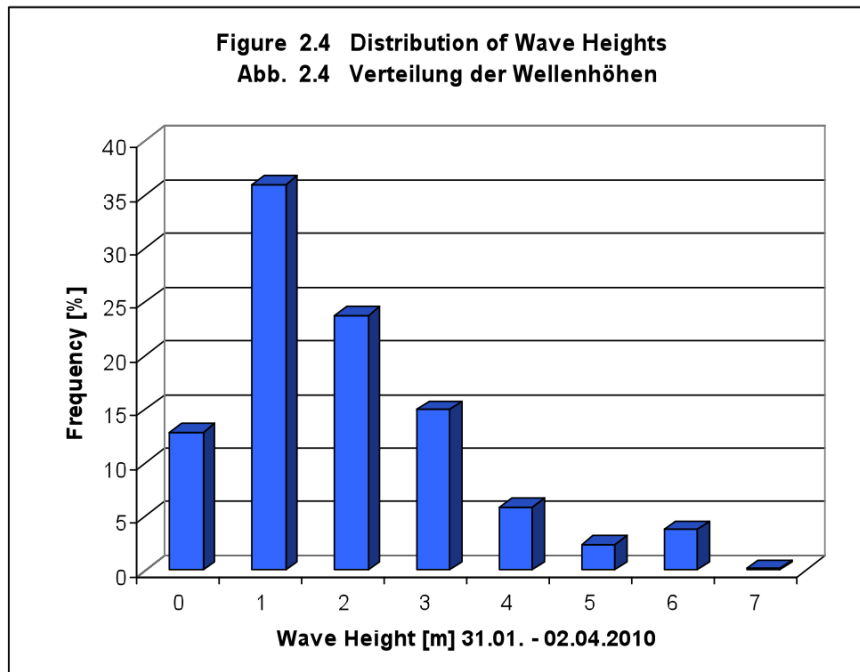
More GPS-instruments had been placed at Pine Island Bay during *Polarstern*'s first stay at end of February. A ridge of high pressure had been announced for the weekend of 13 and 14 March and the beginning of the following week. On Monday (16 March) it had become necessary to retrieve the instruments as soon as possible. Therefore *Polarstern* headed to the inner Pine Island Bay during the night of Tuesday. Although clouds in higher levels of the atmosphere reached the bay, the visibility on the ice shelf was sufficient. Therefore on Tuesday all GPS-instruments could be removed. Additionally geologists were flown to the land with the second helicopter to sample rocks. There was still hope for one more flight to Mt. Murphy on Wednesday (17 March), but was dampened on Tuesday evening though. An attempt to fly was made on Wednesday morning, but was stopped due to bad conditions.

In the evening of 21 March measurements in the outer Pine Island Bay had to be stopped ahead of schedule to go directly northwestward to Marie Byrd Seamounts. Therefore Tuesday, 23 March, was a quiet day to carry out the planned work, because storm was forecasted for Wednesday, which arrived with southerly winds at Bft 7. Against this strong wind we steamed to the South again to complete last measurements.

Finally on 26 March the crossing to Punta Arenas started. First *Polarstern* steamed northwest to $60^{\circ}45' S - 116^{\circ}05' W$ to measure the seabed seismically. While doing so *Polarstern* had temporarily to fight against waves up to 7 meters at a wind force of Bft 8. On the continuation of the journey to the east wind and swell came from aft. A new storm was forecasted for Saturday, requiring the cancellation of the last planned station and to enter the Strait of Magellan earlier. In the morning of Easter Monday, on 5 April 2010, we reached Punta Arenas.

For further statistics of weather parameters see Figs. 2.2 to 2.5.





3. BATHYMETRY

Norbert Ott, Laura Jensen, Sarah Reinshagen
Alfred-Wegener-Institut für Polar- und Meeresforschung, Bremerhaven

Objectives

The main task of the bathymetric group during ANT-XXVI/3 was to perform high resolution multibeam surveys and to monitor the acquisition of bathymetry data during the entire cruise. Bathymetric data is acquired with the multibeam echo sounder Hydrosweep DS-2 manufactured by *ATLAS HYDROGRAPHIC*. Besides data acquisition and data processing, the bathymetric group was also responsible for providing bathymetric maps with additional site and profile information for geophysicists, geologists, and oceanographers. Depth information is used for the selection of stations, sampling sites, and assists the geological and geophysical interpretation in specific areas of interest. Precise depth measurements are indispensable for the generation of high resolution digital terrain models of the seafloor. The complete workflow, starting with data acquisition, cleaning, editing, and final 2-D and 3-D visualization, is performed by the use of a variety of software applications on board. Interpretation of geomorphologic structures based on the maps and models gives information about geological and glacial processes.

Existing data in the Amundsen Sea Embayment are limited due to its remote location and annual sea ice coverage. During previous *Polarstern* expeditions bathymetric data were collected in this region, e.g. ANT-XXIII/4. In order to avoid duplicate measurements of the seafloor topography, the bathymetry group was responsible for a reasonable track planning based on existing track information and multibeam data.

The collected data are a valuable contribution to the world database for oceanic mapping and bathymetric databases and will be included in the Bathymetric grid of the Amundsen Sea, the International Bathymetric Chart of the Southern Ocean (IBCSO) as well as the General Bathymetric Chart of the Oceans (GEBCO).

Work at sea

Data acquisition was carried out during the entire cruise from 31 January 2010 (03:50 UTC) until 4 April 2010 (13:36 UTC).

The deep-sea multibeam echo sounder *Hydrosweep DS2* from *ATLAS HYDROGRAPHIC* was run in the hardbeam mode, sending out a signal with a frequency of 15.5 kHz and a spectrum of 1.2 kHz and receiving the reflected signal in 59 preformed beams per swath. Discussion about the use of the High Definition Bearing Estimation (HDBE) mode, also named softbeam mode, arose during the cruise. Reports from AWI Bathymetry and FIELAX in Bremerhaven clearly

demonstrate that the HDBE mode with DS-2 is not running properly. It was strongly recommended to continue data acquisition in the hardbeam mode with a swath angle of 90° and 120° respectively. In addition to depth, echo amplitudes were converted to (i.) sidescan (4094 pixel per swath) and (ii.) backscatter data (59 values per swath). This data is important for studies of the seafloor texture and helps to discriminate different grain sizes of sediments.

Due to the low resolution and poor data quality associated with an angle of 120° the angle was set to 90° most of the time. The same information was provided by Martin Jakobsson during his visit from *Oden* on *Polarstern*. He experienced a loss of data of about 50 %, whereas our group cleaned 30 % of data acquired with a swath angle of 120°. Fig. 3.1 shows a Fledermaus profile with distance in decimeters and depth in meters of Hydrosweep data (Hardbeam, 120°) with merged global ETOPO1 data in the western Getz Shelf. Systematic data error in the outer beams is up to 100 meters or 20 % of water depth respectively.

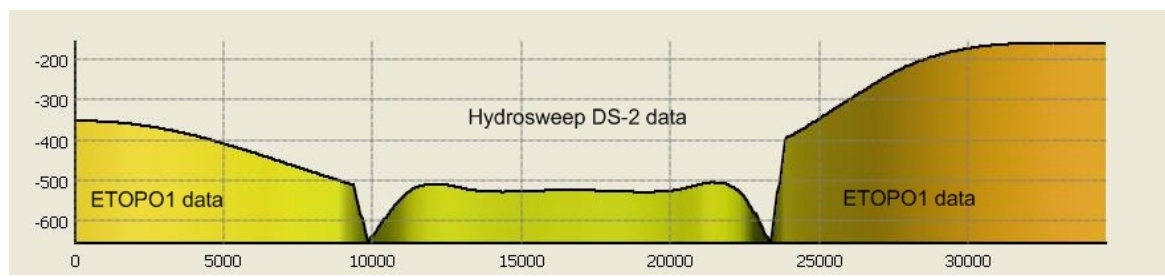


Fig. 3.1: Hydrosweep DS-2 data acquired with a swath angle of 120° in the western Getz Shelf

Abb. 3.1: Hydrosweep DS-2-Daten auf dem westlichen Getz Schelf – Öffnungswinkel von 120°

Using a swath angle of 120° the width is about 3.4 times the water depth. The along track seafloor coverage with the 90° swath has a width about the double water depth. Percentage of cleaned data acquired with a swath angle of 90° is less than 2 %. The accuracy of the measured water depth is about 1 % of the water depth for the center beam and about 2 % for the outer beams. To achieve this accuracy the knowledge of the sound velocity throughout the water column is needed. The Hydrosweep system has a patented function to perform a cross fan calibration for determining the mean sound speed within the water column. During the cruise the system was running in the calibration mode “standard”, accomplishing a cross fan calibration every two nautical miles (nm) most of the time.

A more precise technique to determine the sound velocity throughout the water column is to perform CTD measurements, whereby the sound velocity is calculated from the parameters conductivity, temperature, and pressure. CTD-measurements were conducted by the oceanographers during this cruise leg. Five of them were imported as C-Mean values for the water sound velocity in specific areas such as western Getz Ice Shelf and Pine Island Bay.

The acquisition of multibeam data was conducted using HYDROMAP ONLINE provided by ATLAS HYDROGRAPHIC. The recorded data was amalgamated in eight hour blocks and stored in the ATLAS raw data format SURF (sensor independent raw data format).

During data acquisition the measured bathymetry has outliers in depth values due to ship movements (pitch and roll) or ice floes below the transducers, so the acquired data is edited during the on board processing. This allows production and delivery of high quality bathymetric maps.

At first the navigation data was checked with the programme HYDROMAP OFFLINE, to exclude coarse positioning errors. In fact, only one positioning error occurred during this leg. After converting to the dux-format, blunders and spikes were removed using CARIS HIPS and SIPS version 6.1. The most erroneous data were recorded during surveying through ice floes, where up to 60 % of the beams were flagged.

The cleaned data was converted into ASCII format (longitude, latitude, depth) for map plotting with the Generic Mapping Tools (GMT). Bathymetric maps were provided to other working groups on a daily base, by combining data from previous cruises by *Polarstern*, James Clark Ross and Nathaniel B. Palmer together with currently acquired data. Fig. 3.2 presents the simplified workflow process on board *Polarstern* as it was carried out during this cruise leg.

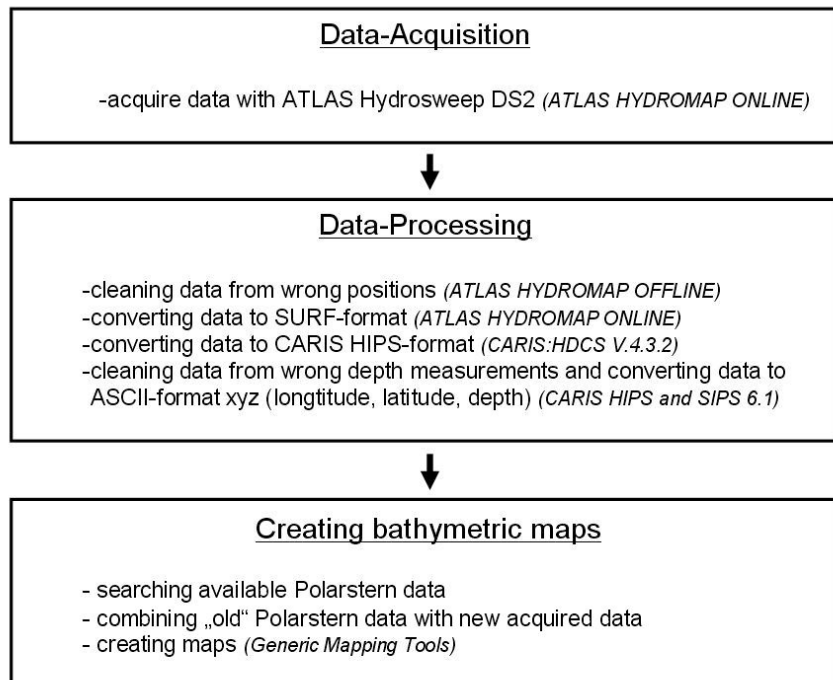


Fig. 3.2: Simplified workflow of the data pre-processing on board *Polarstern*

Abb. 3.2: Flussdiagramm der Datenprozessierung auf *Polarstern*

Preliminary Results

During the cruise a continuous recording of data was achieved, except for data gaps due to unexpected system errors and shutdowns. All data were processed by the end of the cruise except for one 8 hours data block due to aborted conversion. In total 64 days with a track length of 10,349 nm (19,167 km) were recorded. The raw data volume is 4.43 GB with 192 separate files. The data consists of 696,523 pings and 82,066,516 beams in total (before editing). The observed minimum water depth was 79 meters in the Pine Island Bay west of Burke Island. The maximum water depth was 6,450 meters during transit in the South Pacific Abyssal Plain.

Apart from transit data recorded during the entire expedition, several systematic bathymetric surveys were carried out. Fig. 3.3 shows the location of the bathymetric surveys accomplished in conjunction with marine geology and geophysics during this cruise leg.

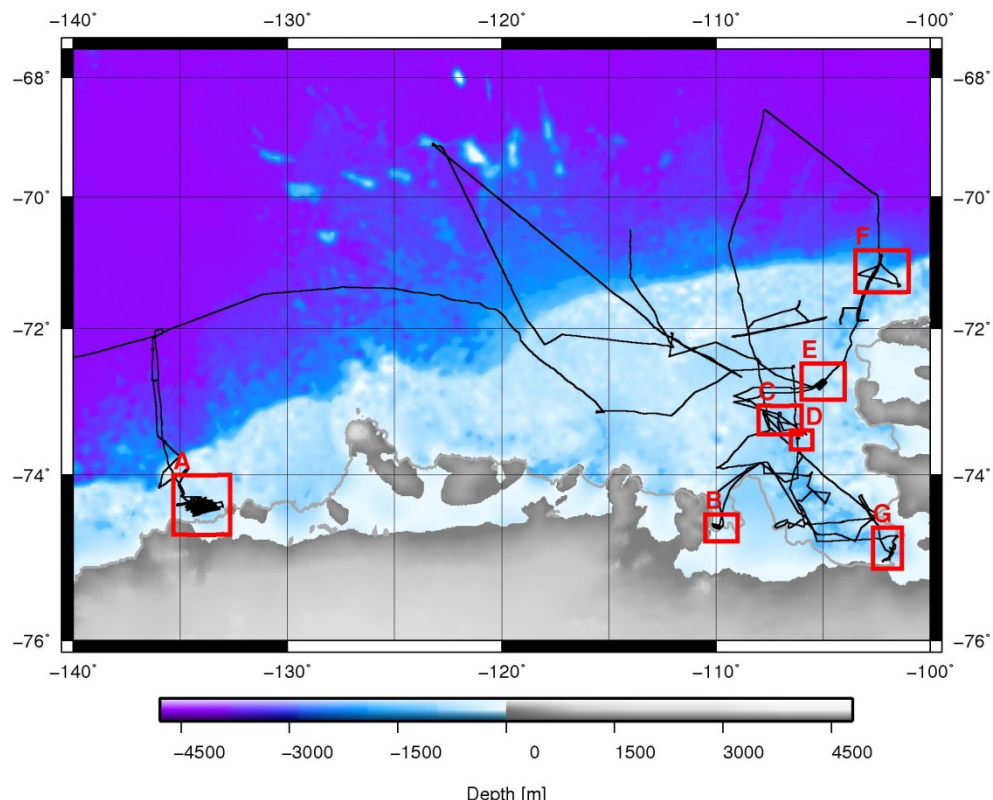


Fig. 3.3: Sketch of the Amundsen Sea Embayment and Pine Island Bay showing track plot and survey areas during ANT-XXVI/3

Abb. 3.3: Übersichtskarte des Amundsenschelfs und der Pine Island Bay mit Schiffskurs und Vermessungsgebiete der ANT-XXVI/3 Expedition

More detailed information about area, date, water depth and data acquisition mode is summarized in Tab. 3.1.

Tab. 3.1: Hydrographical survey areas in the Amundsen Sea during ANT-XXVI/3

Survey Area (Name)	Date (Hydrosweep)	Depth (Min-Max)	Mode (Fan)
A: Getz Ice Shelf	2010/02/17 – 2010/02/21	442-894	HB, 120°
B: Crosson Ice Shelf	2010/03/04	300-1050	HB, 90°
C: "Dippers"	2010/03/18 – 2010/03/19	464-965	HB, 90°
D: "Neptune's Bottle"	2010/02/27 – 2010/02/28	810-845	HB, 90°
	2010/03/05 – 2010/03/06		
E: Burke Island	2010/03/19 – 2010/03/20	550-595	HB, 90°
F: Thurston Island	2010/03/09 – 2010/03/10	450-2225	HB, 90°
G: Pine Island Glacier	2010/02/28 – 2010/03/01	515-1055	HB, 90°

A hydrographical survey of 6 hours was conducted off the Crosson Ice Shelf. This specific area (8.5×4.5 nm) was ice free and allowed surveying with *Polarstern*. The ship approached within the safety distance of 0.5 nm to the ice shelf edge. A color-coded map of the bathymetry with detailed glacial bedforms is shown in Fig. 3.4.

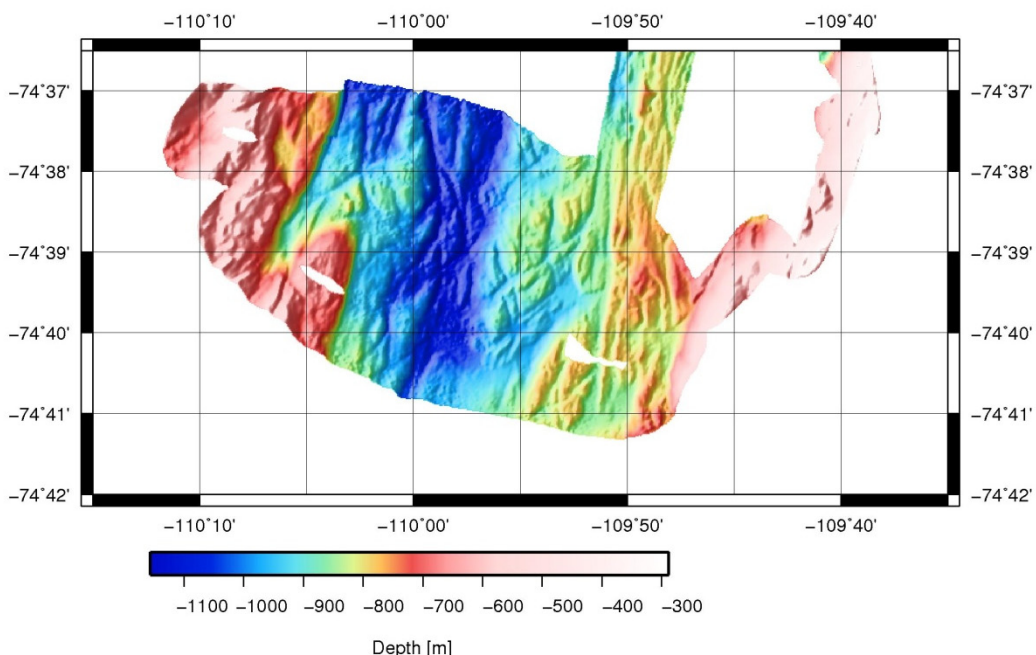


Fig. 3.4: Multibeam data off the Crosson Ice Shelf showing glacial structures
Abb. 3.4: Multibeam Daten mit glazialen Strukturen im Bereich des Crosson-Schelfeises

The seafloor topography is dominated by a trough in North-South direction off the ice shelf; maximum depth of the trough is 1,050 meters. The melt water channel is flanked by shallow areas with depth less than 600 meters. The mapped area shows numbers of grooves oriented in three distinctive directions which form a regular pattern: prominent structures are oriented in North-South direction, while others are oriented in Northeast-Southwest and Northwest-Southeast directions. Note: white gaps are due to occurrence of ice floes and run-around manoeuvre.

4. GEOPHYSICS: TECTONIC, SEDIMENTARY AND GLACIAL PROCESSES OF THE CONTINENTAL MARGIN OF THE AMUNDSEN SEA, WEST ANTARCTICA

Karsten Gohl¹, Frank Brenner¹,
Bryan Davy², Astrid Denk¹,
Thorsten Eggers³, Jürgen Gossler¹,
Thomas Kalberg¹, Norbert Kaul⁴,
Norbert Lensch¹, Ansa Lindeque¹,
Eike Müller¹, Martin Romsdorf¹,
Florian Wobbe¹

¹Alfred-Wegener-Institut für Polar- und
Meeresforschung, Bremerhaven
²GNS Science, Lower Hutt, New Zealand
³Optimare GmbH, Bremerhaven, Germany
⁴University of Bremen, Dept. of
Geosciences, Bremen, Germany

Objectives

West Antarctica exhibits three geoscientific characteristics which are unique in their combination and highly significant for our understanding of the Earth system and for simulations of paleo-climate and climate/sea-level prediction scenarios: As opposed to East Antarctica, this part of the continent (1) has changed its bedrock relief through enormous tectonic change in the Cenozoic, possibly until the Quaternary, by the development of the West Antarctic Rift System (WARS) and the Marie Byrd Land dome, (2) has experienced intense magmatic and volcanic activity until recent times, and (3) has a predominantly submarine based ice sheet even after isostatic rebound adjustment of the lithosphere.

Little is known with regard to the interconnection between the topographic relief development, the West Antarctic Ice Sheet (WAIS) generation and dynamics as well as influences of volcanic/magmatic activity on ice flow behaviour. Since the last glacial maximum, the WAIS has experienced dramatic volume changes within short periods of time. Studies are urgently required to show if these short-term variations can be compared to volume changes in the older geological past.

Next to the ice drainage basins of the Weddell Sea and the Ross Embayment, Pine Island Bay within the Amundsen Sea Embayment forms the third-largest outflow area for the WAIS. The main ice streams from the WAIS into the Pine Island Bay flow through the Pine Island and Thwaites Glacier systems and have followed deeply eroded troughs on the inner to middle shelf. Most of the glacial-marine sediments have been transported onto the outer shelf of the Amundsen Sea Embayment and across the continental slope into the deep sea where they were redistributed by bottom currents. Geophysical surveys of the sedimentary sequences and the underlying basement of the shelf, slope and rise along the continental margin of Marie Byrd Land, the Amundsen Sea Embayment, Pine Island Bay will allow to decipher the tectonic, magmatic and sedimentary processes.

The aim is to reconstruct these processes in time-scales ranging from the rifting and break-up between New Zealand and West Antarctica in the Late Cretaceous to the beginning of major glaciation in the late Paleogene and Neogene and, further, to the youngest glacial cycles in the Quaternary. Accurate models of the geodynamic-magmatic and tectonic history as well as the sedimentary and glacial evolution provide important constraints for our understanding and reconstruction of the paleo-environment of West Antarctica and its impact on global sea-level variations. The following objectives are addressed:

Major boundaries between suspected crustal blocks and volcanic zones in Pine Island Bay have been proposed by various researchers without available data to prove their existence. The glacier troughs and Pine Island Bay itself are thought to have developed along such tectonic boundaries or lineaments. Heli-magnetic, gravimetric and seismic surveys in the Amundsen Sea Embayment provide the necessary data base to map these boundaries and to derive models that link tectonic lineaments to preferential sedimentary and ice stream transport paths.

During and after separation from the Chatham Rise and Campbell Plateau (New Zealand), the continental margin of Marie Byrd Land developed as a rifted margin, accompanied by crustal thinning and intensive volcanism in some parts. The question is whether this volcanism occurred mainly during the rifting process or during post-rift phases, or whether it developed in relation to the West Antarctic rift system. Helicopter-magnetic mapping, gravimetric surveying and seismic profiling of the continental margin of Marie Byrd Land provide data to develop models of the tectonic and magmatic evolution.

Causes for the accelerated retreat of the Pine Island and Thwaites Glaciers are currently being debated. In addition to the influx of warm Antarctic Deep Water into the deep troughs of the Pine Island Bay shelf towards the grounding lines of the glaciers, increased heat flow can be considered to have an additional effect on the sensitivity of this part of the West Antarctic Ice Sheet. Recent volcanism has been identified in the area of the Hudson Mts. Heat flow measurements in sediments of the inner and middle shelf in the vicinity of the Hudson Mts. provides a first estimate on the local geothermal heat flux.

Sedimentary sequences across the shelf, slope and the continental rise contain archives for patterns of pre-glacial/glacial erosional and depositional processes as well as paleo-ocean current systems. Seismic reflection profiles, sub-bottom profiling (Parasound) and multibeam bathymetry (Hydrosweep) are datasets used to derive reconstructions of pre-glacial and glacial sedimentation processes and to derive constraints for glacial-interglacial cyclicity. The data will also be used to support shallow drilling proposals for the Amundsen Sea Embayment.

Reconstructing paleoceanographic and palaeoclimate scenarios are restricted by the lack of realistic paleobathymetric models of the Southern Ocean. Within the international project *Circum-Antarctic Stratigraphy and Paleobathymetry* (CASP), the

seismic data base is being evaluated for a unified circum-Antarctic stratigraphy. During that cruise, we had been filling a major gap of continuous seismic coverage in the western Amundsen Sea in order to correlate the stratigraphy from the Ross Sea to the Amundsen and Bellingshausen Sea.

Seismic pre-site surveys were conducted in the southern Pacific on drill sites proposed in the paleoceanographic IODP proposal no. 625 by Gersonde et al. (see cruise report of ANT-XXVI/2).

Work at sea

Seismic reflection profiling was acquired along the continental margin on the shelf and slope as well as in the deep sea from the eastern Ross Sea to the Amundsen Sea Embayment. Profiling was densified in the Amundsen Sea Embayment to complement the first few multichannel profiles collected during ANT-XXIII/4 in 2006. In addition, seismic pre-site surveys were conducted on three proposed IODP drill sites on the transit from Wellington to the eastern Ross Sea and in the northern Bellingshausen Sea.

Magnetic data were collected using a three-component fluxgate magnetometer as well as the helicopter-towed caesium-vapour aeromagnetic sensor system. Heli-mag surveys were performed at selected locations along the shiptrack on oceanic crust (mapping of seafloor spreading anomalies) and on the shelf of the Amundsen Sea Embayment to complement the first magnetic survey grid of ANT-XXIII/4 in 2006. Gravity data were continuously collected using the ship's gravity meter.

Geo-thermal heat flux measurements were conducted on the shelf of the Amundsen Sea Embayment, in particular in the Pine Island Bay close to the volcanic Hudson Mountains, using heat-flow sensors of University of Bremen.

4.1 Seismics

Karsten Gohl¹, Ansa Lindeque¹,
 Frank Brenner¹, Bryan Davy²,
 Thorsten Eggers³, Jürgen Gossler¹,
 Thomas Kalberg¹, Norbert Lensch¹,
 Eike Müller¹, Martin Romsdorf¹

¹Alfred-Wegener-Institut für Polar- und
 Meeresforschung, Bremerhaven
²GNS Science, Lower Hutt, New Zealand
³Optimare GmbH, Bremerhaven, Germany

Objectives

The objectives for seismic profiling were multi-fold:

(1) Sedimentation into the deep sea of the Ross Sea embayment is expected to be high due to large influx of terrestrial sediments both from pre-glacial and glacial-interglacial times. Seismic profiles extending the existing ones to the north aim to image sediments as far north as terrestrial deposition can be identified. This will provide important constraints on the total pre-glacial and glacial deposition into the deep sea of sediments eroded from the Ross Sea drainage areas.

4.1 Seismics

(2) The Circum-Antarctic Stratigraphy and Paleobathymetry (CASP) project aims to reconstruct the paleodepths of the seafloor at geological times significant for climate change. A major seismic data gap exists between seismic grids of the Ross Sea and the Amundsen Sea which needs to be closed in order to correlate and compare the stratigraphy and depositional character between both regions.

(3) The continental shelf and slope of the Amundsen Sea Embayment is dominated by glacial deposition and erosion processes. As the Amundsen Sea Embayment with its Pine Island Bay is suspected to have exhibited a very dynamic ice-sheet advance and retreat cyclicity, imaging of the shelf sediments and the top of basement will help enable the reconstruction of past West Antarctic ice-sheet dynamics. The data will also be used to identify shallow drilling sites for dating the sedimentary sequences to compare glacial cyclicity of the Amundsen Sea Embayment with observations from the ANDRILL cores from the Ross Sea embayment.

(4) Imaged basement structures along the continental margin from the Ross Sea embayment to the Amundsen Sea will contribute to the understanding of the tectonic breakup process and the identification of the continent-ocean crustal transition.

(5) Deep-sea sediment drifts record the dynamics of past bottom currents. Such drifts have been identified north of the Amundsen Sea Embayment and were further imaged to allow a refined characterisation and reconstruction of suspension bottom flows.

(6) Seismic pre-site surveys in the southern Pacific on drill sites proposed in the paleoceanographic IODP proposal no. 625 by Gersonde et al. (see cruise report of ANT-XXVI/2) need to be conducted.

Work at sea

Instruments

The main recording system consisted of a relatively new 3,000 m long digital solid streamer of 240 channels, type Sentinel by SERCEL (Fig. 4.1). The data were recorded by the SEAL system of SERCEL and stored on parallel LTO-2 tapes and on a NAS disk system for backup. The stored data are in SEG-Y format, ready to be processed with the FOCUS processing software. On-track quality control was done with the eSQC-Pro system displaying every shot record as well as single-channels (ch. 16) along profiles. 12 DigiCourse depth-control birds were mounted on the streamer keeping it at constant 10 m depth. Due to the extremely unusual and favourable sea-ice conditions, we deployed the 3,000 m streamer for most of the profiles.



Fig. 4.1: Winches with the 600 m streamer (in front) and the 3,000 m streamer (in the back) on the working deck.

Abb. 4.1: Winden mit dem 600 m Streamer (vorne) und dem 3,000 m Streamer (hinten) auf dem Arbeitsdeck.

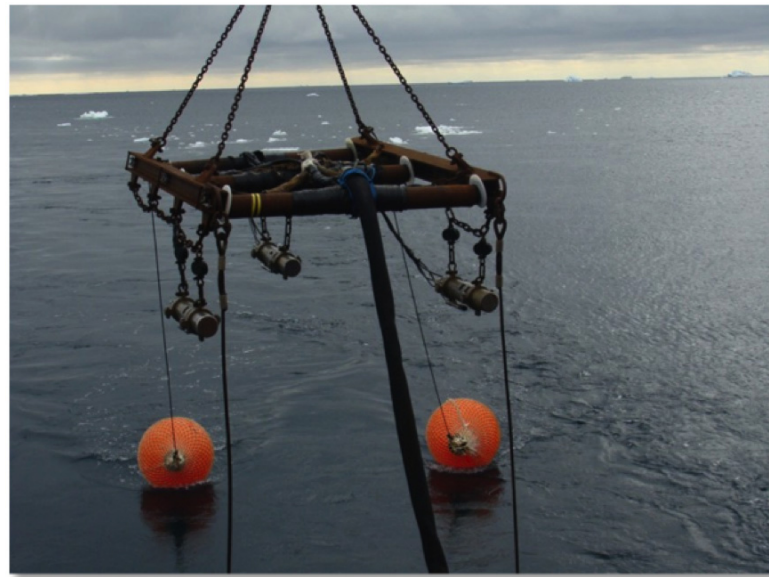
In the few areas of dense sea-ice coverage, we deployed on older 600 m long analogue streamer of 96 channels, made by PRAKLA (Fig. 4.1), and recorded the data with a Geometrics EG&G 2400 recorder with an extension module. The data were stored on 3480 cartridge tapes in SEG-D format and had to be demultiplexed with FOCUS processing software. On-track quality control was performed using a thermoplotter displaying a single channel (ch. 16). The 600 m streamer was deployed without a depth-control bird system.

Along profile AWI-20100100/133 on the outer shelf of Pine Island Bay, we deployed 6 ocean-bottom seismometers (OBS) of type LOBSTER of the DEPAS national pool of OBS systems (Fig. 4.3 and Tab. 4.1). The purpose was to obtain refraction and wide-angle reflection recordings for seismic velocity-depth inversion of the entire sedimentary sequences and top of basement. Each OBS system consists of a Guralp CMG-40T broadband seismometer, a SEND MCS data logger, a KUMquat releaser, a battery pack, floaters, a flash light and a radio beacon. The seismometer is coupled to the top of the steel anchor frame. The sampling rate was set to 250 Hz. All 6 OBS systems recorded the airgun shots on all 4 channels with varying quality.

4.1 Seismics

Fig. 4.2: Airgun configuration, consisting of 3 GI-Guns, before deployment

Abb. 4.2: Airgun-Konfiguration, bestehend aus 3 GI-Guns, vor ihrem Einsatz



The seismic airgun source consisted of a cluster of 3 GI-Guns (by SERCEL) (Fig. 4.2). A single GI-Gun is made of two independent airguns within the same body. The first airgun (“Generator”) produces the primary pulse, while the second airgun (“Injector”) is used to control the oscillation of the bubble produced by the “Generator”. We used the “Generator” with a volume of 0.74 liters (45 in³) and fired the “Injector” with a volume of 1.72 liters (105 in³) with a delay of 33 ms, resulting in an almost bubble-free signal. The GI-Gun cluster was towed 10 m behind the vessel in 5 m water-depth and was fired at a nominal operating pressure of 195 bar at shot intervals between 6 and 12 seconds for seismic reflection surveying and 60 seconds along the seismic refraction OBS profile AWI-20100100. We tried using a single towed G-Gun of 8.5 liters (520 in³) volume in the beginning of the OBS profile, but the umbilical was damaged after one hour of operation. We continued the profile with the GI-Gun cluster instead.



Fig. 4.3: Ocean-bottom seismometer (OBS) after recovery from the sea-floor

Abb. 4.3:
Ozeanbodenseismometer (OBS) nach Rückkehr vom Meeresboden

Seismic data acquisition requires a very precise timing system, because seismic sources and recording systems must be synchronised. A combined electric trigger-clock system was in operation in order to provide the firing signal for the electric airgun valves, to provide the time-control of the seismic data recording and to synchronize the internal clocks of the OBH system.

The seismic acquisition parameters for all profiles are noted in Tab. 4.1.

Mitigation for marine mammals

Mitigation for marine mammals was conducted during seismic profiling. The main procedures include (1) visual observations by marine mammal observers before the start of airgun operations and during seismic profiling, (2) soft-start procedures for the airgun cluster for the duration of 15 minutes and (3) immediate shutdowns of airgun operations in cases of detected marine mammals within a safety distance from the ship.

Seismic profiling

A total of more than 5,000 km of seismic reflection profiles (Fig. 4.4 and Tab. 4.2) were recorded in the northeastern Ross Sea, along the Marie Byrd Land margin, in the southern Amundsen Sea and in the northernmost Bellingshausen Sea. Extremely favourable sea-ice conditions allowed the seismic coverage of large parts of the Amundsen Sea Embayment shelf. Technical problems of the seismic gear were almost negligible, allowing continuous profiling over many days along some profiles. However, frequent shutdowns of airgun operations, due to some whale but mostly seal occurrence close to the ship, caused significant data gaps along many profiles. The data quality is generally at a high level due to relatively favourable weather conditions with calm seas.

It must be noted that the originally planned deep crustal seismic profiles with and without OBS systems could not be conducted because of environmental permitting restrictions on the usage of large-volume airgun configurations.

4.1 Seismics

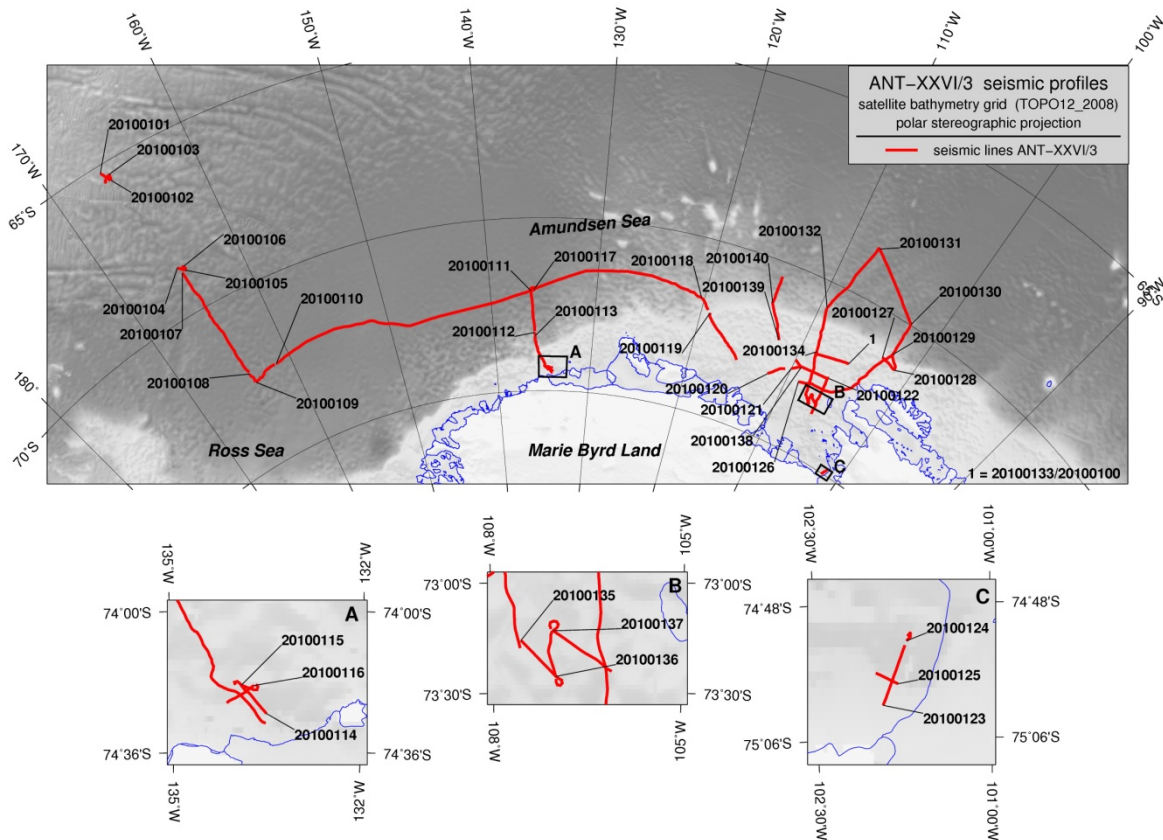


Fig. 4.4: Map with tracks of seismic profiles (red lines). The profile numbers are marked at the beginning of the respective profiles.

Abb. 4.4: Karte mit Lage der seismischen Messprofile (rote Linien). Die Profilnummern sind zum Anfang der jeweiligen Profile hin markiert.

Tab. 4.1: OBS deployments along profile AWI-20100100

Tab. 4.1: OBS-Einsätze entlang des Profils AWI-20100100

No.	Deployed (UTC)	Recovery (UTC)	Latitude South	Longitude West	Depth (m)	Data (MB)	Skew (μsec)	Comment
1	13.03.10 12:44	14.03.10 16:15	72° 04.624'	108° 28.867'	572	170.3	17125	Y comp. offset
2	13.03.10 14:00	14.03.10 18:49	72° 02.546'	107° 54.553'	602	200.8	1625	
3	13.03.10 15:15	14.03.10 20:31	72° 00.466'	107° 20.725'	588	205.0	4437	
4	13.03.10 17:01	14.03.10 23:10	71° 57.931'	106° 40.686'	593	208.0	3937	
5	13.03.10 18:16	15.03.10 00:44	71° 55.938'	106° 11.621'	572	209.8	-1563	high noise level
6	13.03.10 19:33	15.03.10 03:00	71° 53.835'	105° 37.076'	509	218.9	2906	

Tab. 4.2: Summary of seismic reflection profiles**Tab. 4.2:** Zusammenfassung der reflexionsseismischen Profile

PROFILE # AWI...	Start /End	DATE (UTC)	TIME (UTC)	LATITUDE	LONGITUDE	SHOT #	RECORD LENGTH (s)	SAMP. RATE (ms)	SHOT INTERVAL (s)	PROFILE LENGTH (km)	STREAMER	GL-GUN ARRAY	COMMENT
20100101	start	08.02.10	09:08:21	-65.20503	-166.38501	1	9	1	10	39.5	SEAL	3000 m	
	end	08.02.10	13:11:31	-65.52581	-166.03313	1460							3 x 2.7 ltr
20100102	start	08.02.10	13:25:51	-65.51830	-165.98028	1	9	1	10	18.6	SEAL	3000 m	
	en	08.02.10	15:25:41	-65.35717	-165.90292	720							airleak on GI-2
20100103	start	08.02.10	15:38:11	-65.35688	-165.93781	1	9	1	10	30.4	SEAL	3000 m	
	end	08.02.10	18:51:01	-65.52202	-166.37872	1158							3 x 2.7 ltr
20100104	start	09.02.10	19:18:41	-68.63114	-165.07478	1	9	1	10	26.7	SEAL	3000 m	
	end	09.02.10	21:55:31	-68.79328	-164.62947	942							airleak on GI-2
20100105	start	09.02.10	21:55:41	-68.79343	-164.62892	1	9	1	10	15.5	SEAL	3000 m	
	end	09.02.10	23:33:41	-68.68205	-164.59288	589							airleak on GI-2
20100106	start	09.02.10	23:33:51	-68.68186	-164.59308	1	9	1	10	17.5	SEAL	3000 m	
	end	10.02.10	01:26:21	-68.76733	-164.91612	676							airleak on GI-2, airbag on Bird 11 open
20100107	start	10.02.10	02:07:11	-68.82077	-164.92694	1	10	1	12	390.4	SEAL	3000 m	
	end	11.02.10	19:49:24	-72.28503	-164.12152	11920							airleak on GI-2
20100108	start	11.02.10	23:30:00	-72.22564	-164.17555	1	10	2	12	33.9	PFAKLA	600 m	
	end	12.02.10	03:00:00	-72.59175	-164.07619	1002							3 x 2.7 ltr
20100109	start	12.02.10	06:32:00	-72.60656	-164.00705	1	10	2	12	89.4	PFAKLA	600 m	
	end	12.02.10	16:00:47	-72.39858	-161.57855	2695							3 x 2.7 ltr
20100110	start	12.02.10	19:41:24	-72.16236	-154.60963	1	10	1	12	917.6	SEAL	3000 m	
	end	16.02.10	16:10:50	-72.10809	-136.18391	28639							airleak on GI-1 and GI-2, malfunctioned off as from 18.02 on 15.02.2010, FFID 28820
20100111	start	16.02.10	16:11:02	-72.10838	-136.18385	1	10	1	12	132.7	SEAL	3000 m	
	end	17.02.10	05:28:26	-73.28977	-135.873864	3927							2 x 2.7 ltr
20100112	start	17.02.10	07:45:12	-73.31875	-135.87210	1	10	2	12	9.7	PFAKLA	600 m	
	end	17.02.10	08:47:36	-73.40463	-135.866409	251							2 x 2.7 ltr
20100113	start	17.02.10	08:59:00	-73.42221	-135.86317	1	10	2	15	140.4	PFAKLA	600 m	
	end	18.02.10	00:10:59	-74.47894	-134.00412	3402							2 x 2.7 ltr

4.1 Seismics

PROFILE # AWI-...	Start /End	DATE (UTC)	TIME (UTC)	LATITUDE	LONGITUDE	SHOT #	RECORD LENGTH (s)	SAMP. RATE (ms)	SHOT INTERVAL (s)	PROFILE LENGTH (km)	STREAMER	GI-GUN ARRAY	COMMENT
20100114	start	20.02.10	08:25:00	-74.448893	-133.985239	1	8	2	12	28.6	PRAKLA 600 m	3 x 2.7 tr	
	end	20.02.10	11:22:24	-74.315557	-134.480339	859							
20100115	start	20.02.10	11:24:48	-74.315753	-134.46690	1	8	2	12	14.0	PRAKLA 600 m	3 x 2.7 tr	
	end	20.02.10	12:52:24	-74.31692	-134.48848	490							
20100116	start	20.02.10	12:54:24	-74.31858	-134.19818	1	8	2	12	15.9	PRAKLA 600 m	3 x 2.7 tr	
	end	20.02.10	14:36:11	-74.39349	-134.63361	492							
20100117	start	22.02.10	17:05:30	-72.07436	-135.89052	1	10	1	12	571.5	SEAL 3000 m	3 x 2.7 tr	airleak on GI-2, shutdown as from 22.19
	end	25.02.10	03:19:19	-71.72357	-120.28627	14286							on 23.02.2010, FFID 57585, GI-3 leaking as from 03.03 on 25.02.2010, FFID 66203
20100118	start	25.02.10	03:19:31	-71.72365	-120.28551	1	10	1	12	46.5	SEAL 3000 m	2 x 2.7 tr	GI-2 off due to airleak
	end	25.02.10	06:08:31	-72.02328	-119.38563	1445							
20100119	start	25.02.10	09:42:00	-72.08510	-119.16051	1	8	2	10	183.3	PRAKLA 600 m	2 x 2.7 tr	GI-2 off due to airleak
	end	26.02.10	04:42:28	-73.15060	-115.29586	6443							
20100120	start	26.02.10	14:32:30	-73.18657	-111.95014	1	8	2	10	61.9	PRAKLA 600 m	2 x 2.7 tr	GI-2 off due to airleak
	end	26.02.10	20:55:19	-72.84404	-110.51593	2149							
20100121	start	26.02.10	22:56:31	-72.77896	-110.02216	1	10	1	12	128.3	SEAL 3000 m	2 x 2.7 tr	GI-2 off due to airleak
	end	27.02.10	11:40:32	-72.55804	-106.37727	3821							
20100122	start	27.02.10	11:40:43	-72.55795	-106.37662	1	10	1	12	135.6	SEAL 3000 m	2 x 2.7 tr	GI-2 off due to airleak
	end	28.02.10	01:32:43	-73.68115	-106.12699	4161							
20100123	start	01.03.10	05:41:00	-75.02427	-101.93143	1	4	1	6	18.7	PRAKLA 600 m	2 x 2.7 tr	GI-2 off due to airleak
	end	01.03.10	07:38:42	-74.87402	-101.67925	1074							
20100124	start	01.03.10	07:40:30	-74.87302	-101.67158	1	4	1	6	3.8	PRAKLA 600 m	2 x 2.7 tr	GI-2 off due to airleak
	end	01.03.10	08:04:06	-74.88156	-101.71468	215							
20100125	start	01.03.10	08:05:54	-74.88392	-101.71677	1	4	1	6	18.5	PRAKLA 600 m	2 x 2.7 tr	GI-2 off due to airleak
	end	01.03.10	10:04:24	-74.95003	-102.00161	1075							

PROFILE # AWI-...	Start /End	DATE (UTC)	TIME (UTC)	LATITUDE	LONGITUDE	SHOT #	RECORD LENGTH (s)	SAMP. RATE (ms)	SHOT INTERVAL (s)	PROFILE LENGTH (km)	STREAMER	GI-GUN ARRAY	COMMENT
20100126	start	06.03.10	15:29:10	-73.02161	-108.81082	1	10	1	12	356.8	SEAL	3 x 2.7 ltr	
	end	08.03.10	04:21:22	-70.99831	-102.36626	11062				3000 m			
20100127	start	09.03.10	20:18:47	-71.23093	-103.01080	1	10	1	12	69.1	SEAL	3 x 2.7 ltr	
	end	10.03.10	05:03:47	-71.35922	-101.51642	2026				3000 m			
20100128	start	10.03.10	05:03:59	-71.35895	-101.51642	1	10	1	12	52.6	SEAL	3 x 2.7 ltr	
	end	10.03.10	07:58:23	-71.00074	-102.36659	1473				3000 m			
20100129	start	10.03.10	07:58:35	-71.00024	-102.36665	1	10	1	12	112.7	SEAL	3 x 2.7 ltr	
	end	10.03.10	18:41:35	-69.98907	-102.43397	3216				3000 m			
20100130	start	10.03.10	18:41:47	-69.98879	-102.43402	1	10	1	12	263.1	SEAL	3 x 2.7 ltr	
	end	11.03.10	20:11:47	-68.56666	-107.68452	7651				3000 m			
20100131	start	11.03.10	20:11:59	-68.56651	-107.68504	1	10	1	12	257.8	SEAL	3 x 2.7 ltr	
	end	12.03.10	20:50:12	-70.75013	-109.40014	7392				3000 m			
20100132	start	12.03.10	20:50:21	-70.75037	-109.40031	1	10	1	12	145.1	SEAL	3 x 2.7 ltr	
	end	13.03.10	11:13:12	-72.00143	-108.51541	4315				3000 m			
20100133 = OBS refraction profile	start	13.03.10	28:43:00	-71.388370	-105.35043	1	10	1	60	116.8	SEAL	3 x 2.7 ltr	1 x 8.5 ltr G-Gun from 0 ms 23:43 till 00:48 on delay 14.03.10 FFID 112847 - between 112913; G-Gun defect, gen & inj swapped to GI-Guns at 1:19:56 on 14.03.10 FFID 11914
20100134 profile	start	14.03.10	11:24:56	-72.08932	-108.65044	673				3000 m			
20100135	start	18.03.10	07:37:02	-73.28254	-107.54333	1	10	1	12	38.3	SEAL	3 x 2.7 ltr	
	end	18.03.10	11:25:30	-73.42783	-106.99969	1144				3000 m			
20100136	start	18.03.10	11:25:42	-73.42757	-106.99982	1	10	1	12	38.7	SEAL	3 x 2.7 ltr	
	end	18.03.10	15:12:53	-73.22064	-107.03693	1137				3000 m			
20100137	start	18.03.10	15:13:06	-73.22111	-107.03475	1	10	1	12	37.5	SEAL	3 x 2.7 ltr	
	end	18.03.10	18:50:30	-73.41077	-106.07990	1088				3000 m			

4.1 Seismics

PROFILE # AWI-...	Start /End	DATE (UTC)	TIME (UTC)	LATITUDE	LONGITUDE	SHOT #	RECORD LENGTH (s)	SAMP. RATE (ms)	SHOT INTERVAL (s)	PROFILE LENGTH (km)	STREAMER	GI-GUN ARRAY	COMMENT
20100138	start	21.03.10	12:08:39	-72.61945	-109.18191	1	10	1	12	30.6	SEAL	3 x 2.7 tr	
	end	21.03.10	15:10:00	-72.33129	-111.02989	928				3000 m			
20100139	start	26.03.10	03:40:28	-72.16039	-112.21904	1	10	1	12	121.3	SEAL	3 x 2.7 tr	
	end	26.03.10	15:43:15	-71.24501	-113.99800	3539				3000 m			
20100140	start	26.03.10	15:43:27	-71.24480	-113.99822	1	10	1	12	91.0	SEAL	3 x 2.7 tr	
	end	27.03.10	01:10:03	-70.43445	-113.99964	2834				3000 m			
20100141	start	30.03.10	02:58:00	-60.85415	-115.87140	1	10	1	12	26.3	PRAKLA	3 x 2.7 tr	
	end	30.03.10	05:36:12	-60.71203	-116.12053	712				600 m			
20100142	start	30.03.10	05:38:12	-60.71505	-116.11849	1	10	1	12	13.4	PRAKLA	3 x 2.7 tr	
	end	30.03.10	06:55:35	-60.83373	-116.10765	1068				600 m			
20100143	start	30.03.10	06:57:35	-60.83631	-116.10215	1	10	1	12	32.8	PRAKLA	3 x 2.7 tr	
	end	30.03.10	09:52:59	-60.67949	-115.62551	1869				600 m			
							Total length =	5031.8	km				

Preliminary results

A total of 5,032 km of multichannel seismic profiles were collected from the Ross Sea, along the continental rise of the Marie Byrd Land margin, across the shelf of western Wrigley Gulf, in the Amundsen Sea Embayment and Pine Island Bay, in the Amundsen Sea continental rise, and in the northwestern Bellingshausen Sea (Fig. 4.4 and Tab. 4.2). The display of single channels of the multichannel data provided continuously instant results along the profiles (example in Fig. 4.5). An overview of very preliminary results includes:

1. Undulating basement structures and very dynamic sediment depositional processes are revealed on the continental rise of the northern and northeastern Ross Sea.
2. Very thick and undisturbed layered strata show on continental rise along the Marie Byrd Land margin. These data will enable the correlation and comparison of pre-glacial to glacial sedimentation processes between the Ross Sea and Amundsen Sea sectors of Antarctica.
3. A clearly defined boundary between oceanward dipping sedimentary sequences and outcropping basement is identified on the shelf of western Wrigley Gulf.
4. Most of Amundsen Sea Embayment and Pine Island Bay is now covered with key seismic profiles which enable seismic horizon mapping and an analysis of stratigraphic processes at pre-glacial and glacial times.
5. Oceanward dipping sequences which outcrop near or at the seafloor are observed at various locations of middle shelf in Pine Island Bay. The data direct to ideally suitable locations for future shallow drilling of dipping strata and grounding zone wedges.
6. Tectonic basement features infer a renewed interpretation of the continent-ocean boundary/transition of the Amundsen Sea continental margin and the continental breakup process between West Antarctica and New Zealand.
7. Sediment drifts are imaged on continental rise of Amundsen Sea. The records will enable the reconstruction of drift-building processes in relation to bottom-current dynamics in this area.
8. Seismic pre-site surveys in the northernmost Ross Sea and the northwestern Bellingshausen Sea provide records for supporting the IODP drilling proposal 625.

4.2 Magnetics and gravimetry

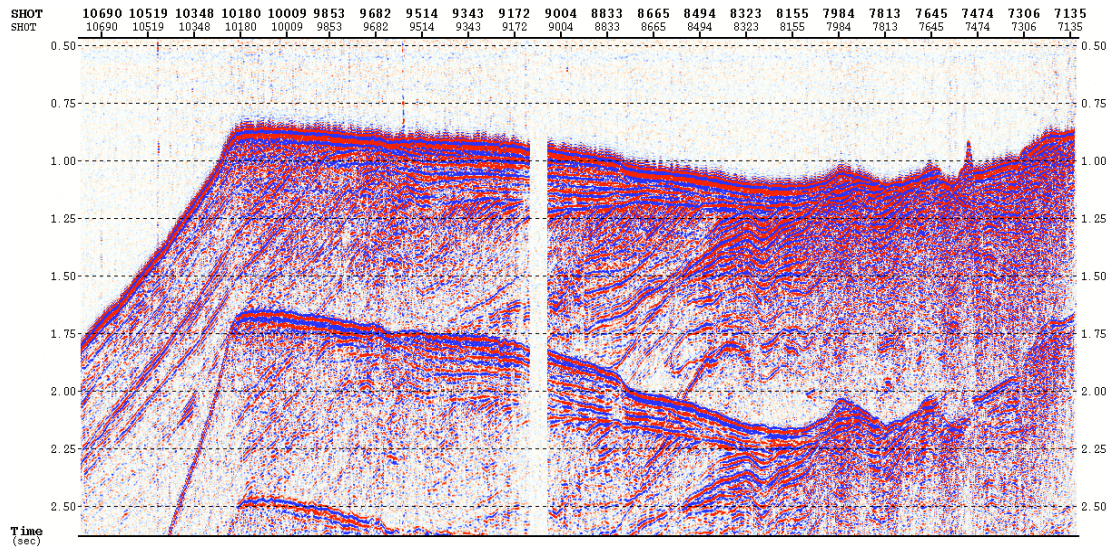


Fig. 4.5: Example of a 100 km long seismic record from the outer shelf of Pine Island Bay. The Fig. shows a single-channel display of the multi-channel data of the 3,000-m-streamer system. The vertical axis is two-way travel-time in seconds.

Abb. 4.5: Beispiel einer 100 km langen seismischen Datenaufnahme vom äußeren Schelf der Pine-Island-Bucht. Die Abbildung zeigt eine Einkanaldarstellung der Mehrkanaldaten des 3,000-m-Streamersystems. Auf der Vertikalachse ist die Zweiweglaufzeit in Sekunden aufgetragen.

4.2 Magnetics and gravimetry

Florian Wobbe, Astrid Denk, Thomas Kalberg, Karsten Gohl
Alfred-Wegener-Institut für Polar- und Meeresforschung, Bremerhaven

Objectives

Accurate models of the geodynamic-tectonic evolution contain some of the most important parameters for understanding and reconstruction of the palaeo-environment. Magnetic and gravimetric surveys of the abyssal plain, the continental shelf and slope of the southern Amundsen Sea and Pine Island Bay allow plate tectonic and continental crustal reconstructions. The objectives are:

- Identifying magnetic sea-floor spreading anomalies of the oldest oceanic crust along the continental margin of the Ross Sea and Marie Byrd Land;
- identification and characterisation of the continental-ocean transition and the boundaries between suspected crustal blocks and volcanic zones in the Amundsen Sea Embayment and Pine Island Bay;
- inverting gravity data for modelling crustal thickness and tectonic features of the continental shelf and the continent-ocean transition.

Work at sea

The work plan for surveying during the expedition consisted of:

- Collection of magnetic data using the ship's permanently installed three-component fluxgate magnetometer as well as the helicopter-towed caesium vapour aeromagnetic sensor system;
- processing the helicopter magnetometer data by removing the geomagnetic variation and electromagnetic noise;
- processing the ship's magnetometer data by compensating for perturbations due to magnetic fields caused by the ship's hull and superstructure, filtering, removing the geomagnetic variations and level the data with the helicopter magnetics;
- collection of gravity data with the ship's marine gravity meter.

Shipborne magnetics

Ship borne magnetic measurements were made by two fluxgate vector magnetometers, which were permanently mounted at the crow's nest. The data were directly saved in the ship's archiving system, DSHIP, at 1-second intervals. To take account of the influence of the metallic bulk of the ship, the ship undertook 8 compensation loops on 31 Jan., 2 Feb., 7 Feb., 12 Feb., 22 Feb., 26 Feb., 8 Mar. and 19 Mar. 2010. In the small area of a compensation loop the variations of the magnetic field due to crustal magnetisation are assumed to be negligible. The loops thus provide coefficients that relate the ship's heading, roll, and pitch movements to the variations in magnetometer measurements that they cause. Using these coefficients, it is possible to correct the ship borne magnetic measurements in the wider area around the compensation loop. This compensation process was completed using a MATLAB routine written by Matthias König (formerly at AWI).

Helicopter magnetics

AWI's Scintrex caesium vapour magnetometer, towed 30 m below the helicopter to avoid magnetic disturbances, was used to collect aeromagnetic data. Inside the cockpit, this magnetometer was connected to the AGIS (Airborne Geophysical Information System, PICO ENVIROTEC INC.) data acquisition system, consisting of three computers with further connections to a GPS-receiver and radio altimeter. The different computers share the tasks of processing the signals of the Scintrex sensor, displaying the received data (data control unit), display the flight track on the Pilot Guidance Unit (PGU) and the operator's navigation screen (AGIS software), and recording the collected data on hard disk.

The caesium vapour magnetometer sensor is enclosed in a redesigned towed bird, which is considerably heavier and larger than the old one used during the *Polarstern* expedition ANT-XXIII/4 in 2006. This redesign of the bird is supposed to allow for a steadier flight and thus reduce measuring errors due to strong vibration and turbulence.

Daily flight planning was done using a compilation of ArcGIS, PICO's PEIConvert software and several algorithms, written during the cruise, which allow interactive project management. This capability is essential in an area like the Amundsen Sea where changeable ice and weather conditions meant that the ship's itinerary was often altered on short notice. This capability is intended to improve the flexibility of

4.2 Magnetics and gravimetry

the flight operator's response to situations in which the flight plan needs to be changed during acquisition.

Data acquisition went smoothly most of the time, although we experienced problems caused by HF communication with *Polarstern* when the magnetometer cable was placed near the HF antenna on the left hand side of the helicopter. This problem was resolved by passing the cable through the door on the right hand side. Occasionally tracks had to be rerouted during flight, especially during extended periods of local snowfall.

The AGIS system is intended for survey plans that stretch over large areas with more than one Universal Transverse Mercator (UTM) zone. The software on the measuring unit in the helicopter is fed with precompiled project files before the flight. Unfortunately, changing or adding of new waypoints to the flight path during the measurement is unsupported. However, the survey area can be subdivided into an arbitrary number of parallel survey and tie lines at constant distance and particular angle. During the flight any desired line can be selected and displayed on the PGU, which is very convenient when rerouting an ongoing flight. Even though our target research area, the Amundsen Sea embayment, covers several UTM zones, we mostly used UTM 12S coordinates, in which the project lines are only negligibly distorted.

The bird and cable have been affected during the operation on two incidents. The first event took place during take-off, when the magnetometer cable was caught on the box, which was subsequently torn off its bearing on deck. The mantle of the cable was injured during this accident. The flight and data acquisition continued normally, though. The second incident took place upon landing in unfavorable visibility conditions. During landing, the bird crashed onto deck and the tail section was separated from the main body. The tubing was destroyed and parts of the wings were torn off (Fig. 4.8). However, the sensor and electronics survived and the tail section could successfully be rebuilt within three days, using spare parts from the ship (e.g. sewage pipe, glass fiber surfacer, polyester resin).

Gravimetry

Gravity data were continuously acquired during the expedition (with the exception of the EEZ of Chile) using the ship's permanently mounted Bodenseewerke KSS31 gravity meter. The data were directly transmitted to the D-SHIP system in one-second intervals. The gravity data acquisition operated without any problems for most of the cruise leg, except for short periods when the gravity meter failed several times within a few hours for unknown reasons. Several restarts were necessary before the system operated again continuously.

We conducted calibration measurements (referencing) with the LaCoste & Romberg gravity meter G-877 at the pier of Wellington Port and at the Madones Pier of Punta Arenas.

Preliminary results

Ship borne magnetics

The ship's magnetometer data were downloaded from DSHIP and processed in blocks located close to compensation circles. As well as compensation for the ship's field, processing consisted of an IGRF correction, data reduction and filtering of high frequency chatter. Regardless of which set of compensation parameters is used, some data retain long wavelength residual anomalies after the processing. This is attributable to the high gradient in the geomagnetic field in the study area, meaning a set of compensation coefficients quickly becomes inadequate for full compensation as the ship progresses (between 500 and 1,500 km during this cruise). This point can easily be determined by comparing the compensated data from upper and lower sensor. When the difference between both increases steadily the set of compensation coefficients is insufficient to compensate the magnetic readings (Fig. 4.6).

Because it was impractical to complete a large number of compensation loops, these long wavelength anomalies were removed by levelling the data to the helicopter magnetics with the software GEOSOFT OASIS montaj. At this stage, the data are useable, although in some cases there remain artefacts in the data. Comparison with helicopter magnetic profiles shows that the ship borne data are reliable in that they show similar anomalies with similar amplitudes.

Helicopter magnetics

Although unfavourable weather conditions did not allow the helicopter magnetic programme to perform equally well as during the *Polarstern* expedition ANT-XXIII/4 in 2006, and many flights had to be cancelled or flight time had to be reduced, a total of about 15,300 km (Amundsen Sea Embayment) of new data were delivered (as opposed to 20,900 km in 2006). During the N-S transect from New Zealand to the Ross Sea another 6,905 km of helicopter magnetic data were collected.

A first test flight on the Campbell Plateau did not yield in usable magnetic data because of a misconfiguration of the sensor. The sensor electronics were switched to southern hemisphere operation thereafter and the data acquisition performed well. A comparison between the data from the old system of 2006 and the data from the new one utilised on this cruise shows a considerable improvement in data quality. During the operation in 2006 problems with static electricity caused system malfunction and the data shows a lot of high frequency noise and outliers that have to be manually removed. These obstacles have been resolved in the meantime and the new system clearly outperforms the old one: the ratio between total flight time vs. data acquisition time could be diminished by 50 %. In addition, the increased weight of the new bird causes a steadier flight and thus reduces high frequency noise due to vibrations. Since the measuring system is operates in a stable way and is not influenced by static electricity, the editing and the filtering of the recorded data is not necessary any more.

4.2 Magnetics and gravimetry

Tab. 4.3 - 4.5 and Fig. 4.7 - 4.9 give an overview of the heli-magnetic flights. At the beginning of February, the first tracks were flown during the North-South transect from New Zealand to the Eastern Ross Sea, revealing seafloor-spreading anomalies. During the West-East transect towards the Amundsen Sea a series of North-South directed profiles could be completed perpendicular to the ship's track. Upon reaching the Amundsen Sea embayment, regular flight patterns were flown over the continental shelf, filling up the gaps with no data left over from the 2006 cruise from the North-West to the South-East.

The fundamental division between the magnetic styles of the inner and outer shelf that has been detected during the season in 2006 could be confirmed on additional profiles: short wavelength anomalies characterise the inner shelf and neighbouring land, but longer wavelength anomalies are visible in the North. Further, parallel belts of similar magnetic signature could be identified on the outer shelf. These linear features extend up to 500 km long and strike approximately South-West, North-East. Similar but less distinct features exist in a direction perpendicular to the former.

The aim to connect the helicopter magnetic grid to the AGASEA data over the main land, acquired by the University of Texas (USA) and British Antarctic Survey (UK) in 2005, could not be realised. However, there is one line from AWI's flights in 2006, reaching far enough south to provide the possibility of connecting the two data sets. In this region, high amplitude short wavelength magnetic anomalies appear to be related to granitic island groups that lie along NW-oriented gravity anomaly trends, but at this stage the NW trend itself is not strongly evident in the magnetic data.

After leaving Pine Island Bay we resumed flights over the continental shelf North of Thurston Island, extending AWI's 2006 helicopter magnetics data set to the North-East. The new data reveals a prolongation of the North-East striking linear features reaching out from central Pine Island Bay to the shelf break. The oceanic crust to the North displays inhomogeneous magnetic patterns that do not appear to correlate with those on parallel profile lines. In addition, the shelf break itself is not well defined by magnetic signatures along lines that cross the outer shelf to the open sea. This seems to be the case in the North-West corner of the Amundsen Sea Embayment as well, where data were acquired on several flight tracks at the end of March.

During a short excursion into the Marie Byrd Seamounts province a densification of the 2006 flight tracks was attempted. However, due to bad weather conditions only few data acquired on a short flight could be added.

In summary, we can see that even at this early stage the newly acquired potential field data are undoubtedly of scientific value. In the future, after further data reduction and modelling of source body distributions, the ship's magnetic data will be useful adjuncts to the interpretation of the seismic refraction profiles, as these are co-located. After further processing and levelling, the helicopter magnetic data will also contribute to these studies, as they provide information on the spatial extent of

features crossed by the profiles. In the absence of extensive rock outcrops, these data will also provide key information on the near surface geology of Pine Island Bay.

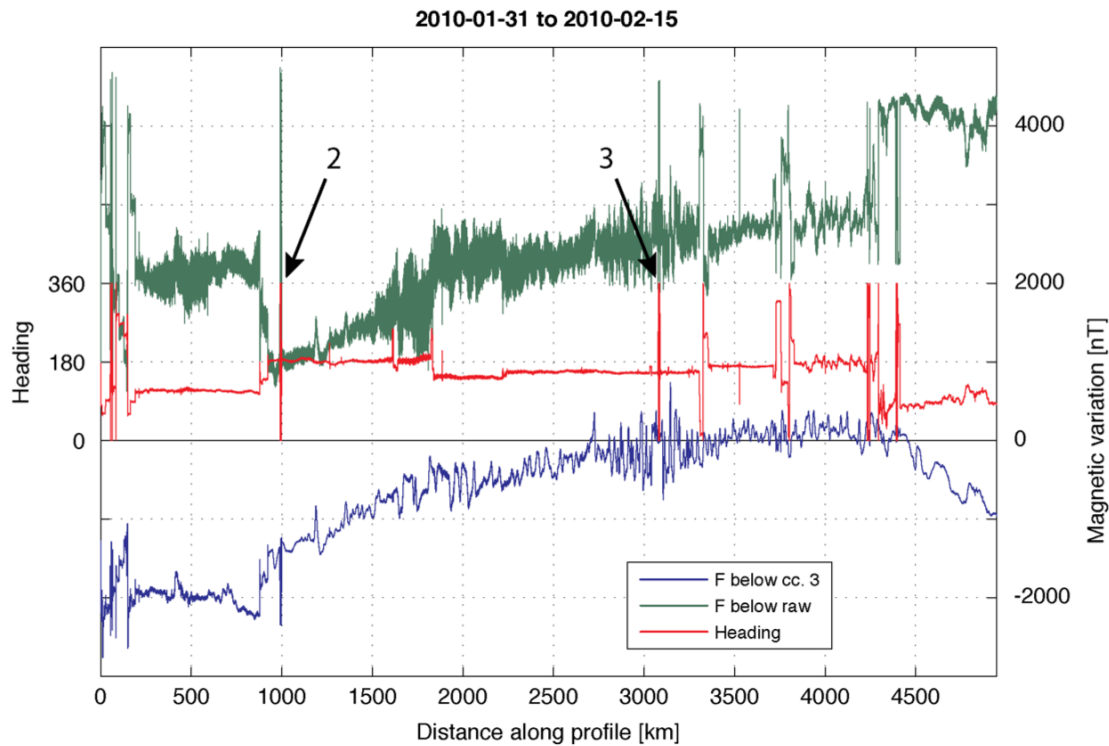


Fig. 4.6: Ship's magnetometer data (unprocessed: green; compensated with 3rd compensation circle coefficients: blue; heading: red). Arrows indicate position of 2nd and 3rd compensation loop along the ship's profile.

Abb. 4.6: Schiffsmagnetische Messdaten (unbearbeitet: grün; kompensiert mit Koeffizienten des 3. Kompensationskreises: blau; Kurs: rot). Pfeile markieren die Lage der 2. und 3. Kompensationskreise entlang der Schiffsroute.

4.2 Magnetics and gravimetry

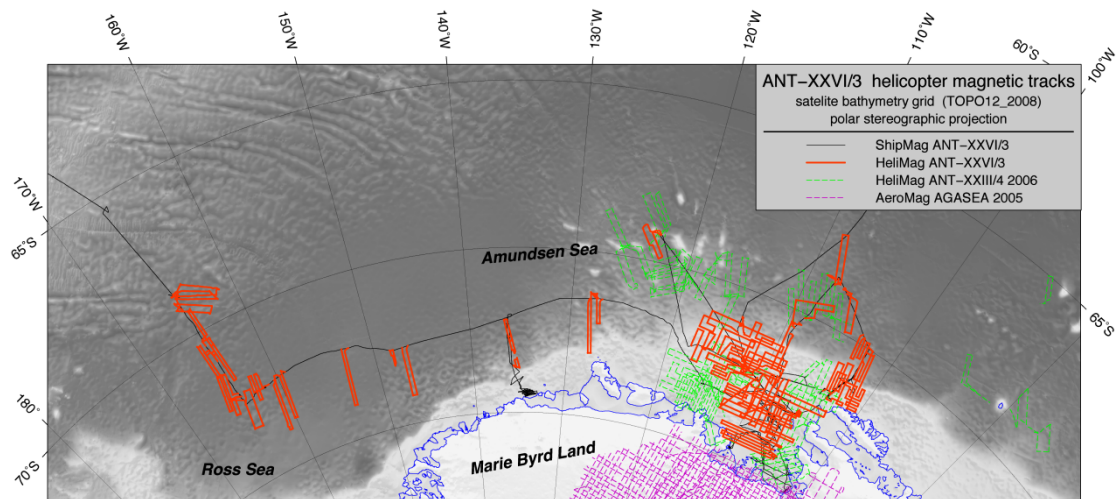


Fig. 4.7: All magnetic survey tracks along the West Antarctic margin from this expedition (red lines) and previous expeditions by AWI and BAS/Univ. Texas (over main land).

Abb. 4.7: Magnetische Vermessungsprofile entlang des westantarktischen Kontinentalrandes von dieser Expedition (rote Linien) und von früheren Expeditionen des AWI und BAS/Univ. of Texas (über dem Festland).

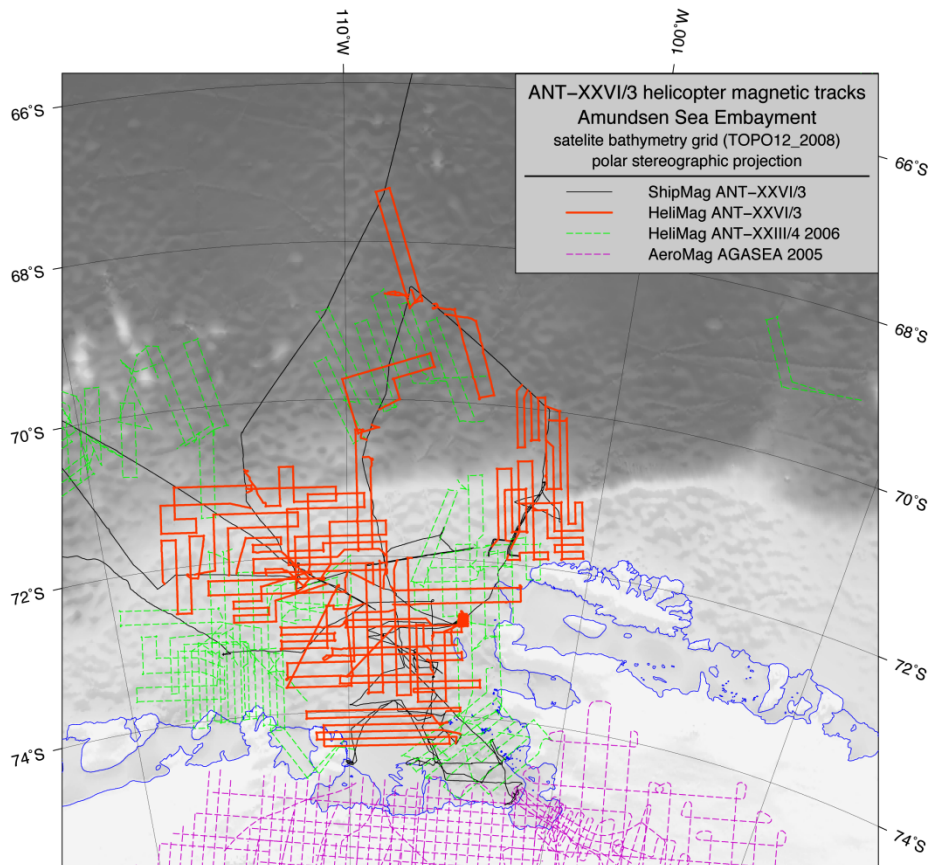


Fig. 4.8: Magnetic survey tracks in Amundsen Sea Embayment from this expedition (red lines) and previous expeditions by AWI and BAS/Univ. Texas (over main land). Abb. 4.8: Magnetische Vermessungsprofile im Amundsen Sea Embayment von dieser Expedition (rote Linien) und von früheren Expeditionen des AWI und BAS/Univ. of Texas (über dem Festland).



*Fig. 4.9: Photography of the broken and repaired bird's tail section
Abb. 4.9: Fotos der gebrochenen und reparierten Flugkörpersektion*

Tab. 4.3: Magnetic compensation circles

Tab. 4.3: Magnetische Kompensationskreise

No	Date, UTC	Time, UTC	Lon	Lat
1	2010-01-31	04:18 – 05:16	-173	-44
2	2010-02-02	08:03 – 09:03	-178	-47
3	2010-02-07	21:39 – 22:55	-168	-64
4	2010-02-12	16:26 – 17:32	-161	-72
5	2010-02-22	13:33 – 14:30	-137	-72
6	2010-02-26	06:48 – 07:45	-115	-73
7	2010-03-08	05:48 – 06:51	-102	-71
8	2010-03-19	04:16 – 05:16	-108	-73

Tab. 4.4: Statistics of helicopter-magnetics

Tab. 4.4: Statistik der Helikopter-Magnetik

Number of flights:	58
Total flight distance:	22594 km
Total flight distance in Amundsen Sea Embayment:	15291 km
Total flight hours:	136.8 h
Time of actual data acquisition:	134.6 h
Mean flight velocity:	167.8 km/h
Overhead (due to start/ landing/ system malfunction):	1.6 %

4.2 Magnetics and gravimetry

Tab. 4.5: Helicopter magnetic data acquisition flight details

Tab. 4.5: Details der helikopter-magnetischen Datenaufnahme

Campbell Plateau, New Zealand:

No	Project Filename	Date (UTC)	Raw Data File	UTM Zone	Time [min]	distance [km]
1	f001a	2010-02-02 02:15	B0020202.P15	1S	142.8	73.4
		2010-02-02 02:54	B0020202.P54			4.4
		2010-02-02 02:55	B0020202.P55			2
		2010-02-02 02:56	B0020202.P56			37.7
		2010-02-02 03:08	B0020203.P08			114.2
		2010-02-02 03:45	B0020203.P45			165.6

Bollons Seamount area, New Zealand:

No	Project Filename	Date (UTC)	Raw Data File	UTM Zone	Time [min]	Distance [km]
2	f002	2010-02-03 02:10	B0020302.P10	1S	160.4	417.5

Transect New Zealand to eastern Ross Sea:

No	Project Filename	Date (UTC)	Raw Data File	UTM Zone	Time [min]	Distance [km]
3	f003a	2010-02-09 19:50	B0020919.P50	3S	165.6	425.3
4	f004a	2010-02-10 01:36	B0021001.P36	3S	131.6	361.6
5	f004a	2010-02-10 04:37	B0021004.P37	3S	121.8	334
6	2010-02-10	2010-02-10 19:55	B0021019.P55	3S	146.7	399
7	2010-02-10	2010-02-11 00:10	B0021100.P10	3S	135.2	357.8
8	2010-02-10	2010-02-11 02:53	B0021102.P53	3S	139.3	377.1
9	2010-02-11	2010-02-11 18:58	B0021118.P58	3S	127.1	362.1
10	2010-02-11	2010-02-11 23:24	B0021123.P24	3S	131.0	364.7
11	2010-02-11	2010-02-12 02:28	B0021202.P28	3S	131.1	349.5

Transect from eastern Ross Sea to western Amundsen Sea:

No	Project Filename	Date (UTC)	Raw Data File	UTM Zone	Time [min]	Distance [km]
12	2010_02_12	2010-02-12 18:48	B0021218.P48	3S	136.7	394
13	2010_02_12	2010-02-12 23:10	B0021223.P10	3S	145.9	408
14	2010_02_12	2010-02-13 02:03	B0021302.P03	3S	124.7	355
15	2010_02_13	2010-02-14 01:14	B0021401.P14	5S	152.1	417.9
16	2010_02_13	2010-02-14 18:03	B0021418.P03	5S	49.2	130.3
17	2010_02_13	2010-02-14 22:33	B0021422.P33	5S	127.6	359.3

Western Wrigley Gulf area:

No	Project Filename	Date (UTC)	Raw Data File	UTM Zone	Time [min]	Distance [km]
18	2010_02_16	2010-02-16 22:39	B0021622.P39	8S	107.2	294.2
19	2010_02_21	2010-02-21 19:23	B0022119.P23	8S	42.8	111
20	2010_02_23a	2010-02-23 21:35	B0022321.P35	8S	147.3	439
21	2010_02_23a	2010-02-24 00:37	B0022400.P37	8S	91.6	248

Western Amundsen Sea:

No	Project Filename	Date (UTC)	Raw Data File	UTM Zone	Time [min]	Distance [km]
22	2010_02_25	2010-02-26 22:49	B0022622.P49	11S	187.9	493.1
		2010-02-27 01:49	B0022701.P49			20.8
23	2010_02_27	2010-02-27 16:03	B0022716.P03	11S	136.4	393.7
24	2010_02_27	2010-02-27 20:19	B0022720.P19	11S	164.6	478.4
25	2010_02_27	2010-02-27 23:21	B0022723.P21	11S	173.7	500

Amundsen Sea Embayment:

No	Project Filename	Date (UTC)	Raw Data File	UTM Zone	Time [min]	Distance [km]
26	2010_02_27	2010-03-03 16:21	B0030316.P21	11S	152.3	433.1
27	2010_02_27	2010-03-03 20:19	B0030320.P19	11S	147.1	426
28	2010_03_03	2010-03-03 23:11	B0030323.P11	12S	162.9	466.2
29	2010_03_03	2010-03-08 17:04	B0030817.P04	12S	150.6	435.3
30	2010_03_03	2010-03-08 20:25	B0030820.P25	12S	145.7	409.4
31	2010_03_03	2010-03-09 19:35	B0030919.P35	12S	150.8	427.9
32	2010_03_09a	2010-03-10 14:56	B0031014.P56	12S	156.5	457.3
33	2010_03_09a	2010-03-10 19:33	B0031019.P33	12S	166.9	189.1
34	2010_03_09a	2010-03-10 22:51	B0031022.P51	12S	66.2	477.3
35	2010_03_09a	2010-03-11 14:16	B0031114.P16	12S	132.5	372.6
36	2010_03_09b	2010-03-11 18:32	B0031118.P32	12S	142.2	420
37	2010_03_09b	2010-03-11 21:35	B0031121.P35	12S	28.7	77.8
38	2010_03_09b	2010-03-12 13:57	B0031213.P57	12S	138.4	416.8
39	2010_03_09a	2010-03-12 18:21	B0031218.P21	12S	138.7	392.1
40	2010_03_03	2010-03-14 14:02	B0031414.P02	12S	147.7	413.4
41	2010_03_03	2010-03-14 18:16	B0031418.P16	12S	147.6	424.4
42	2010_03_03	2010-03-15 13:53	B0031513.P53	12S	152.0	424.3
43	2010_03_03	2010-03-15 18:20	B0031518.P20	12S	161.8	424.9
44	2010_03_03	2010-03-15 21:43	B0031521.P43	12S	166.4	462.3
45	2010_03_03	2010-03-19 20:52	B0031920.P52	12S	149.7	424.2
46	2010_03_03	2010-03-19 23:33	B0031923.P33	12S	113.9	334.4
47	2010_03_03	2010-03-20 14:10	B0032014.P10	12S	156.5	443.2
48	2010_03_03	2010-03-20 17:01	B0032017.P51	12S	158.8	434.6
49	2010_03_03	2010-03-20 21:03	B0032021.P03	12S	150.2	423.7
50	2010_03_03	2010-03-21 14:50	B0032114.P50	12S	149.8	408.1
51	2010_03_03	2010-03-21 18:27	B0032118.P27	12S	162.5	459.5
52	2010_03_03	2010-03-21 21:35	B0032121.P35	12S	134.3	418.7

Marie Byrd Seamounts:

No	Project Filename	Date (UTC)	Raw Data File	UTM Zone	Time [min]	Distance [km]
53	2010_03_22	2010-03-23 15:47	B0032315.P47	11S	126.2	358.6

Amundsen Sea Embayment:

No	Project Filename	Date (UTC)	Raw Data File	UTM Zone	Time [min]	Distance [km]
54	2010_03_03	2010-03-25 14:45	B0032514.P45	12S	172.8	450.6
55	2010_03_03	2010-03-25 14:45	B0032518.P07	12S	157.3	428.1
56	2010_03_03	2010-03-25 14:45	B0032521.P17	12S	140.4	364.8
57	2010_03_03	2010-03-26 14:17	B0032614.P17	12S	163.3	455.7
58	2010_03_03	2010-03-26 17:43	B0032617.P43	12S	167.1	450.6

4.3 Geothermal heat-flow measurements

4.3 Geothermal heat-flow measurements

Norbert Kaul¹, Frank Brenner²,
Karsten Gohl²

¹University of Bremen, Dept. of Geosciences,
Bremen, Germany

²Alfred-Wegener-Institut für Polar- und
Meeresforschung, Bremerhave

Objectives

Recent volcanism has been identified in the area of the Hudson Mountains. Heat flow measurements in sediments of the inner and middle shelf of Pine Island Bay in the vicinity of the Hudson Mts provide a first estimate on the local geothermal heat flux. As information on geothermal heat flow in this region is unknown, the survey is designed as a regional test survey to obtain a first impression of the general heat flow distribution.

Work at sea

During that cruise a number of 29 positions were selected to conduct heat flow measurements. For heat flow density determination, information of the undisturbed temperature gradient is essential as well as of the thermal conductivity of the respective material. During that cruise temperature gradient was measured by using a temperature gradient lance as a tool (see Fig. 4.9). Thermal conductivity k is measured on core material, sampled near or at the positions of the gradient lance positions (see Fig. 4.10).



Fig. 4.9: Temperature gradient probe equipped with five temperature loggers on the lance and one on the head for bottom water reference temperature.

Abb. 4.9: Temperaturgradienten-Lanze, hier ausgerüstet mit fünf Loggern an der Lanze und einem zusätzlichen, der die Bodenwassertemperatur misst.



Fig. 4.10: Thermal conductivity measurement on split cores using the KD2 Pro instrument
Abb. 4.10: Wärmeleitfähigkeitsmessungen am geöffneten Kern mit dem KD2 Pro Messgerät

For temperature measurements five ANTARES autonomous temperature loggers are mounted onto the lance of a dedicated tool plus one additional for bottom water reference. These loggers have a resolution of app. 0.001 K and an accuracy of app. 0.1 K. They are calibrated against the on-board CTD during this cruise, yielding an absolute accuracy of +/-0.002 K. The relative z-positions on the instrument are:

4.54, 3.84, 3.14, 2.44, 1.74, 0 m with respect to the uppermost water sensor resulting in 0.7 m spacing within the ground.

For thermal conductivity measurements the DECAGON DEVICES thermal properties meter KD2 Pro is employed together with the KS-1, 1.3 mm single-needle. The instrument is rated at 5 % accuracy in conductivity.

4.3 Geothermal heat-flow measurements

Tab. 4.6: Geothermal heat-flow measurement stations

Tab. 4.6: Stationen geothermischer Wärmeflussmessungen

PS station	HF station	latitude S	longitude W	water-depth (m)
PS75/129-2	H1001	74°30.524'	134°07.354'	893
PS75/132-2	H1002	74°22.022'	134°23.066'	724
PS75/136-4	H1003	74°23.241'	134°36.040'	722
PS75/139-3	H1004	74°05.993'	135°03.162'	430
PS75/162-2	H1005	74°49.99'	103°29.94'	1021
PS75/163-2	H1006	74°44.476'	104°23.539'	1104
PS75/164-2	H1007	74°44.84'	105°12.03'	1302
PS75/165-2	H1008	74°40.176'	106°36.387'	1184
PS75/166-2	H1009	74°36.099'	106°36.677'	1353
PS75/169-2	H1010	74°20.00'	106°00.00'	1386
PS75/170-2	H1011	74°12.530'	105°32.996'	1644
PS75/173-2	H1012	74°08.33'	106°43.82'	1468
PS75/174-2	H1013	74°00.913'	105°41.536'	1037
PS75/178-2	H1014	74°05.48'	106°45.019'	604
PS75/179-2	H1015	74°02.500'	106°11.08'	1111
PS75/180-4	H1016	73°31.426'	106°12.025'	806
PS75/181-1	H1017	73°31.716'	106°11.866'	813
PS75/182-1	H1018	73°31.12'	106°12.09'	814
PS75/184-2	H1019	73°31.256'	106°12.09'	795
PS75/185-1	H1020	73°31.085'	106°12.296'	795
PS75/190-2	H1021	71°52.775'	103°23.241'	752
PS75/192-3	H1022	71°44.689'	103°19.69'	768
PS75/194-2	H1023	71°27.205'	103°00.432'	626
PS75/195-2	H1024	71°03.975'	102°22.00'	1447
PS75/210-2	H1025	71°53.776'	105°37.126'	496
PS75/214-2	H1026	74°32.050'	102°36.700'	611
PS75/216-3	H1027	74°36.679'	105°51.131'	626
PS75/230-2	H1028	72°49.962'	106°30.131'	577
PS75/260-1	H1029	70°21.858'	113°57.436'	3496

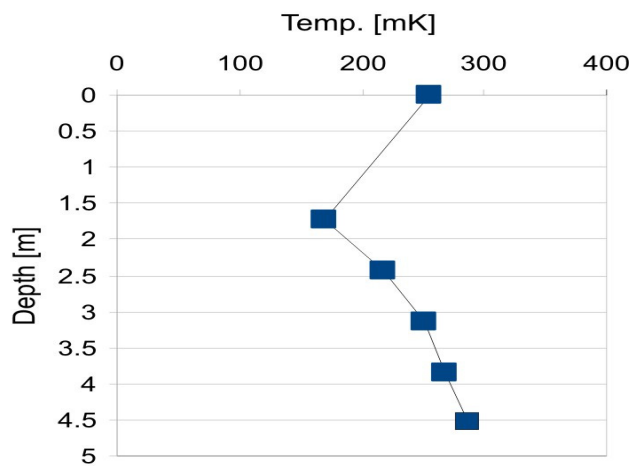
Preliminary results

In Wrigley Gulf, the geothermal temperature gradients often suffer from vigorous ocean bottom currents, an example is given in Fig. 4.11, indicating a temperature decrease in the recent past and an actual temperature increase of 0.1°C. Similar hints come from oceanographic measurements, showing strong thermal layering near the seafloor in some places. In Pine Island Bay, stable gradients are met at most sites, allowing the calculation of heat flow values (Fig. 4.12). Penetration is good or very good at almost all locations.

H1001

Fig. 4.11: Example of a disturbed temperature gradient of Wrigley Gulf. Seafloor is at 1 m.

Abb. 4.11: Beispiel für einen gestörten Temperaturgradienten aus dem Wrigley-Golf. Die Grenze Wasser-Boden ist bei 1 m.



H1010

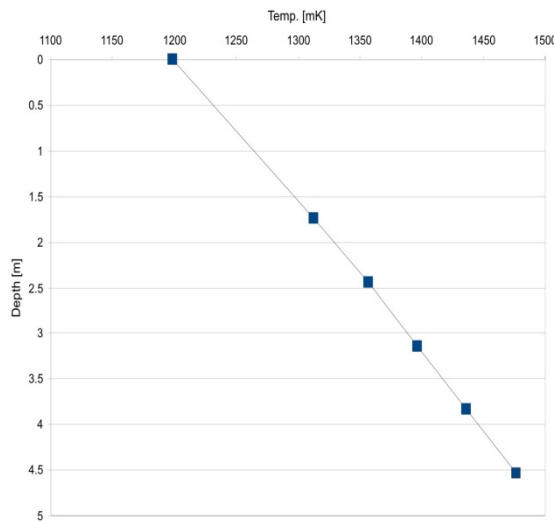


Fig. 4.12: Example of a linear temperature gradient of Pine Island Bay. Seafloor is at 1 m.

Abb. 4.12: Beispiel für einen linearen Temperaturgradienten aus der Pine Island Bucht. Die Grenze Wasser-Boden ist bei 1 m.

5. MARINE-SEDIMENTARY GEOLOGY: WEST ANTARCTIC CONTINENTAL MARGIN SEDIMENTS AS RECORDED OF VARIABILITY OF THE WEST ANTARCTIC ICE SHEET AND PALAEOCLIMATIC CHANGES DURING THE QUATERNARY

Gerhard Kuhn¹, Claus-Dieter Hillenbrand², Marcus Gutjahr³, Daniel Baqué¹, Matthias Forwick⁴, Patrycja Ewa Jernas^{4,5}, Johann Philipp Klages¹, Norbert Lensch¹, Ian MacNab², James A. Smith², Steffen Wiers¹

¹Alfred-Wegener-Institut für Polar- und Meeresforschung, Bremerhaven

²British Antarctic Survey, Cambridge, UK

³Department of Earth Sciences, University of Bristol, UK

⁴Department of Geology, University of Tromsø, Norway

⁵Norwegian Polar Institute, Tromsø, Norway

Objectives

Late Quaternary dynamics of the West Antarctic Ice Sheet

The collapse of the West Antarctic Ice Sheet (WAIS) would result in a global sea-level rise between 3.3 and 5 m. At present it is not clear to what extent current retreat of WAIS grounding lines observed in the Amundsen Sea Embayment (ASE), in particular in Pine Island Bay, is part of ongoing recession that started before ca. 14.5 ka, or if it reflects more recent climatic changes. During cruise ANT-XXIII/4 with *Polarstern* in 2006 and cruises JR141 and JR179 with RRS *James Clark Ross* in 2006 and 2008, respectively, AWI and BAS collected marine sediment cores, swath bathymetry and high-resolution seismic data from the ASE and the adjacent continental margin. Primary aims of this work were the reconstruction of the poorly known deglaciation history in this sector of West Antarctica since the Last Glacial Maximum (LGM) and finding evidence of a possible WAIS collapse during the Quaternary. Up to now, geophysical and geological data from these expeditions have indicated that grounded ice advanced to the shelf break in the ASE at the LGM. Furthermore, they revealed a complex pattern of glacial bedforms on the shelf, which resulted from variabilities in subglacial substrate, basal ice conditions and ice-flow rate. Results from marine sediment cores have shown that the inner shelf in the western ASE deglaciated before ca. 13 ka and that some of the meltwater channels there pre-date the last WAIS advance. The analysis of an older sediment core, which had been collected by *Polarstern* from the continental rise offshore from Pine Island Bay in 2001, revealed a depositional anomaly from ca. 620-480 ka that might be related to a Mid-Quaternary collapse of the WAIS. Work on the data sets collected in 2006 and 2008 is ongoing, and the results constraining post-LGM grounding-line retreat in the ASE will be coupled with glaciological models to improve understanding of the stability and climate sensitivity of the WAIS. Nevertheless, some crucial gaps in

the geographical coverage of the ASE shelf with geomorphological data and sediment cores that fully penetrated the post-LGM sediments have become obvious. The main objective on cruise ANT-XXVI/3 was to collect marine geological and geophysical data for closing these gaps in the ASE and to collect new data from the Marie Byrd Land shelf to determine:

- 1) The LGM extent of the WAIS between the easternmost Ross Sea and Pine Island Bay,
- 2) the extent of fast ice flow in the former WAIS, and controls on the location and onset position of fast ice flow,
- 3) the post-LGM retreat history of the WAIS,
- 4) the timing and forcing of a possible WAIS collapse during the Quaternary.

Cold water deep-sea coral sampling at the Marie Byrd Seamounts

While late Holocene pre-industrial atmospheric CO₂ contents were on the order of 280 ppm, during the LGM the atmospheric CO₂ concentration was as low as 180 ppm. Despite two decades of research, the reasons for this change in an important greenhouse gas are still poorly understood. The Southern Ocean is a key region for palaeoclimatic research generally, but especially with regard to these glacial-interglacial atmospheric CO₂ concentration changes. Deep water can store significantly more dissolved inorganic carbon (DIC) than surface water, and upwelling waters around Antarctica at present-day degas substantial amounts of previously dissolved deep water-bound DIC. Changes in the large-scale Southern Ocean circulation around Antarctica have been suggested to play a significant role in controlling these variations. Several previous studies suggested decreased rates of upwelling around Antarctica during the last glacial period, either due to extended sea ice cover or northward shifted Westerlies. As yet, however, only few rigorous tests of these ideas have been carried out due to the lack of suitable archives.

One potential test is the measurement of the modern and past deep-water boron isotopic composition recorded in deep-sea corals from seamounts around Antarctica. Oceanic abyssal basins isolated from major vertical water exchange rich in respired carbon are prime candidates to store the extra amount of atmospheric CO₂ that was drawn from the atmosphere during the last glacial period. Boron is a minor element in seawater. It occurs as ¹¹B and ¹⁰B, and the ¹¹B/¹⁰B isotopic composition of deep-sea corals living in intermediate water depths depends on the pH of ambient seawater in which these corals grow. Since the seawater pH in turn is dependent on the total alkalinity and ultimately the amount of DIC, the comparison of modern, deglacial and fully glacial coral ¹¹B/¹⁰B yields essential information about the amount of DIC at a given time. These calcitic scleractonian deep-sea corals from the Marie Byrd Seamounts can be radiocarbon-dated providing the base for key palaeoceanographic and palaeoclimatic reconstructions during major climatic transitions such as the last deglaciation. We are ultimately interested in identifying periods of deep ocean total alkalinity- and pH re-adjustments that accompanied periods of fossil carbon degassing from the deep sea into the atmosphere. Corals dredged during *Polarstern*

cruise ANT-XXIII/4 in 2006, as well as those sampled during cruise ANT-XXVI/3 will be characterised for their elemental composition using a laser ablation device connected to a Thermo-Finnigan Element 2. The boron isotopic compositions will be determined using a Thermo-Finnigan Neptune MC-ICP-MS. All analyses are carried out within the Bristol Isotope Group at the University of Bristol, UK.

Seawater sampling for neodymium isotopic analyses

Neodymium (Nd) is a trace metal that belongs to the Rare Earth Elements (REE). Neodymium-143 is the radiogenic daughter of Samarium-147 with a half-life of 106 Gyr. In open seawater Nd behaves semi-conservative with a residence time ranging from 500 to 1,500 years. Because of this intermediate residence time in seawater it serves as an excellent tracer for inter-basin deep-water exchange and it is increasingly used for past deep-water reconstructions in a similar manner to classical palaeoceanographic proxies such as carbon isotopes. Conversely to carbon isotopes, the Nd isotopic composition of seawater is not affected by productivity. Neodymium is supplied to the oceans through riverine continental input and particle-seawater exchange along continental margins through the so-called boundary exchange. Labrador Seawater in the North Atlantic has the least radiogenic (lowest $^{143}\text{Nd}/^{144}\text{Nd}$) and North Pacific water the most radiogenic (highest $^{143}\text{Nd}/^{144}\text{Nd}$) Nd isotope compositions. Southern Ocean water is intermediate between these end-member compositions. Although most parts of the world oceans have been mapped for their Nd isotopic compositions over the past two decades there is a clear lack of data from remote locations such as the Ross Sea or along the West Antarctic margin. The aim of our work here is therefore twofold: (a) to provide water column Nd isotope compositions within the Ross Sea and along the West Antarctic margin, and (b) to investigate the effect of boundary exchange for the bottom water Nd isotopic composition at the sediment-bottom water interface at locations on the West Antarctic shelf in the ASE. All water samples taken during this cruise will be analysed for their $^{143}\text{Nd}/^{144}\text{Nd}$, $^{147}\text{Sm}/^{144}\text{Nd}$, as well as their Nd concentrations within the Bristol Isotope Group at the University of Bristol, UK.

Work at sea

Sub-bottom echosounding with the Parasound DS III - P70 system

The most important tool on board for the identification, characterization and quantification of seafloor sediments is the hull mounted Parasound sub-bottom echosounder (Atlas Hydrographic, Bremen, Germany). On cruise ANT-XXVI/3 a distance of 10,250 nautical miles was profiled. Parasound is a high-resolution sub-bottom echosounder, which operates with two high primary frequencies (PHF) generating a parametric differential frequency in the water column. This effect results in a secondary low frequency (SLF) variable from 0.5 to 6 kHz, which can be used for sub-bottom profiling, depending on the scientific objective. During the whole leg the following settings were used: SLF Frequency 4 kHz, 2 Periods/Pulse length, rectangular pulse shape; and sensor operation mode "Quasi Equidistant Transmission" with time intervals between 1,000 and 2,000 ms between signal transmissions was used in water depths below ca. 1,500 m and "Single Pulse" in

shallower waters. At some geological stations, the SLF was set to 6 kHz for minimizing the noise generated by the ship's thrusters. The secondary high frequency (SHF) is a sum signal of the two high primary frequencies and was only recorded during a short time from 05/03/10 17:33 UTC to 06/03/10 03:45 UTC to search for gas escape structures at the seafloor and in the bottom water. Such features were, however, not detected.

Two software packages operate the Parasound system on a PC under Windows XP. ATLAS HYDROMAP CONTROL (Vers. 2.2.4) sets the control parameter, modes of operation and ranges of the echosounder. ATLAS PARASTORE-3 (Vers. 3.5.6) is an acquisition, visualisation, processing, conversion, quality control, print and data storage software. With this software a replay of recorded data and further processing is possible as well. ATLAS HYDROMAP CONTROL SERVER (Vers. 2.1.0) runs in the background and provides the data exchange and communication with the signal processor unit and transceiver electronics. The software was running stable; some computer reboots were necessary as a result of printing or operating system errors. Two hardware failures occurred and were replaced by spare parts: a broken optical port on one Blackfin-Processor-Board and a broken power-plug part for a DIP.

Data acquisition and storage of the PHF and SLF signal was switched on after leaving the port of Lyttelton on 31 January at 04:41 UTC and switched off on April 4 before entering the Chilean EEZ. Both frequencies were stored in ASD (Atlas Sound Data) format. This is a raw file xml data format storing the complete sounding profiles. In addition, the SLF signal was stored as SEG-Y and PS3 format. Navigation data and general Parasound and PARASTORE-3 settings were stored in daily ASCII format files and printouts. SLF profiles were printed on DIN A4 pages and screenshots were taken. During ANT-XXVI/3 the system was controlled by an operator around the clock, who took records of time, navigational data, basic settings and illustrated the sub-bottom profile by hand. All SLF data recorded in the New Zealand EEZ (also from the previous cruise) were stored in SEG-Y format and given onboard to the NZ observer Bryan Davy for cooperative investigations.

South of 60°00'S whale watching was carried out. No whale with a calf was observed closer than 100 m to the vessel, so that an immediate switch-off was not required. At station work not relevant for geological sampling, the system was switched off.

Sub-bottom profiling is not only a tool for gathering information about sediment accumulation and erosion but it is also used for locating coring positions. Parasound was particularly useful for the identification of core sites on the inner West Antarctic shelf, where a very patchy spatial distribution of sediments had been recorded. The acoustic information from Parasound at each coring location can be compared with physical properties measured on the sediment cores with the multi-sensor core logger (MSCL), thus allowing the correlation of acoustic data with core data.

Physical properties of sediment cores

Physical properties of the sediments such as wet bulk density, p-wave velocity, magnetic susceptibility and electrical resistivity were detected on the collected sediment cores with two GEOTEK multi-sensor core loggers (MSCL). In addition, core diameter and temperature were measured for the calculation of these values. The parameters listed in the logger settings of the MSCL software (version 6) and given in Tab. 5.1 were used for calibration. The AWI MSCL device (MSCL#14) was used for continuous whole-core measurement at 1 cm resolution. On the device of the Geological Department of the University of Bremen (GeoB) the whole-core measurements were taken with 2 cm resolution and 30 cm spacers between the core sections for zero corrections.

All physical property data still have to be graphically corrected, and faulty values, e.g. at core section boundaries, have to be deleted.

In addition, magnetic susceptibility was measured with an F-sensor at 1-cm intervals on the surfaces of the split cores with the GeoB device. Furthermore, an image was scanned with a line scan camera (RGB values), and visual color reflectance from 400 to 700 nm (10 nm channels) was measured with a hand held Minolta spectrophotometer. The data will be stored in the database PANGAEA (www.pangaea.de) after verification. The shear strength of sediments was measured with a hand held shear vane on the work halves of gravity cores recovered from the shelf.

Giant box corer (GBC), multiple corer (MUC), TV grab (TVG), piston corer (PC) and gravity corer (GC)

During ANT-XXVI/3 a giant box corer (GBC) (50 x 50 x 60 cm) was used at eight sites and a multiple corer (MUC) with tubes of 10 cm and 6.7 cm diameter, respectively, was used at five sites to recover undisturbed surface sediments (Tab. 5.2). A Van Veen-type grab connected to a camera-light system (TVG) was deployed at a single site on the inner shelf of the Amundsen Sea (PS75/151-1), where its grab failed to trigger. Two piston corers (PC), including two trigger corers (TC), and 39 gravity corers (GC) with a total core barrel length of 282 m were deployed to recover long sedimentary sequences. The deployment of the gear types and the length of the coring devices were chosen based on lithological information derived from sediment acoustic profiles provided by the Parasound echosounding system. With the exception of one unsuccessful GBC deployment (PS75/180-2), where the trigger mechanism obviously became entangled in the wire, two unsuccessful MUC (\varnothing 10 cm) deployments (PS75/195-3, PS75/254-1) and two unsuccessful GC deployments (PS75/134-1, PS75/193-1), where the corer apparently fell over and sticky diamicton did not intrude the barrel, respectively, all deployments were successful and resulted in a total core recovery of 173 m including 1.9 m core length recovered with the TC (Tab. 5.2). However, only one MUC (\varnothing 6.7 cm) deployment (PS75/216-2) was fully successful with recovery of 11 tubes, while the other two deployments of this MUC (PS75/143-3, PS75/254-2) resulted in recovery of 7 tubes each.

Two 25 and 20 m long piston corers (PC) were deployed to recover both pelagic, biogenic sediments and hemipelagic-terrigenous sedimentary sequences. Their recoveries were 21.7 m in the Ross Sea (PS75/113-1) and 15.9 m on the Antarctic continental rise in the Amundsen Sea (PS75/143-2), providing recovery rates (ratio of core recovery to penetration depth) of 85 % and 80 %, respectively. Core recoveries of the trigger corer (TC) varied between 0.9 m and 1.0 m. The gravity corer (GC) was used for coring glaciomarine and subglacial deposits on the shelf north of the westernmost Getz Ice Shelf (Fig. 5.1), on the ASE shelf (Fig. 5.2) and on the abyssal plain of the Amundsen Sea. The GC deployments were carried out with 3 m to 15 m long barrels. The successful deployments recovered sediment cores with lengths between 0.3 m (PS75/194-1) and 9.8 m (PS69/262-1; Tab. 5.2). At site PS75/161-1 in Pine Island Bay a GC with a 5 m-long barrel recovered a 6.8 m long sediment core (1.8 m of sediment were recovered from within the weight set). As a consequence a second GC with a 10 m-long barrel was deployed (PS75/214-1), which recovered a 7.7 m-long sediment core. At site PS75/136-3 north of the westernmost Getz Ice Shelf bending of the 10 m long GC at ca. 2 m depth below the seafloor resulted in low core recovery of only 2.1 m. In general, the recovery rate for the GC spanned a wide range from 5 % to 98 %.

The sediment cores taken with piston and gravity corers were cut onboard *Polarstern* into ≤ 1 m-long sections. After the measurement of physical properties with the multi-sensor core logger, PC and GC sections and subcores taken from the GBC, which were not opened onboard, were stored in a reefer container at a temperature of +4°C and transported to Bremerhaven.

Sampling and documentation

During ANT-XXVI/3 two surface sediment samples (approx. 400 cm³) were taken from the giant box cores for various sedimentological analyses and AMS ¹⁴C dating on acid-insoluble organic matter (AIO) and/or calcareous (micro-)fossils. Two subcores (\varnothing 12.5 cm) for sedimentological studies and archiving were recovered from the box cores. Two additional subcores (\varnothing 6.7 cm) were taken and immediately cut into 1 cm thick slices for the measurement of water content and the analysis of benthic foraminifera assemblages. Another subcore (\varnothing 6.7 cm) was frozen as archive core for geochemical investigations. Sediment from GBCs deployed at near-coastal sites north of the westernmost Getz Ice Shelf and in the eastern ASE (PS75/130-2, PS75/132-1, PS75/133-1, PS75/192-2, PS75/215-1, PS75/219-2) were washed through sieves on deck to collect pebbles and cobbles for petrological and geochemical studies.

Three subcores taken from GBCs (PS75/130-2, PS75/132-1, PS75/133-1), four GCs (PS75/129-1, PS75/132-3, PS75/136-3, PS75/160-1) and one PC including its TC (PS75/143-2) corresponding to 30.6 core meters were opened and sub-sampled during the expedition. After opening and splitting, the sections were photographed. High-resolution colour scans and measurements of magnetic susceptibility (at 1-cm intervals using a point-sensor) as well as a sediment description were carried out on

the archive half. Microscopical analyses of smear slides were also used to classify the main lithologies in the cores. Sediment colours were determined using a “Munsell Soil Color Chart”.

Sampling procedures of the cores followed standard methods at AWI and were exclusively carried out on the work half. Sampling types and intervals (usually 5, 10, or 15 cm) varied in response to the identified lithologies of the recovered sediments. The general sampling plan included sampling of a 25 x 10 x 1 cm sediment slab for X-raying. Samples (10 cm³ in volume each) for the determination of bulk parameters (water content, density, CaCO₃, total organic carbon and opal content) and grain-size distribution (including clay mineral analysis) were taken with syringes and stored in whirlpak bags, which were pre-weighed in the case of bulk samples. Sediment slices (ca. 40 cm³ volume) for investigations on the coarse grained (>63 µm) fraction were sampled with a spatula and stored in whirlpak bags. All samples taken from GC PS75/160-1 for analysing the coarse grained fraction were washed through 2 mm and 63 µm sieves during the cruise. Further laboratory analyses on all cores will be carried out on the individual samples at AWI, BAS and the University of Tromsø. Information regarding the lithological descriptions, sample types and volumes will be made available in the PANGAEA database at AWI (<http://www.pangaea.de>).

Preliminary results

Seafloor mapping and sediment coring on the West Antarctic continental margin

Initially, a swath bathymetry survey combined with a sediment core transect had been planned for a large glacial trough located in Wrigley Gulf, north of the Marie Byrd Land coast. Because of intense sea-ice cover and time constraints, however, a minor glacial trough extending north from the westernmost Getz Ice Shelf had to be surveyed as an alternative target (Fig. 5.1). Multi-beam mapping focused mainly on the inner and middle shelf and revealed iceberg furrows, mega-scale glacial lineations (MSGL), a large grounding-zone wedge (GZW), grooves and meltwater channels. Eight gravity and three box cores were deployed at sites that had been selected on the basis of their geographical location within the trough or their position in relation to sub- and proglacial bedforms (Fig. 5.1, Tab. 5.2). One gravity core (PS75/134-1) located on top of a GZW recovered only a core catcher sample, while another core (PS75/136-3) recovered successfully stratified sediments of possibly pre-LGM age, even though the core barrel at this site was bent. Surveying of the outer shelf was limited to two ship tracks, and the main axis of the trough could not be mapped.

Other targets for multi-beam surveys were the shelf north of Burke Island, where a drumlin field was mapped and two gravity cores were deployed (PS75/233-1, PS75/234-1), and a glacial trough extending from the present Abbot Ice Shelf NNE of Thurston Island (Fig. 5.2). In the latter survey area a set of five gravity cores including one box core was recovered (PS75/190-3 to PS75/194-3). The swath bathymetry mapping north of Thurston Island, which is the continuation of an earlier multi-beam

survey (carried out on cruise ANT-XXIII/4) towards the shelf break in the NE, recorded mainly MSGLs and iceberg furrows. On the outer shelf the survey comprised just three ship tracks, and here only the eastern trough flank could be mapped.

The remaining core sites in the eastern ASE (Fig. 4.2) targeted locations in inner Pine Island Bay, proximal to the ice fronts of Pine Island Glacier, Thwaites Glacier and Crosson Ice Shelf, GZWs on the middle and outer shelf in eastern Pine Island Trough (PS75/211-1, PS75/212-1, PS75/235-2, PS75/236-1, PS75/237-1) and subtle MSGLs on the outer shelf in western Pine Island Trough (PS75/242-1). Two cores (PS75/223-1, PS75/225-1) were deployed to recover dipping sedimentary strata on the mid-shelf, which obviously underlie till of LGM-age as observed in Parasound and reflection seismic profiles (see chapter 4). Apparently, they failed to penetrate the Holocene and LGM sediment cover. In addition, two gravity cores (PS75/255-1, PS75/257-1) were collected from outer shelf areas characterised by only minor iceberg scouring in the Dotson-Getz Trough of the western ASE.

Three multiple corers were deployed on the upper continental slope offshore from the Thurston and the Dotson-Getz troughs. Only one MUC (PS75/254-2) recovered sediments, which will be used for the study of living benthic foraminifera species. Just four deep-sea sites were targeted during cruise ANT-XXVI/3. One piston core from the northern Ross Sea (PS75/113-1) was a redeployment of a gravity core (PS75/088-6) collected during cruise ANT-XXVI/2. Another piston core (PS75/143-2) was recovered from the upper continental rise in the Amundsen Sea, offshore from the trough north of the westernmost Getz Ice Shelf. Two gravity cores (PS75/261-1, PS75/262-1) were collected from the flank and the centre of a dome-like seabed feature on the abyssal plain of the Amundsen Sea. Both cores recovered diatomaceous ooze.

Cold water deep-sea coral sampling at the Marie Byrd Seamounts

To date the distribution and abundance of exotic calcitic cold water scleractonian deep-sea corals is not well known. Therefore we selected our sampling sites close to dredge sites of *Polarstern* cruise ANT-XXIII/4 that collected most corals (Fig. 5.3). On cruise ANT-XXVI/3, a grabber with a video camera (attached 3 m above the camera) was deployed throughout the first 24 hours at Haxby Seamount in order to obtain a first insight on the *in-situ* occurrence of these corals. Video material was collected that contained both footage of sites bare of corals but also from one site that showed abundant coral patches (PS75/249-1, Tab. 5.3). Since the video grabbing device was directly connected to the ship and sampling difficult in heavy sea conditions a series of six dredge runs was also carried out to sample as much fossil coral material as possible (Tab. 5.3). Two deployments of the dredge recovered only dropstones, other rock fragments and ferromanganese crusts, and four dredge stations recovered coral material. Corals were visually inspected, photographed and packed for shipping to the University of Bristol. Some modern coral fragments will be taken to AWI (Bremerhaven) for biological research, frozen at -80°C. A large number of fossil coral

fragments and few modern specimens were recovered during this cruise (Figs. 5.4, 5.5). From visual observation most corals appear to be of Holocene age, but several specimens seem to be older, coated with thick Mn-oxide coatings. Few fossil specimens were recolonised by modern corals (Fig. 5.6).

Seawater sampling for neodymium isotopic analyses

Three water column sections have been sampled and bottom water from the West Antarctic shelf has been collected at further sites within the ASE (Tab. 5.4, Fig. 5.7). The first water column section was chosen in the Ross Sea to sample both Ross Gyre waters and the Ross Sea-derived Antarctic Bottom Water (AABW) at depth. The second station was chosen at the West Antarctic continental rise to trace the southernmost extent of the Antarctic Circumpolar Current (ACC) close to the shelf. Finally, the third station was placed at the Marie Byrd Seamounts in order to cross-calibrate coral Nd isotopic compositions obtained from the deep-sea corals. Within the ASE bottom water samples were taken at five locations in the central-eastern part (Tab. 5.4, Fig. 5.7) to complement an ongoing project based at the University of Bristol and the British Antarctic Survey (Carter et al., in prep.). Since exchange processes at the sediment-bottom water interface are of prime importance for this project, the CTD was lowered as much as possible, usually down to one or two metres above the seafloor (Tab. 5.4). The volume of seawater taken varied between 11 and 16 l per sample, using either one or two Niskin bottles per sampled depth. Samples were pre-treated on board, Nd and Sm co-precipitated in a FeCl_3 matrix and the supernatant discarded. The final volume of about 200 ml per sample will be shipped to the University of Bristol for further purification and isotopic analyses.

Potential temperature and salinity characteristics of all open water column depth profiles show values typical for Circumpolar Deep Water (CDW) over most of the water column. The Ross Sea AABW could be identified in the lowermost few hundred metres above the seafloor at the Ross Sea station. Bottom water on the shelf of the ASE also bears strong resemblance of CDW upwelling onto the West Antarctic shelf. This observation is key since CDW is fairly homogenous in its Nd isotopic composition, and any local exchange between particulate and dissolved fraction should be clearly detectable.

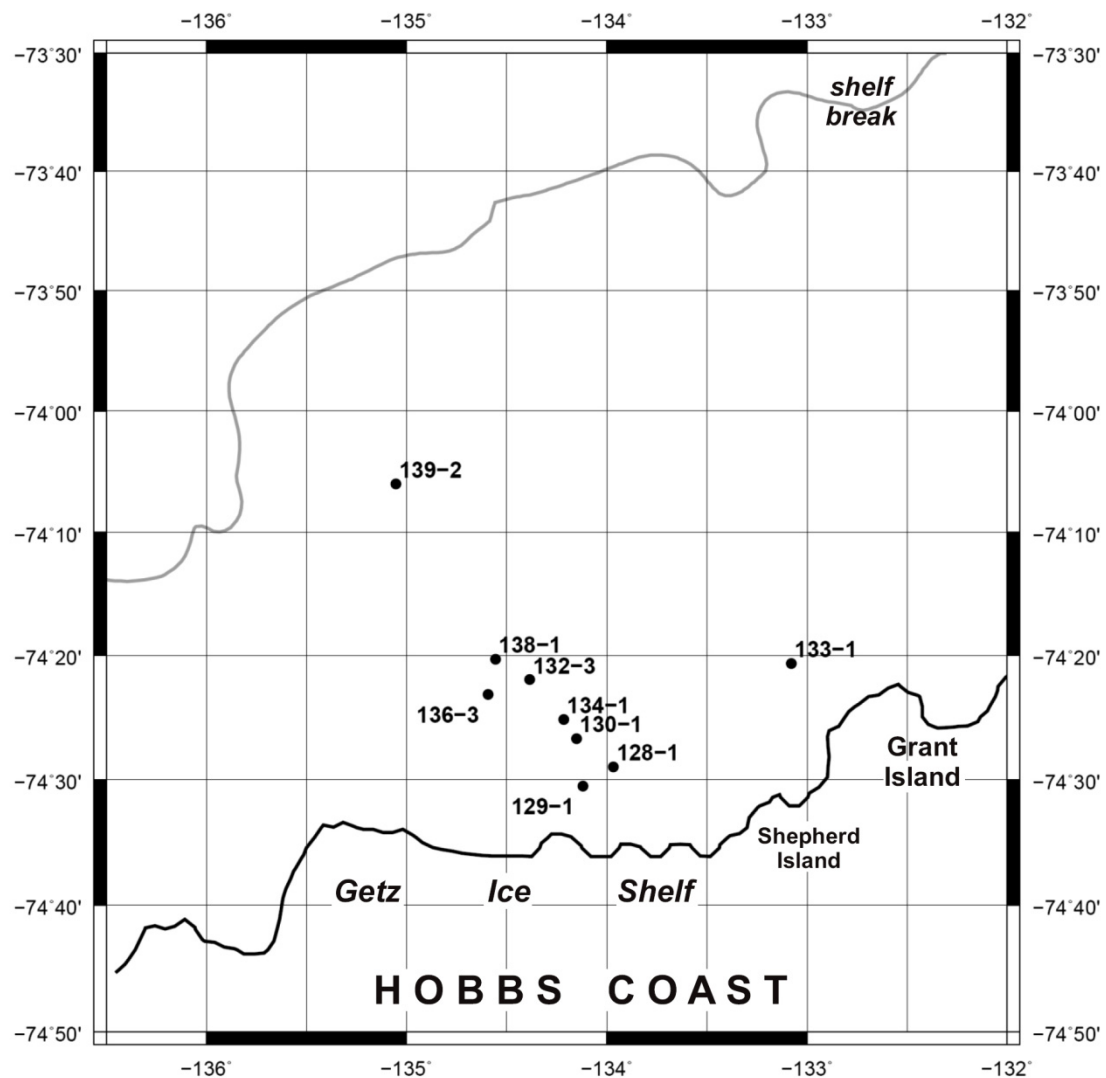


Fig. 5.1: Map of core locations on the shelf north of the westernmost Getz Ice Shelf, Marie Byrd Land

Abb. 5.1: Karte mit Kernlokationen auf dem Schelf nördlich des westlichsten Getz-Schelfeises, Marie Byrd Land

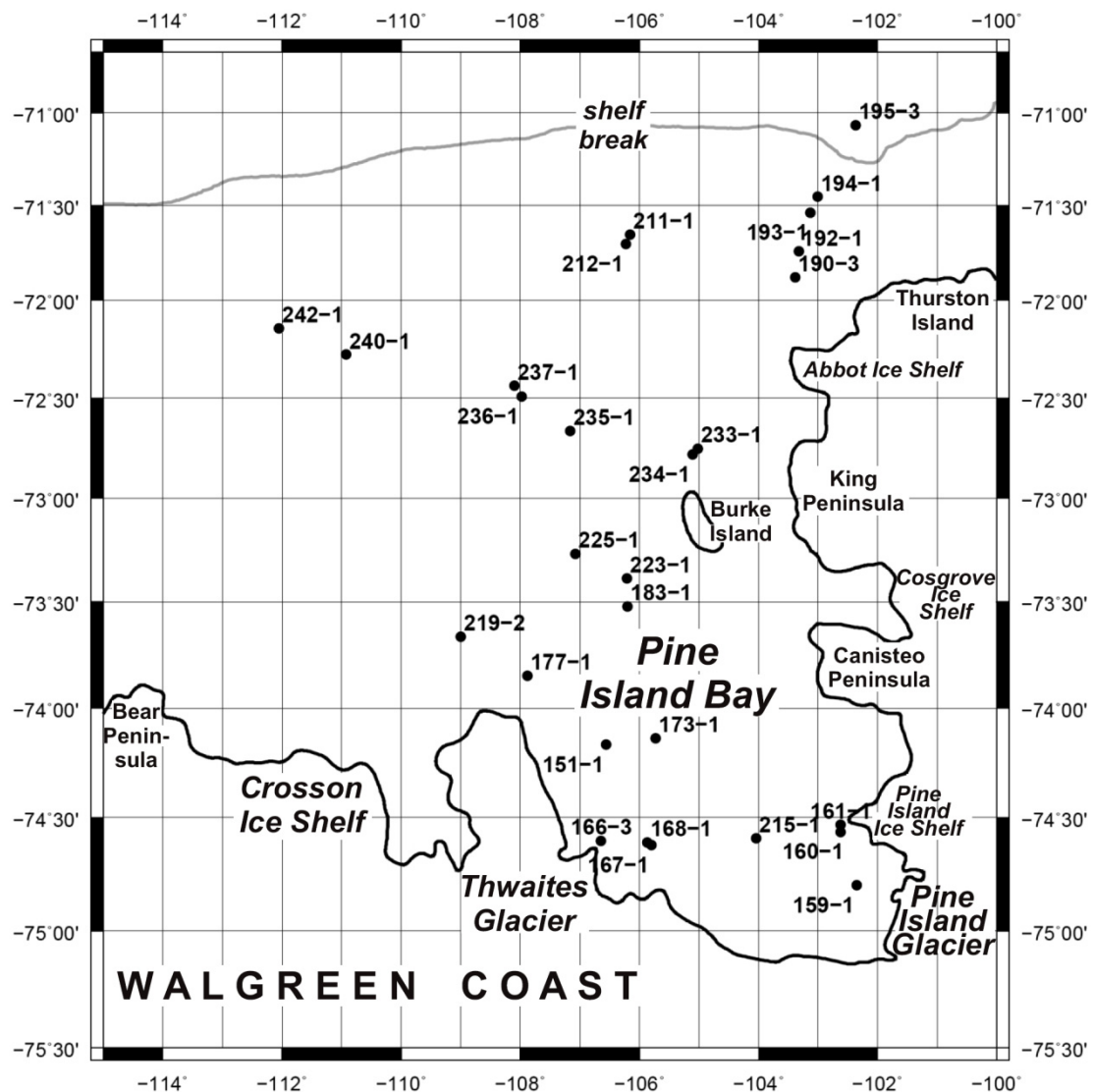


Fig. 5.2: Map of core locations on the shelf of the eastern Amundsen Sea Embayment

Abb. 5.2: Karte mit Kernlokationen auf dem Schelf des östlichen Amundsenmeer-Embayments

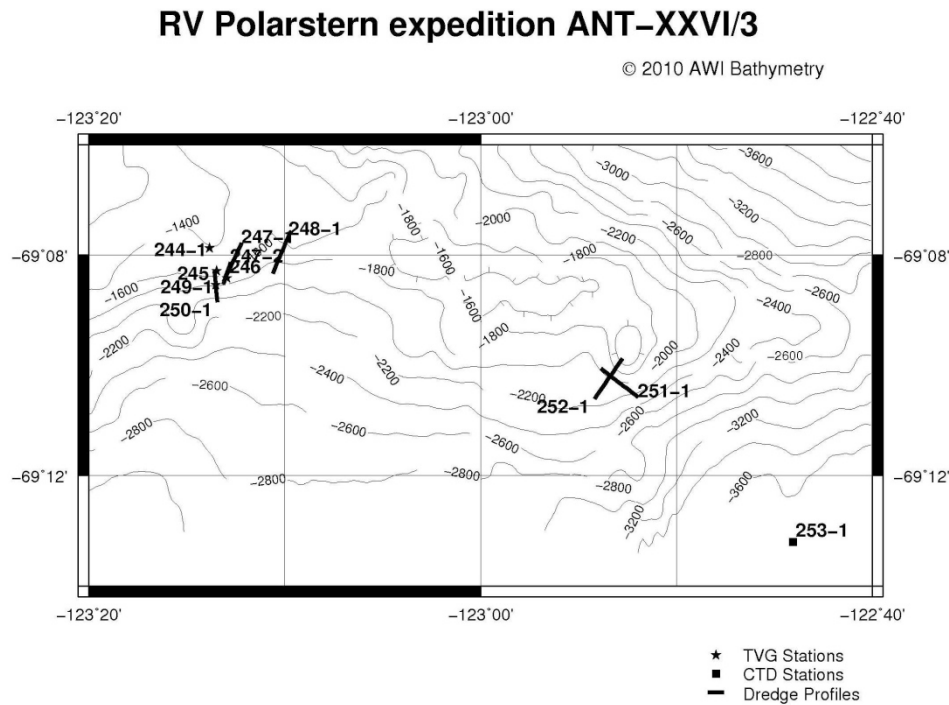


Fig. 5.3: Map of TV grabber and dredge locations on Polarstern cruise ANT-XXVI/3 at Haxby Seamount, Marie Byrd Seamounts. Also shown is the location of CTD station PS75/253-1.

Abb. 5.3: Karte der TV-Greifer und Dredge-Stationen am Haxby Seamount (Marie Byrd Seamounts) während Polarstern-Expedition ANT-XXVI/3. CTD-Station PS75/253-1 ist ebenfalls dargestellt.



Fig. 5.4: Fossil deep-sea corals recovered from dredge site PS75/247-2
Abb. 5.4: Fossile Tiefseekorallen, beprobt an der Dredge-Lokation PS75/247-2



Fig. 5.5: Fossil deep-sea corals recovered from dredge site PS75/251-1
Abb. 5.5: Fossile Tiefseekorallen, beprobt an der Dredge-Lokation PS75/251-1



Fig. 5.6: Modern deep-sea corals recolonising fossil coral branches, recovered from dredge site PS75/247-1

Abb. 5.6: Moderne Tiefseekorallen-Rekolonialisation auf fossilen Korallenstümpfen, beprobt an der Dredge-Lokation PS75/247-1

RV Polarstern expedition ANT-XXVI/3

© 2010 AWI Bathymetry

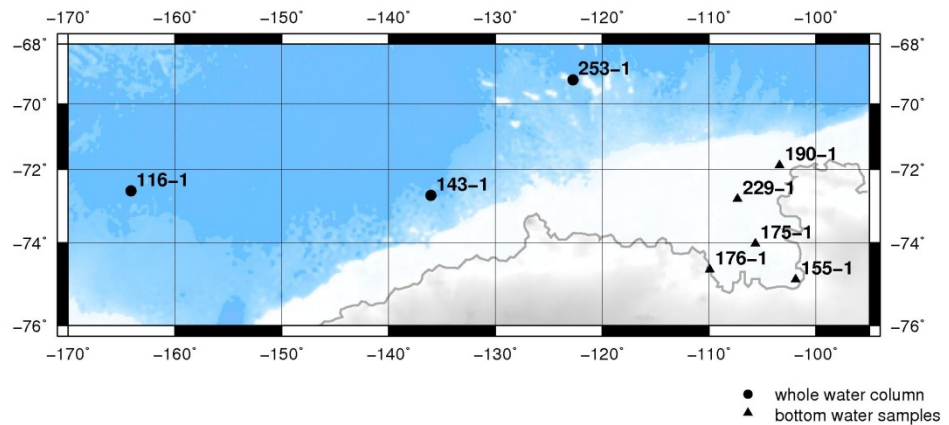


Fig. 5.7: Seawater sampling stations on cruise ANT-XXVI/3. Open ocean stations recovered water samples throughout the water column, whereas those on the Antarctic shelf only recovered bottom water samples.

Abb. 5.7: Meerwasser-Probenstationen während Polarstern-Ausfahrt ANT-XXVI/3. Tiefsee-Stationen dienten der Wasserprobennahme durch die gesamte Wassersäule, während nur Bodenwasserproben an den Schelf-Stationen beprobt wurden.

Tab. 5.1: Sensors and parameter settings for measurements with the GEOTEK multi-sensor core logger during ANT-XXVI/3

Tab. 5.1: Verwendete Sensoren und Einstellungen von Parametern für Messungen mit der GEOTEK Multi-Sensor Kernmessbank während Expedition ANT-XXVI/3

<i>P-wave velocity and core diameter</i>
plate-transducers diameter: 4 cm
transmitter pulse frequency: 500 kHz
pulse repetition rate: 1 kHz
recorded pulse resolution: 50 ns
gate: 2800
delay: 10 μ s
P-wave travel time offset: 8.09 μ s (PC, 2*2.7 mm liner thickness, PS75/113 and 143)
P-wave travel time offset: 7.60 μ s (GC and GBC, 2*2.5 mm liner thickness, all other cores)
temperature = 20 °C, salinity = 35 psu, not corrected for water depth and <i>in-situ</i> temperature; calibrated with water core of known temperature and theoretical sound velocity
<i>Temperature</i>
bimetal sensor, calibrated with Hg-thermometer
<i>Density</i>
gamma ray source: Cs-137; activity: 356 MBq; energy: 0.662 MeV
aperture diameter: 5.0 mm (PC, GC and GBC archive cores)
gamma ray detector: Gammasearch2, Model SD302D, Ser. Nr. 3047, John Caunt Scientific Ltd.; count time 10 s
Gamma ray attenuation measurement and density calculation with equation type $y=Ax^2+Bx+C$, (Coefficients A, B, and C determined with measurements on calibration cores PC (PS75/113 and 143) A=0.0002, B=-0.0659, C=10.058
GC and GBC archive cores (all other cores) A=-0.00006, B=-0.0646, C=9.9847
<i>Fractional porosity</i>
Mineral grain density = 2.65, water density = 1.026
<i>Magnetic susceptibility</i>
coil sensor: BARTINGTON MS-2C, Ser. Nr. 208, and F-Sensor on GeoB device
nominal inner coil diameter: 14 cm
coil diameter: 14.8 cm
alternating field frequency: 565 Hz, count time 10 s, precision $0.1 * 10^{-5}$ (SI)
magnetic field strength: ca. 80 A/m RMS
Krel: 0.69 (PC, 8.46 cm core-ø); 1.56 (GC and GBC, 12 cm core-ø)
coil sensor correction factor: 14.584 (PC), 6.391 (GC and GBC); for 10^{-6} (SI)
<i>Core thickness measurement</i>
Penny + Giles, Type HLP 190..., Ser #. 92730147, calibrated with distance pieces
<i>Electrical resistivity measurements on GeoB device</i>
Inductive non contact sensor, averaging about 12 cm core length, calibrated with salty solutions.
Porosity calculations after MSCL manual, Zero corrections after each section possible

Tab. 5.2: Coring sites on cruise ANT-XXVI/3. GBC: giant box corer, GC: gravity corer, PC: piston corer, TC: trigger corer, TVG: video grab. *: on the ground, #: hoisting.

Tab. 5.2: Kernstationen der Expedition ANT-XXVI/3. GBC: Gross-Kastengreifer, GC: Schwerelot, PC: Kolbenlot, TC: Voreil-Lot, TVG: Videogreifer. *: Auf Grund, #: Hieven.

Station	Gear	Area	Latitude	Longitude	Water depth depth (m)	Penetration core length (m)	Core recovery (m)	Remarks
PS75/113-1	TC	northern Ross Sea	68° 43.82' S	164° 48.17' W	3878	1.05/1.00	1.00	(ca. 5 cm of surface lost)
PS75/113-1	PC	northern Ross Sea	68° 43.82' S	164° 48.17' W	3878	25.5/25	21.69	
PS75/128-1	GC	westernmost Getz Trough, inner shelf	74° 28.98' S	133° 58.04' W	895	3.1/3	2.20	
PS75/129-1	GC	westernmost Getz Trough, inner shelf	74° 30.54' S	134° 07.25' W	923	3.5/5	2.58	
PS75/130-1	GC	westernmost Getz Trough, inner shelf	74° 26.71' S	134° 09.17' W	794	3.8/5	3.19	
PS75/130-2	GBC	westernmost Getz Trough, inner shelf	74° 26.73' S	134° 09.16' W	793	n/a	0.23	
PS75/132-1	GBC	westernmost Getz Trough, inner shelf	74° 22.00' S	134° 23.17' W	750	n/a	0.54	
PS75/132-3	GC	westernmost Getz Trough, inner shelf	74° 21.97' S	134° 23.16' W	750	2.7/5	1.26	
PS75/133-1	GBC	westernmost Getz Trough, inner shelf	74° 20.65' S	133° 04.68' W	474	n/a	0.33	
PS75/134-1	GC	westernmost Getz Trough, inner shelf	74° 25.17' S	134° 12.99' W	654	0.3	0.00	probably fallen over
PS75/136-3	GC	westernmost Getz Trough, inner shelf	74° 23.15' S	134° 35.59' W	752	2.2/10	2.12	bent at ca. 2.2 m; surface disturbed
PS75/138-1	GC	westernmost Getz Trough, inner-middle shelf	74° 20.30' S	134° 33.42' W	703	2/5	0.95	
PS75/139-2	GC	westernmost Getz Trough, outer shelf	74° 06.01' S	135° 03.31' W	449	3.5/3	2.23	
PS75/143-2	TC	Amundsen Sea, upper continental rise	72° 44.01' S	136° 01.99' W	3812	1.03/1.00	0.94	(ca. 5 cm of surface lost)
PS75/143-2	PC	Amundsen Sea, upper continental rise	72° 44.01' S	136° 01.99' W	3812	20/20	15.94	(ca. 7 cm of surface washed out)
PS75/143-3	MUC (6.7cm)	Amundsen Sea, upper continental rise	72° 44.02' S	136° 02.15' W	3814	n/a	0.43	7 tubes filled
PS75/151-1	TVG	Pine Island Bay, subglacial meltwater channel	74° 10.11' S	106° 33.48' W*	1311*	n/a	0.00	failed to trigger
			74° 10.27' S#	106° 43.06' W#	1308#			
PS75/159-1	GC	Pine Island Bay, inner shelf	74° 47.99' S	102° 21.31' W	1046	11/10	8.62	
PS75/160-1	GC	Pine Island Bay, inner shelf	74° 33.83' S	102° 37.44' W	337	11/10	6.68	
PS75/161-1	GC	Pine Island Bay, inner shelf	74° 31.90' S	102° 37.44' W	646	6.8/5	6.78	sediment within weight head (recovered)
PS75/163-3	GC	Pine Island Bay, inner shelf	74° 36.28' S	106° 38.59' W	1385	12/15	7.44	
PS75/167-1	GC	Pine Island Bay, inner shelf	74° 37.37' S	105° 48.11' W	526	12/10	9.34	
PS75/168-1	GC	Pine Island Bay, inner shelf	74° 36.71' S	105° 51.96' W	652	11/10	7.44	
PS75/173-1	GC	Pine Island Bay, inner shelf	74° 08.34' S	105° 43.82' W	1507	3/5	2.34	cobble stuck in core cutter
PS75/177-1	GC	Pine Island Bay, middle shelf	73° 51.04' S	107° 52.97' W	740	6.5/5	4.44	
PS75/180-2	GBC	Pine Island Bay, middle shelf	73° 31.43' S	106° 11.98' W	831	n/a	0.00	failed to trigger
PS75/180-3	GBC	Pine Island Bay, middle shelf	73° 31.44' S	106° 11.92' W	829	n/a	0.53	
PS75/183-1	GC	Pine Island Bay, middle shelf	73° 31.44' S	106° 12.16' W	827	2.5/5	1.38	
PS75/190-3	GC	Thurston Trough, inner shelf	71° 52.72' S	103° 23.15' W	775	5.7/5	2.96	

PS75/192-1	GC	Thurston Trough, inner-middle shelf	71° 44' 65"S	103° 19' 56"W	793	3.85	2.14
PS75/192-2	GBC	Thurston Trough, inner-middle shelf	71° 44.65"S	103° 19.61"W	793	n/a	0.59
PS75/193-1	GC	Thurston Trough, middle-outer shelf	71° 32.44"S	103° 07.75"W	676	4/5	0.00
PS75/194-1	GC	Thurston Trough, outer shelf	71° 27.25"S	103° 00.46"W	652	3/5	0.25
PS75/194-3	GC	Thurston Trough, outer shelf	71° 27.32"S	103° 00.73"W	656	3/3	1.18
PS75/195-3	MUC (10cm)	upper continental slope, offshore Thurston Trough	71° 04.02"S	102° 22.37"W	1443	0.4	0.00
PS75/211-1	GC	E Pine Island Trough, outer shelf	71° 39.36"S	106° 09.21"W	578	3.5/3	2.94
PS75/212-1	GC	E Pine Island Trough, outer shelf	71° 42.25"S	106° 13.81"W	568	3/3	2.70
PS75/214-1	GC	Pine Island Bay, inner shelf	74° 31.96"S	102° 37.28"W	641	10.5/10	7.72
PS75/215-1	GBC	Pine Island Bay, inner shelf	74° 35.50"S	104° 02.52"W	556	n/a	0.62
PS75/216-2	MUC (6.7cm)	Pine Island Bay, inner shelf	74° 36.66"S	105° 51.25"W	654	0.6	0.59
PS75/219-2	GBC	Pine Island Bay, middle shelf	73° 39.97"S	108° 59.95"W	458	n/a	0.43
PS75/223-1	GC	Pine Island Bay, middle shelf	73° 23.29"S	106° 12.38"W	773	3.5/3	1.17
PS75/225-1	GC	Pine Island Bay, middle shelf	73° 16.20"S	107° 04.43"W	874	2/3	1.51
PS75/233-1	GC	N Burke Island	72° 45.25"S	105° 00.99"W	555	2.9/3	2.34
PS75/234-1	GC	N Burke Island	72° 47.05"S	105° 06.29"W	583	1.5/3	0.85
PS75/235-1	GC	E Pine Island Trough, outer shelf	72° 39.95"S	107° 09.93"W	752	5.5/5	0.40
PS75/235-2	GC	E Pine Island Trough, outer shelf	72° 39.94"S	107° 10.08"W	751	5.5/5	3.85
PS75/236-1	GC	E Pine Island Trough, outer shelf	72° 29.60"S	107° 58.82"W	622	1.5/5	0.57
PS75/237-1	GC	E Pine Island Trough, outer shelf	72° 26.33"S	108° 05.87"W	649	3.7/5	2.62
PS75/240-1	GC	W Pine Island Trough, outer shelf	72° 16.78"S	110° 55.56"W	569	2/5	1.30
PS75/242-1	GC	W Pine Island Trough, outer shelf	72° 08.70"S	112° 02.93"W	545	2/5	2.39
PS75/254-1	MUC (10cm)	upper continental slope, offshore Dotson-Getz Trough	71° 52.59"S	118° 50.00"W	1318	ca. 0.4	0.02
PS75/254-2	MUC (6.7cm)	upper continental slope, offshore Dotson-Getz Trough	71° 52.60"S	118° 50.03"W	1317	ca. 0.4	0.40
PS75/255-1	GC	Dotson-Getz Trough, close to shelf edge	72° 00.11"S	118° 29.86"W	512	3/5	2.39
PS75/257-1	GC	Dotson-Getz Trough, outer shelf	72° 10.91"S	117° 39.90"W	542	3/5	2.61
PS75/261-1	GC	Amundsen Sea, abyssal plain	64° 33.39"S	107° 04.88"W	5002	13/15	8.14
PS75/262-1	GC	Amundsen Sea, abyssal plain	64° 32.40"S	107° 04.71"W	4999	13/15	9.79

Tab. 5.3: TV grab and dredge stations on cruise ANT-XXVI/3. Also shown are the details for CTD station 253-1.

Tab. 5.3: TV-Greifer und Dredge-Stationen während der Expedition ANT-XXVI/3. CTD-Station 253-1 ist ebenfalls dargestellt.

Station	Gear	Latitude.	Longitude	Depth [m]	Action / Comments
PS75/244-1	Grab, TV	69° 7.98' S	123° 13.71' W	1391	in the water
PS75/244-1	Grab, TV	69° 7.87' S	123° 13.84' W	1364	on ground/max depth
PS75/244-1	Grab, TV	69° 7.75' S	123° 13.99' W	1312	on deck
PS75/245-1	Grab, TV	69° 8.29' S	123° 13.68' W	1479	in the water
PS75/245-1	Grab, TV	69° 8.32' S	123° 13.58' W	1492	triggered during descent at around 550 m
PS75/245-1	Grab, TV	69° 8.30' S	123° 13.50' W	1482	at surface
PS75/245-1	Grab, TV	69° 8.29' S	123° 13.51' W	1480	on deck
PS75/245-2	Grab, TV	69° 8.30' S	123° 13.51' W	1483	in the water
PS75/245-2	Grab, TV	69° 8.28' S	123° 13.50' W	1480	aborted, grabber closed at 500 m during descent
PS75/245-2	Grab, TV	69° 8.30' S	123° 13.53' W	1484	at surface
PS75/245-2	Grab, TV	69° 8.30' S	123° 13.55' W	1485	on deck
PS75/245-3	Grab, TV	69° 8.28' S	123° 13.56' W	1472	in the water
PS75/245-3	Grab, TV	69° 8.29' S	123° 13.48' W	1484	on ground/max depth
PS75/245-3	Grab, TV	69° 8.30' S	123° 13.49' W	1481	hoisting
PS75/245-3	Grab, TV	69° 8.30' S	123° 13.51' W	1483	at surface
PS75/245-3	Grab, TV	69° 8.28' S	123° 13.51' W	1475	on deck
PS75/246-1	Grab, TV	69° 8.41' S	123° 13.00' W	1603	in the water
PS75/246-1	Grab, TV	69° 8.42' S	123° 12.94' W	1644	triggered during descent at around 560 m
PS75/246-1	Grab, TV	69° 8.42' S	123° 12.93' W	1640	hoisting
PS75/246-1	Grab, TV	69° 8.37' S	123° 12.92' W	1598	on deck
PS75/246-2	Grab, TV	69° 8.38' S	123° 12.96' W	1597	in the water
PS75/246-2	Grab, TV	69° 8.37' S	123° 12.98' W	1587	aborted, video camera failure during descent
PS75/246-2	Grab, TV	69° 8.37' S	123° 12.98' W	1587	hoisting
PS75/246-2	Grab, TV	69° 8.42' S	123° 12.85' W	1647	on deck
PS75/247-1	Dredge	69° 9.48' S	123° 14.02' W	2284	in the water
PS75/247-1	Dredge	69° 8.48' S	123° 13.11' W	1681	on ground/max depth
PS75/247-1	Dredge	69° 8.48' S	123° 13.11' W	1681	profile start
PS75/247-1	Dredge	69° 8.04' S	123° 12.60' W	1509	profile end, max. rope length: 2741 m
PS75/247-1	Dredge	69° 7.98' S	123° 12.56' W	1507	hoisting / dredging
PS75/247-1	Dredge	69° 7.78' S	123° 12.19' W	1507	detach from ground
PS75/247-1	Dredge	69° 7.49' S	123° 11.64' W	1498	on deck
PS75/247-2	Dredge	69° 9.82' S	123° 14.23' W	2357	in the water
PS75/247-2	Dredge	69° 8.53' S	123° 13.13' W	1734	on ground/max depth
PS75/247-2	Dredge	69° 8.50' S	123° 13.09' W	1708	profile start
PS75/247-2	Dredge	69° 8.14' S	123° 12.73' W	1504	profile end, max. rope length: 2937 m
PS75/247-2	Dredge	69° 8.13' S	123° 12.76' W	1502	hoisting / dredging
PS75/247-2	Dredge	69° 8.16' S	123° 12.80' W	1499	at surface

5. Marine-sedimentary Geology

Station	Gear	Latitude.	Longitude	Depth [m]	Action / Comments
PS75/247-2	Dredge	69° 8.17' S	123° 12.79' W	1498	on deck
PS75/248-1	Dredge	69° 8.36' S	123° 10.64' W	1894	in the water
PS75/248-1	Dredge	69° 8.34' S	123° 10.61' W	1887	on ground/max depth
PS75/248-1	Dredge	69° 8.33' S	123° 10.59' W	1878	profile start
PS75/248-1	Dredge	69° 7.70' S	123° 9.85' W	1522	profile end, max. rope length: 2907 m
PS75/248-1	Dredge	69° 7.65' S	123° 9.81' W	1517	hoisting / dredging
PS75/248-1	Dredge	69° 7.64' S	123° 9.78' W	1518	detach from ground
PS75/248-1	Dredge	69° 7.63' S	123° 9.82' W	1517	on deck
PS75/249-1	Grab, TV	69° 8.55' S	123° 13.48' W	1739	in the water
PS75/249-1	Grab, TV	69° 8.54' S	123° 13.52' W	1724	on ground/max depth
PS75/249-1	Grab, TV	69° 8.49' S	123° 13.59' W	1678	on deck
PS75/250-1	Dredge	69° 8.86' S	123° 13.38' W	2025	in the water
PS75/250-1	Dredge	69° 8.86' S	123° 13.44' W	2014	on ground/max depth
PS75/250-1	Dredge	69° 8.32' S	123° 13.46' W	1499	hoisting / dredging, max. rope length: 2775 m
PS75/250-1	Dredge	69° 8.29' S	123° 13.58' W	1479	detach from ground
PS75/250-1	Dredge	69° 8.43' S	123° 13.57' W	1572	on deck
PS75/251-1	Dredge	69° 10.62' S	122° 52.10' W	2254	in the water
PS75/251-1	Dredge	69° 10.58' S	122° 51.95' W	2235	on ground/max depth
PS75/251-1	Dredge	69° 9.86' S	122° 52.71' W	1500	hoisting / dredging, max. rope length: 3022 m
PS75/251-1	Dredge	69° 10.06' S	122° 53.86' W	1935	detach from ground
PS75/251-1	Dredge	69° 10.25' S	122° 54.50' W	2087	at surface
PS75/251-1	Dredge	69° 10.26' S	122° 54.56' W	2098	on deck
PS75/252-1	Dredge	69° 10.58' S	122° 54.24' W	2158	in the water
PS75/252-1	Dredge	69° 10.61' S	122° 54.18' W	2163	on ground/max depth
PS75/252-1	Dredge	69° 10.57' S	122° 54.11' W	2154	profile start
PS75/252-1	Dredge	69° 9.94' S	122° 52.87' W	1521	profile end
PS75/252-1	Dredge	69° 9.88' S	122° 52.78' W	1502	hoisting / dredging, max. rope length: 2807 m
PS75/252-1	Dredge	69° 9.88' S	122° 52.76' W	1502	detach from ground
PS75/252-1	Dredge	69° 9.91' S	122° 52.79' W	1506	at surface
PS75/252-1	Dredge	69° 9.92' S	122° 52.78' W	1508	on deck
PS75/253-1	CTD	69° 13.00' S	122° 44.10' W	3712	in the water
PS75/253-1	CTD	69° 13.04' S	122° 44.13' W	3715	on ground/max depth, CTD depth: 3657 m (bottom -2 m)
PS75/253-1	CTD	69° 13.09' S	122° 43.91' W	3715	on deck

Tab. 5.4: CTD stations sampled for Nd isotopic analyses during ANT-XXVI/3.

Tab. 5.4: Beprobte CTD-Stationen für Nd-Isotopen Analysen während Expedition ANT-XXVI/3.

Station		Latitude	Longitude	Water depth [m]	Sampled depths [m]
<i>Water column depth transects</i>					
PS75/116-1	Ross Sea Station	72° 36.61' S	164° 05.31' W	4227	11, 101, 254, 668, 1420, 2102, 2948, 3361, 3875, 4210, 4225 (bottom -2 m)
PS75/143-1	Continental Rise Station	72° 44.04' S	136° 02.13' W	3823	10, 202, 606, 1015, 1521, 2184, 2746, 3309, 3772, 3818 (bottom -5 m)
PS75/253-1	Haxby Seamount Station	69° 13.04' S	122° 44.13' W	3728	10, 505, 1013, 1521, 2029, 2541, 3051, 3555, 3726 (bottom -1.5 m)
<i>Shelf bottom water sampling stations</i>					
PS75/155-1		74° 54.77' S	101° 53.37' W	1045	1043 (bottom - 2 m)
PS75/175-1		74° 01.00' S	105° 40.66' W	1088	1067 (bottom -1 m)
PS75/176-1		74° 40.40' S	109° 54.84' W	945	943 (bottom -1.5 m)
PS75/190-1		71° 52.75' S	103° 23.44' W	759	757 (bottom -1.5 m)
PS75/229-1		72° 50.02' S	107° 20.04' W	656	655 (bottom -1.5 m)

6. OCEANOGRAPHY

Michael Schröder¹, Andreas Wisotzki¹,
Ralph Timmermann¹, Lutz Sellmann¹,
Sandra Esther Brunnabend¹, Hartmut H.
Hellmer¹ (not on board), Oliver Huhn²
(not on board)

¹Alfred-Wegener-Institut für Polar- und
Meeresforschung, Bremerhaven

²Tracer Oceanography, University of
Bremen, Germany

Objectives

This oceanographic project has three main objectives:

- Determination of CDW routes and properties from the continental slope to the ice shelf fronts fringing the Amundsen Sea;
- measurement of shelf water characteristics to detect freshwater input due to ice shelf basal melting;
- extension of collaborations with international colleagues who investigate the ocean's role in the mass loss of WAIS (West Antarctic Ice Sheet).

In 2002 the WAIS community outlined a study plan, emphasizing the need for better information about the ocean circulation, ice thickness, sea floor morphology, and atmospheric forcing, along with improved numerical modelling of WAIS interactions with its surroundings. For the Amundsen Sea it is entirely plausible that ocean influence on the WAIS could increase from changes in ocean temperature, heat transport and vertical thermohaline structure, in response to altered atmospheric forcing, sea ice production on the continental shelf, and ice shelf morphology.

The first oceanographic stations occupied on the Amundsen continental shelf in 1994 have since been supplemented by late summer measurements in 2000, 2003, 2006, 2007, 2008, and 2009. This work has revealed that the ‘warm,’ salty CDW gains access to the continental shelf near the sea floor, particularly in the eastern sector, filling up the glacially scoured troughs that extend to the ice shelf front and deep beneath the ice shelves. Where the ice shelves have deep grounding zones, they can be exposed to seawater more than 4°C above the *in-situ* melting point. This drives basal ice shelf melting orders of magnitude faster than beneath the large ice shelves in Weddell and Ross Seas. Substantial thermohaline variability is apparent in some of the repeated late summer observations, but little is yet known about the seasonal cycle or interannual variability. Also lacking is information about the strength of the ocean circulation, heat transport to the ice shelf caverns, and how efficiently that heat is used for basal melting. Ocean warming documented at distant locations like the Antarctic Circumpolar Current (ACC) may be transmitted directly to the exposed glacial ice, or weakened in mixing across the Antarctic Slope Front. Heat transport from the continental shelf break to the ice shelf caverns may also be

influenced by mixing over the rough bottom topography, tidal currents, winds, sea ice production, icebergs, and melt water impacts on the pycnocline.

Work at sea

The programme consisted of measurements from the ship using a Seabird 911+ CTD (SN 561) connected to a carousel (SBE 32, SN 202) with 24-(12-l) water bottles. This instrument system contains two sensor pairs of conductivity (SBE 4, SN 3607, SN 3590) and temperature (SBE 3, SN 1373, SN 2629), a high precision pressure sensor Digiquartz 410K-105 (SN 68997), one oxygen sensor (SBE 43, SN 743 until station no. 143 and SN 880 from station no. 147 on), one oxygen sensor (Rinko SN 10, optode), a fluorometer (Wetlab ECO-AFL/FL, SN 1365) and a Benthos altimeter Model PSA 916 (SN 1228).

The conductivity and temperature sensor calibration were performed before and after the cruise at Seabird Electronics. The accuracy of the temperature sensors can be given to 2 mK. The readings for the pressure sensors are better than 2 dbar.

The conductivity was corrected using salinity measurements from water samples. IAPSO Standard Seawater from the P-series P149 ($K_{15} = 0.99984$) was used. A total of 77 water samples were measured using a Guildline Autosal 8400B. On the basis of the water sample correction, salinity is measured to an accuracy of 0.002 (see also Fig. 6.1).

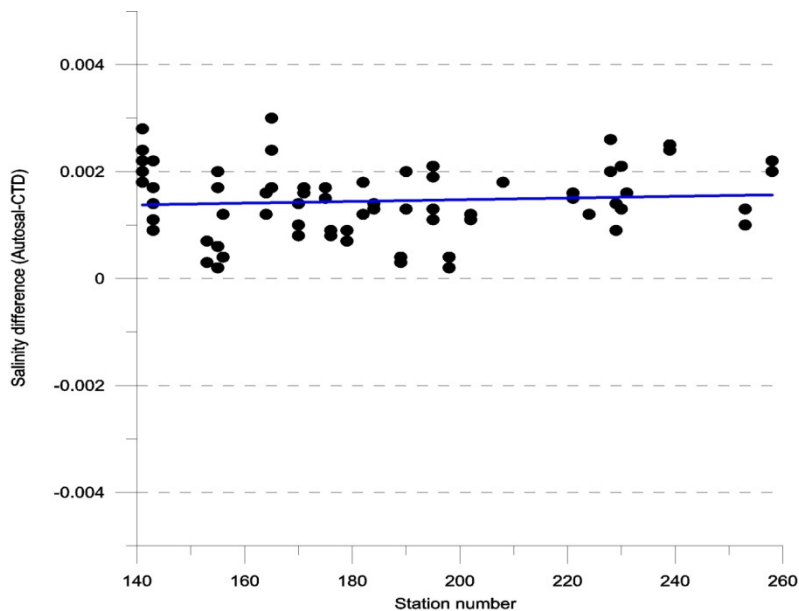


Fig. 6.1: Salinity difference of water samples measured with Autosal minus CTD salinity over station number equivalent to time. There is only a negligible trend of less than 0.0001 detectable.

Fig. 6.1: Salzgehaltsdifferenzen zwischen Wasserprobe, gemessen mit dem Salinometer und Meßwerten aus der CTD aufgetragen über die Stationsnummer bzw. Zeit. Es ist nur ein vernachlässigbarer zeitlicher Trend von weniger als 1/10,000 sichtbar.

The oxygen was corrected from water samples by using the Winkler method with a Dissolved Oxygen Analyser (DOA, SIS type). 202 water samples were measured which had no trend with time (Fig. 6.2) but still have to be corrected for the hysteresis under increasing pressure.

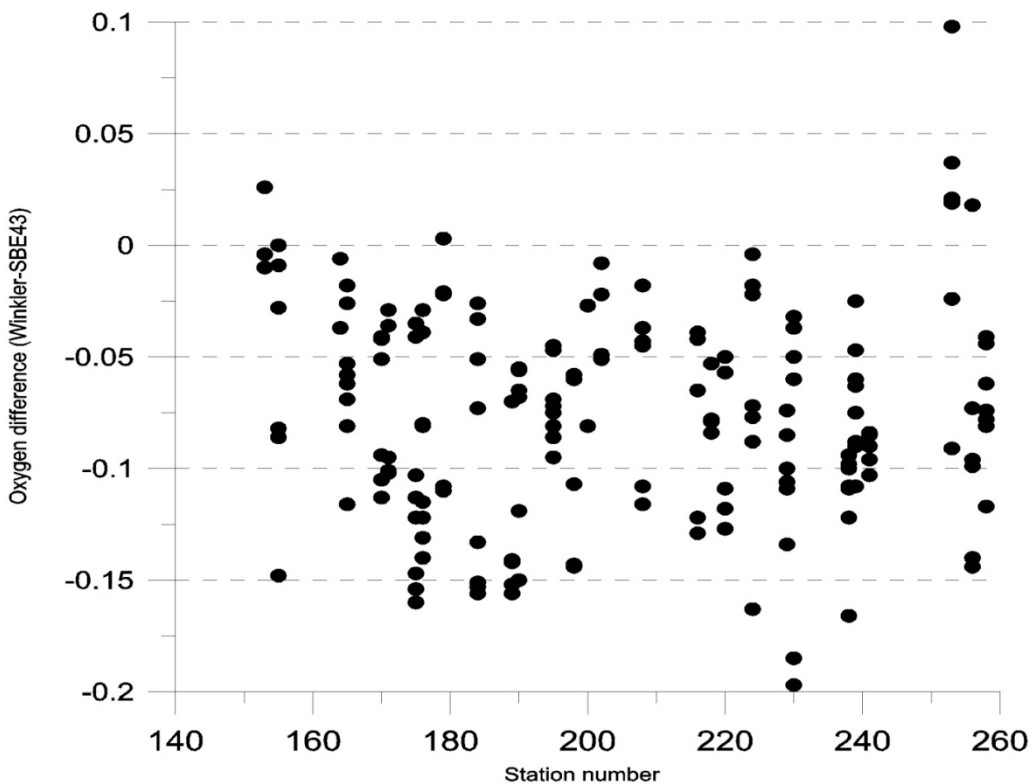


Fig. 6.2: Oxygen difference between water samples measured by Winkler method minus CTD oxygen sensor values over station number (time)

Fig. 6.2: Differenzen von gelöstem Sauerstoff aus Wasserproben, gemessen mit der Winkler Methode und Werten des Sauerstoffsensors der CTD aufgetragen über die Stationsnummer bzw. Zeit

For the identification of meltwater coming out of the cavity beneath the Pine Island glacier 20 Helium samples were taken out of the water samples from the CTD casts. They were sealed in copper tubes and will be analysed at the University of Bremen after the cruise (for details see Tab. 6.3).

In total 61 CTD profiles were measured on this cruise. 3 in water depths of more than 3,000 m, 13 between 1,000 m and 2,000 m, 35 in the range of 500 m to 1,000 m, and 10 in water depths of less than 500 m. The deepest cast was at 4,206 m, the shallowest cast at 362 m.

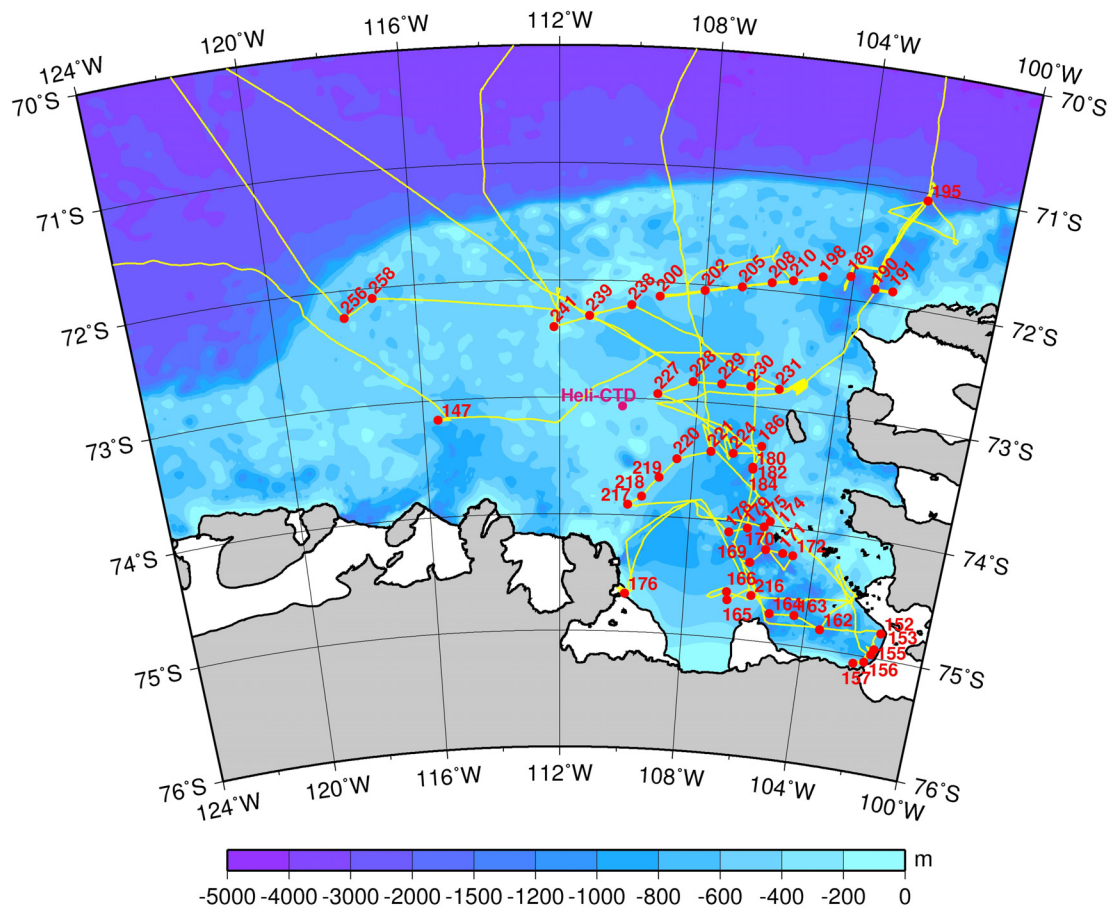


Fig. 6.3: Position of 51 CTD stations in the eastern Amundsen Sea. 8 additional CTD stations in the Wrigley Gulf are shown below (Fig. 6.8). 2 other (1 in the Ross Sea and 1 at Marie Byrd seamounts) are not shown. For more details see Tab. 6.2.

Fig. 6.3: Position der 51 CTD Stationen im östlichen Amundsen Meer. 8 zusätzliche CTD Stationen im Wrigley Gulf sind nicht zu sehen (Fig. 6.8). 2 andere (1 im Ross und 1 an den Marie Byrd Kuppen) sind ebenfalls nicht zu sehen. Für weitere Details siehe auch Tabelle 6.2.

Underway measurements with the vessel-mounted narrow band ADCP (Acoustic Doppler Current Profiler) from RDI Instruments type Ocean Surveyor with 153.6-kHz transducer were done to provide current data of the top 150 - 300 m. The data will be processed at AWI by means of the CODAS software.

To supply the ship with surface temperature and salinity values the two ships SBE 21/SBE 38 thermosalinographs were used, one in 6 m depth in the bow thruster tunnel and one in 11 m depth in the keel. Both instruments were controlled by taking water samples which are measured on board.

During the cruise a Helicopter CTD system was in use which consists of an analogue high precision instrument system as on the ship. It contains a Seabird 911+ CTD (SN

287) without carousel, two sensor pairs of conductivity (SBE 4, SN 3290, SN 2470) and temperature (SBE 3, SN 5027, SN 5104), a high precision pressure sensor Digiquartz 410K-105 (SN 51197), and a Benthos altimeter model PSA 916 (SN 46617). It is able to measure profiles up to 1800 m water depth via continuous data acquisition with a 3.14 mm single wired cable.

The whole system will be calibrated using the pre and post calibration values from Seabird. The accuracy for temperature is better than 2 mK, for salinity it is better than 0.002, and the pressure sensor measured with an accuracy better than 2 dbar.

Helicopter CTD – portable CTD system with autonomous winch

Accurate profiles of the physical parameters of seawater as temperature, conductivity/salinity and pressure could only be measured throughout the water column, including the bottom boundary layer, with the aid of a single wire cable. In ice covered waters this is only possible on a ship or from ice floes, if one has the possibility to lower large wire length's from the ice to the sea floor. Wire lengths of more than 1,500 m are needed to measure not only within the shallow (< 500 m) shelf areas but also along the steep slope at shelf break into the deep sea.

At AWI a portable instrument system was developed which can be carried by the helicopter (type BO-105) from the ship onto an ice floe in a range of 60 nm. There is only a need of ice floes of sufficient size (50 m radius) and thickness (~0.5 m) to get ship independent hydrographic profiles. The whole system consists of two aluminium sledges for the generator and the winch which are fixed together under a lift off frame and carried as outside load underneath a helicopter (Fig. 5.4). In total the system weighs 525 kg.



Fig. 6.4: Portable CTD system carried by a helicopter. For protection all components are covered by a canvas.

Fig. 6.4: Mobiles CTD System transportiert als Außenlast unter dem Helikopter. Zum Schutz sind alle Komponenten mit einer Persennig abgedeckt.

The measuring system itself now consists of a Seabird 911+ with double paired sensors for conductivity and temperature and a Benthos altimeter. It has the same accuracy as the ships system. It is also possible to connect a 5 l bottle to the wire to get water samples for tracer analysis from the bottom layer. The bottle can be closed by use of a messenger.

The measurements had to be done in leads at the edge of an ice floe (Fig. 6.5) so that no drilling equipment has to be carried as additional gear with the helicopter. The built up and rebuilt of the system on the ice floe takes 1.5 hours each, which together with a 30 min. profile sums up to a total amount of time of 3.5 hours on the floe (Fig. 6.6). Tested first during the ISPOL campaign 2004 - 2005 in front of the Larsen ice shelf with a modified SBE 19 and lower resolution and data quality, this cruise was the first successful field test for the modified, high precision version.



*Fig. 6.5: Touchdown of the portable CTD system at the edge of an ice floe
Fig. 6.5: Absetzen des mobile CTD Systems am Rande einer Meereisscholle*

Due to the extremely low sea ice concentration in the whole Amundsen shelf area only one helicopter CTD profile could be done. Even so it demonstrates the great benefit in completing hydrographic sections in ice covered regions. On this cruise it extends section 2 about 20 nm to the west (see below). A second station has to be cancelled due to unsafe ice conditions and increasing wind speeds, which exceed 15 m/s (Bft 7).



Fig. 6.6: Fully rigged up measuring system on site 26-01. It consists of a tent, the winch, and a maneuverable mast. Online data acquisition is done via the deck unit on a laptop in the tent. The mast allows the CTD to hang aside the floe without touching the ice. For transportation the mast can be disassembled into 4 pieces of 1m length. The generator sledge is not seen.

Fig. 6.6: Fertig aufgebautes Meßsystem an Station 26-01. Es besteht aus einem Zelt, der mobilen Winde und einem beweglichen Gittermast. Im Zelt erfolgt die Datenerfassung über ein Bordgerät auf einen Laptop. Mit Hilfe des Mastes wird die CTD Sonde über die Eiskante ins Wasser gebracht. Zum Transport wird der Mast in 4 Teile a 1 m zerlegt. Der Generatorschlitten steht außerhalb des Bildes.

Preliminary results

The experiment represents an important contribution to the long-term monitoring of CDW characteristics on the Amundsen Sea continental shelf and the freshwater input due to ice shelf basal melting, continuously conducted by colleagues in the US (LDEO) and UK (BAS), as part of the international ASEP (**A**mundsen **S**e **E**mbayment **P**roject) and the WAIS initiative. It also provides additional hydrographic data for the validation of the coupled ice-ocean global finite element model FESOM focused on the Southern Ocean as part of AWI's research programme PACES (T1WP1.1 - Impact of Ice Sheets on the Earth System) and the EU (FP7-ENV.2008.1.1.1.1) project ICE2SEA - Estimating the Future Contribution of Continental Ice to Sea-Level Rise. The latter represents a cooperation with 22 European partners, involving various glaciological disciplines, all interested in the prediction of global sea level rise in a warmer climate.

Surface measurements with the ships thermosalinograph

By using the information of the ships thermosalinograph the changes in temperature and salinity near the surface are visible. The interpretation of the data could be of greater importance for the marine mammal and bird observing group in analyzing

fluctuations in the abundance of species and comparing it to the frontal zones of the ACC or the Ross gyre (Fig. 6.7).

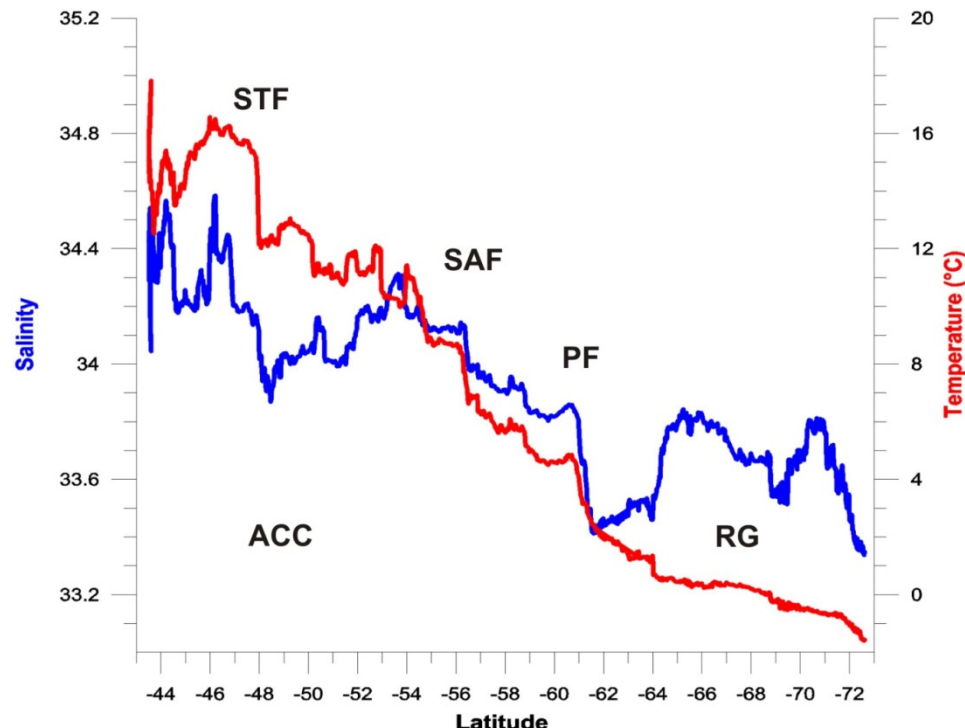
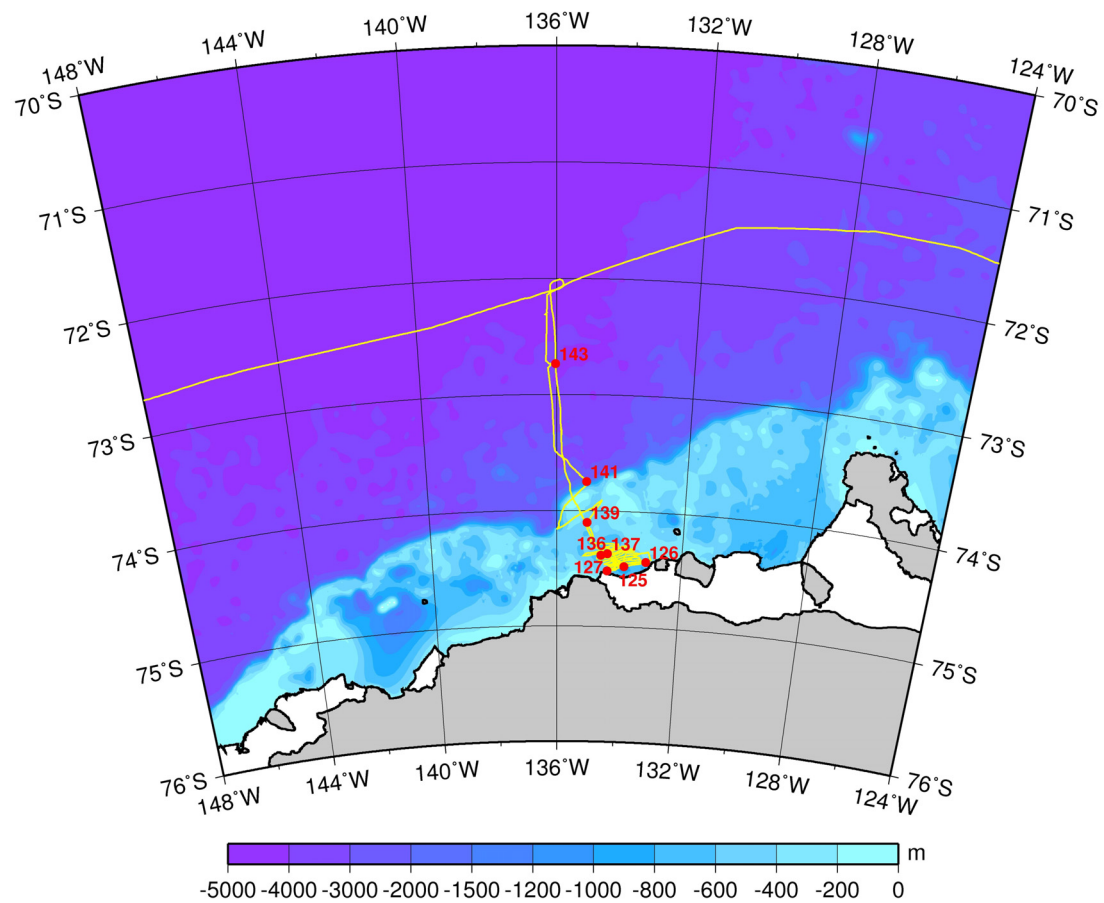


Fig. 6.7: Surface (11m) temperature and salinity on the leg Wellington-Ross Sea over latitude. The position of fronts in the Antarctic Circumpolar Current (ACC) are shown. STF – Subtropical front, SAF – Subantarctic front, PF – Polar front, RG – Ross gyre.

Fig. 6.7: Oberflächentemperatur und Salzgehalt (11m) auf dem Schnitt von Wellington ins Ross Meer aufgetragen über die Breite. Die Lage der Fronten im Antarktischen Zirkumpolarstrom (ACC) wird sichtbar. STF – Subtropenfront, SAF – Subantarktis Front, PF – Polarfront, RG – RossWirbel.

Physical properties of the western Wrigley Gulf embayment

Between 132° W and 136° W slightly west of Shepard Island, 8 CTD stations were done in front of the ice shelf and on the way to the shelf break as shown in Fig. 6.8. Here, 3 profiles of potential temperature, salinity and dissolved oxygen content are shown to illustrate the highly variable bottom layer. The position of these 3 profiles is shown in Fig. 6.9.



*Fig. 6.8: Position of 8 CTD stations in the western Wrigley Gulf
Fig. 6.8: Position der 8 CTD Stationen im westlichen Wrigley Gulf*

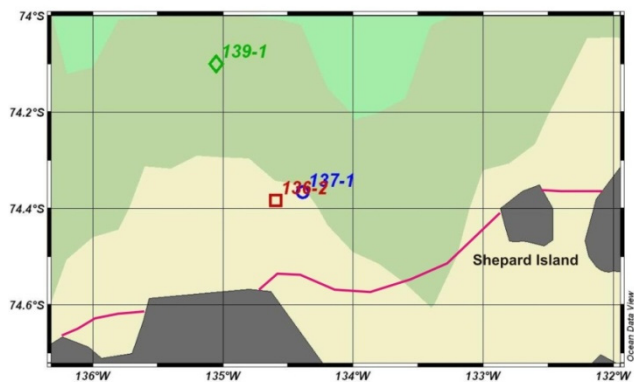


*Fig. 6.9: Position of CTD stations 136, 137, and 139 west of Shepard Island
Fig. 6.9: Position der CTD Stationen 136, 137 und 139 westlich von Shepard Island*

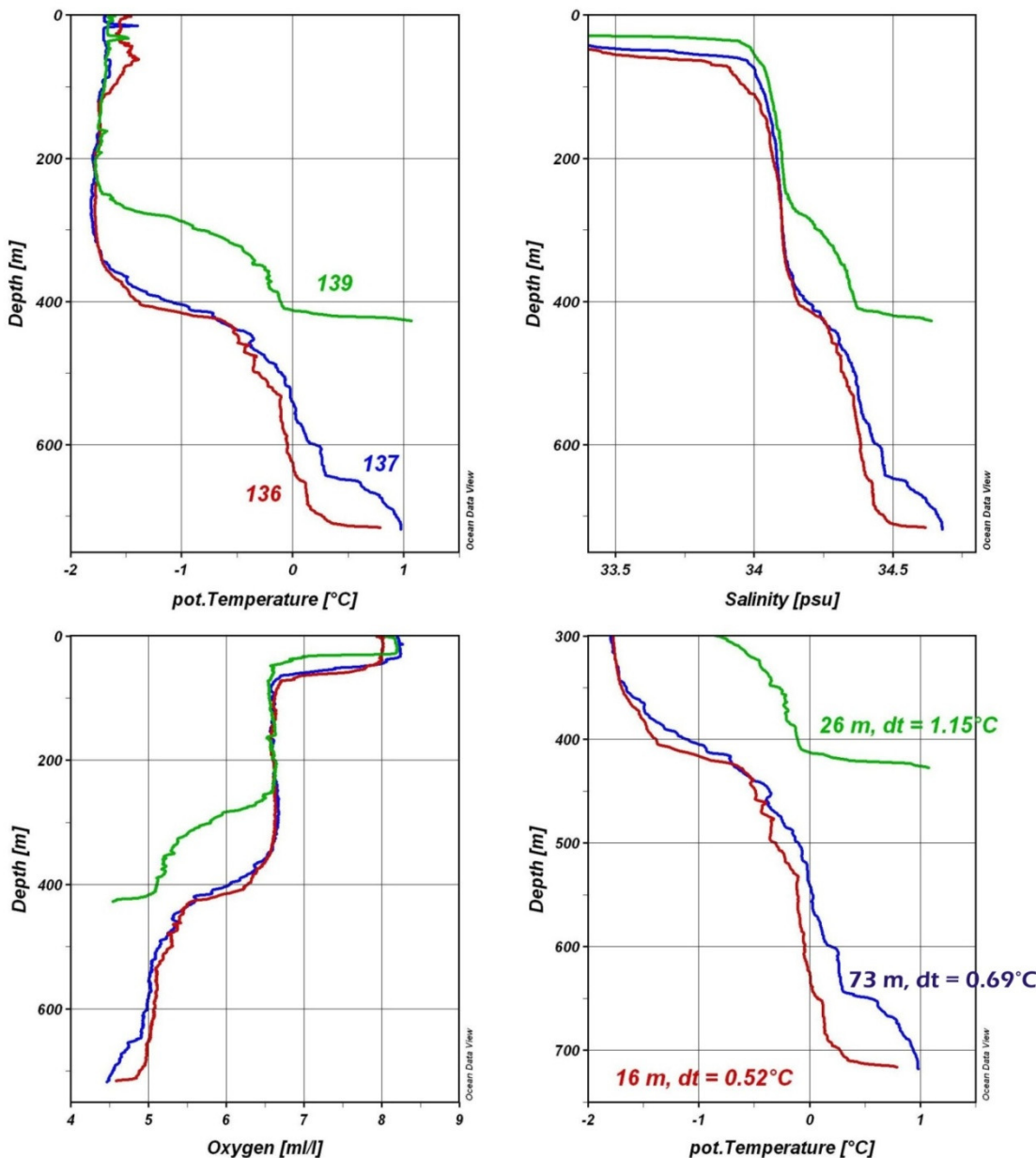


Fig. 6.10: Profiles of potential temperature (top left), salinity (top right), and dissolved oxygen content (lower left) for CTD stations 136 (red), 137 (blue), and 139 (green) west of Shepard Island. In addition the enlarged depth between 300 m and 750 m of each profile is shown (lower right). The temperature change within the bottom boundary layer (BBL) of each profile is given together with the thickness of the BBL.

Fig. 6.10: Profile der potentiellen Temperatur (oben links), des Salzgehalt (oben rechts) und des gelösten Sauerstoffs (unten links) für die CTD Stationen 136 (rot), 137 (blau) und 139 (grün) westlich von Shepard Island. Zusätzlich ist vergrößert der Tiefenbereich zwischen 300 m und 750 m jedes Profils gezeigt (unten links). Zusätzlich ist die Temperaturänderung innerhalb der Bodengrenzschicht (BBL) von jedem Profil zusammen mit der Schichtdicke der BBL angegeben.

Station 136 and 137 are only 3.5 nm apart with nearly the same water depth of 717 m / 721 m but totally different bottom temperatures ($+0.7^{\circ}\text{C}$, $+1.0^{\circ}\text{C}$) and bottom layer thicknesses (16 m, 73 m) (Fig. 6.10). The profiles of the oxygen content emphasizes this contrast. For comparison station 139 with a by far bigger gradient is shown, although here the depth is shallower (429 m) and the position is 15 nm north of station 137 on the outer shelf. The temperature increase at station 139 is 1.15°C within the lowest 26 m above the bottom.

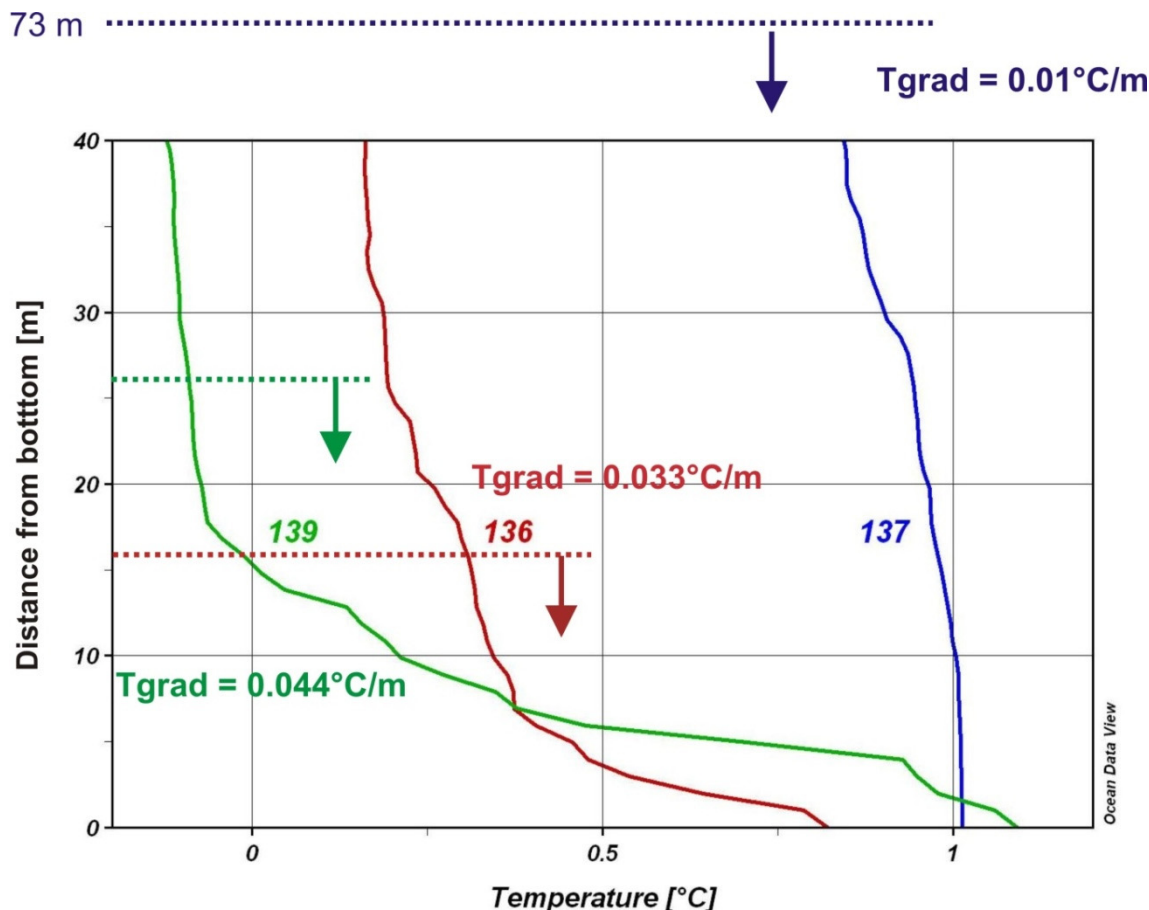


Fig. 6.11: For a better resolution of the BBL the temperature profiles of CTD stations 136 (red), 137 (blue), and 139 (green) are plotted counting the distance from the bottom on the y-axis. Here the different temperature gradients are added together with the thickness of the boundary layer.

Fig. 6.11: Zur besseren Auflösung der BBL sind hier die Temperaturprofile der Stationen 136 (rot), 137 (blau) und 139 (grün) über den Abstand vom Boden aufgetragen. Hier wird zusätzlich der Temperaturgradient pro Meter mit der Dicke der Bodengrenzschicht angegeben.

For a better resolution of the bottom boundary layer the temperature files of the stations 136, 137, and 139 are plotted against the distance from the bottom (Fig. 6.11). The temperature gradient is highest at station 139 with $\text{Tgrad} = 0.044^{\circ}\text{C}/\text{m}$ followed by station 136 with $\text{Tgrad} = 0.033^{\circ}\text{C}/\text{m}$. Only 30 % of that value was measured at station 137. Because of this large gradient at the bottom it is highly

recommended to drive the CTD as close to the bottom as possible otherwise a lot of information is lost.

At all these stations a comparison with measurements of the heat probe will be done (see also Chapter 4, Geophysics).

Hydrography and Physical Properties of the Pine Island Embayment and the Amundsen Shelf

The eastern embayment shelf is dominated by deep troughs (up to 1,600 m depth) and a variety of sills and shallow areas (some around 350 m depth) in between. Therefore 6 hydrographic sections across the trough axis were made between the northern shelf break and the Pine Island glacier in the south. A total of 48 CTD casts were measured from the ship and 1 cast was lowered with the portable helicopter CTD (see also Fig. 6.3).

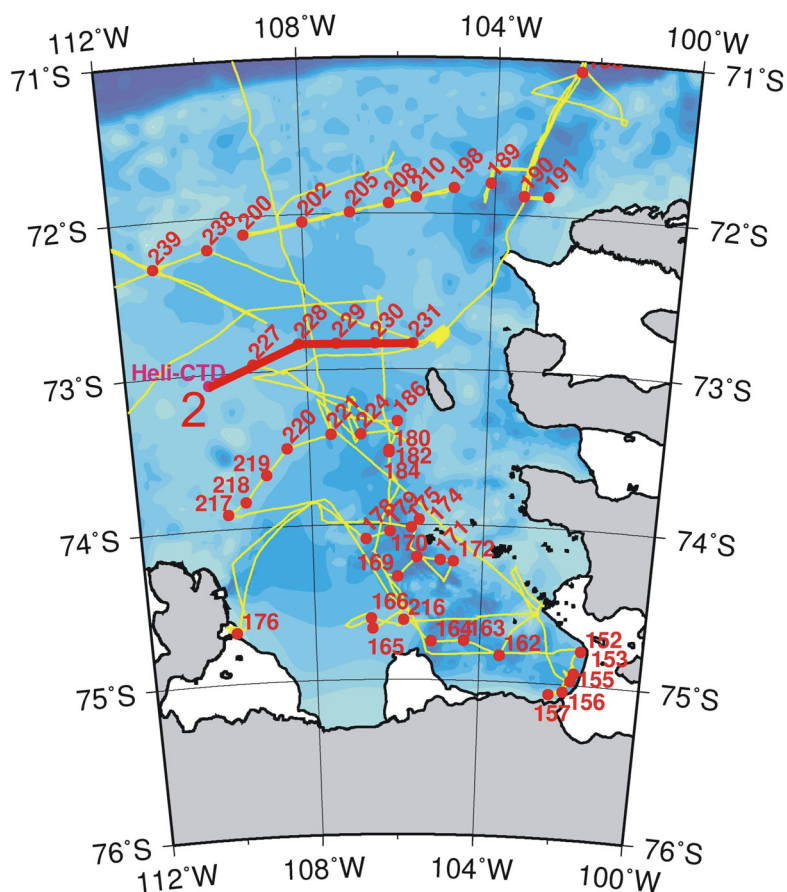


Fig. 6.12: Position of hydrographic section 2 north of Burke Island. The westernmost station was done with the portable helicopter CTD.

Fig. 6.12: Position des hydrographischen Schnittes 2 nördlich von Burke Island. Das westlichste Profil wurde mit der mobile Helikopter CTD aufgenommen.

Section 2 was chosen as an example of the hydrographic conditions of the northern shelf. It is also at a position where the deep trough of the eastern embayment splits into a western and an eastern part, when looking from south to north in direction to the shelf break. Therefore, all warm CDW water flowing towards the south should be detected on this section.

The cross section 2 northwest of Burke Island shows the great pool of warm water (pot. temperatures $>1.0^{\circ}\text{C}$) in water depths greater than 400 m on the eastern flank of the depression as shown at station 230 and 231 in Fig. 6.13a. This water mass with circumpolar origin flows to the south and is seen on all transects. It is the densest water mass on the shelf due to its high salinity content of more than 34.70 (station 230 and 231 in Fig. 6.13b).

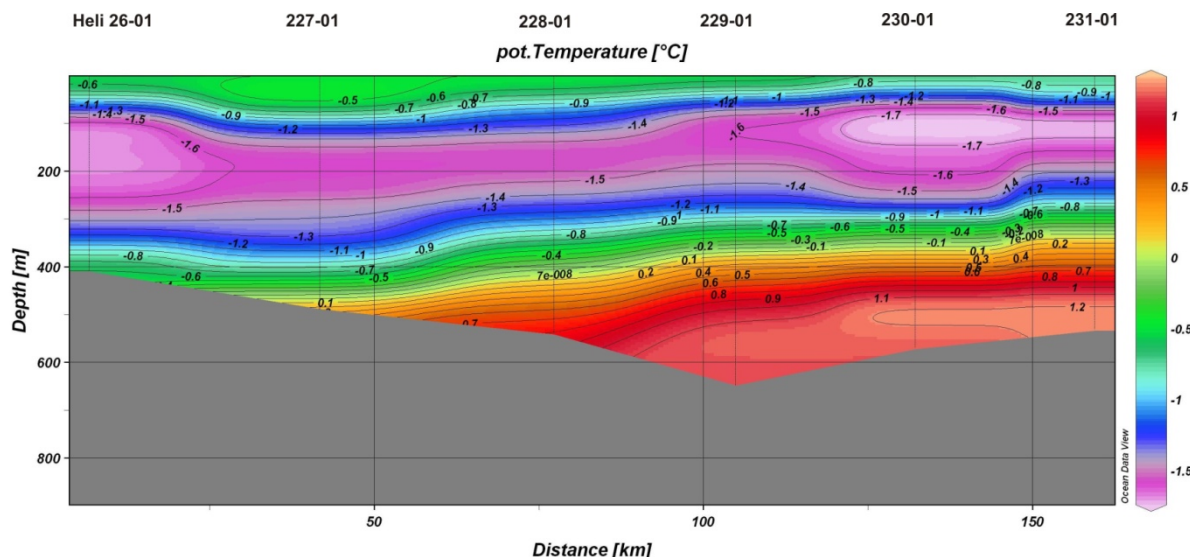


Fig. 6.13a: Potential temperature on hydrographic section 2 northwest of Burke Island. The warm deep water of circumpolar origin fills the depression on the eastern flank (right).

Fig. 6.13a: Potentielle Temperatur auf dem hydrographischen Schnitt 2 nordwestlich von Burke Island. Das warme Tiefenwasser mit zirkumpolarem Ursprung füllt den gesamten östlichen Teil der Rinne (rechte Seite).

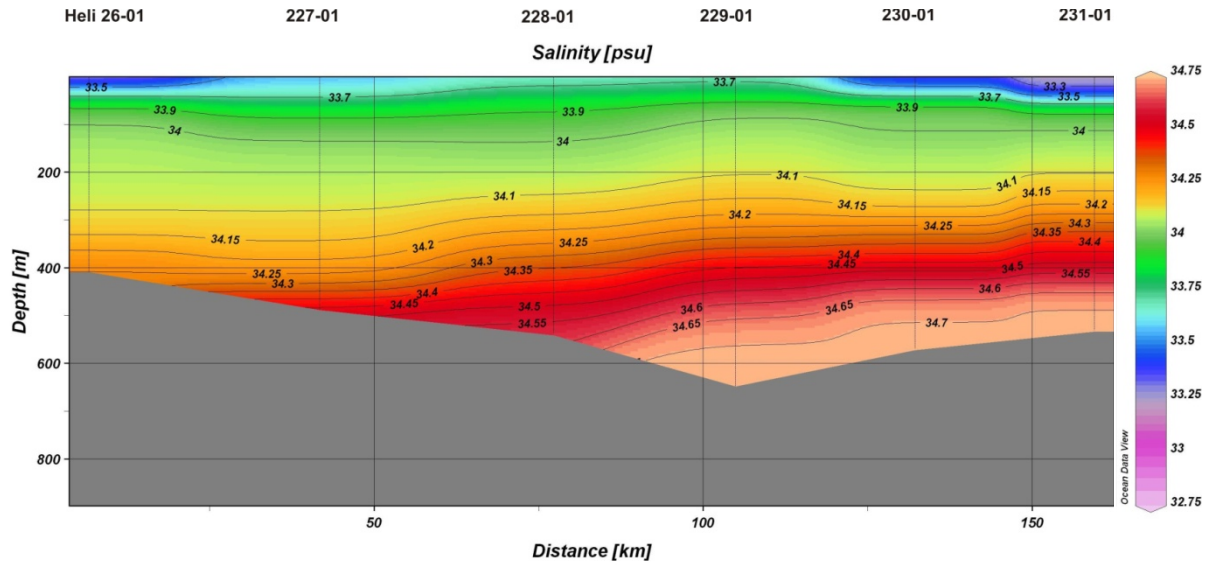


Fig. 6.13b: Salinity on hydrographic section 2 northwest of Burke Island. The warm and salty deep water of circumpolar origin fills the depression on the eastern flank (right).

Fig. 6.13b: Salzgehalt auf dem hydrographischen Schnitt 2 nordwestlich von Burke Island. Das warme, salzreiche Tiefenwasser mit zirkumpolaren Ursprung füllt den gesamten östlichen Teil der Rinne (rechte Seite).

It has to be proven with data from recent cruises, if there is any change in temperature or salt content.

Section 6 along the ice shelf front of Pine Island glacier was chosen to show the hydrographic conditions of inflowing and outflowing water masses right in front of the cavity of this small ice shelf (Fig. 6.14). This transect was possible because of the extreme low ice conditions this year. It covers almost the entire 48 km wide front of the flowing ice shelf.

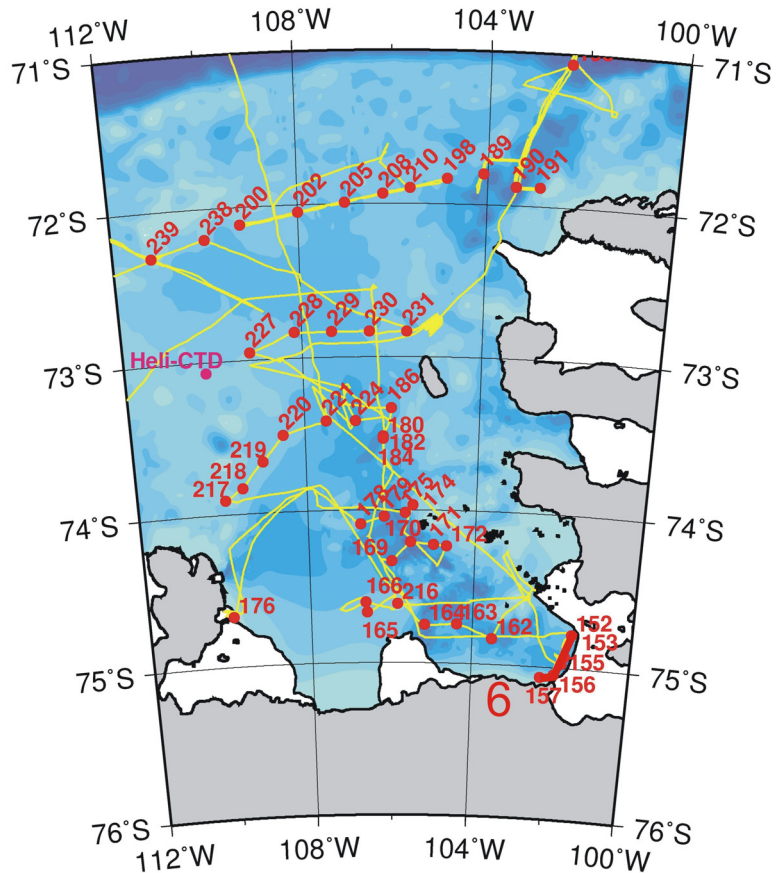


Fig. 6.14: Position of hydrographic section 6 in front of Pine Island glacier

Fig. 6.14: Position des hydrographischen Schnittes 6 an der Schelfeisfront des Pine Island Gletscher

Here the entire water column below 400 m depth is filled with warm and saline water of circumpolar origin flowing in from the north deep into the cavity underneath the ice shelf, where it is responsible for the large melting rates from below. Station 155 is the deepest station with a water depth of 1,029 m. The potential temperature at the bottom is 1.165°C with a salinity of 34.684. This temperature is approximately 3.8 °C higher than the in-situ freezing point near the grounding line as given by Hellmer et al. (1998).

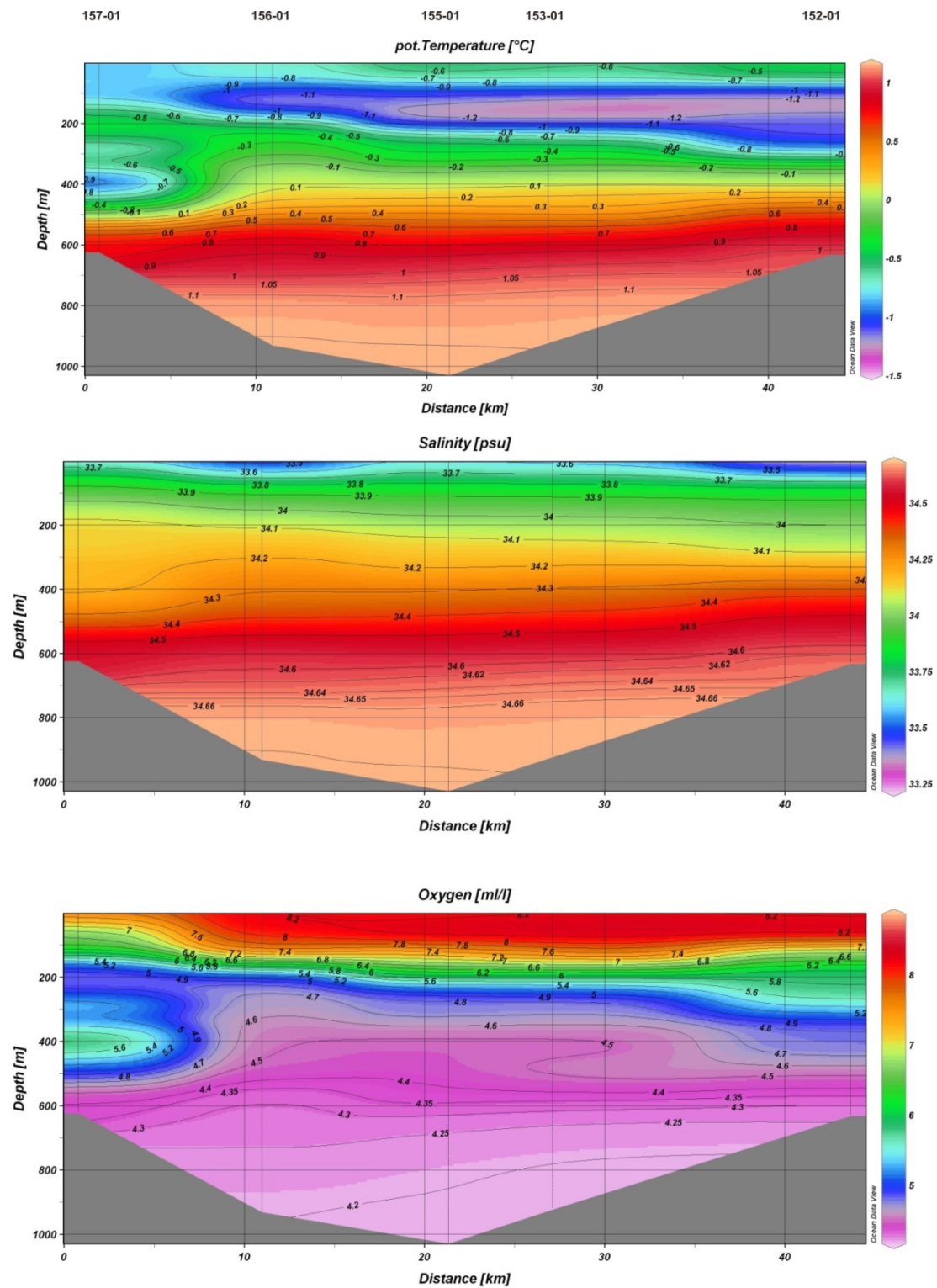


Fig. 6.15 a,b,c: Potential temperature, salinity and dissolved oxygen on hydrographic section 6 along Pine Island glacier

Fig. 6.15 a,b,c: Potentielle Temperatur, Salzgehalt und gelöster Sauerstoff auf dem hydrographischen Schnitt 6 entlang der Schelfeisfront des Pine Island Gletscher

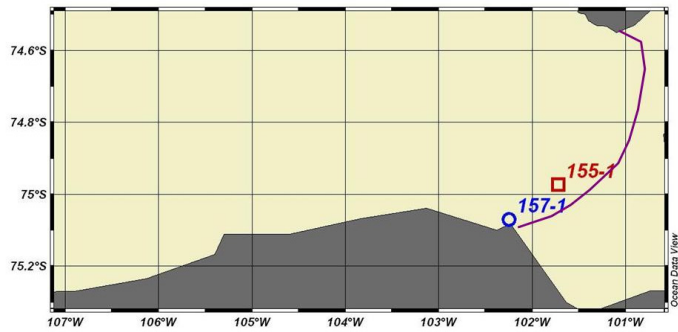


Fig. 6.16: Position of station 157 and 155 near Pine Island glacier
 Fig. 6.16: Position der Stationen 157 und 155 nahe dem Pine Island Gletscher

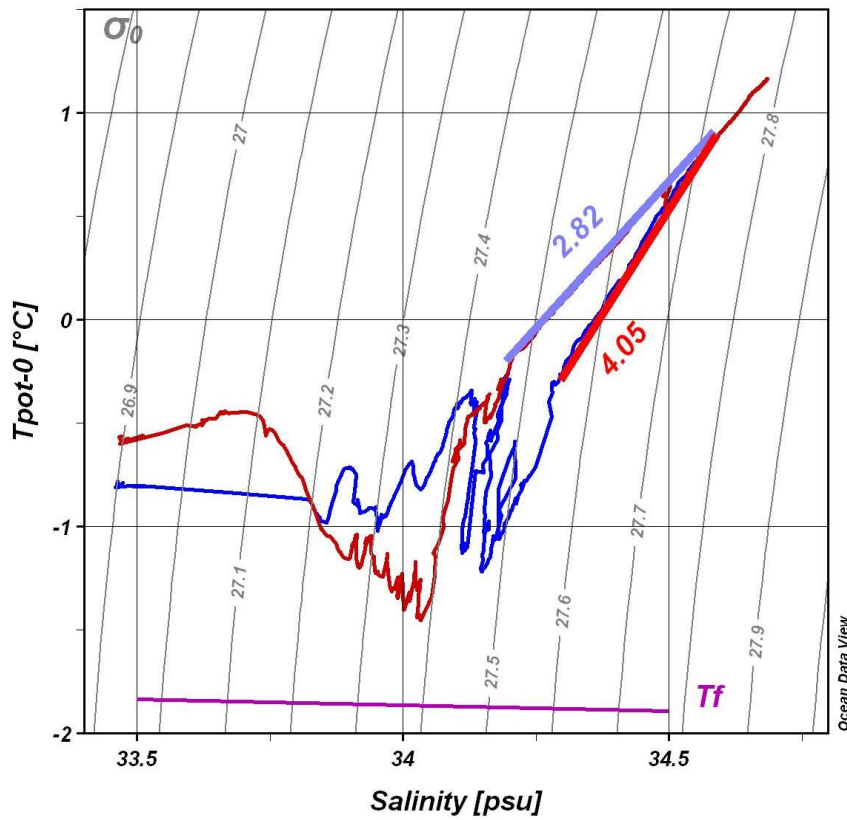


Fig. 6.17: Theta-S diagram of stations 157 and 155 near Pine Island glacier showing the different slopes of inflowing (4.05) and outflowing water (2.82). Tf denotes the surface freezing point.

Fig. 6.17: Theta-S Diagram der Stationen 157 und 155 nahe dem Pine Island Gletscher. Die unterschiedlichen Steigungen zeigen die einfließende Wassermasse (4.05) und die ausfließende Wassermasse (2.82). Tf gibt die Gerade des Oberflächengefrierpunkts an.

As an example for the heterogeneous composition of the water column the two profiles of station 157 (blue) and 155 (red) (Fig. 6.16) are shown in a theta-S diagram to illustrate, that the inflowing warm water is detectable by slopes of around 4 to 5 whereas the outflowing meltwater has slopes of around 2.8 (Fig. 6.17). Mixing ratios and estimates of melting rates and volumina of meltwater contents are possible analyzing the helium samples, which were taken at specific depths on each station at section 6. This analysis will be done after the cruise at the University of Bremen (Oliver Huhn).

References

Hellmer, H.H., S. S. Jacobs, A. Jenkins, 1998. Oceanic erosion of a floating antarctic glacier in the Amundsen Sea. Antarctic Res. Series, Vol. 75, pp. 83-99

ARGO Floats

In cooperation with the University of Washington (Steve Riser) and the Lamont-Doherty Earth Observatory of Columbia University (Xiaojun Yuan) four ARGO floats were deployed in the Ross gyre. The corresponding data is listed in Tab. 6.1.

Tab. 6.1: Data of four ARGO floats deployed during ANT-XXVI/3

Float S/N	Date/ UTC	Time/ UTC	Latitude	Longitude	Water depth [m]
6393	09-Feb-2010	04:08	66° 59,850' S	165° 45,400' W	3680
6101	14-Feb-2010	12:10	72° 28,300' S	150° 00,240' W	4197
6394	15-Feb-2010	05:32	72° 34,922' S	145° 00,472' W	4172
6396	15-Feb-2010	22:40	72° 24,800' S	139° 59,850' W	4213

Mooring recovery

Two attempts were made to recover two moorings (BSR 6, BSR 4), deployed in 2009 by the US ship *Nathaniel B. Palmer*. In cooperation with the Lamont-Doherty Earth Observatory of Columbia University (Stan Jacobs) we were asked to recover these moorings. Unfortunately both trials failed and the moorings did not come up to the surface. It is not clear what the reason was, because each releaser answered but not in a distinct way. In both cases the range could be measured. Even after more than an hour the range was identical to the water depth, which implies that the mooring is still at depth at their position.

Sea ice observation

Sea ice observations were conducted from the bridge of *Polarstern* on an hourly basis. They contribute to the Antarctic Sea Ice Processes and Climate (ASPeCt) programme, which aims at an improved understanding of the role of Antarctic sea ice in the global climate system. According to the ASPeCt protocol, the thickness, concentration and morphology (ridge height, areal fraction of ridged ice, floe size;

snow thickness) of the three dominant ice types within a 1 km radius from the ship were recorded while the ship moved through the drifting ice. Data contribute to a circumantarctic ice thickness dataset which (until remote-sensing data become available on an operational basis) is the only comprehensive ice thickness information available for the Southern Ocean.

As the 2009/2010 summer season in Amundsen Sea featured an extraordinarily small sea ice coverage, most of the cruise was conducted in open water and only a total of 150 ice observations were recorded. In the northern Ross and western Amundsen Seas, we crossed fields of scattered multi-year ice floes, with total coverage only between 5 and 20 % in vast areas (Fig. 6.18). This is an interesting observation in particular if we consider that computational algorithms for the detection of the ice edge in remote sensing data or models use a threshold value of typically 15 % for the boundary between ice and open water. In many regions and conditions, the choice of this threshold value is not critical because gradients at the ice edge are rather sharp; here, instead, a variation of the threshold value by 15 % would make a huge difference to the ice extent computed.

Small areas with ice concentrations between 60 and 90 % consisted of roughly equal fractions of heavily deformed floes with 20 - 100 m size, and smaller, almost undeformed floes of mostly less than 20 m size; plus a small fraction of brash and broken ice. Among the heavily deformed floes, it was not uncommon to find a level ice thickness (including a probably significant proportion of ice that has been converted from flooded snow) of 1.5 m and more. Ridges with a sail height of more than 3 m were observed. Vast floes (i.e. floes with a size of more than 100 m), which might have been able to slow down *Polarstern*'s progress, were not found.

Although most of the floes were in an advanced state of decay, melt ponds or other clear indications of melting snow were found only on very few occasions. The state of decay became obvious, however, by the fact that the floes broke into pieces very easily as soon as *Polarstern* touched them. Broken floes revealed a typical summer structure with large salt channels and high concentrations of ice algae. Concave floe edges with ice eroded at water surface level and overhanging snow cover indicated that melting of Antarctic sea ice mainly uses the heat from solar radiation absorbed at the open water surface and then transported to the ice floes by the floes' own drift.

An exception to this general view was the small region of very large (exceeding several kms), mostly undeformed ice floes in which the only Heli-CTD station was successfully carried out. These floes were surrounded and apparently protected by an array of stranded icebergs. While these floes were not fast ice in the strict sense, their properties were very similar. Although level ice thickness was hardly more than 1 m (with about 30 cm of snow), the virtual absence of fracture zones (less than 5 % of the area was covered by ridges) gave them a structure stable enough to support the CTD equipment and crew in a safe way.

First observations of newly formed sea ice were recorded on 21 March when we crossed large areas of freshly frozen frazil and grease ice north of Pine Island Bay after air temperature (at the ship's position) had dropped from -3.5°C to -11°C within 24 hours. When returning from our excursion to the Marie Byrd Seamounts on 25 March, we found the ocean covered with pancake ice on a 250 km long section a bit further to the west (about 72°S, 117°W). While pancakes where still undeformed and self-contained near the ice edge in the north, we found them to be rafted and partly cemented further south (Fig. 6.19). In most of the area ice coverage was between 90 and 100 % with distinct polynyas on the leeside of icebergs. We found very few polynyas not associated with icebergs; given that their size did not exceed a few 100 m and that Circumpolar Deep Water (CDW) is readily available in this area, it is reasonable to assume that these polynyas were of the sensible-heat type, i.e. kept open by turbulent vertical flux of sensible heat from the deeper ocean.

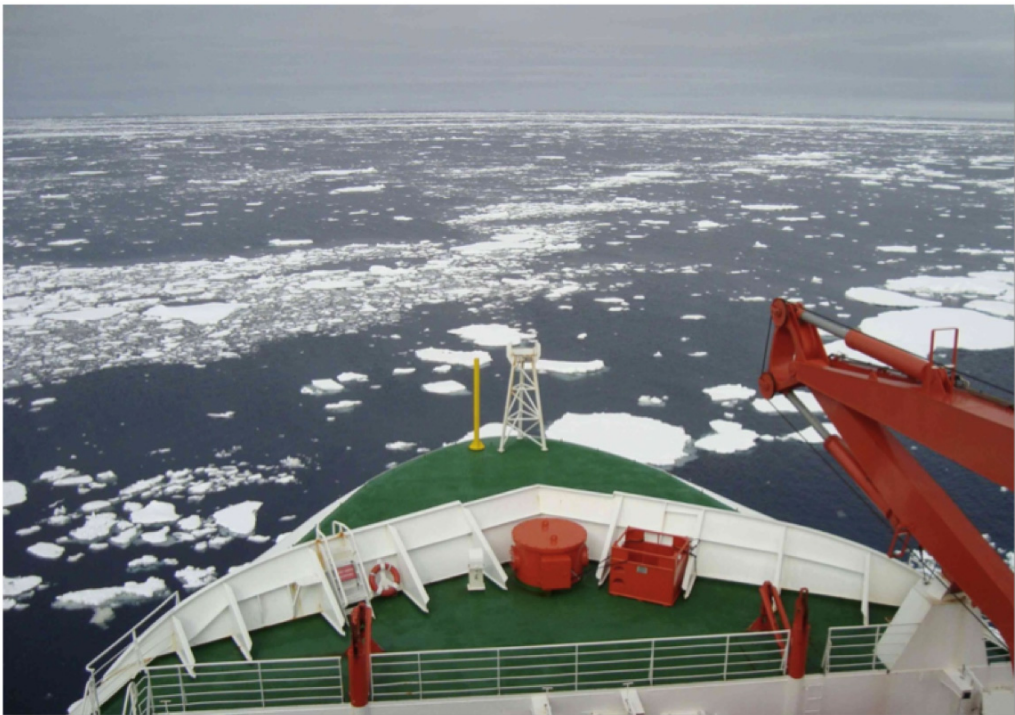


Fig. 6.18: Sea ice concentration of about 20 % in the western Amundsen Sea (16.02.2010)
Fig. 6.18: Meereiskonzentration von etwa 20 % in der westlichen Amundsen Sea (16.02.2010)



Fig. 6.19: Pancake ice in the northern Amundsen Sea (25.03.2010)

Fig. 6.19: Pfannkucheneis in der nördlichen Amundsen Sea (25.03.2010)

Tab. 6.2: All CTD stations of ANT-XXVI/3

Tab. 6.2: CTD Stationen während ANT-XXVI/3

Station	Cast	Date	Time/UTC	Latitude	Longitude	Pressure max.	Waterdepth m
116	01	12-Feb-2010	03:28:00	72 36.619 S	164 5.296 W	4226	4143
125	01	18-Feb-2010	00:59:00	74 28.662 S	133 50.559 W	941	935
126	02	18-Feb-2010	03:27:00	74 25.937 S	133 9.042 W	458	457
127	01	18-Feb-2010	06:49:00	74 31.046 S	134 23.024 W	467	467
136	02	20-Feb-2010	16:46:00	74 22.999 S	134 35.614 W	725	717
137	01	20-Feb-2010	19:58:00	74 22.019 S	134 22.985 W	727	721
139	01	21-Feb-2010	03:33:00	74 5.991 S	135 3.197 W	432	429
141	01	21-Feb-2010	16:51:00	73 44.814 S	135 4.891 W	1224	1217
143	01	22-Feb-2010	02:53:00	72 44.027 S	136 2.130 W	3821	3752
147	01	26-Feb-2010	06:01:00	73 10.012 S	115 35.100 W	791	783
152	01	28-Feb-2010	18:51:00	74 46.825 S	101 30.982 W	636	633
153	01	28-Feb-2010	20:47:00	74 55.514 S	101 38.890 W	931	924
155	01	01-Mar-2010	00:28:00	74 58.429 S	101 43.182 W	1043	1034
156	01	01-Mar-2010	02:02:00	75 2.756 S	101 54.063 W	939	932
157	01	01-Mar-2010	03:29:00	75 4.216 S	102 14.588 W	628	625
162	01	02-Mar-2010	05:46:00	74 49.999 S	103 30.065 W	1040	1031
163	01	02-Mar-2010	09:03:00	74 44.496 S	104 23.520 W	1120	1111
164	01	02-Mar-2010	12:17:00	74 45.026 S	105 11.735 W	1365	1351
165	01	02-Mar-2010	17:31:00	74 40.195 S	106 36.358 W	1182	1173
166	01	02-Mar-2010	22:49:00	74 36.220 S	106 38.560 W	1347	1333
169	01	03-Mar-2010	08:01:00	74 20.006 S	106 0.035 W	1382	1368
170	01	03-Mar-2010	11:25:00	74 12.506 S	105 33.125 W	1650	1631

ANT-XXVI/3

Station	Cast	Date	Time/UTC	Latitude	Longitude	Pressure max.	Waterdepth m
171	01	03-Mar-2010	14:50:00	74 13.511 S	105 0.099 W	1369	1353
172	01	03-Mar-2010	16:40:00	74 14.025 S	104 40.990 W	682	678
174	01	04-Mar-2010	01:26:00	73 57.937 S	105 30.210 W	684	681
175	01	04-Mar-2010	02:41:00	74 1.003 S	105 40.662 W	1068	1055
176	01	04-Mar-2010	16:01:00	74 40.361 S	109 54.838 W	943	933
178	01	05-Mar-2010	09:32:00	74 5.515 S	106 44.840 W	601	599
179	01	05-Mar-2010	12:00:00	74 2.596 S	106 11.030 W	1126	1116
180	01	05-Mar-2010	19:29:00	73 31.486 S	106 12.006 W	813	804
182	02	06-Mar-2010	00:37:00	73 32.141 S	106 12.106 W	820	815
184	01	06-Mar-2010	02:15:00	73 31.173 S	106 12.047 W	797	792
186	01	06-Mar-2010	05:46:00	73 20.116 S	106 0.485 W	676	669
189	01	08-Mar-2010	17:00:00	71 48.000 S	104 4.973 W	672	669
190	01	08-Mar-2010	21:08:00	71 52.748 S	103 23.431 W	757	749
191	01	09-Mar-2010	00:31:00	71 52.676 S	102 53.840 W	563	561
195	01	09-Mar-2010	13:49:00	71 4.007 S	102 22.035 W	1426	1408
198	01	13-Mar-2010	21:22:00	71 50.066 S	104 50.336 W	590	585
200	01	14-Mar-2010	13:36:00	72 7.025 S	109 13.741 W	518	515
202	01	14-Mar-2010	17:26:00	72 2.882 S	107 59.981 W	588	585
205	01	14-Mar-2010	21:30:00	71 59.518 S	106 59.918 W	598	596
208	01	15-Mar-2010	00:54:00	71 55.980 S	106 11.802 W	553	551
210	01	15-Mar-2010	03:07:00	71 53.768 S	105 37.165 W	493	491
216	01	17-Mar-2010	03:29:00	74 36.847 S	105 51.304 W	630	624
217	01	17-Mar-2010	19:30:00	73 54.526 S	109 55.506 W	363	361
218	01	17-Mar-2010	21:02:00	73 50.024 S	109 30.127 W	384	382
219	01	17-Mar-2010	23:01:00	73 40.013 S	108 59.883 W	442	439
220	01	18-Mar-2010	01:30:00	73 29.994 S	108 30.073 W	547	542
221	01	18-Mar-2010	04:11:00	73 25.042 S	107 30.000 W	747	739
224	01	18-Mar-2010	23:00:00	73 25.077 S	106 50.038 W	909	902
227	01	19-Mar-2010	06:38:00	72 57.052 S	109 9.933 W	493	489
228	01	19-Mar-2010	09:15:00	72 49.956 S	108 9.932 W	544	542
229	01	19-Mar-2010	11:21:00	72 50.011 S	107 20.016 W	656	649
230	01	19-Mar-2010	13:29:00	72 49.940 S	106 30.057 W	576	573
231	01	19-Mar-2010	16:16:00	72 50.033 S	105 40.732 W	537	534
238	01	20-Mar-2010	17:11:00	72 11.963 S	110 0.160 W	490	488
239	01	20-Mar-2010	20:17:00	72 18.009 S	111 10.138 W	550	548
241	01	21-Mar-2010	00:24:00	72 23.941 S	112 10.050 W	489	485
253	01	24-Mar-2010	08:18:00	69 13.004 S	122 44.072 W	3728	3659
256	01	25-Mar-2010	12:50:00	72 13.984 S	118 0.315 W	501	500
258	01	25-Mar-2010	16:08:00	72 5.176 S	117 11.072 W	488	485
Heli 26	01	27-Feb-2010	00:57:00	73 4.213 S	110 10.338 W	413	410

Tab. 6.3: Helium samples taken during the cruise ANT-XXVI/3

Tab. 6.3: Helium Probennahme während ANT-XXVI/3

Station	Bottle no.	Depth (m)
153	1	800
	4	480
	6	316
	7	170
155	4	550
	6	320
	8	200
156	2	300
	3	160
157	1	372
	2	287
164	4	270
165	3	800
	6	270
176	3	900
	6	250
218	1	340
	2	295
220	2	400
	4	315

7. LAND GEOLOGY: EXHUMATION AND DEGLACIATION HISTORY OF COASTAL MARIE BYRD LAND AND ELLSWORTH LAND

Cornelia Spiegel¹, James Smith²,
Julia Lindow¹, Ian MacNab²

¹University of Bremen, Dept. of
Geosciences, Bremen, Germany

²British Antarctic Survey,
Cambridge, UK

Objectives

West Antarctica and particularly Marie Byrd Land is a geodynamically active area with Cenozoic rifting, a relatively hot lithospheric, high heat flow, and recent volcanic activity. Most of West Antarctica is covered by the West Antarctic Ice Sheet (WAIS), parts of which are undergoing rapid thinning and retreat. For example, the Pine Island and Thwaites glaciers exhibit the most rapid elevation change/ice thinning and grounding-line retreat in Antarctica. Indeed, it has been suggested that this area may be the most likely site for the initiation of collapse of the two million km² WAIS, which would result in a global sea-level rise of 5 to 6 m. Our project has two main goals: (1) to reconstruct the exhumation history of Marie Byrd and Ellsworth Land using thermochronological analysis, and (2) to reconstruct the deglaciation history of Marie Byrd and Ellsworth Land by using surface exposure dating. Due to the remoteness and challenging accessibility, only very few data on long-term glacial thinning (Johnson et al., 2008) and no thermochronology data exist so far from our study area, which stretches over ~1400 km along the West Antarctic coast.

Surface Exposure Dating

Surface exposure dating, which relies on the abundance of the cosmogenic nuclide ¹⁰Be in pure quartz grains separated from rock, will be used to determine the thinning history of the West Antarctic Ice Sheet in the Amundsen Sea Region. During glacial periods, the several metres of ice that overlies bedrock stops the penetration of cosmic rays, thereby halting the production of cosmogenic nuclides within the rock. With the subsequent onset of deglaciation, retreating ice deposits the debris (erratics) and exposes bedrock surface. These are then exposed to cosmic radiation and accumulation of ¹⁰Be begins. Therefore, cosmogenic isotopes are a useful tool for determining deglaciation ages in Antarctica. Our main objective for surface exposure dating during cruise ANT-XXVI/3 is to collect rock samples (erratics and bedrock surfaces) from nunataks and ice free Islands along altitudinal transects. These samples will be used to constrain the vertical thinning of the WAIS through time.

Thermochronology

Thermochronology (zircon fission track, apatite fission track and apatite (U-Th)/He analysis) provides cooling paths through the upper ~10 km of the earth's crust, thus recording movements, tectonic activity and erosion of the shallow crust and close to the surface. Our main objectives for thermochronological analyses during cruise ANT-XXVI/3 were (i) reconstructing the thermotectonic evolution of West Antarctica in response to Gondwana breakup, rifting of the West Antarctic Rift System, uplift of the Marie Byrd Land dome and potential differential movements between the Marie Byrd Land and Thurston Island / Ellsworth Land crustal blocks, and (ii) testing whether the geodynamic activity of the underlying lithosphere (i.e. fault movements, differential exhumation rates, differential paleo-geothermal gradients) influences the dynamics of the West Antarctic ice sheet. For this we will relate the newly generated thermochronological data to glacial thinning rates extracted from surface exposure dating.

Work on land

Only about 2 % of bedrocks in Marie Byrd Land are exposed to the surface and can thus be accessed for sampling. During ANT-XXVI/3, potential sites within helicopter range to the ship's position were along the Hobbs Coast in western Marie Byrd Land (Mac Donald Heights, Mt Prince and Holmes Bluff area, Shepard Island), along the Walgreen Coast in eastern Marie Byrd Land (Kohler Range, Bear Peninsula, Mt. Murphy), in western Ellsworth Land (Hudson Mountains, Thurston Island), and along the many small islands of the eastern Pine Island Bay, most of them unnamed (Fig. 7.1).

For both, surface exposure dating and thermochronological analysis, our main priority was sampling altitude profiles, since they allow direct extraction of glacial thinning rates and exhumation rates from age-elevation-relationships. An additional goal was collecting iso-altitude horizontal profiles, because we can derive lateral glacial retreat rates from them, and they reveal information on fault movements, crustal tilting, and paleotopography. For thermochronological analysis, we also collected the coarse-grained detrital fraction from the upper c. 1 m of ocean sediment recovered using a box-corer by the marine geology group (see chapter 5). Dating of this ice rafted debris yields age patterns that reflect the cooling and exhumation history integrated over the whole source area.

Main priority was on coring sites that can be related to well-defined glacial catchments. For surface exposure dating, we sampled erratic boulders and / or glacially-eroded bedrock, (ideally striated). Because surface exposure dating relies on the accumulation of ^{10}Be in quartz, quartz-bearing lithologies such as granites, granodiorites, and gneisses were collected. Most of ^{10}Be production occurs in the upper few centimetres of a rock, which is why particularly the surfaces of exposed rocks are analysed. Since these are difficult to sample from unweathered, rounded bedrock or boulders, we used a fuel-powered Stihl rocksaw to cut grids into the rock's surface. After sawing, the samples were removed from the surface by

hammering and chiselling (Fig. 7.2). For thermochronology, we collected *in-situ* bedrock samples. Our thermochronological dating methods are based on the radioactive decay of U (and Th and Sm) in the minerals apatite and zircon; accordingly we sampled apatite and zircon bearing rocks, which involves essentially the same lithologies as required for surface exposure dating. Apart from sample collection we also included observations on structural evolution, tectonic activity and glacial geomorphology in our fieldwork.

Preliminary results

Due to mostly unstable weather conditions, time in the field was limited, and particularly higher elevated areas were often inaccessible because of deep clouds. However, for thermochronology, we were able to collect 39 samples from 21 different land sites and 6 box corers, while for surface exposure dating, 50 (MUY13-15 only for site characterisation) samples from 12 sites were collected (Tab. 7.1 & 7.2, Fig. 7.1). These samples will allow us to generate the first thermochronological data from this part of West Antarctica, which in turn will provide important information on its exhumation history and tectonic evolution. Furthermore, we will be able to gather new data on the long-term dynamics and thinning history of the West Antarctic Ice Sheet, and on the general process of lithosphere – ice sheet interaction.

Hobbs Coast area

Our first priority area, Mac Donald Heights and Cape Burks, could not be reached because of strong winds and low lying clouds. Instead, we headed for Holmes Bluff, where a relatively large variety of igneous basement rocks was exposed. Some of the rocks showed evidence of late brittle deformation, with epidote mineralisations on fault surfaces. We sampled different lithologies (granite, granodiorite, and gabbro), because the quality of apatite grains may vary between the different rock types, and also because this leaves us the possibility to also study the earlier history of magmatic activity during Gondwana breakup or even earlier episodes by applying high-temperature dating systems such as U-Pb on zircon. In addition, we sampled one relatively small erratic boulder. This sample, however, is probably not suitable for surface exposure dating, because we cannot exclude that it has rolled over. Because of deteriorating weather conditions we were not able to collect additional samples or visit further sites. In a second attempt to reach land, we visited Shepard Island, with *Polarstern* positioned relatively close to the coast so that only a short distance had to be travelled by helicopter. However, the island consists of basaltic rocks, which are not suitable for thermochronological analysis, and also our main goal – finding erratics – proved unsuccessful. Most of the island was covered by a penguin colony and many of the exposed rocks were covered by a uniformly thin layer of guano. In an attempt to date the onset of penguin colonisation we took one sample at the contact between the basaltic bedrock and the guano accumulation.

Marie Byrd Land, West-Antarctica

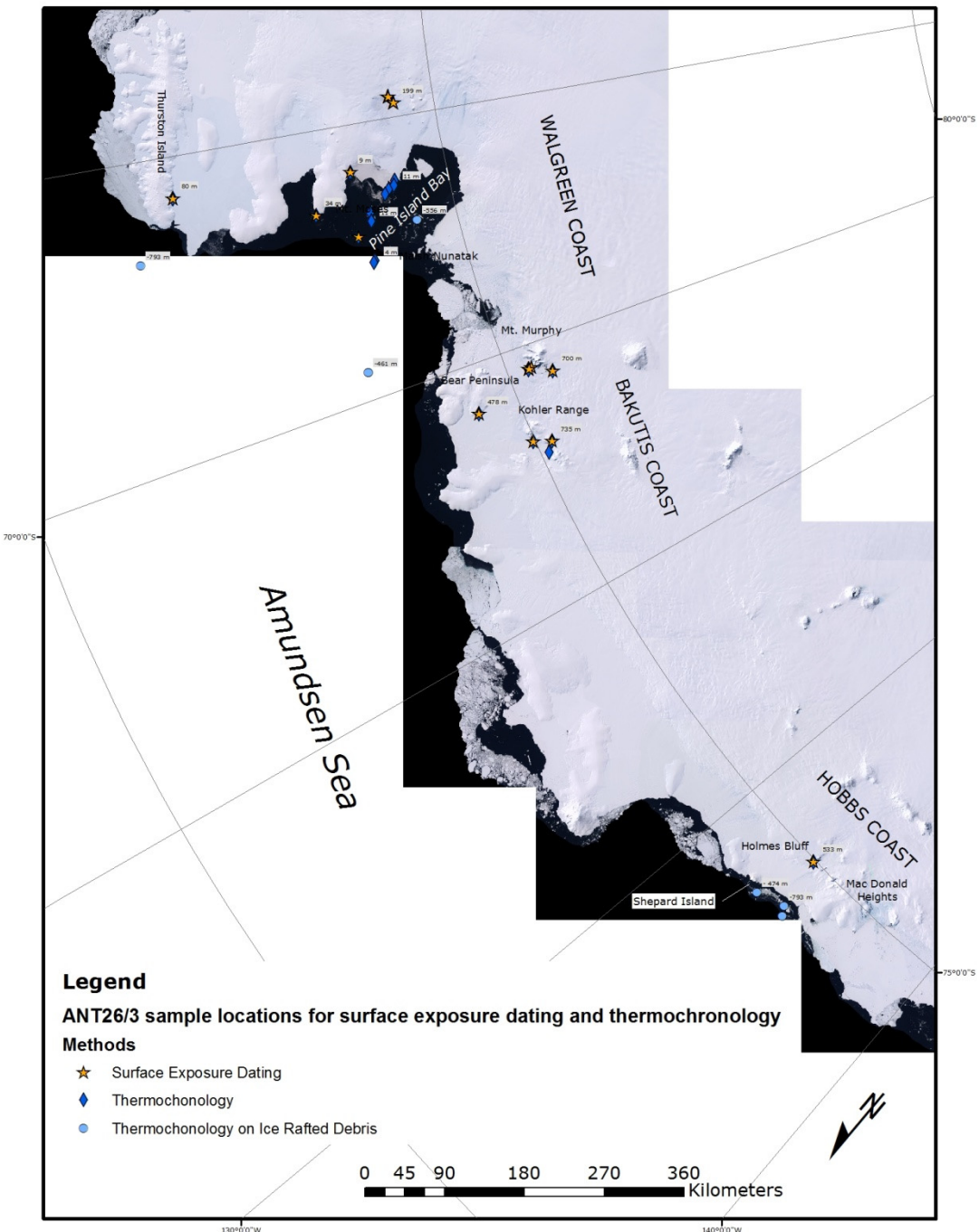


Fig. 7.1: Study area of the land geology team during ANT-XXVI/3 with sample locations
 Abb. 7.1: Arbeitsgebiet der Landgeologie während Ausfahrt ANT-XXVI/3 mit Beprobungspunkten



Fig. 7.2: Sampling for surface exposure dating. A: Example of a granite erratic from Maish Nunatak. The erratic sits on a low elevation WSW-ESE trending ridge composed of basaltic talus (Photo: James Smith). The difference in lithology shows that the boulder has not come from a local source. B: Petrol-powered Stihl saw in use on granite boulder at Maish Nunatak (Photo: Ian McNab). C: Gridded rock samples are then removed using a hammer and chisel (Photo: Florian Wobbe). C: 'T' marks the upper surface of each block (Photo: James Smith).

Abb. 7.2: Probennahme für Oberflächen-Expositionsalter. A: Granitischer Findling, Maish Nunatak (Foto: James Smith). Dieser Findling wurde auf einem basaltischen WSW-ESE-streichenden Rücken beprobt. B: Beprobung eines granitischen Findlings am Maish Nunatak mit der Gesteinssäge von Stihl. (Foto: Ian MacNab). C: Die herausgesägten Blöcke werden mit Hammer und Meißel aus dem Gestein geschlagen (Foto: Florian Wobbe). D: „T“ markiert die Oberflächen der einzelnen Blöcke (Foto: James Smith).

Islands in Pine Island Bay

12 islands of the eastern Pine Island Bay were sampled, forming two >100 km horizontal profiles in north-south-direction (across strike of main morphological features) and east-west-direction (along strike of main morphological features). The profiles are situated in the approximate area of the boundary between the Marie Byrd Land and Ellsworth Land crustal blocks, and are adjacent to the main trough of the Pine Island Glacier. The large majority of the islands consists of coarse-grained granites, often containing mafic xenoliths ranging in size between several cm and >1 m (Fig. 7.3). Particularly in the area of the Brownson Islands, the granites were cut by up to several m thick basaltic dykes (Fig. 7.3). The only exceptions from the rather

monotonous granitic lithologies are the three westernmost islands, which are composed of slightly foliated quartz-diorites, and, at the western end of the profile, of partly brecciated mafic rocks with larger plagioclase phenocrysts, and of a steeply-dipping, east-west-striking, high-grade mylonitic paragneiss (Fig. 7.3).

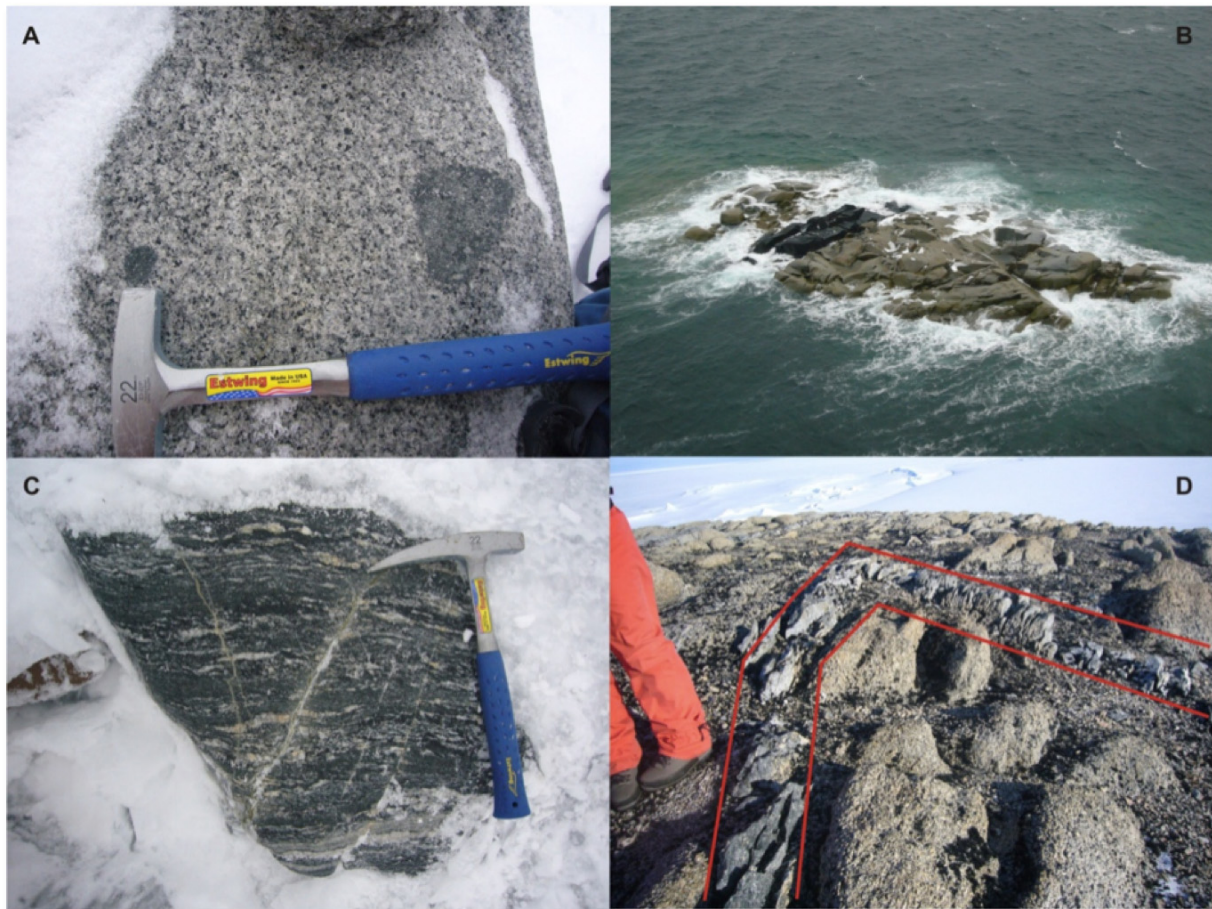


Fig. 7.3: Sampling for thermochronology. A: Coarse-grained granite with rounded mafic xenoliths, unnamed island, Pine Island Bay (sample MBL-12-10). B: Small granitic island with basaltic dyke, Pine Island Bay. C: Strongly deformed gneiss, exposed on Clark Island at the western end of the profile across Pine Island Bay. D: Dyke of intermediate composition cutting the granitic bedrock along the two directions of fault systems measured on Thurston Island (Photos: Cornelia Spiegel).

Abb. 7.3: Probennahme für thermochronologische Datierungen. A: Grobkörniger Granit mit gerundeten mafischen Xenolithen auf einer unbenannten Insel in der Pine Island Bay (Probe MBL-12-10). B: Kleine granitische Insel, die von einem basaltischen Gang durchschlagen wird (Pine Island Bay). C: Stark deformierter Gneis auf Clark Island, am westlichen Ende des Profils über die Pine Island Bay. D: Granitisches Gestein auf Thurston Island, durchschlagen von einem intermediären Gang. Dieser Gang folgt den beiden auf Thurston Island eingemessenen Störungssystemen (Fotos: Cornelia Spiegel).

Samples for surface exposure dating were collected from three of the islands (ISL-01 to 04). Coarse-grained granite/diorite bedrock was sampled at two elevations from one island (ISL-01 & 02) and at one altitude from a second island (ISL-03). An additional erratic cobble (ISL-04) was collected from a third island by Matthias Forwick, although the context of this sample is somewhat unclear so may not be suitable for dating. These samples will be used to investigate the interplay between sea-level rise/isostatic rebound and ice sheet retreat.



Fig. 7.4: Example of striated bedrock from an unnamed bluff on the southern coast of Thurston Island (Photo: Ian MacNab).

Abb. 7.4: Granitisches Gestein mit Gletscherstriemung, Süd-Küste von Thurston Island (Foto: Ian MacNab).

Kohler Range and Bear Peninsula

Apart from sampling elevation profiles, our main goal for this area was collecting samples of approximately the same altitude from both sides of the Kohler glacier in order to detect potential fault zones along the glacial valley. However, weather conditions were again unstable, so that we had less than two hours for sampling. During that time we were able to visit two sites on the eastern side of the glacier and collected two samples for thermochronology plus five erratic boulders for surface exposure dating, covering an altitude difference of approximately 250 m. At equivalent altitudes of the western side, basaltic rocks (no sample taken) and gabbroic rocks (one sample for thermochronology) were exposed. Our profile was complemented by one sample from Bear Peninsula collected for us by the GPS team (see chapter 8).

Samples for surface exposure dating were also taken from Bear Peninsula, taking advantage of the return trip to this site to collect one of the GPS stations. Limited time meant that we only had chance to collect samples immediately outside the helicopter landing site, approximately 20 m to the east of the GPS site. We collected 4 granite bedrock samples and one granite erratic boulder all within a 2 m radius of one another. It is hoped these samples will help verify whether this area of Bear Peninsula was ice covered during the Last Glacial Maximum.

Mount Murphy

For the Mt. Murphy region, an altitude profile covering ~500 m was sampled for thermochronology. Two samples are from the northwestern ridge below the actual volcanic edifice and consist of a biotite-rich migmatic basement gneiss associated with (meta-) gabbroic rocks and intruded by a fine-grained leucogranite. In addition, one coarse-grained gabbro sample from Dorrel Rock outcropping at the southwestern edge of Mt Murphy was provided by the GPS team.

Sampling for surface exposure dating was focussed on the Kay Peaks, an east-west (lower elevation sites) to southeast-northwest (higher elevation site) trending ridge in the Mt. Murphy range. The workable part of the ridge extends up to c:800 m. Due to time pressure and the availability of safe and suitable landing sites, sampling was initially focussed on low elevation sites (< 350 m) along the main ridge and then on the north facing flank. Both areas were characterised by basaltic talus/rubble covered slopes. The distribution of suitable erratics (mainly granite) was sparse and sampling was clustered into three elevations; 324 m (MUY-08 to 11) 338 m (MUY-01 to 07) and 361 m (MUY-12) with multiple samples taken from the lower two elevations. We were limited to just 20 minutes of sampling time at our second and higher (c. 730 m) elevation landing site, because the helicopter needed to return to the ship. Unfortunately no suitable erratics were seen at this elevation nor did we see any suitable outcrops of granite bedrock. We did however sample three hyaloclastic erratics (MUY-13 to 15) as a record of the general context of the site. The GPS team also provided 3 additional samples from Dorrel Rock for surface exposure dating. Unfortunately a second flight to Mt. Murphy on the 18/03/2010 had to be aborted due to bad weather.

Hudson Mountains

Two sites were visited in the Hudson Mountains for surface exposure dating, Mt. Moses and Maish Nunatak. Both nunataks were characterised by basaltic talus/rubble covered slopes. Mt. Moses was recently visited by a BAS colleague (Dr. Mike Bentley, BAS and Durham University) who collected multiple erratic boulders for surface exposure dating between c. 800 - 350 m elevation. Thus we focussed our sampling at low elevation sites (below 350 m) in the main saddle between the ridge of Mt. Moses to the east and the Lucchitta Glacier west. In total 6 erratic cobbles/boulders were collected (MTM-01 to 06) between 224 and 366 m elevation. Samples mainly consisted of light coloured granites and gneisses. The lowermost erratic boulder was very large (2 x 1.5 m) and was sampled using the Stihl saw (Fig. 7.2). On our first flight to Mt. Moses we circled Maish Nunatak to look for suitable landing sites. It was hoped we would stop at this site on our return from Mt. Moses. However, bad weather and a need to return to the ship prevented this. Instead we returned to Maish Nunatak later in the expedition. We focussed our sampling on the WNW-ESE trending ridge collecting granite erratic boulders from three main altitudes 286 m, 268 m and 255 m (JF-01 to 04). We had a very brief (20 minute) stop at one of the lower WNW-ESE elevation ridges, taking a paired sample of granite erratics at 200 m (JF-05 & 06) and one additional sample at 187 m (JF-07). Many more erratics

were recorded at this site, but lack of time prevented us from taking further samples. It is likely that the samples from Mt. Moses and Maish Nunatak will be combined to provide a thinning history of the Lucchitta Glacier.

Thurston Island

Three attempts were made to reach Thurston Island. Two times helicopter landing was not possible due to low-lying clouds and poor visibility, but during one visit we could at least reach the low-elevation areas along the coast. Our first goal was a nunatak on the western tip of Thurston Island, but this proved inaccessible because of steep slopes. We finally found a landing spot on a small nunatak on the southern coast of Thurston Island, adjacent to the Abbot Ice Shelf. Main lithology was again a coarse-grained granite, cut by at least 3 generations of dykes with different compositions (see Tab. 7.1). Two different fault systems were measured, one running north-south along strike of geological units on Thurston Island, the other one running ESE to WNW, approximately parallel to Thurston Island, King Peninsula and Canisteo Peninsula. No crosscutting relationships were observed, but one granodioritic dyke was following the direction of the two fault systems (Fig. 7.3) indicating that at least some of the intrusives postdate fault activities.

Two sets of paired samples were taken for surface exposure dating, one at 80 m (THUR-01 to 02) and the other at 90 m elevation (THUR-03 to 04). At 80 m we sampled the coarse-grained granite bedrock and the finer-grained granite dyke. We sampled the same coarse-grained granite at the 90 m site but the bedrock at sample site THUR-04 was characterised by a finer-grained cap (c. 2 cm thick) that was finely striated (Fig. 7.4). All bedrock samples were taken using the Stihl saw. It is hoped that these samples will provide information on the recent thinning of the Abbott Ice Shelf.

Box corer

For thermochronology, our land samples were complemented by marine-deposited clastic sediments, which were sourced in our study area and transported to the sea by glacial activity. Altogether, sediments from 6 box corers were sieved in order to obtain the coarse clastic material >2 mm. For a more detailed description of the sites we refer to chapter 4, names of marine stations are given in Tab. 7.1. 3 Box corers were taken off the Getz Ice Shelf at the westernmost end of Wrigley Gulf, 1 west of Thurston Island sourced from the Abbot Ice Shelf / Thurston Island, 1 from the main trough of the Pine Island Glacier, and one off the Crosson Ice Shelf in an area formerly covered by the Thwaites Iceberg Tongue. Most of the box corers were rich in coarse material, with single dropstones up to 20 cm in size. Most clasts were granitic, rhyolitic, and basaltic, plus some (meta-) sedimentary rocks. Slightly surprising was the sample from the Pine Island glacial catchment, which was almost entirely composed of red granitic clasts, with nearly no volcanic material. Sediments from off the Crosson Ice Shelf showed a distinct colour zonation, with the upper ~10 cm consisting of brown sediment and few coarse material, while the lower part of the box corer was composed of a stiff grey clay very rich in coarse clasts. We assumed

that the upper part was deposited after the retreat of the Thwaites Iceberg Tongue and thus sampled the upper and the lower part separately.

References

Johnson, J., Bentley, M., Gohl, K., 2008: First exposure ages from the Amundsen Sea Embayment, West Antarctica: the late Quaternary context for recent thinning of Pine Island, Smith, and Pope Glaciers. *Geology* 36, 223-226.

Tab. 7.1: Samples collected for thermochronology

Location	Latitude	Longitude	Elevation	Code	Lithology
<i>Hobbs Coast Area</i>					
Holmes Bluff	S 74° 58.868'	W 133° 43.137'	533 m	MBL-15-10	coarse-grained granite
Holmes Bluff	S 74° 58.868'	W 133° 43.137'	533 m	MBL-04-10	gabbro
Holmes Bluff	S 74° 58.868'	W 133° 43.137'	533 m	MBL-13-10	granodiorite
<i>Eastern Pine Island Bay</i>					
Unnamed Island	S 74° 27.593'	W 102° 23.146'	09 m	MBL-01-10	coarse-grained granite
Unnamed Island	S 74° 27.593'	W 102° 23.146'	09 m	MBL-06-10	coarse-grained granite
Unnamed Island	S 74° 26.604'	W 102° 33.045'	11 m	MBL-08-10	coarse-grained granite
Unnamed Island	S 74° 26.604'	W 102° 33.045'	11 m	MBL-10-10	coarse-grained granite
Unnamed Island	S 74° 22.859'	W 102° 39.944'	19 m	MBL-12-10	coarse-grained granite
Unnamed Island	S 74° 20.169'	W 102° 48.743'	17 m	MBL-14-10	coarse-grained granite
Unnamed Island	S 74° 08.665'	W 103° 22.160'	13 m	MBL-05-10	coarse-grained granite
Unnamed Island	S 74° 08.387'	W 103° 39.933'	121 m	MBL-11-10	coarse-grained granite plus basalt dyke
Unnamed Island	S 74° 08.021'	W 103° 41.124'	11 m	MBL-09-10	coarse-grained granite
Unnamed Island	S 73° 36.121'	W 103° 01.274'	29 m	MBL-70-10	coarse-grained granite
Unnamed Island	S 73° 36.121'	W 103° 01.274'	29 m	MBL-71-10	gabbro
Unnamed Island	S 73° 58.160'	W 104° 08.090'	17 m	MBL-72-10	Qtz-diorite, slightly foliated
Unnamed Island	S 74° 03.298'	W 105° 11.587'	31 m	MBL-73-10	basalt
Unnamed Island	S 74° 01.932'	W 101° 44.546'	13 m	MBL-74-10	coarse-grained granite
Unnamed Island	S 74° 01.932'	W 101° 44.546'	13 m	MBL-75-10	gabbro
Clark Island	S 74° 04.380'	W 105° 09.081'	4 m	MBL-76-10	mylonitic paragneiss
<i>Kohler Range</i>					
Barter Bluff	S 75° 09.592'	W 113° 58.702'	735 m	MBL-51-10	granite
Morrison Bluff	S 75° 05.099'	W 114° 19.502'	488 m	MBL-57-10	gabbro
Mt. Isherwood	S 74° 58.993'	W 113° 41.630'	480 m	MBL-55-10	coarse white granite

Tab. 7.1 (continued): Samples collected for thermochronology

Location	Latitude	Longitude	Elevation	Code	Lithology
<i>Mt. Murphy</i>					
Ridge N Kay Peak	S 75° 13.048'	W 110° 57.800'	192 m	MBL-59-10	migmatitic gneiss
Ridge N Kay Peak	S 75° 13.048'	W 110° 57.800'	192 m	MBL-63-10	fine-grained leucogranite
Ridge N Kay Peak	S 75° 13.048'	W 110° 57.800'	192 m	MBL-53-10	gabbro/granulite
Ridge N Kay Peak	S 75° 13.23'	W 110° 57.58'	335 m	MBL-60-10	migmatitic gneiss
Dorrel Rock	S 75° 26.67'	W 111° 22.06'	698 m	MBL-61-10	gabbro
<i>Bear Peninsula</i>					
close to Hunt Bluff	S 74° 34.75'	W 111° 53.27'	474 m	MBL-62-10	granite
<i>Thurston Island</i>					
S, cls. Abbot Ice Shelf	S 72° 12.558'	W 101° 23.588'	80 m	MBL-65-10	coarse-grained granite
S, cls. Abbot Ice Shelf	S 72° 12.558'	W 101° 23.588'	80 m	MBL-66-10	fine-grained granitic dyke
S, cls. Abbot Ice Shelf	S 72° 12.558'	W 101° 23.588'	80 m	MBL-67-10	basic dyke, rel. coarse-grained
S, cls. Abbot Ice Shelf	S 72° 12.558'	W 101° 23.588'	80 m	MBL-68-10	porphyric granodiorite, dyke
<i>Box Corer</i>					
W Wrigley Gulf	S 74° 26.73'	W 134° 09.16'	-793 m	MBL-30-10	IRD>2 mm, PS 75 / 130-2
W Wrigley Gulf	S 74° 22.03'	W 134° 22.95'	-750 m	MBL-31-10	IRD>2 mm, PS 75 / 132-1
W Wrigley Gulf	S 74° 20.64'	W 133° 04.68'	-474 m	MBL-32-10	IRD>2 mm, PS 75 / 133-1
W of Thurston Island	S 71° 44.69'	W 103° 19.61'	-793 m	MBL-33-10	IRD>2 mm, PS 75 / 192-2
S Pine Island Bay	S 74° 35.51'	W 104° 02.51'	-556 m	MBL-34-10	IRD>2 mm, PS 75 / 215-1
N Crosson Ice Shelf	S 73° 40.00'	W 108° 59.96'	-461 m	MBL-35-10	IRD>2 mm, PS 75 / 219-2, lower part
N Crosson Ice Shelf	S 73° 40.00'	W 108° 59.96'	-461 m	MBL-35-10-A	IRD>2 mm, PS 75 / 219-2, upper 10 cm

Tab. 7.2: Samples collected for surface exposure dating

Location	Latitude	Longitude	Elevation	Code	Lithology
<i>Hobbs Coast Area</i>					
Holmes Bluff	S 74° 58.868'	W 133° 43.137'	533 m	MBL-02-10	small granite erratic
<i>Kohler Range</i>					
Barter Bluff	S 75° 09.592'	W 113° 58.702'	735 m	MBL-50-10	rounded granitic boulder
Barter Bluff	S 75° 09.592'	W 113° 58.702'	735 m	MBL-52-10	large granitic boulder
Mt. Isherwood	S 74° 58.993'	W 113° 41.630'	480 m	MBL-54-10	granite
Mt. Isherwood	S 74° 58.993'	W 113° 41.630'	480 m	MBL-58-10	mylonite
Mt. Isherwood	S 74° 58.993'	W 113° 41.630'	480 m	MBL-56-10	granite
<i>Hudson Mountains</i>					
Mt. Moses	74°33'032"	99°11'561"	351 m	MTM-01	Coarse-grained granite erratic
Mt. Moses	74°33'02.8"	99°11'21.2"	366 m	MTM-02	Granite erratic. Sample broken into two pieces
Mt. Moses	74°33'154"	99°11'499"	310 m	MTM-03	Gneissic erratic
Mt. Moses	74°33'11.6"	99°11'57.1"	247 m	MTM-04	Fine-grained granite erratic
Mt. Moses	74°33'225"	99°11'794"	244 m	MTM-05	Coarse-grained granite erratic
Mt. Moses	74°33'10.3"	99°12'07.5"	224 m	MTM-06	Large gneiss/syenite erratic boulder
Maish Nunatak	74° 35.33	99° 27.06	286 m	JF-01	Large coarse-granite erratic
Maish Nunatak	74° 35.36	99° 26.93	268 m	JF-02	Coarse-grained granite erratic
Maish Nunatak	74° 35.343	99° 26.956	268 m	JF-03	Coarse-grained granite. ~3m north of JF-02
Maish Nunatak	74° 35.43	99° 26.44	255 m	JF-04	Large, fine-grained granite erratic.
Maish Nunatak	74° 35.82	99° 27.33	200 m	JF-05	Medium-grained granite erratic
Maish Nunatak	74° 35.80	99° 27.33	200 m	JF-06	Coarse-grained granite erratic
Maish Nunatak	74°35.835	99° 27.032	187 m	JF-07	Coarse-grained granite erratic
<i>Mt. Murphy</i>					
Kay Peak	75°13.248	110°57.590	338 m	MUY-01	Small coarse-grained granite erratic
Kay Peak	75°13.250	110°57.595	338 m	MUY-02	Small coarse-grained granite erratic
Kay Peak	75°13.245	110°57.583	334 m	MUY-03	Small fine-grained granite
Kay Peak	75°13.239	110°57.559	328 m	MUY-04	Fine-grained granite bedrock (dyke)

Tab. 7.2 (continued): Samples collected for surface exposure dating

Location	Latitude	Longitude	Elevation	Code	Lithology
Kay Peak	75°13'237	110°57.570	338 m	MUY-05	Fine-grained granite bedrock (dyke)
Kay Peak	75°13.242	110°57.557	339 m	MUY-06	Gneissic erratic
Kay Peak	75°13.243	110°57.548	334 m	MUY-07	Striated fine-grained granite bedrock (dyke)
Kay Peak	75°13.228	110°57.670	326 m	MUY-08	Medium-grained granite erratic
Kay Peak	75°13.232	110°57.669	324 m	MUY-09	Medium-granite granite erratic
Kay Peak	75°13.233	110°57.663	324 m	MUY-10	Medium-granite granite erratic
Kay Peak	75°13.229	110°57.649	327 m	MUY-11	Medium-granite granite erratic
Kay Peak	75°13.340	110°57.761	361 m	MUY-12	Small quartzite erratic
Kay Peak	75°15.079	110°55.863	717 m	MUY-13	Hyaloclastite (?) erratic (same as MUY-13 & 14)
Kay Peak	75°15.116	110°55.897	725 m	MUY-14	Hyaloclastite erratic
Kay Peak	75°15.115	110°55.896	725 m	MUY-15	Hyaloclastite erratic
Dorrel Rock	75°26.67	111°22.10	700 m	DOR-1	Coarse-grained gabbro bedrock
Dorrel Rock	75°26.67	111°22.07	699 m	DOR-2	Fine grained granite
Dorrel Rock	75°26.67	111°22.05	699 m	DOR-3	Coarse-grained gabbro bedrock
<i>Eastern Pine Island Bay</i>					
Unnamed Island	73° 36.102	103° 00.962	27 m	ISL-01	Med to coarse-grained granite bedrock
Unnamed Island	73° 36.130	103° 01.011	34 m	ISL-02	Med to coarse-grained granite bedrock
Unnamed Island	73° 58.159	104° 08.091	26 m	ISL-03	Coarse-grained granite/qtz-diorite bedrock
Unnamed Island	74°01.946	101°44.511	9 m	ISL-04	Small granite erratic sitting on bedrock
<i>Thurston Island</i>					
S,cls. Abbot Ice Shelf	72° 12.564	101° 23.620	80 m	THUR-01	Coarse-grained granite bedrock
S,cls. Abbot Ice Shelf	72°12.567	101° 23.614	78 m	THUR-02	Fine-grained granite dyke
S,cls. Abbot Ice Shelf	72° 12.545	101° 23.539	90 m	THUR-03	Coarse-grained granite bedrock
S,cls. Abbot Ice Shelf	72° 12.542	101° 23.529	90 m	THUR-04	Striated granite bedrock
<i>Bear Peninsula</i>					
close to Hunt Bluff	74° 34.745	111° 53.226	478 m	BR-01	Coarse-granite bedrock
close to Hunt Bluff	74° 34.747	111° 53.214	477 m	BR-02	Coarse-granited granite erratic
close to Hunt Bluff	74° 34.750	111° 53.210	477 m	BR-03	Coarse granite bedrock
close to Hunt Bluff	74° 34.742	111° 53.214	477 m	BR-04	Coarse-granited granite bedrock
close to Hunt Bluff	74° 34.745	111° 53.224	477 m	BR-05	Coarse-granited granite bedrock

8. GPS OBSERVATIONS IN WEST ANTARCTICA FOR THE DETERMINATION OF VERTICAL AND HORIZONTAL DEFORMATIONS OF THE EARTH'S CRUST AND FOR THE INVESTIGATION OF THE TIDAL DYNAMICS OF ICE SHELVES

Mirko Scheinert, Ralf Rosenau

Technical University of Dresden, Inst. of Planet. Geodesy, Germany

Objectives

In order to deepen the knowledge on the glacial history and on the tectonic state of Antarctica it is important to investigate recent deformations of the earth's crust. Vertical deformations are caused by changing ice loads, hence they are connected with glacial history and with recent ice mass changes. West Antarctica shows larger changes of its (marine based) ice sheet, which leads to an expectation of vertical deformations up to ten times larger than in East Antarctica. Especially the Pine Island Bay area features the largest mass imbalance in entire Antarctica. The large outlet glaciers Pine Island Glacier and Thwaites Glacier show significant variations of their flow regime as well as of the ice mass changes. Their negative mass imbalance causes significant vertical deformations. Altogether, the viscoelastic effect due to the glacial history and the elastic effect due to the recent ice mass changes may result in a vertical uplift of up to 10 mm/year. During the 2006 ANT-XXIII/4 cruise of *Polarstern* the TUD group set up four sites on bedrock in the Pine Island Bay area. These sites have now been reoccupied. From the repeated observations we will obtain coordinate changes over the time span of four years, from which statements on the vertical deformation shall be inferred. Also, possible horizontal deformations will be analysed to yield an independent view of the tectonic situation in the area of interest.

Furthermore, ice shelves and outlet glaciers, respectively, shall be investigated with regard to their motion and flow regime. The largest impact is excited by ocean tides, which the floating ice follows immediately by 100 % (depart of a small-scale region at the grounding zone). Realizing direct GPS observations of the floating ice the tidal dynamics can be investigated. Combining these observations with analyses of remote sensing data (ICESat laser data, feature tracking and/or SAR interferometry of optical and microwave data) the flow regime of the outlet glaciers and ice shelves will be determined. For this goal, it was anticipated to concentrate on ice shelves of the Pine Island Bay area.

Work at sea

As described above, the main goal was to re-occupy GPS sites on bedrock which were measured for the first time in 2006. By means of the ship-based helicopters

three of the four sites could be visited, and the GPS equipment was successfully installed, namely at BEAR in the western part and at PIG2 and MANT in the eastern part of Pine Island Bay. The GPS equipment was left there to gain data for at least five days before it was re-collected again. At the site MURP it was decided not to install the GPS equipment. Due to the bad weather conditions prevailing throughout the cruise we would risk of not being able to get there again to re-collect the equipment. This decision proved to be correct. Likewise, it was not possible to set up further GPS sites at ice shelf locations according to the scientific objections as originally planned.

The locations, coordinates and observation times of the GPS bedrock sites are summarized in Tab. 8.1. The overview map of the area of interest is shown in Fig. 8.1. Examples of the installation of the GPS equipment are shown in Fig. 8.2.

There was only one position on an ice shelf where a GPS site was set up in order to measure the vertical motion due to ocean tides and eventually to compare it with the predictions from ocean tide models (see Fig. 8.3). This site GET1 was established at the western end of the Getz Ice shelf on February 17, 2010 (Fig. 8.4). It is situated between Grant Island and the coast at approx. $131^{\circ}51'28''W$ and $74^{\circ}40'24''S$. An attempt to re-collect the equipment on February 20, 2010, was not successful. Due to low clouds and bad visibility the helicopter had to return just about nine miles before reaching the position. Further chances to reach the site again had not occurred. Therefore, the equipment had to be left at the ice shelf. Possible options to re-collect the equipment in the forthcoming season are subject to further considerations.

Preliminary results

The data analysis will be done at the home institution during the so-called post-processing since further data like re-analysed precise GPS orbits have to be utilized. Therefore, preliminary results cannot be presented in this report.

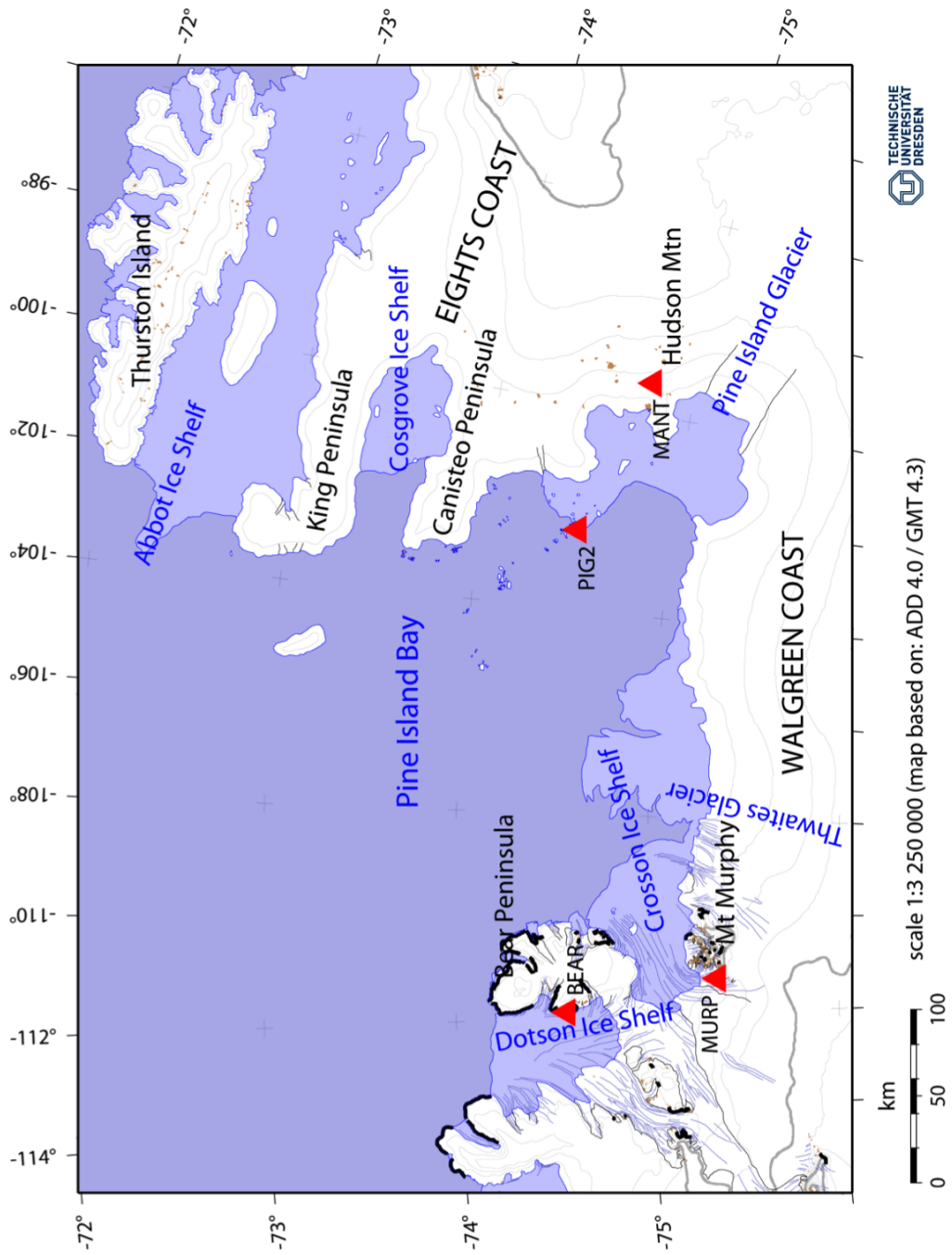


Fig. 8.1: Overview map of the area of interest. The GPS sites are situated at the coastal region of the Pine Island Bay. They are marked by special bolts fixed into bedrock. All sites were measured in 2006 and could be re-occupied during this cruise, except the site MURP.

Abb. 8.1: Karte des Arbeitsgebietes. Die GPS-Stationen befinden sich in der Küstenregion der Pine-Island-Bucht und sind mit Hilfe eines Spezialbolzen im anstehenden Gestein vermarkt. Bis auf die Station MURP konnten alle Stationen, die 2006 zum ersten Mal gemessen wurden, wieder besetzt werden.

Tab. 8.1: Geographical location, coordinates and observation time of the GPS bedrock sites [set-up: date of the set-up of the equipment; recoll.: date of the recollection of the equipment; days: number of days with complete 24h measurements (24h sessions)].

Tab. 8.1: Geographische Lage, Koordinaten und Beobachtungszeit der GPS-Stationen auf Fels.

ID	geographical location	approximate coordinates		observation time		
		longitude (west)	latitude (south)	set-up	recoll.	days
BEAR	west coast of Bear Peninsula (Hunt Bluff), eastern side of Dotson Ice Shelf	111° 53' 16"	74° 34' 45"	02-26-2010	03-04-2010	5
MANT	lower cliff at north-west side of Mt. Manthe, Hudson Mts.	99° 22' 05"	74° 46' 46"	02-28-2010	03-16-2010	15
PIG2	Rock island at northwestern tip of Pine Island Northern Ice Shelf	102° 26' 22"	74° 30' 40"	03-01-2010	03-16-2010	14



Fig. 8.2: Installation of the GPS equipment at the sites MANT (upper left), BEAR (upper right) and PIG2 (lower left). The lower-right photography shows the typical set-up of receiver, batteries and auxiliary devices within the Zarges aluminium box.

Abb. 8.2: Aufbau der GPS-Ausrüstung (MANT: oben links, BEAR: oben rechts, PIG2: unten links). Die typische Installation mit Empfänger, Batterie und zusätzlichen Geräten innerhalb der Zargesbox ist unten rechts zu sehen.

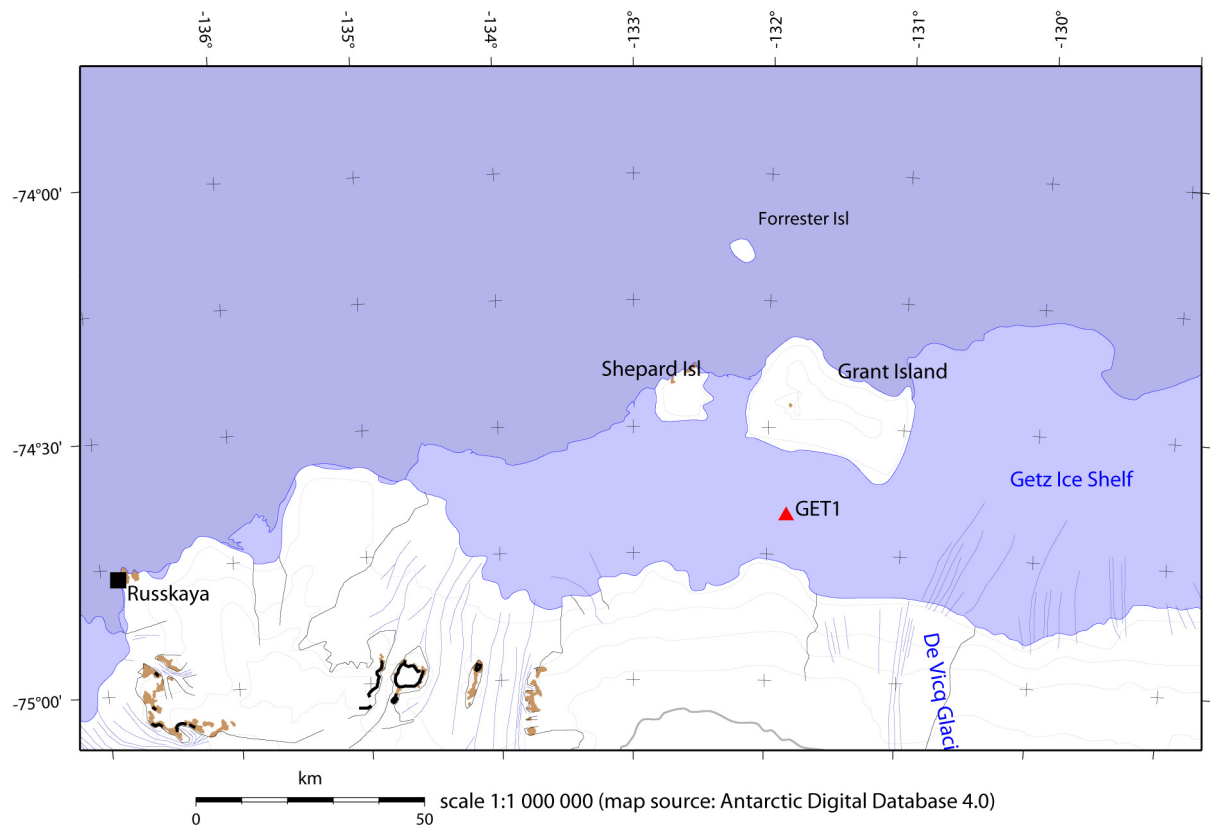


Fig. 8.3: Location of GPS site GET1 on the Getz Ice Shelf
Abb. 8.3: Lage der GPS-Station GET1 auf dem Getz-Eisschelf



Fig. 8.4: Set-up of the GPS equipment at site GET1 on the Getz Ice Shelf
Abb. 8.4: Aufbau der GPS-Ausrüstung der Station GET1 auf dem Getz-Eisschelf

9. CLIMATE INDUCED CHANGES AND BIODIVERSITY OF ANTARCTIC PHYTOPLANKTON

Christian Wolf

Alfred-Wegener-Institut für Polar- und Meeresforschung, Bremerhaven

Objectives

The polar oceans appear to be very sensitive to global warming. The once dominant cold, dry continental Antarctic climate will be replaced by a trend towards later sea-ice advance, earlier retreat and shorter sea-ice season. This will cause multi-level responses in the marine ecosystem. The changing environmental conditions will affect the composition and distribution of species and will allow the intrusion of temperate key species, such as *E. huxleyi*.

The aim of the current project is to answer the following researchable questions:

- 1) Do we observe a further southward intrusion of *E. huxleyi* in the Antarctic?

E. huxleyi is a key species in biogeochemical cycles in the world ocean. Current investigations have shown a moving of *E. huxleyi* into Polar Regions. The previous observed distribution of *E. huxleyi* is considered to be a result of a temperature barrier. With ongoing warming and intrusion of warmer water into the polar habitats we expect *E. huxleyi* to extend its distribution into these regions and to become a common member of the Antarctic phytoplankton.

- 2) Will other key species in the Antarctic be affected by climate change?

Global warming will allow more temperate species to evolve into polar habitats and typical polar species will lose their habitat, because they are usually stenotherm. We expect a shift in the composition of Antarctic phytoplankton with ongoing global warming due to more competition and unfavorable growth conditions.

- 3) How do the phytoplankton composition and distribution in the Pacific sector of the Southern Ocean look like?

The ongoing global warming will have an effect on the biodiversity and distribution of phytoplankton in the Antarctic. To detect and assess these effects we have to know its current biodiversity and distribution. Especially about the diversity and distribution of picophytoplankton, the smallest phytoplankton fraction (0.2 - 2 µm), not much is known. Due to difficulties in identifying picophytoplankton down to species level with conventional methods (microscopy), we apply molecular approaches (sequencing of rDNA, fingerprinting methods). These approaches approved to be a good opportunity to get information about the diversity of this small fraction. This study shall deliver a

ground-based data set of the biodiversity and distribution of phytoplankton in the Pacific sector of the Southern Ocean.

- 4) How do Cryptophyceae contribute to the biodiversity of Antarctic phytoplankton?

This study is dedicated to assess the abundance and diversity of Cryptophyceae in the Antarctic. This will involve surveillance of Cryptophyceae via high performance liquid chromatography (HPLC) and molecular approaches (sequencing of rDNA, phylochips and fingerprinting methods). The data set will contribute to further illuminate the ecological role of Cryptophyceae in the marine environment.

- 5) Can we monitor the changes of PFTs with satellite data in the Antarctic?

Field studies have the problem of only covering limited space and time. A major new advantage would be to identify Phytoplankton Functional Groups (PFTs) via satellite. This study shall deliver the ground-based data set for the development and validation of the PhytoDOAS method.

Work at sea

To achieve our goals filter samples for pigment analyses (HPLC), DNA analyses and phytoplankton absorption measurements (PAB) were taken during the cruise. For a better quantification of the plankton groups water samples for flow cytometry were also taken. Additionally some water samples were taken into culture for microscopy analyses.

Surface water samples were taken every 3 to 4 hours from the moon pool during all transects of the cruise (Figs. 9.1 and 1.2).

In the Amundsen Sea embayment depth profiles were taken from 32 CTD casts with a resolution of 6 samples (Fig. 9.3). The sample depths were chosen after the fluorescence profile, to ensure that the profiles contain the layer with the chlorophyll maximum.

For the pigment analyses (HPLC) 1 - 4 l of the water sample were filtered through a GF/F filter (25 mm Ø) and stored immediately at -80°C.

For the flow cytometry analyses 4.5 ml of the water sample were fixed with 20 µl gluteraldehyde and stored immediately at -80°C.

For the phytoplankton absorption measurements (identifying of PFTs) 0.5 - 2 l of the water sample were filtered through a GF/F filter (47 mm Ø) and stored immediately at -80°C.

For the DNA analyses a fractioning was performed. Two liters of the water sample were first filtered through a membrane filter with a pore size of 10 µm. Then the flow

9. Climate induced changes and biodiversity of Antarctic phytoplankton

trough was filtered through a membrane filter with a pore size of 3 μm and finally the flow trough of the last filtration was filtered through a membrane filter with a pore size of 0.2 μm . Finally there are three size fractions of phytoplankton for analyses from every water sample taken, above 10 μm , between 3 and 10 μm and between 0.2 μm and 3 μm . The samples were stored immediately at -80°C.

Preliminary results

No results can be presented at this time, because all samples will have to be analyzed in the home laboratory in Bremerhaven.

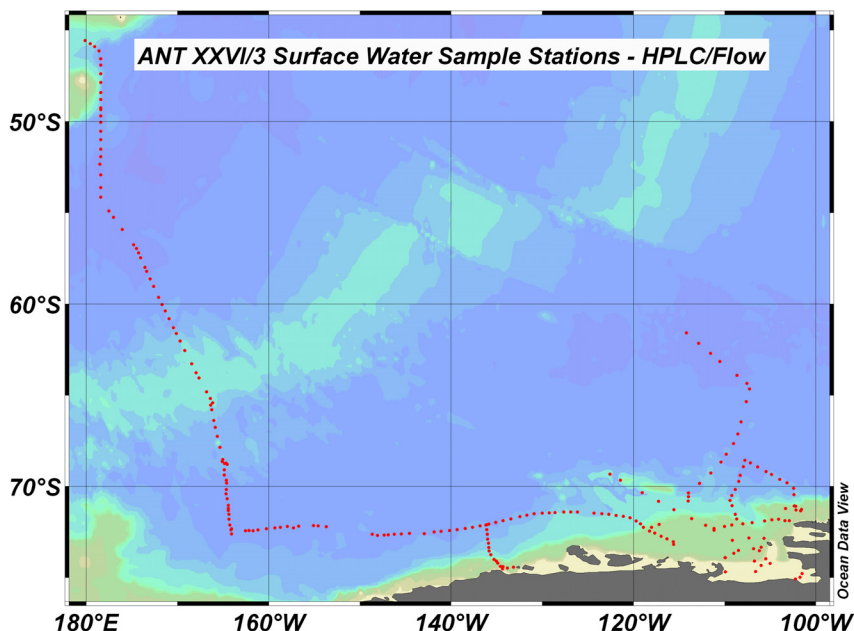


*Fig. 9.1: Stations where surface water samples were taken for HPLC and flow cytometry (red dots).
Abb. 9.1: Stationen an denen Oberflächenwasserproben für HPLC und Flow Cytometrie genommen wurden (rote Punkte).*

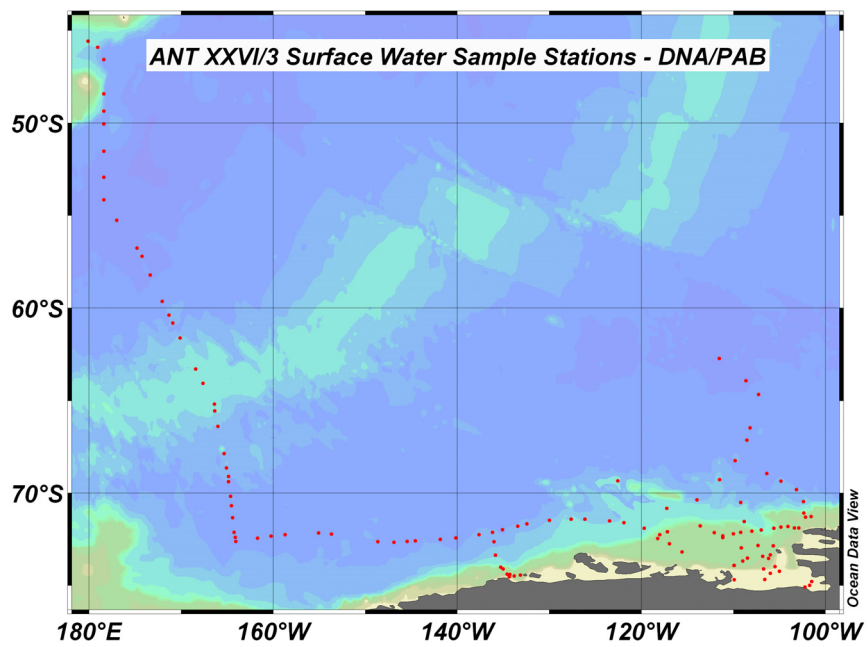


Fig. 9.2: Stations where surface water samples were taken for DNA analyses and PAB (red dots).
Abb. 9.2: Stationen an denen Oberflächenwasserproben für die DNA-Analyse und PAB genommen wurden (rote Punkte).

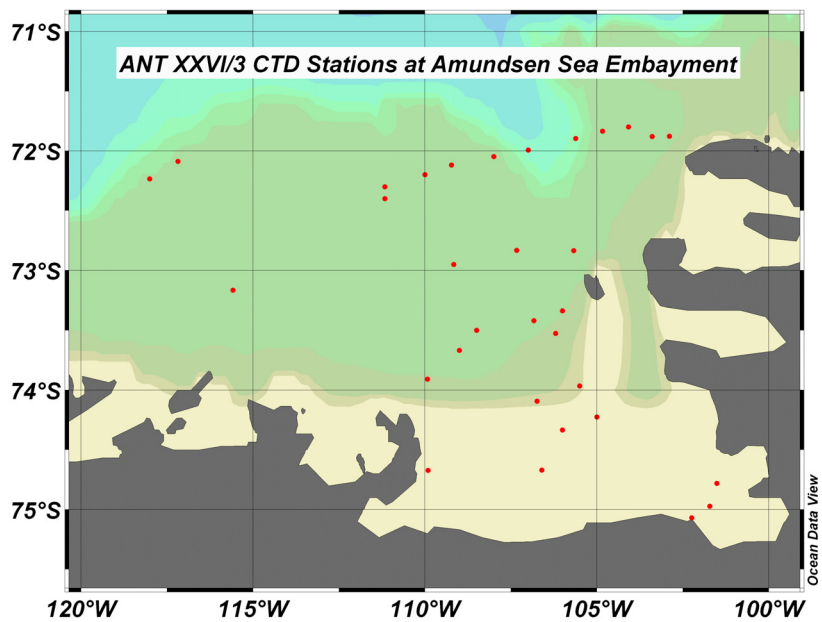


Fig. 9.3: CTD stations at Amundsen Sea Embayment (red dots)
Abb. 9.3: CTD-Stationen im Amundsenmeer (rote Punkte)

10. METHANE IN-SITU PRODUCTION IN SURFACE WATER DURING THE PHYTOPLANKTON BLOOM IN THE AMUNDSEN SEA

Ellen Damm, Ellen Lichte, Christine Cychon

Alfred-Wegener-Institut für Polar- und Meeresforschung, Bremerhaven

Objectives

Recent climate change may have profound effects on natural biogeochemical cycles in seawater. Special feedback effects to pathways of climatically relevant biogases like DMS and methane will loom large in the equation of change. The present marine methane cycle is influenced mainly by atmospheric methane transported by downward diffusion and convective ventilation into the deeper ocean, by fossil methane released from gas venting sites at the sea floor, microbial *in-situ* methane production in the surface ocean and microbial oxidation in the whole water column. A methane surplus relative to the atmospheric equilibrium concentration is a persistent feature of most ocean surface water. Although it is evident that microbial induced production within the photic zone generates this super-saturation, the mechanism remains poorly understood. Methanogens may form methane via various pathways commonly classified with respect to the type of carbon precursor utilized, e.g. the methylo trophic pathway indicates the intact conversion of a methyl group to methane. Hence a principal pathway by which methane can be formed is methyl trophic methanogenesis. The contribution of methylated substrates is potentially large in the surface ocean, however, the direct evidence of the link between degradation of methylated substrates and production of the greenhouse gas methane is still lacking.

DMSP (dimethylsulfoniopropionate) is an abundant methylated substrate and large amounts are produced annually by marine phytoplankton. Its turnover plays a significant role in carbon and sulphur cycling in the surface ocean. DMSP degradation occurs via a demethylation and a cleavage pathway. Cleavage of DMSP can be carried out by bacteria or by phytoplankton, and leads to formation of DMS (dimethylsulfide). DMS partly escapes to the atmosphere where it is oxidized to sulphuric acid and methanesulfonic acid. These sulphur-containing aerosols serve as cloud condensation nuclei altering the global radiation budget. Thus DMS may exert a cooling (negative) effect to earth's climate. However bacteria in the water column oxidize a large amount of the DMS before it can be released to the atmosphere. Anaerobic metabolism of DMS and further degradation production results in the production of methane. Hence, DMSP catabolism may also have a positive (warming) effect on earth's climate due to the formation of the greenhouse gas, methane. To expand the knowledge about the cycling of methane and DMS and a potential coupling between both our project has two main objectives:

(1) Measurements of methane, DMS, DMSP and nutrients to study different DMSP degradation pathways during and after a phytoplankton bloom in the Amundsen Sea embayment. (2) Microcosm experiments to induce a methane production in Antarctic surface water supplemented with DMSP and without DMSP. To detect changes in the bacterial community structure sampling for CARD-FISH were carried out during the experiments.

Work at sea

Water samples were collected at 36 stations along the oceanographic transects in the Amundsen Sea embayment (Tab.10.1). Water samples were taken from the Niskin bottles mounted on a rosette sampler from the sea surface up to 200 m water depths. The dissolved gases dimethylsulphide and methane are immediately extracted after sampling and analysed by gas chromatographs equipped with a flame-photometer detector (PFPD) and a flame ionization detector (FID), respectively. Further, water samples are taken for analysing particular and dissolved DMSP (dimethylsulfoniopropionate) and nutrients. Gas samples are collected for analyses of the stable carbon isotopic signature of methane. These measurements will be carried out in the home lab.

Three microcosm experiments were set up to study the ability of natural Antarctic bacterial communities to produce methane from DMSP. Sea water sampling, incubation and methane measurements were conducted with surface water from the stations 126, 191 and 224. Seawater was transferred from 10 L Niskin bottles into sterile 1 liter glass flasks with silicone membranes. Immediately after water sampling bottles were spiked with 50 μ M DMSP (1st experiment) and with 500 nM (2nd and 3rd experiment). A second sequence of bottles served as blank which were free of DMSP supplements. The concentration of methane, DMS, DMSP and oxygen was measured on board. Subsamples are taken for analyzing nutrients and the isotopic carbon signature of methane in the home lab. Measurements were conducted at the beginning of the experiment and after 2, 4, 6, 8 and 10 days each in one bottle spiked with DMSP and at one bottle with blank sea water. The incubation was carried out at approximately *in-situ* temperature in artificial daylight, in darkness and in a daily change between daylight (12 h) and darkness (12 h) to simulate different light conditions. For CARD-FISH as well as DGGE-analysis, sub-samples (600ml) were used to determine the composition and changing of the bacterial communities developed in the bottles spiked with DMSP.

Preliminary results

Until now only raw data are available and therefore no results can be shown.

10. Methane in-situ production in surface water during the phytoplankton bloom in the Amundsen Sea

Tab. 10.1: CTD stations with water sampling for analyzing methane, DMS, DMSP, nutrients.

Station	Cast	Date	Time/UTC	Latitude	Longitude	Pressure max.	Water depth m
116	01	12-Feb-2010	03:28:00	72 36.619 S	164 5.296 W	4226	4143
125	01	18-Feb-2010	00:59:00	74 28.662 S	133 50.559 W	941	935
126	02	18-Feb-2010	03:27:00	74 25.937 S	133 9.042 W	458	457
127	01	18-Feb-2010	06:49:00	74 31.046 S	134 23.024 W	467	467
136	02	20-Feb-2010	16:46:00	74 22.999 S	134 35.614 W	725	717
137	01	20-Feb-2010	19:58:00	74 22.019 S	134 22.985 W	727	721
139	01	21-Feb-2010	03:33:00	74 5.991 S	135 3.197 W	432	429
147	01	26-Feb-2010	06:01:00	73 10.012 S	115 35.100 W	791	783
152	01	28-Feb-2010	18:51:00	74 46.825 S	101 30.982 W	636	633
155	01	01-Mar-2010	00:28:00	74 58.429 S	101 43.182 W	1043	1034
157	01	01-Mar-2010	03:29:00	75 4.216 S	102 14.588 W	628	625
165	01	02-Mar-2010	17:31:00	74 40.195 S	106 36.358 W	1182	1173
169	01	03-Mar-2010	08:01:00	74 20.006 S	106 0.035 W	1382	1368
171	01	03-Mar-2010	14:50:00	74 13.511 S	105 0.099 W	1369	1353
174	01	04-Mar-2010	01:26:00	73 57.937 S	105 30.210 W	684	681
176	01	04-Mar-2010	16:01:00	74 40.361 S	109 54.838 W	943	933
178	01	05-Mar-2010	09:32:00	74 5.515 S	106 44.840 W	601	599
180	01	05-Mar-2010	19:29:00	73 31.486 S	106 12.006 W	813	804
186	01	06-Mar-2010	05:46:00	73 20.116 S	106 0.485 W	676	669
189	01	08-Mar-2010	17:00:00	71 48.000 S	104 4.973 W	672	669
190	01	08-Mar-2010	21:08:00	71 52.748 S	103 23.431 W	757	749
191	01	09-Mar-2010	00:31:00	71 52.676 S	102 53.840 W	563	561
198	01	13-Mar-2010	21:22:00	71 50.066 S	104 50.336 W	590	585
200	01	14-Mar-2010	13:36:00	72 7.025 S	109 13.741 W	518	515
202	01	14-Mar-2010	17:26:00	72 2.882 S	107 59.981 W	588	585
205	01	14-Mar-2010	21:30:00	71 59.518 S	106 59.918 W	598	596
210	01	15-Mar-2010	03:07:00	71 53.768 S	105 37.165 W	493	491
217	01	17-Mar-2010	19:30:00	73 54.526 S	109 55.506 W	363	361
219	01	17-Mar-2010	23:01:00	73 40.013 S	108 59.883 W	442	439
220	01	18-Mar-2010	01:30:00	73 29.994 S	108 30.073 W	547	542
224	01	18-Mar-2010	23:00:00	73 25.077 S	106 50.038 W	909	902
227	01	19-Mar-2010	06:38:00	72 57.052 S	109 9.933 W	493	489
229	01	19-Mar-2010	11:21:00	72 50.011 S	107 20.016 W	656	649
231	01	19-Mar-2010	16:16:00	72 50.033 S	105 40.732 W	537	534
238	01	20-Mar-2010	17:11:00	72 11.963 S	110 0.160 W	490	488
239	01	20-Mar-2010	20:17:00	72 18.009 S	111 10.138 W	550	548
241	01	21-Mar-2010	00:24:00	72 23.941 S	112 10.050 W	489	485

11. MARINE MAMMALS AND SEABIRDS

Claude R. Joiris, Alejandro Cammareri
Laboratory for Polar Ecology (PoLE), Ramillies, Belgium

Objectives

Our main aim was to establish the quantitative at-sea distribution of marine mammals and seabirds in the poorly known Pacific sector of the Southern “Ocean”, particularly its western section, between NE Ross and NW Amundsen seas. The ecological interpretation being made as function of the main hydrological factors: water masses, recognized on the basis of water temperature and salinity, and ice coverage, with special attention to fronts and ice edge.

A more applied aspect concerns the possible effects of seismological studies (airgun explosions) on the presence and behaviour of marine mammals – mainly cetaceans (whales), but also swimming pinnipeds (seals). In parallel, our role as MMO's (Marine Mammals Observers) was to detect their presence close to the ship (less than 1 km for whales, 500 m for seals) and interrupt seismic activity for 1 hour or 15 min respectively (mitigation). This last part was supported by the presence of a team of voluntary observers during seismic activity, in order to be able to simultaneously survey both sides of the ship with 2 observers.

Work at sea

Continuous transect counts were realized from the bridge, *i.e.* when *Polarstern* was moving, visibility conditions allowing (interruptions at night, and in few cases for heavy fog/ snow showers). No width limitation was applied: if these data were to be expressed as densities, a species specific conversion factor should be applied, the detection limit depending on the jizz of each species, as defined and applied earlier in polar marine ecosystems by this team. Many of the birds, however, - especially the albatrosses - were obviously followers accompanying the ship or at least came to her by “curiosity”: such data should obviously not be calculated as densities. Each count lasted 30 min. Detection was essentially visual, binoculars (10 x 40, Zeiss; 8 x 40, Nikon) being used to complete and confirm identification at a longer range.

Preliminary results

A total of 1,500 counts were realized (as on March 29). Total numbers registered were very low, in comparison *e.g.* with the Weddell Sea: 215 cetaceans, 2,400 pinnipeds and 12,200 seabirds – ship observations only. Taking into account the different water masses we met, numbers in the actual sub-Antarctic and Antarctic domains were even much lower, the highest densities of seabirds being encountered in the sub-tropical water. See chapter 6, Oceanography, for more information about

hydrological structure, definition and position of the water masses and fronts, etc. Many counts were “empty”, *i.e.* without any contact in half an hour; in the vast majority, less than 5 contacts were registered.

Sub-tropical water

This zone was characterized by high concentrations of albatrosses: 140 wanderers (New Zealand and antipodean), 200 royal (N and S), and the locally abundant Salvin's (430). Similarly, locally abundant shearwater species were: 60 Buller's, 400 Hutton's and 480 short-tailed. Few marine mammals were encountered: 12 endemic Hector's dolphins and 4 common dolphins close to the coast (Christchurch), 7 individual New-Zealand fur seals drafting (*i.e.* resting at the surface) and 1 sea-lion at sea.

Antarctic domain

An obvious North-South gradient was observed, from the sub-tropical front (approximative position during the first, long N-S transect: 48°S), passing sub-Antarctic water to the sub-Antarctic front (56°S), entering the Antarctic domain at the Polar front (61°S), and recognizing the Ross gyre (64 to 72°S). The few data presented here concern this first transect, and the same structure in birds and mammal distribution was basically found back during the next N-S transects. The succession was, from N to S (seabirds, main species): Westland and white-chinned petrels (40 & 200), very local prions (70) and storm-petrels (270 white-faced, 7 grey-backed and 6 black-bellied), and further south: southern giant (30), soft-plumaged (225) and mottled petrels (28); then: Cape, Antarctic and snow petrels (160, 790 & 25) and finally, 44 Adélie penguins closer to the ice and small, low icebergs. Cetaceans encountered during the same transect were: 2 blue, 1 Antarctic minke, 7 fin whales and 17 humpbacks. Forty seals were counted, of which 35 crabeaters and 5 leopards.

During the rest of the expedition, bird numbers remained proportionally similar in the same water masses and fronts, with southern observations of light-mantled albatross (43) and emperor penguin (240 for a total of 1,810 Adélie penguins). South polar skuas (100) were observed in the vicinity of the small islands on which they breed.

Among the cetaceans, numbers of Antarctic minke whales increased eastward, especially in the eastern part of Pine Island Bay, to reach a total of 134. Their distribution was very patchy, with 10 to 15 days without any contact, followed by 1 or a few days with more small pods, apparently grouped into larger super-pods. The maximal size of pods was 10 to 20, and a group of 40. Numbers of fin and humpbacks (26 each), on the contrary, strongly decreased eastward. The same patchy structure was noted, *e.g.* with 9 fin whales in 3 pods during half-a-day, close to a front between water masses (change in water temperature and salinity). Two sperm whales were encountered. One pod of 4 orca's was noted close to the ice shelf, 3 others from helicopter. Worth noting is a pod of 12 very rare Arnoux's beaked whales, from the helicopter, eastern Pine Island Bay.

Among the pinnipeds, crabeaters were, as expected, by far the most numerous species (2300, for a total of 2400 seals). They were bound to small floes in drifted ice, and around small icebergs. A few concentrations of 100 and more on the ice were detected from ship and helicopter, while a huge concentration of 10.000 was seen twice from helicopter during 20 min of flight, *i.e.* covering 50 to 60 km, in the NW part of Pine Island Bay, at the northern limit of a huge ice field with medium sized pack ice floes. It seems that the extremely poor ice coverage in the bay was the cause of such a gathering. Few small groups were swimming far from any ice, often attracted by the ship. An extreme case was when tens of such groups came behind the ship from different directions during more than 10 hours (interruption of the observations due to obscurity!). The first ones arrived while seismic activity was running; they kept arriving for hours, with a "silent" streamer behind *Polarstern*. They did not stay long behind her, so that not more than 25 to 50 exemplars were following at any time, while the total number of arriving crabeaters was above 400 for the whole period.

The other species were 40 Weddell, 10 leopard and 3 rare Ross seals (plus 1 from helicopter); numbers of these 3 species are however probably underestimates, due to the difficulty of detecting them in groups of 100 crabeaters and more.

Complementary observations concern: age classes (crabeater, Adélie penguin, grey-headed albatross at the end of the expedition, giant petrel), with a critical discussion on what is described in the literature as juvenile plumage by birds, and moult by the birds (penguins, Antarctic petrel mainly).

Effects of seismic activity

Data deserve more detailed analysis and discussion: within a given zone, as defined here above, numbers and behaviour will be compared in function of the seismic activity. Special attention will be paid to the short N-S transect to the western bay (140°W), which was run twice, without and with seismic respectively.

A first general impression is now as follows:cetaceans: the majority (mainly minke whales) were apparently not influenced by the ship, with or without seismic activity, and kept swimming in the same direction – this must however be confirmed later by detailed analysis of the data. Most of them were surface feeding or slowly swimming, without many deep dives. On a few occasions, however, a minke whale coming closer to the ship during seismic suddenly changed its direction, made a 90-degree-turn and took distance from the ship.

Seals: swimming crabeaters were regularly attracted by *Polarstern*, without or with seismic activity – but never the ones hauled out on the ice. Here again, on 1 or 2 occasions, a few crabeaters were swimming toward the back of the ship with seismic, but then turned back to avoid her.

References

- Joiris CR. 1991. Spring distribution and ecological role of seabirds and marine mammals in the Weddell Sea, Antarctica. *Polar Biol.* **11**: 415-424.
- Joiris CR. 2000. Summer at-sea distribution of seabirds and marine mammals in polar ecosystems: a comparison between the European Arctic seas and the Weddell Sea, Antarctica. *J. Mar. Syst.* **27**: 267-276.

12. MAPS: MARINE MAMMAL PERIMETER SURVEILLANCE

Daniel P. Zitterbart, Olaf Boebel (not on board), Lars Kindermann (not on board)
Alfred-Wegener-Institut für Polar- und Meeresforschung, Bremerhaven

Objectives

The detection of marine mammals in the vicinity of ships to either collect data for cetacean research or for mitigation purposes during the operation of some hydroacoustic instruments is a strenuous, personnel- and time-intensive task. The MAPS projects aim at making maximum use of ship-whale encounters through systematic logging of opportunistic sightings by the ship's nautical officers (MAPS-vis) and by developing an automatic detections system based on thermal imaging (MAPS-IR).

Whales may be detected by infrared thermography on the basis of the thermal anomaly generated by a whale's blow, which strongly contrasts the cold Antarctic environment. To achieve this, a scanning, high-resolution thermal imaging system, FIRST-Navy, was installed on the ship's crow's nest prior to this expedition. This system, representing the state-of-the-art in infrared imaging, provides 360° thermal images at a 5Hz full frame refresh rate to computer monitors on the ship's bridge and in the operator's lab.

The primary purpose of our participation in this cruise was to test the sensor's endurance under polar environmental conditions during a seismic cruise and to improve and test various system software components which acquire, archive and analyze thermal images. In addition the efficiency of auto-detection algorithms were to be tested and improved by comparison with concurrent marine mammal observations conducted by the ship's nautical officers and additional marine mammal observers.

Work at sea

Early in the cruise, the FIRST thermal imager was operated for 21 days (437 h in total), starting with a maximum of 9 days of uninterrupted operation, (Tab. 12.1). Thereafter, sensor hardware problems repeatedly caused internally triggered shutdowns, resulting in reduced operation periods ranging from only minutes to days, while presenting increasing problems when trying to restart the system. Finally, attempts to uphold a continuous operation of the system were terminated and activities thereafter focused on error identification.

12. MAPS: Marine mammal perimeter surveillance

These efforts were conducted on the basis of instructions from the sensor producer, Rheinmetall Defense Electronics, which were exchanged via satellite communication. To access internal sensor parameters and be able to preheat the sensor, additional cabling was installed between the outside sensor and the crow's nest interior. To check for and remove moisture from inside the sensor head, the FIRST thermal imager was dismounted on 2010-03-02, dismantled, cleaned and reassembled in the lab before reinstalling the system 2010-03-09 in the crow's nest for further testing.

Tab. 12.1: Timetable showing the operation periods of the FIRST-navy. Start-ups which were preceded by a preheating phase are indicated by an asterix (*).

Start	End	Hours operational [hhh:mm:ss]
2010.01.31 02:00	2010.02.09 07:27	221:27
2010.02.09 07:27	2010.02.09 19:02	11:35
2010.02.12 20:44	2010.02.13 22:26	25:42
2010.02.13 22:26	2010.02.14 00:04	1:38
2010.02.14 00:04	2010.02.14 02:06	2:02
2010.02.14 02:06	2010.02.14 05:35	3:29
2010.02.14 05:35	2010.02.14 09:05	3:30
2010.02.14 09:05	2010.02.15 05:18	20:13
2010.02.15 05:18	2010.02.15 15:51	10:33
2010.02.15 15:51	2010.02.16 04:00	12:09
2010.02.16 04:00	2010.02.16 15:00	11:00
2010.02.16 15:00	2010.02.17 17:37	26:37
2010.02.17 20:00	2010.02.18 23:29	27:29
2010.02.18 02:50	2010.02.18 04:38	1:48
2010.02.19 21:40	2010.02.21 02:11	28:31
2010.02.21 02:16	2010.02.21 06:20	4:04
2010.02.21 18:46	2010.02.22 17:20	22:34
2010.02.22 17:20	2010.02.22 17:34	0:14
2010.02.22 17:52	2010.02.22 18:20	0:28
2010.02.22 18:20	2010.02.22 18:28	0:08
2010.02.22 18:28	2010.02.22 18:33	0:05
2010.03.01 18:37	2010.03.01 19:00	0:23
2010.03.02 21:18		FIRST dismounted
2010.03.09 15:37		FIRST remounted
2010.03.09 15:09	2010.03.09 16:01	0:52
2010.03.10 19:58	2010.03.10 20:18	0:20
2010.03.16 19:42	2010.03.16 19:48	0:06
		Σ 436:58

In parallel, the development, implementation and testing of software modules for pattern recognition and data management was performed throughout the cruise. Onboard development thereby is particularly important, as conclusive testing of the *real-time* system behavior can only be conducted aboard when using the actual hardware setup:

The pattern recognition software for automatic detection of whale blows was rewritten from scratch to meet the demanding *real-time* data processing requirements.

New filtering kernels for blow detection and new classification methods were tested, resulting in a first promising result of 19 of 20 known blows being detected by the algorithm.

The graphical user interface and visualization software was modified for use by marine mammal observers as possibility to observe the ship's perimeter while seismic profiling during the night. Unfortunately, after the first eight days, the FIRST did not run stable enough for operational use, which prevented its use in the mitigation context. The user interface provides semi-automatic features, like single-button start-up, auto-contrast leveling, optical notification in case of events, and manual event trigger possibilities.

The time span for retained images during events has been implemented to automatically vary with the ships speed.

The data management software was improved to allow hot-plug storage capacity expansions. This was necessary due to the FIRST Navy imager's high data rate, which leads to a necessary allocation of several 100 GB of storage space if sightings occur while the ship is on station (see previous item).

The data management system saves IR data whenever sightings are reported via the ship's Walog interface (used for systematic logging of opportunistic sightings by the ship's nautical officers) or via a customized web-interface (used by independent marine mammal observers). During the operation of FIRST-Navy, 19 ship-whale encounters occurred, which led to a total of 2.7 TB of data saved. This data was visually (i.e. via the fvi-browser's computer display) inspected for the occurrence of infrared signatures of whale blows (Fig. 12.1).

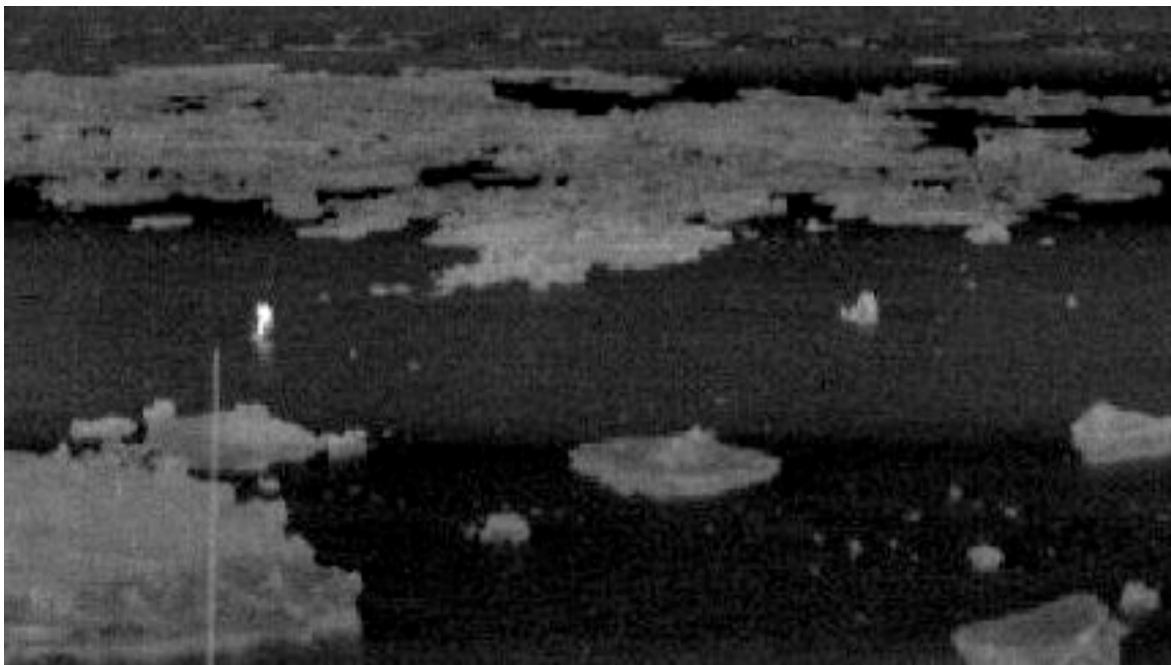


Fig. 12.1: Thermographic image of a minke whale spout (white) at about 320 m distance from the ship.
Dark grey to black areas represent open water, light grey depicts ice floes.

Abb. 12.1: Blas eines Zwerghals im thermographischen Bild, in ungefähr 320 m Entfernung zum Schiff. Das Meer ist in dunkelgrau bis schwarz dargestellt, Eisschollen erscheinen hellgrau.

Preliminary results

As noted above, the FIRST thermal imager had been running for 21 days before hardware problems forced its shutdown. The technical examinations performed at sea revealed, that:

- Internally, the sensor head contained moisture;
- debris was found on positioning unit of the sensor head;
- the motor software was disturbed by the debris on the sensor head;
- one ball bearing seems to be damaged, the cause of which remains unknown.

Monitoring of the system parameters during internally triggered shut-down events revealed a slow increase in sensor head temperature. The possible cause – or causes – for this behavior are yet unclear and further testing will be performed by Rheinmetall Defense Electronics once the sensor is returned to Germany. In contrast to a test system which is operated uninterrupted by RDE on their facilities for several months, our system was exposed to the marine environment for 4 months on *Polarstern's* cruise from Bremerhaven to Wellington (including a crossing of the equator). During this time, the system was subject to the (unquantified) ship's vibrations and sun, wind and humidity, yet protected by a tarpaulin.

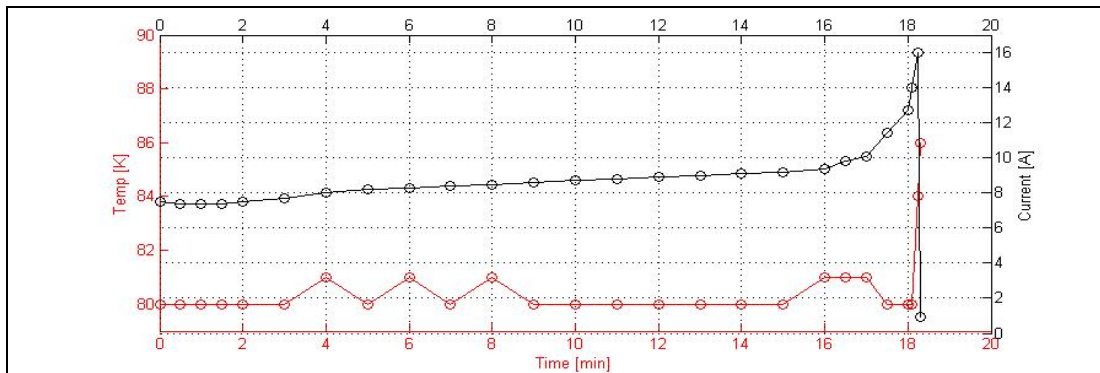


Fig. 12.2: Temporal evolution of sensor temperature and motor current. The time series begins with the system's startup and ends with the system's internally triggered shutdown.

Abb. 12.2: Zeitlicher Verlauf von Sensortemperatur und Motorstrom. Die Zeitserie endet mit der intern getriggerten Systemabschaltung.

Despite these problems, 2700 GB of high quality thermal imaging data were acquired and a total of 19 ship-whale encounters recorded.

Tab. 12.2: ship-whale encounter events (manually triggered)

Date	IR timestamp
2010-02-08	18:42:18
2010-02-08	22:13:32
2010-02-08	22:22:00
2010-02-13	01:34:05
2010-02-13	03:22:00
2010-02-13	13:20:00
2010-02-13	14:01:00
2010-02-14	02:11:00
2010-02-14	02:38:00
2010-02-14	02:58:00
2010-02-18	05:00:00
2010-02-19	22:25:00
2010-02-19	22:34:21
2010-02-19	23:40:00
2010-02-20	05:31:00
2010-02-21	05:50:00
2010-02-21	14:05:00
2010-02-22	00:47:00
2010-02-22	18:48:00

During each event, multiple detections of blows usually occur. These instances allow tracking of individual whales or spatially coherent pods (Fig. 12.3) relative to the ship,

and by using the ship's navigational data, the calculation of georeferenced blow positions.

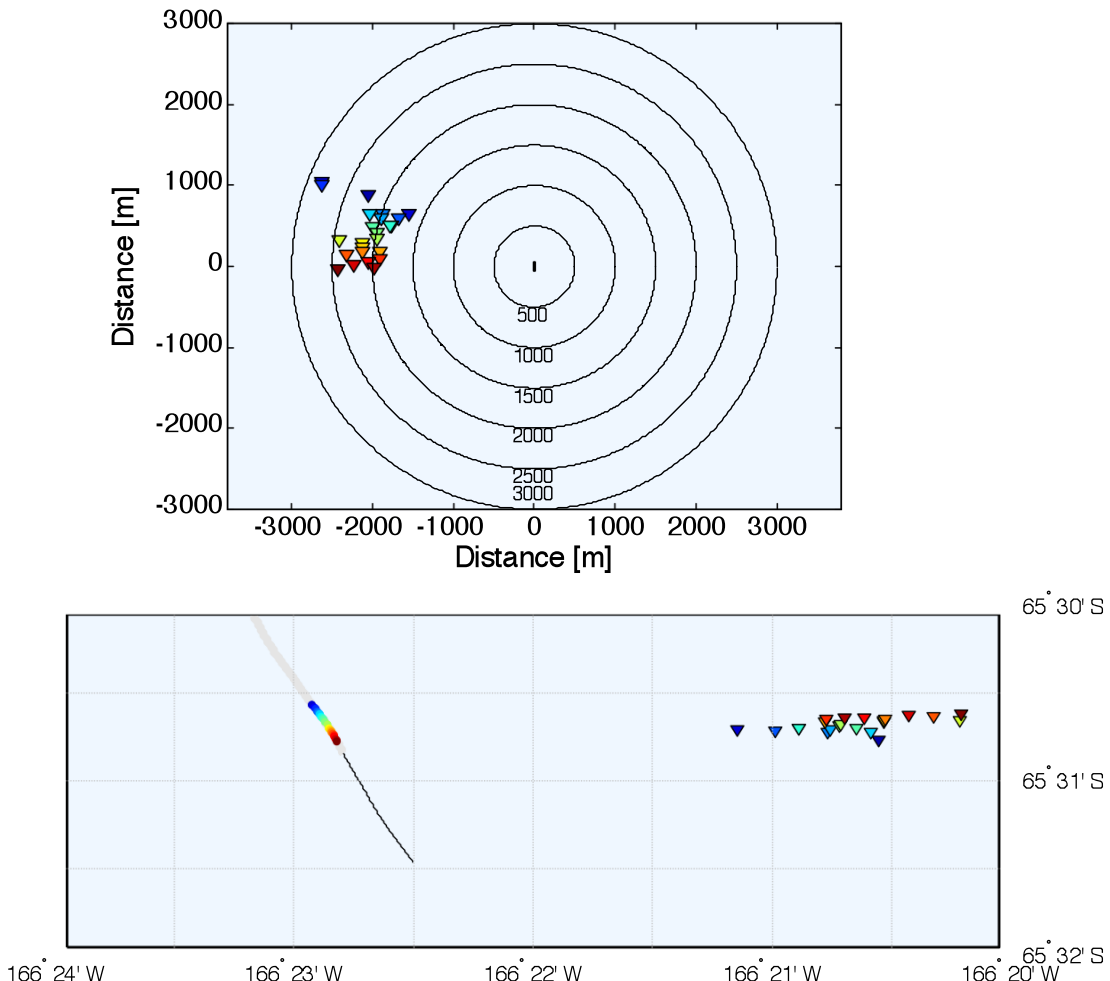


Fig. 12.3: Top: Locations of multiple blows (triangles) relative to ship (centre). The ship is outlined at scale. Bottom: Geo-referenced locations of multiple blows (triangles) and ship positions (dots) during a single ship-whale encounter. Matching color codes corresponding to detection time (blue to red).

Abb. 12.3: Oben: Positionen mehrere Walblase (Dreiecke) relativ zum Schiff (Zentrum). Die Schiffgröße entspricht dem Maßstab. Unten: Georeferenzierte Positionen mehrere Walblase (Dreiecke) des Schiffs (Punkte) während eines Sichtungseignisses. Korrespondierende Farben entsprechen gleichen Zeiten (Blau nach Rot).

The collected data is expected to help improving detection and classification algorithms, while the data acquisition and management software has now reached a state allowing an autonomous operation without a dedicated operator. Further automation requires pending hardware improvements (focus control, image counter, and system parameter output) to be implemented by the sensor manufacturer before the next expedition ANT-XXVII/2 (2010/11).

In addition to these MAPS-IR activities, the WALOG software, used by the nautical officers to log whale sightings for MAPS-vis, worked smoothly throughout the cruise. Only one bug had to be fixed: Using a Canon EOS 50D digital photo camera (150-500 mm lens) pictures are taken for species identification and documentation purposes by the ship's officers. The pictures are transferred automatically from the camera via WLAN to the WALOG software and logged therein. Some of these pictures, however, did not contain a proper EXIF date, causing the WALOG software to hang up. Once this bug had been corrected, no further problems occurred with the WALOG software.

APPENDIX

A.1 PARTICIPATING INSTITUTIONS

A.2 CRUISE PARTICIPANTS

A.3 SHIP'S CREW

A.4 STATION LIST

A.1 TEILNEHMENDE INSTITUTE / PARTICIPATING INSTITUTIONS

Address	
AWI	Stiftung Alfred-Wegener-Institut für Polar- und Meeresforschung in der Helmholtz-Gemeinschaft Postfach 120161 D-27515 Bremerhaven Germany
BAS	British Antarctic Survey High Cross, Madingley Road Cambridge, CB3 0ET UK
Brazil Navy	Brazilian Navy Directorate of Hydrography and Navigation Rua Baraō de Jaceguai, sem número Niterói, Rio de Janeiro Brazil
DWD	Deutscher Wetterdienst Geschäftsbereich Wettervorhersage Seeschifffahrtsberatung Bernhard-Nocht-Str. 76 D-20359 Hamburg Germany
GNS	GNS Science 1 Fairway Drive, Avalon Lower Hutt, 5010 New Zealand
HeliService	HeliService International GmbH Am Luneort 15 D-27572 Bremerhaven Germany
H&J Film	Hoferichter & Jacobs Film- und Fernsehproduktionsgesellschaft mbH Alte Schönhauser Str. 9 D-10119 Berlin Germany

Address

Marybio	Marybio Foundation Conaniyeu 475, dept 4 8521 Las Grutas, Rio Negro Argentina
NPI	Norwegian Polar Institute Polar Environmental Center N-9296 Tromsø Norway
Optimare	Optimare GmbH Am Luneort 15a D-27572 Bremerhaven Germany
PolE	Polar Ecology Rue du Fodia 18 B-1367 Ramillies-Offus Belgium
TU Dresden	Technische Universität Dresden Institut für Planetare Geodäsie D-01062 Dresden Germany
University of Bremen	Universität Bremen Fachbereich Geowissenschaften Klagenfurter Str. D-28359 Bremen Germany
University of Bristol	University of Bristol Dept. of Earth Sciences Wills Memorial Building Queen's Road Bristol, BS8 1RJ UK
University Tromsø	University of Tromsø Department of Geology N-9037 Tromsø Norway

A.2 FAHRTTEILNEHMER / CRUISE PARTICIPANTS

Name	Vorname/ First Name	Institut/ Institute	Beruf/	Profession
Baque	Daniel	AWI	Student, geology	
Brenner	Frank	AWI	Student, geophysics	
Brunnabend	Sandra-Esther	AWI	PhD student, oceanography	
Cammareri	Alejandro	PoLE & Marybio	Biologist	
Cychon	Christine	AWI	PhD student, biogeochem.	
Damm	Ellen	AWI	Biogeochemist	
Davy	Bryan	GNS	Geophysicist	
Denk	Astrid	AWI	Student, geophysics	
Eggers	Thorsten	Optimare	Technician, geophysics	
Forwick	Matthias	UNIVERSITY OF Tromsø	Geologist	
Gall	Fabian	HeliService	Technician, helicopter	
Gohl	Karsten	AWI	Geophysicist	
Gomes do Nascimento	Guilherme	Brazil Navy	Hydrographer	
Gossler	Jürgen	AWI	Geophysicist	
Gutjahr	Marcus	UNIVERSITY OF Bristol	Geologist	
Hammrich	Klaus	HeliService	Pilot, helicopter	
Heckmann	Hans-Hilmar	HeliService	Pilot, helicopter	
Heckmann	Markus	HeliService	Technician, helicopter	
Hillenbrand	Claus-Dieter	BAS	Geologist	
Jensen	Laura	AWI	Student, geodesy	
Jernas	Patrycja	NPI & UNIVERSITY OF Tromsø	PhD student, geology	
Joiris	Claude	PoLE	Biologist	
Kalberg	Thomas	AWI	PhD student, geophysics	
Kaul	Norbert	UNIVERSITY OF Bremen	Geophysicist	
Kilbert	Guido	H&J Film	Journalist	
Klages	Johann Philip	AWI	Student, geology	
Kuhn	Gerhard	AWI	Geologist	
Lensch	Norbert	AWI	Technician, geophysics	
Lichte	Ellen	AWI	Technician, biogeochemistry	
Lindeque	Ansa	AWI	PhD student, geophysics	
Lindow	Julia	University Bremen	PhD student, geology	
MacNab	Ian	BAS	Technician, geology	
Miller	Max	DWD	Meteorologist	
Müller	Eike	AWI	PhD student, geophysics	
Ott	Norbert	AWI	Geodesist	
Pimentel	Vitor	Brazil Navy	Hydrographer	

Name	Vorname/ First Name	Institut/ Institute	Beruf/	Profession
Reinshagen	Sarah	AWI	Student, geodesist	
Romsdorf	Martin	AWI	Student, geophysics	
Rosenau	Ralf	TU Dresden	PhD student, geodesy	
Scheinert	Mirko	TU Dresden	Geodesist	
Schröder	Michael	AWI	Oceanographer	
Sellmann	Lutz	AWI	Oceanographer	
Smith	James	BAS	Geologist	
Sonnabend	Hartmut	DWD	Technician, meteorology	
Spiegel	Cornelia	UNIVERSITY OF Bremen	Geologist	
Timmermann	Ralph	AWI	Oceanographer	
Voigtländer	Kai	H&J Film	Journalist	
Wiers	Steffen	AWI	Geologist	
Wisotzki	Andreas	AWI	Oceanographer	
Wobbe	Florian	AWI	PhD student, geophysics	
Wolf	Christian	AWI	Biologist	
Paranhos Zitterbart	Daniel	AWI	PhD student, physics	

A.3 SCHIFFSBESATZUNG / SHIP'S CREW

No.	Name	Rank
1.	Pahl, Uwe	Master
2.	Grundmann, Uwe	1. Offc.
3.	Ziemann, Olaf	Ch. Eng.
4.	Hering, Igor	2. Offc.
5.	Ritter, Michael	2. Offc.
6.	Janik, Michael	3. Offc.
7.	Meuschke, Felix	Doctor
8.	Koch, Georg	R. Offc.
9.	Kotnik, Herbert	2. Eng.
10.	Schnürch, Helmut	2. Eng.
11.	Westphal, Henning	2. Eng.
12.	Holtz, Hartmut	Elec. Eng.
13.	Dimmler, Werner	ELO
14.	Feiertag, Thomas	ELO
15.	Muhle, Helmut	ELO
16.	Nasis, Ilias	ELO
17.	Clasen, Burkhard	Boatsw.
18.	Neisner, Winfried	Carpenter
19.	Burzan, Gerd-Ekkehard	A.B.
20.	Hartwig-Labahn, Andreas	A.B.
21.	Kreis, Reinhard	A.B.
22.	Kretzschmar, Uwe	A.B.
23.	Moser, Siegfried	A.B.
24.	Sandmann, Rainer	A.B.
25.	Schmidt, Uwe	A.B.
26.	Schröder, Norbert	A.B.
27.	Schultz, Ottomar	A.B.
28.	Beth, Detlef	Storek.
29.	Dinse, Horst	Mot-man
30.	Fritz, Günter	Mot-man
31.	Kliem, Peter	Mot-man
32.	Krösche, Eckard	Mot-man
33.	Watzel, Bernhard	Mot-man
34.	Fischer, Matthias	Cook
35.	Tupy, Mario	Cooksmate
36.	Völske, Thomas	Cooksmate
37.	Dinse, Petra	1. Stwdess
38.	Hennig, Christina	Stwdess/Nurse
39.	Hischke, Peggy	2. Stwdess
40.	Hu, Guo Yong	2. Steward
41.	Streit, Christina	2. Stwdess
42.	Sun, Yong Sheng	2. Steward
43.	Wartenberg, Irina	2. Stwdess
44.	Ruan, Hui Guang	Laundrym.

A.4 STATIONSLISTE / STATION LIST PS 75/106-75/263

Station PS75/	Date	Time	Position Lat	Position Lon	Depth [m]	Gear	Action
106-1	31.01.10	04:16	43°31,57'S	173°20,43'E	22,8	Magnetic Turn Circle	profile Start
106-1	31.01.10	04:42	43°31,54'S	173°20,83'E	64,4	Magnetic Turn Circle	action
106-1	31.01.10	05:09	43°31,50'S	173°20,68'E	64,3	Magnetic Turn Circle	action
106-1	31.01.10	05:10	43°31,53'S	173°20,78'E	64,4	Magnetic Turn Circle	on ground/max depth
106-1	31.01.10	05:10	43°31,53'S	173°20,78'E	64,4	Magnetic Turn Circle	profile End
107-1	02.02.10	08:02	46°54,06'S	178°24,40'W	4506,0	Magnetic Turn Circle	profile Start
107-1	02.02.10	08:30	46°54,15'S	178°24,44'W	4501,0	Magnetic Turn Circle	action
107-1	02.02.10	09:10	46°55,70'S	178°24,39'W	4466,0	Magnetic Turn Circle	profile End
107-1	02.02.10	09:11	46°55,85'S	178°24,39'W	4466,0	Magnetic Turn Circle	on ground/ max depth
108-1	03.02.10	00:28	49°15,39'S	178°24,73'W	4591,0	Releaser Test	in the water
108-1	03.02.10	01:52	49°15,38'S	178°25,50'W	4602,0	Releaser Test	on ground/max depth
108-1	03.02.10	01:54	49°15,39'S	178°25,49'W	4603,0	Releaser Test	action
108-1	03.02.10	02:26	49°15,35'S	178°25,70'W	4586,2	Releaser Test	action
108-1	03.02.10	02:28	49°15,35'S	178°25,71'W	4586,9	Releaser Test	hoisting
108-1	03.02.10	03:29	49°15,18'S	178°25,78'W	4618,0	Releaser Test	on deck
109-1	05.02.10	20:20	56°52,36'S	174°39,00'W	5033,0	Seismic reflection profile	in the water
109-1	05.02.10	22:10	56°58,23'S	174°30,25'W	4915,0	Seismic reflection profile	profile Start
109-1	05.02.10	22:11	56°58,28'S	174°30,18'W	4911,0	Seismic reflection profile	profile End
109-1	05.02.10	22:12	56°58,33'S	174°30,10'W	4903,0	Seismic reflection profile	hoisting
109-1	05.02.10	23:25	57°1,40'S	174°25,53'W	4873,0	Seismic reflection profile	on deck
110-1	07.02.10	21:41	63°45,89'S	167°58,00'W	2546,0	Magnetic Turn Circle	profile Start
110-1	07.02.10	22:56	63°46,43'S	167°57,39'W	2535,0	Magnetic Turn Circle	on ground/max depth
110-1	07.02.10	22:57	63°46,53'S	167°57,28'W	2575,0	Magnetic Turn Circle	profile End
110-1	07.02.10	22:57	63°46,53'S	167°57,28'W	2575,0	Magnetic Turn Circle	on deck
111-1	08.02.10	07:05	65°4,27'S	166°32,31'W	2949,0	Seismic reflection profile	in the water
111-1	08.02.10	08:58	65°11,51'S	166°23,79'W	2978,0	Seismic reflection profile	in the water
111-1	08.02.10	09:09	65°12,37'S	166°23,04'W	2991,0	Seismic reflection profile	profile Start
111-1	08.02.10	11:42	65°24,67'S	166°9,30'W	3532,0	Seismic reflection profile	action
111-1	08.02.10	13:07	65°31,26'S	166°2,50'W	3201,0	Seismic reflection profile	action
111-1	08.02.10	15:32	65°21,25'S	165°55,21'W	2980,0	Seismic reflection profile	action

ANT-XXVI/3

Station PS75/	Date	Time	Position Lat	Position Lon	Depth [m]	Gear	Action
111-1	08.02.10	16:50	65°24,60'S	166°9,10'W	3542,0	Seismic reflection profile	action
111-1	08.02.10	17:55	65°27,13'S	166°20,80'W	3275,0	Seismic reflection profile	action
111-1	08.02.10	18:10	65°28,06'S	166°22,71'W	3128,0	Seismic reflection profile	profile End
111-1	08.02.10	18:51	65°31,33'S	166°22,72'W	3137,0	Seismic reflection profile	action
111-1	08.02.10	19:08	65°32,73'S	166°22,05'W	3206,0	Seismic reflection profile	action
111-1	08.02.10	20:26	65°36,25'S	166°20,15'W	3113,0	Seismic reflection profile	on deck
112-1	09.02.10	04:08	66°59,85'S	165°45,40'W	3680,0	Argos buoy	in the water
112-1	09.02.10	04:09	66°59,86'S	165°45,34'W	3677,0	Argos buoy	on ground/max depth
113-1	09.02.10	13:45	68°43,80'S	164°48,00'W	3877,0	Piston corer	in the water
113-1	09.02.10	15:08	68°43,82'S	164°48,17'W	3878,0	Piston corer	on ground/max depth
113-1	09.02.10	15:09	68°43,82'S	164°48,18'W	3876,0	Piston corer	hoisting
113-1	09.02.10	16:18	68°43,69'S	164°48,60'W	3879,0	Piston corer	at surface
113-1	09.02.10	16:30	68°43,62'S	164°48,71'W	3874,0	Piston corer	on deck
114-1	09.02.10	17:53	68°33,82'S	165°16,33'W	3746,0	Seismic reflection profile	in the water
114-1	09.02.10	19:03	68°37,14'S	165°6,95'W	3940,0	Seismic reflection profile	action
114-1	09.02.10	19:11	68°37,49'S	165°5,72'W	3944,0	Seismic reflection profile	action
114-1	09.02.10	19:19	68°37,90'S	165°4,41'W	3905,0	Seismic reflection profile	profile Start
114-1	09.02.10	20:46	68°43,27'S	164°49,59'W	3887,0	Seismic reflection profile	information
114-1	09.02.10	21:58	68°47,72'S	164°37,21'W	3689,0	Seismic reflection profile	profile End
114-1	09.02.10	23:42	68°40,47'S	164°36,80'W	3934,0	Seismic reflection profile	action
114-1	09.02.10	23:54	68°40,90'S	164°39,24'W	3954,0	Seismic reflection profile	profile Start
114-1	10.02.10	00:45	68°43,79'S	164°48,04'W	3871,0	Seismic reflection profile	information
114-1	10.02.10	01:27	68°46,08'S	164°55,11'W	4012,0	Seismic reflection profile	profile End
114-1	10.02.10	01:39	68°46,95'S	164°56,08'W	4159,0	Seismic reflection profile	profile Start
114-1	11.02.10	06:03	71°6,87'S	164°26,42'W	4216,0	Seismic reflection profile	action
114-1	11.02.10	06:53	71°10,81'S	164°26,65'W	4184,0	Seismic reflection profile	action
114-1	11.02.10	17:56	72°6,68'S	164°16,77'W	4219,0	Seismic reflection profile	action
114-1	11.02.10	18:27	72°9,19'S	164°14,78'W	4218,0	Seismic reflection profile	action

Station list PS 75

Station PS75/	Date	Time	Position Lat	Position Lon	Depth [m]	Gear	Action
114-1	11.02.10	18:37	72°10,00'S	164°13,96'W	4216,0	Seismic reflection profile	action
114-1	11.02.10	19:09	72°12,65'S	164°11,50'W	4215,0	Seismic reflection profile	action
114-1	11.02.10	19:49	72°15,89'S	164°7,32'W	4217,0	Seismic reflection profile	profile End
114-1	11.02.10	19:55	72°16,31'S	164°6,74'W	4210,0	Seismic reflection profile	hoisting
114-1	11.02.10	21:04	72°19,61'S	164°3,77'W	4209,0	Seismic reflection profile	on deck
115-1	11.02.10	22:36	72°13,66'S	164°10,56'W	4212,0	Seismic reflection profile	in the water
115-1	11.02.10	22:52	72°14,96'S	164°10,12'W	4212,0	Seismic reflection profile	in the water
115-1	11.02.10	22:54	72°15,12'S	164°10,10'W	4213,0	Seismic reflection profile	profile Start
115-1	12.02.10	03:00	72°35,52'S	164°4,59'W	4207,0	Seismic reflection profile	profile End
115-1	12.02.10	03:03	72°35,75'S	164°4,81'W	4203,0	Seismic reflection profile	action
115-1	12.02.10	03:04	72°35,83'S	164°4,88'W	4200,0	Seismic reflection profile	action
115-1	12.02.10	03:08	72°36,10'S	164°5,12'W	4203,0	Seismic reflection profile	hoisting
115-1	12.02.10	03:17	72°36,51'S	164°5,42'W	4199,0	Seismic reflection profile	on deck
116-1	12.02.10	03:27	72°36,61'S	164°5,31'W	4201,0	CTD/rosetteWaterSa mpler	in the water
116-1	12.02.10	04:50	72°36,60'S	164°6,00'W	4199,0	CTD/rosetteWaterSa mpler	on ground/max depth
117-1	12.02.10	06:12	72°36,39'S	164°5,93'W	4202,0	Seismic reflection profile	in the water
117-1	12.02.10	06:13	72°36,38'S	164°5,77'W	4198,0	Seismic reflection profile	lowering
117-1	12.02.10	06:32	72°36,40'S	164°0,38'W	4202,0	Seismic reflection profile	profile Start
117-1	12.02.10	15:59	72°23,97'S	161°35,12'W	4248,0	Seismic reflection profile	profile End
117-1	12.02.10	16:04	72°24,00'S	161°33,99'W	4250,0	Seismic reflection profile	action
117-1	12.02.10	16:09	72°24,05'S	161°33,04'W	4247,0	Seismic reflection profile	hoisting
117-1	12.02.10	16:17	72°24,14'S	161°31,84'W	4250,0	Seismic reflection profile	on deck
118-1	12.02.10	16:28	72°24,81'S	161°29,96'W	4249,0	Magnetic Turn Circle	profile Start
118-1	12.02.10	16:59	72°25,09'S	161°29,85'W	4249,0	Magnetic Turn Circle	action
118-1	12.02.10	17:30	72°25,33'S	161°29,93'W	4252,0	Magnetic Turn Circle	profile End
118-1	12.02.10	17:30	72°25,33'S	161°29,93'W	4252,0	Magnetic Turn Circle	on ground/max depth
119-1	12.02.10	18:25	72°25,88'S	161°49,10'W	4248,0	Seismic reflection profile	in the water

ANT-XXVI/3

Station PS75/	Date	Time	Position Lat	Position Lon	Depth [m]	Gear	Action
119-1	12.02.10	19:38	72°24,22'S	161°28,23'W	4252,0	Seismic reflection profile	action
119-1	12.02.10	19:39	72°24,20'S	161°27,95'W	4253,0	Seismic reflection profile	action
119-1	12.02.10	19:41	72°24,17'S	161°27,39'W	4251,0	Seismic reflection profile	profile Start
119-1	12.02.10	21:40	72°22,10'S	160°52,30'W	4256,0	Seismic reflection profile	action
119-1	12.02.10	22:16	72°21,24'S	160°42,25'W	4249,0	Seismic reflection profile	action
119-1	13.02.10	01:30	72°17,74'S	159°48,24'W	4266,0	Seismic reflection profile	action
119-1	13.02.10	02:16	72°16,76'S	159°35,35'W	4280,0	Seismic reflection profile	action
119-1	13.02.10	03:03	72°16,08'S	159°22,19'W	4294,0	Seismic reflection profile	action
119-1	13.02.10	03:23	72°15,80'S	159°16,82'W	4304,0	Seismic reflection profile	action
119-1	13.02.10	03:55	72°15,41'S	159°7,56'W	4308,0	Seismic reflection profile	action
119-1	13.02.10	14:01	72°9,95'S	156°15,32'W	4357,0	Seismic reflection profile	action
119-1	13.02.10	14:35	72°9,90'S	156°5,82'W	4358,0	Seismic reflection profile	action
119-1	14.02.10	02:57	72°15,01'S	152°31,57'W	4185,0	Seismic reflection profile	action
119-1	14.02.10	03:28	72°15,31'S	152°22,58'W	4178,0	Seismic reflection profile	action
119-1	14.02.10	12:08	72°28,27'S	150°0,76'W	4199,0	Seismic reflection profile	action
120-1	14.02.10	12:10	72°28,30'S	150°0,24'W	4197,0	Argos buoy	in the water
120-1	14.02.10	12:11	72°28,30'S	150°0,06'W	4201,0	Argos buoy	on ground/max depth
119-1	14.02.10	12:13	72°28,32'S	149°59,61'W	4198,0	Seismic reflection profile	action
119-1	15.02.10	05:30	72°34,96'S	145°0,83'W	4197,0	Seismic reflection profile	action
122-1	15.02.10	05:30	72°34,96'S	145°0,83'W	4197,0	Argos buoy	in the water
119-1	15.02.10	05:32	72°34,93'S	145°0,25'W	4196,0	Seismic reflection profile	action
122-1	15.02.10	05:32	72°34,93'S	145°0,25'W	4196,0	Argos buoy	on ground/max depth
119-1	15.02.10	22:38	72°24,82'S	140°0,39'W	4212,0	Seismic reflection profile	action
123-1	15.02.10	22:40	72°24,80'S	139°59,85'W	4213,0	Argos buoy	in the water
123-1	15.02.10	22:40	72°24,80'S	139°59,85'W	4213,0	Argos buoy	on ground/max depth
119-1	15.02.10	22:42	72°24,78'S	139°59,38'W	4210,0	Seismic reflection profile	action
119-1	16.02.10	13:08	72°5,25'S	135°55,41'W	4149,0	Seismic reflection	action

Station list PS 75

Station PS75/	Date	Time	Position Lat	Position Lon	Depth [m]	Gear	Action
						profile	
119-1	16.02.10	16:10	72°6,42'S	136°11,06'W	4143,0	Seismic reflection profile	action
119-1	16.02.10	19:53	72°26,52'S	136°3,96'W	4007,0	Seismic reflection profile	action
119-1	16.02.10	20:31	72°29,94'S	136°3,12'W	3740,0	Seismic reflection profile	action
119-1	17.02.10	00:35	72°51,51'S	136°0,62'W	3735,0	Seismic reflection profile	action
119-1	17.02.10	01:05	72°54,15'S	135°59,56'W	3714,0	Seismic reflection profile	action
119-1	17.02.10	02:14	73°0,27'S	135°56,76'W	3620,0	Seismic reflection profile	action
119-1	17.02.10	02:47	73°3,20'S	135°55,12'W	3619,0	Seismic reflection profile	action
119-1	17.02.10	03:45	73°8,35'S	135°53,57'W	3568,0	Seismic reflection profile	action
119-1	17.02.10	04:15	73°10,82'S	135°53,51'W	3511,0	Seismic reflection profile	action
119-1	17.02.10	05:29	73°17,33'S	135°52,41'W	3453,0	Seismic reflection profile	profile End
119-1	17.02.10	05:30	73°17,41'S	135°52,38'W	3453,0	Seismic reflection profile	action
119-1	17.02.10	05:32	73°17,57'S	135°52,35'W	3458,0	Seismic reflection profile	hoisting
119-1	17.02.10	06:39	73°21,03'S	135°51,87'W	3356,0	Seismic reflection profile	on deck
124-1	17.02.10	07:15	73°18,01'S	135°51,39'W	3435,0	Seismic reflection profile	in the water
124-1	17.02.10	07:43	73°18,94'S	135°52,36'W	3447,0	Seismic reflection profile	action
124-1	17.02.10	07:44	73°19,03'S	135°52,35'W	3447,0	Seismic reflection profile	profile Start
124-1	17.02.10	16:37	74°2,14'S	135°13,80'W	426,9	Seismic reflection profile	action
124-1	17.02.10	17:10	74°4,53'S	135°9,36'W	434,8	Seismic reflection profile	action
124-1	17.02.10	20:40	74°19,34'S	134°42,65'W	675,2	Seismic reflection profile	action
124-1	17.02.10	21:17	74°20,34'S	134°33,98'W	705,4	Seismic reflection profile	action
124-1	18.02.10	00:11	74°28,74'S	134°0,20'W	795,6	Seismic reflection profile	profile End
124-1	18.02.10	00:24	74°28,88'S	133°57,69'W	869,1	Seismic reflection profile	action
124-1	18.02.10	00:30	74°28,94'S	133°56,77'W	879,0	Seismic reflection profile	on deck
125-1	18.02.10	00:56	74°28,67'S	133°50,51'W	1023,0	CTD/rosetteWaterSampler	in the water
125-1	18.02.10	01:22	74°28,64'S	133°51,47'W	972,5	CTD/rosetteWaterSampler	on ground/max depth
125-1	18.02.10	01:44	74°28,64'S	133°52,27'W	962,2	CTD/rosetteWaterSampler	on deck

ANT-XXVI/3

Station PS75/	Date	Time	Position Lat	Position Lon	Depth [m]	Gear	Action
						sampler	
126-1	18.02.10	01:58	74°28,50'S	133°50,05'W	1023,0	HydroSweep/ParaSound profile	profile Start
126-1	18.02.10	03:23	74°25,96'S	133°8,86'W	496,7	HydroSweep/ParaSound profile	action
126-2	18.02.10	03:25	74°25,96'S	133°8,92'W	496,7	CTD/rosetteWaterSampler	in the water
126-2	18.02.10	03:43	74°25,96'S	133°9,15'W	480,8	CTD/rosetteWaterSampler	on ground/max depth
126-2	18.02.10	03:45	74°25,96'S	133°9,15'W	481,8	CTD/rosetteWaterSampler	hoisting
126-2	18.02.10	04:00	74°25,96'S	133°9,30'W	478,0	CTD/rosetteWaterSampler	on deck
126-1	18.02.10	04:01	74°25,96'S	133°9,33'W	478,5	HydroSweep/ParaSound profile	action
126-1	18.02.10	06:44	74°31,02'S	134°23,17'W	502,9	HydroSweep/ParaSound profile	action
127-1	18.02.10	06:47	74°31,04'S	134°22,99'W	538,1	CTD/rosetteWaterSampler	in the water
127-1	18.02.10	07:03	74°31,01'S	134°23,22'W	497,7	CTD/rosetteWaterSampler	on ground/max depth
127-1	18.02.10	07:13	74°31,01'S	134°23,18'W	498,6	CTD/rosetteWaterSampler	hoisting
127-1	18.02.10	07:17	74°31,01'S	134°23,14'W	497,0	CTD/rosetteWaterSampler	at surface
127-1	18.02.10	07:19	74°31,01'S	134°23,13'W	497,4	CTD/rosetteWaterSampler	on deck
126-1	18.02.10	07:23	74°31,01'S	134°23,10'W	497,6	HydroSweep/ParaSound profile	action
126-1	18.02.10	13:16	74°29,45'S	134°23,98'W	439,4	HydroSweep/ParaSound profile	action
126-1	18.02.10	13:49	74°27,46'S	134°12,44'W	665,2	HydroSweep/ParaSound profile	action
126-1	18.02.10	14:20	74°28,14'S	134°28,86'W	597,3	HydroSweep/ParaSound profile	action
126-1	18.02.10	17:42	74°22,29'S	133°21,11'W	490,9	HydroSweep/ParaSound profile	action
126-1	18.02.10	18:36	74°21,82'S	133°50,04'W	697,2	HydroSweep/ParaSound profile	profile End
128-1	18.02.10	20:02	74°28,74'S	133°58,75'W	853,7	Gravity corer	in the water
128-1	18.02.10	20:25	74°28,93'S	133°58,23'W	885,7	Gravity corer	lowering
128-1	18.02.10	20:37	74°28,98'S	133°58,04'W	895,2	Gravity corer	on ground/max depth
128-1	18.02.10	20:38	74°28,99'S	133°57,99'W	897,7	Gravity corer	hoisting
128-1	18.02.10	20:50	74°29,10'S	133°58,62'W	937,2	Gravity corer	at surface
128-1	18.02.10	20:51	74°29,10'S	133°58,72'W	938,2	Gravity corer	on deck
129-1	18.02.10	22:27	74°30,55'S	134°7,04'W	921,7	Gravity corer	in the water
129-1	18.02.10	22:40	74°30,54'S	134°7,25'W	923,0	Gravity corer	on ground/max depth

Station list PS 75

Station PS75/	Date	Time	Position Lat	Position Lon	Depth [m]	Gear	Action
129-1	18.02.10	22:55	74°30,52'S	134°7,48'W	924,0	Gravity corer	at surface
129-1	18.02.10	22:59	74°30,50'S	134°7,54'W	925,5	Gravity corer	on deck
129-2	18.02.10	23:12	74°30,52'S	134°7,23'W	923,8	Heat Flow	in the water
129-2	18.02.10	23:30	74°30,52'S	134°7,36'W	923,5	Heat Flow	on ground/max depth
129-2	18.02.10	23:40	74°30,52'S	134°7,37'W	924,5	Heat Flow	hoisting
129-2	18.02.10	23:56	74°30,47'S	134°7,72'W	925,5	Heat Flow	at surface
129-2	18.02.10	23:58	74°30,47'S	134°7,74'W	924,0	Heat Flow	on deck
130-1	19.02.10	01:02	74°26,72'S	134°9,23'W	791,9	Gravity corer	in the water
130-1	19.02.10	01:20	74°26,71'S	134°9,17'W	794,3	Gravity corer	on ground/max depth
130-1	19.02.10	01:35	74°26,72'S	134°9,20'W	793,4	Gravity corer	on deck
130-2	19.02.10	02:01	74°26,72'S	134°8,98'W	795,3	Box corer	in the water
130-2	19.02.10	02:15	74°26,73'S	134°9,16'W	793,4	Box corer	on ground/max depth
130-2	19.02.10	02:29	74°26,75'S	134°9,16'W	790,7	Box corer	on deck
131-1	19.02.10	03:21	74°27,71'S	134°10,07'W	664,7	HydroSweep/ParaSound profile	profile Start
131-1	19.02.10	18:40	74°20,21'S	134°30,33'W	699,0	HydroSweep/ParaSound profile	profile End
131-1	19.02.10	18:41	74°20,19'S	134°30,05'W	699,3	HydroSweep/ParaSound profile	on deck
132-1	19.02.10	19:17	74°22,08'S	134°22,86'W	750,1	Large Box Corer	in the water
132-1	19.02.10	19:19	74°22,05'S	134°22,91'W	750,1	Large Box Corer	lowering
132-1	19.02.10	19:30	74°22,00'S	134°23,17'W	750,3	Large Box Corer	on ground/max depth
132-1	19.02.10	19:31	74°22,00'S	134°23,18'W	749,7	Large Box Corer	hoisting
132-1	19.02.10	19:41	74°21,97'S	134°23,29'W	750,0	Large Box Corer	at surface
132-2	19.02.10	19:43	74°21,99'S	134°23,29'W	749,5	Geothermic corer	in the water
132-1	19.02.10	19:44	74°21,99'S	134°23,29'W	749,5	Large Box Corer	on deck
132-2	19.02.10	20:04	74°22,03'S	134°22,95'W	750,4	Geothermic corer	lowering
132-2	19.02.10	20:18	74°21,99'S	134°23,22'W	749,7	Geothermic corer	on ground/max depth
132-2	19.02.10	20:28	74°21,97'S	134°23,27'W	749,5	Geothermic corer	off ground
132-2	19.02.10	20:29	74°21,97'S	134°23,29'W	749,4	Geothermic corer	hoisting
132-2	19.02.10	20:39	74°21,90'S	134°23,37'W	749,8	Geothermic corer	at surface
132-2	19.02.10	20:40	74°21,90'S	134°23,40'W	750,3	Geothermic corer	on deck
132-3	19.02.10	20:57	74°21,98'S	134°22,97'W	750,8	Gravity corer	in the water
132-3	19.02.10	21:08	74°21,97'S	134°23,16'W	750,3	Gravity corer	on ground/max depth
132-3	19.02.10	21:20	74°21,96'S	134°23,55'W	749,4	Gravity corer	at surface
132-3	19.02.10	21:23	74°21,96'S	134°23,66'W	748,8	Gravity corer	on deck
133-1	20.02.10	01:27	74°20,64'S	133°4,46'W	472,5	Large Box Corer	in the water
133-1	20.02.10	01:34	74°20,65'S	133°4,68'W	473,7	Large Box Corer	on ground/max depth
133-1	20.02.10	01:43	74°20,68'S	133°4,63'W	471,2	Large Box Corer	on deck

ANT-XXVI/3

Station PS75/	Date	Time	Position Lat	Position Lon	Depth [m]	Gear	Action
134-1	20.02.10	06:44	74°25,15'S	134°12,78'W	650,4	Gravity corer	in the water
134-1	20.02.10	06:47	74°25,16'S	134°12,86'W	652,1	Gravity corer	lowering
134-1	20.02.10	06:57	74°25,17'S	134°12,99'W	653,7	Gravity corer	on ground/max depth
134-1	20.02.10	06:58	74°25,17'S	134°12,97'W	654,0	Gravity corer	hoisting
134-1	20.02.10	07:07	74°25,16'S	134°12,90'W	653,4	Gravity corer	at surface
134-1	20.02.10	07:10	74°25,16'S	134°13,06'W	676,8	Gravity corer	on deck
135-1	20.02.10	08:00	74°27,81'S	134°3,85'W	779,4	Seismic reflection profile	in the water
135-1	20.02.10	08:04	74°27,85'S	134°3,55'W	777,5	Seismic reflection profile	lowering
135-1	20.02.10	08:20	74°28,03'S	134°0,18'W	795,0	Seismic reflection profile	in the water
135-1	20.02.10	08:25	74°28,14'S	133°59,07'W	825,0	Seismic reflection profile	information
135-1	20.02.10	08:50	74°26,29'S	134°0,18'W	786,5	Seismic reflection profile	profile Start
135-1	20.02.10	10:44	74°18,97'S	134°24,10'W	691,3	Seismic reflection profile	profile End
135-1	20.02.10	11:37	74°18,98'S	134°24,12'W	691,1	Seismic reflection profile	action
135-1	20.02.10	12:52	74°19,00'S	134°11,26'W	652,5	Seismic reflection profile	profile Start
135-1	20.02.10	14:36	74°23,61'S	134°38,31'W	749,1	Seismic reflection profile	profile End
135-1	20.02.10	14:46	74°24,07'S	134°39,98'W	727,0	Seismic reflection profile	action
135-1	20.02.10	14:48	74°24,12'S	134°40,37'W	725,0	Seismic reflection profile	hoisting
135-1	20.02.10	14:56	74°24,33'S	134°41,89'W	676,4	Seismic reflection profile	on deck
135-1	20.02.10	15:00	74°24,44'S	134°42,66'W	680,8	Seismic reflection profile	on deck
136-1	20.02.10	15:43	74°23,01'S	134°35,30'W	751,6	Releaser Test	in the water
136-1	20.02.10	15:45	74°22,99'S	134°35,40'W	750,9	Releaser Test	action
136-1	20.02.10	16:00	74°22,92'S	134°35,29'W	752,7	Releaser Test	on ground/max depth
136-1	20.02.10	16:17	74°22,87'S	134°35,48'W	750,1	Releaser Test	hoisting
136-1	20.02.10	16:28	74°22,86'S	134°35,47'W	749,8	Releaser Test	at surface
136-1	20.02.10	16:29	74°22,86'S	134°35,48'W	749,7	Releaser Test	on deck
136-2	20.02.10	16:44	74°23,00'S	134°35,63'W	752,6	CTD/rosette Water Sampler	in the water
136-2	20.02.10	16:44	74°23,00'S	134°35,63'W	752,6	CTD/rosette Water Sampler	lowering
136-2	20.02.10	17:05	74°22,96'S	134°35,87'W	751,7	CTD/rosette Water Sampler	on ground/max depth
136-2	20.02.10	17:06	74°22,96'S	134°35,88'W	750,9	CTD/rosette Water Sampler	hoisting
136-2	20.02.10	17:26	74°22,96'S	134°35,78'W	751,9	CTD/rosette Water Sampler	at surface

Station list PS 75

Station PS75/	Date	Time	Position Lat	Position Lon	Depth [m]	Gear	Action
136-2	20.02.10	17:28	74°22,96'S	134°35,74'W	752,3	CTD/rosetteWaterSa mpler	on deck
136-3	20.02.10	17:47	74°23,14'S	134°35,59'W	753,3	Gravity corer	in the water
136-3	20.02.10	17:50	74°23,15'S	134°35,53'W	752,6	Gravity corer	lowering
136-3	20.02.10	18:00	74°23,15'S	134°35,59'W	752,1	Gravity corer	on ground/max depth
136-3	20.02.10	18:02	74°23,15'S	134°35,61'W	752,1	Gravity corer	hoisting
136-3	20.02.10	18:13	74°23,14'S	134°35,79'W	754,0	Gravity corer	at surface
136-3	20.02.10	18:19	74°23,16'S	134°35,86'W	754,8	Gravity corer	on deck
136-4	20.02.10	18:31	74°23,24'S	134°36,02'W	754,3	Geothermic corer	in the water
136-4	20.02.10	18:33	74°23,24'S	134°36,04'W	753,7	Geothermic corer	lowering
136-4	20.02.10	18:45	74°23,24'S	134°36,10'W	753,2	Geothermic corer	on ground/max depth
136-4	20.02.10	18:56	74°23,24'S	134°36,12'W	753,4	Geothermic corer	hoisting
136-4	20.02.10	18:58	74°23,23'S	134°36,13'W	752,8	Geothermic corer	off ground
136-4	20.02.10	19:09	74°23,19'S	134°36,17'W	752,6	Geothermic corer	at surface
136-4	20.02.10	19:11	74°23,17'S	134°36,20'W	752,7	Geothermic corer	on deck
137-1	20.02.10	19:55	74°22,05'S	134°22,99'W	750,1	CTD/rosetteWaterSa mpler	in the water
137-1	20.02.10	19:56	74°22,04'S	134°22,99'W	752,0	CTD/rosetteWaterSa mpler	lowering
137-1	20.02.10	20:16	74°22,01'S	134°23,16'W	749,8	CTD/rosetteWaterSa mpler	on ground/max depth
137-1	20.02.10	20:29	74°22,04'S	134°23,26'W	749,8	CTD/rosetteWaterSa mpler	at surface
137-1	20.02.10	20:30	74°22,04'S	134°23,27'W	750,4	CTD/rosetteWaterSa mpler	on deck
138-1	20.02.10	21:10	74°20,30'S	134°33,36'W	703,0	Gravity corer	in the water
138-1	20.02.10	21:22	74°20,30'S	134°33,42'W	702,5	Gravity corer	on ground/max depth
138-1	20.02.10	21:40	74°20,30'S	134°33,31'W	703,0	Gravity corer	on deck
139-1	21.02.10	03:32	74°5,99'S	135°3,25'W	448,5	CTD/rosetteWaterSa mpler	in the water
139-1	21.02.10	03:46	74°6,00'S	135°3,16'W	449,6	CTD/rosetteWaterSa mpler	on ground/max depth
139-1	21.02.10	04:00	74°6,00'S	135°3,21'W	449,6	CTD/rosetteWaterSa mpler	at surface
139-1	21.02.10	04:02	74°6,01'S	135°3,23'W	449,0	CTD/rosetteWaterSa mpler	on deck
139-2	21.02.10	04:09	74°6,02'S	135°3,30'W	449,6	Gravity corer	in the water
139-2	21.02.10	04:10	74°6,02'S	135°3,31'W	449,3	Gravity corer	lowering
139-2	21.02.10	04:16	74°6,01'S	135°3,31'W	448,7	Gravity corer	on ground/max depth
139-2	21.02.10	04:17	74°6,01'S	135°3,31'W	448,2	Gravity corer	hoisting
139-2	21.02.10	04:26	74°6,02'S	135°3,34'W	448,4	Gravity corer	at surface
139-2	21.02.10	04:26	74°6,02'S	135°3,34'W	448,4	Gravity corer	on deck
139-3	21.02.10	04:37	74°6,00'S	135°3,16'W	449,3	Geothermic corer	in the water

ANT-XXVI/3

Station PS75/	Date	Time	Position Lat	Position Lon	Depth [m]	Gear	Action
139-3	21.02.10	04:38	74°6,00'S	135°3,15'W	449,2	Geothermic corer	lowering
139-3	21.02.10	04:45	74°6,02'S	135°3,11'W	449,2	Geothermic corer	on ground/max depth
139-3	21.02.10	04:55	74°6,05'S	135°3,24'W	449,2	Geothermic corer	hoisting
139-3	21.02.10	04:55	74°6,05'S	135°3,24'W	449,2	Geothermic corer	off ground
139-3	21.02.10	05:05	74°6,10'S	135°3,41'W	451,9	Geothermic corer	at surface
139-3	21.02.10	05:05	74°6,10'S	135°3,41'W	451,9	Geothermic corer	on deck
140-1	21.02.10	05:17	74°5,97'S	135°2,85'W	450,6	HydroSweep/ParaSo und profile	profile Start
140-1	21.02.10	07:48	73°54,43'S	134°36,01'W	452,9	HydroSweep/ParaSo und profile	alter course
140-1	21.02.10	16:45	73°44,81'S	135°4,86'W	1299,0	HydroSweep/ParaSo und profile	profile End
141-1	21.02.10	16:49	73°44,80'S	135°4,91'W	1311,0	CTD/rosetteWaterSa mpler	in the water
140-1	21.02.10	16:49	73°44,80'S	135°4,91'W	1311,0	HydroSweep/ParaSo und profile	on deck
141-1	21.02.10	16:50	73°44,80'S	135°4,91'W	1308,0	CTD/rosetteWaterSa mpler	lowering
141-1	21.02.10	17:19	73°44,91'S	135°4,81'W	1233,0	CTD/rosetteWaterSa mpler	on ground/max depth
141-1	21.02.10	17:20	73°44,91'S	135°4,81'W	1232,0	CTD/rosetteWaterSa mpler	hoisting
141-1	21.02.10	17:38	73°44,90'S	135°4,50'W	1211,0	CTD/rosetteWaterSa mpler	at surface
141-1	21.02.10	17:39	73°44,90'S	135°4,52'W	1208,0	CTD/rosetteWaterSa mpler	on deck
142-1	21.02.10	17:42	73°44,91'S	135°4,49'W	1204,0	HydroSweep/ParaSo und profile	profile Start
142-1	21.02.10	21:14	73°29,01'S	136°3,87'W	3278,0	HydroSweep/ParaSo und profile	alter course
142-1	22.02.10	02:20	72°45,00'S	136°16,00'W	3840,0	HydroSweep/ParaSo und profile	alter course
142-1	22.02.10	02:48	72°44,10'S	136°2,13'W	3812,0	HydroSweep/ParaSo und profile	profile End
143-1	22.02.10	02:51	72°44,04'S	136°2,13'W	3812,0	CTD/rosetteWaterSa mpler	in the water
143-1	22.02.10	02:52	72°44,04'S	136°2,13'W	3813,0	CTD/rosetteWaterSa mpler	lowering
143-1	22.02.10	04:06	72°44,02'S	136°2,34'W	3811,0	CTD/rosetteWaterSa mpler	on ground/max depth
143-1	22.02.10	04:07	72°44,02'S	136°2,35'W	3814,0	CTD/rosetteWaterSa mpler	hoisting
143-1	22.02.10	05:08	72°44,00'S	136°2,16'W	3814,0	CTD/rosetteWaterSa mpler	at surface
143-1	22.02.10	05:09	72°44,01'S	136°2,15'W	3815,0	CTD/rosetteWaterSa mpler	on deck
143-2	22.02.10	05:18	72°44,01'S	136°2,00'W	3811,0	Piston corer	in the water
143-2	22.02.10	05:28	72°44,05'S	136°2,08'W	3812,0	Piston corer	lowering
143-2	22.02.10	06:37	72°44,01'S	136°1,99'W	3812,0	Piston corer	on

Station list PS 75

Station PS75/	Date	Time	Position Lat	Position Lon	Depth [m]	Gear	Action
							ground/max depth
143-2	22.02.10	06:37	72°44,01'S	136°1,99'W	3812,0	Piston corer	hoisting
143-2	22.02.10	06:39	72°44,03'S	136°1,99'W	3813,0	Piston corer	off ground
143-2	22.02.10	07:35	72°44,03'S	136°2,01'W	3811,0	Piston corer	at surface
143-2	22.02.10	07:53	72°43,98'S	136°2,03'W	3811,0	Piston corer	on deck
143-3	22.02.10	08:16	72°44,05'S	136°2,06'W	3811,0	Multi corer	in the water
143-3	22.02.10	09:07	72°44,02'S	136°2,15'W	3814,0	Multi corer	on ground/max depth
143-3	22.02.10	09:09	72°44,02'S	136°2,17'W	3814,0	Multi corer	off ground
143-3	22.02.10	09:59	72°44,01'S	136°2,35'W	3811,0	Multi corer	at surface
143-3	22.02.10	10:02	72°44,00'S	136°2,37'W	3815,0	Multi corer	on deck
144-1	22.02.10	13:33	72°18,32'S	136°16,86'W	4076,0	Magnetic Turn Circle	profile Start
144-1	22.02.10	14:00	72°18,29'S	136°16,77'W	4076,0	Magnetic Turn Circle	action
144-1	22.02.10	14:29	72°17,93'S	136°17,08'W	4079,0	Magnetic Turn Circle	profile End
144-1	22.02.10	15:21	72°9,98'S	136°16,25'W	3920,0	Magnetic Turn Circle	on ground/max depth
145-1	22.02.10	15:36	72°8,01'S	136°15,31'W	4150,0	Seismic reflection profile	action
145-1	22.02.10	15:46	72°7,75'S	136°13,79'W	4145,0	Seismic reflection profile	in the water
145-1	22.02.10	16:59	72°4,74'S	135°55,12'W	4173,0	Seismic reflection profile	action
145-1	22.02.10	17:02	72°4,61'S	135°54,31'W	4161,0	Seismic reflection profile	action
145-1	22.02.10	17:02	72°4,61'S	135°54,31'W	4161,0	Seismic reflection profile	action
145-1	22.02.10	17:05	72°4,48'S	135°53,52'W	4159,0	Seismic reflection profile	profile Start
145-1	22.02.10	18:43	72°0,53'S	135°27,61'W	4108,0	Seismic reflection profile	action
145-1	22.02.10	19:27	71°59,14'S	135°15,62'W	4090,0	Seismic reflection profile	action
145-1	22.02.10	19:47	71°58,53'S	135°10,30'W	4071,0	Seismic reflection profile	action
145-1	22.02.10	20:21	71°57,46'S	135°1,23'W	4053,0	Seismic reflection profile	action
145-1	23.02.10	11:10	71°30,00'S	131°7,86'W	3821,0	Seismic reflection profile	alter course
145-1	24.02.10	00:40	71°23,65'S	127°28,15'W	3480,0	Seismic reflection profile	alter course
145-1	24.02.10	09:18	71°24,61'S	125°6,22'W	3361,0	Seismic reflection profile	alter course
145-1	25.02.10	02:16	71°42,72'S	120°34,57'W	2605,0	Seismic reflection profile	action
145-1	25.02.10	02:54	71°42,88'S	120°24,04'W	2534,0	Seismic reflection profile	action
145-1	25.02.10	03:18	71°43,39'S	120°17,50'W	2485,0	Seismic reflection profile	action
145-1	25.02.10	03:25	71°43,62'S	120°15,64'W	2461,0	Seismic reflection profile	action

ANT-XXVI/3

Station PS75/	Date	Time	Position Lat	Position Lon	Depth [m]	Gear	Action
145-1	25.02.10	03:55	71°45,12'S	120°8,38'W	2395,0	Seismic reflection profile	action
145-1	25.02.10	04:38	71°47,66'S	119°58,98'W	2269,0	Seismic reflection profile	action
145-1	25.02.10	04:45	71°48,07'S	119°57,48'W	2248,0	Seismic reflection profile	action
145-1	25.02.10	08:09	72°1,45'S	119°23,03'W	1481,0	Seismic reflection profile	profile End
145-1	25.02.10	08:10	72°1,50'S	119°22,88'W	1477,0	Seismic reflection profile	hoisting
145-1	25.02.10	09:18	72°3,71'S	119°12,03'W	1276,0	Seismic reflection profile	action
145-1	25.02.10	09:21	72°3,84'S	119°11,74'W	1265,0	Seismic reflection profile	on deck
146-1	25.02.10	09:26	72°3,96'S	119°11,58'W	1256,0	Seismic reflection profile	in the water
146-1	25.02.10	09:41	72°5,03'S	119°9,62'W	1174,0	Seismic reflection profile	in the water
146-1	25.02.10	09:43	72°5,20'S	119°9,65'W	1165,0	Seismic reflection profile	profile Start
146-1	25.02.10	14:04	72°22,42'S	118°30,16'W	517,2	Seismic reflection profile	action
146-1	25.02.10	22:23	72°46,97'S	116°42,59'W	640,2	Seismic reflection profile	action
146-1	25.02.10	22:34	72°47,51'S	116°39,78'W	649,3	Seismic reflection profile	action
146-1	26.02.10	04:45	73°9,19'S	115°17,13'W	811,8	Seismic reflection profile	profile End
146-1	26.02.10	04:46	73°9,25'S	115°16,89'W	812,0	Seismic reflection profile	hoisting
146-1	26.02.10	04:49	73°9,41'S	115°16,20'W	811,9	Seismic reflection profile	action
146-1	26.02.10	05:05	73°10,01'S	115°13,69'W	816,7	Seismic reflection profile	on deck
147-1	26.02.10	05:57	73°10,02'S	115°35,11'W	817,5	CTD/rosetteWaterSampler	in the water
147-1	26.02.10	06:00	73°10,01'S	115°35,12'W	818,5	CTD/rosetteWaterSampler	lowering
147-1	26.02.10	06:21	73°10,02'S	115°35,08'W	818,8	CTD/rosetteWaterSampler	on ground/max depth
147-1	26.02.10	06:22	73°10,01'S	115°35,13'W	818,8	CTD/rosetteWaterSampler	hoisting
147-1	26.02.10	06:39	73°10,08'S	115°35,37'W	820,8	CTD/rosetteWaterSampler	at surface
147-1	26.02.10	06:40	73°10,09'S	115°35,37'W	820,5	CTD/rosetteWaterSampler	on deck
148-1	26.02.10	06:49	73°10,09'S	115°33,23'W	827,8	Magnetic Turn Circle	profile Start
148-1	26.02.10	07:15	73°10,13'S	115°32,77'W	831,1	Magnetic Turn Circle	on ground/max depth
148-1	26.02.10	07:43	73°10,11'S	115°31,96'W	824,8	Magnetic Turn Circle	profile End
148-1	26.02.10	07:44	73°10,09'S	115°31,56'W	828,0	Magnetic Turn Circle	on deck

Station list PS 75

Station PS75/	Date	Time	Position Lat	Position Lon	Depth [m]	Gear	Action
149-1	26.02.10	14:03	73°12,98'S	112°3,39'W	440,2	Seismic reflection profile	action
149-1	26.02.10	14:04	73°12,94'S	112°3,25'W	439,9	Seismic reflection profile	in the water
149-1	26.02.10	14:22	73°11,82'S	111°59,35'W	429,5	Seismic reflection profile	in the water
149-1	26.02.10	14:32	73°11,21'S	111°57,04'W	421,2	Seismic reflection profile	profile Start
149-1	26.02.10	17:10	73°1,49'S	111°23,87'W	332,9	Seismic reflection profile	action
149-1	26.02.10	17:21	73°0,82'S	111°21,73'W	334,0	Seismic reflection profile	action
149-1	26.02.10	17:58	72°58,48'S	111°13,85'W	331,3	Seismic reflection profile	action
149-1	26.02.10	18:19	72°57,34'S	111°9,55'W	364,0	Seismic reflection profile	action
149-1	26.02.10	18:33	72°56,45'S	111°6,94'W	406,6	Seismic reflection profile	action
149-1	26.02.10	18:43	72°55,81'S	111°5,14'W	428,0	Seismic reflection profile	action
149-1	26.02.10	19:40	72°53,08'S	110°51,73'W	439,3	Seismic reflection profile	alter course
149-1	26.02.10	21:00	72°50,44'S	110°29,75'W	465,7	Seismic reflection profile	profile End
149-1	26.02.10	21:14	72°49,96'S	110°26,94'W	482,5	Seismic reflection profile	action
149-1	26.02.10	21:15	72°49,93'S	110°26,75'W	481,0	Seismic reflection profile	on deck
150-1	26.02.10	21:24	72°49,62'S	110°24,97'W	484,5	Seismic reflection profile	in the water
150-1	26.02.10	22:54	72°46,23'S	110°1,97'W	495,9	Seismic reflection profile	in the water
150-1	26.02.10	22:58	72°46,08'S	110°0,88'W	501,8	Seismic reflection profile	profile Start
150-1	26.02.10	23:15	72°45,41'S	109°56,27'W	508,7	Seismic reflection profile	action
150-1	27.02.10	02:13	72°36,04'S	109°13,35'W	514,6	Seismic reflection profile	action
150-1	27.02.10	03:08	72°35,77'S	108°57,44'W	523,6	Seismic reflection profile	action
150-1	27.02.10	04:20	72°35,48'S	108°36,74'W	552,0	Seismic reflection profile	action
150-1	27.02.10	11:37	72°33,55'S	106°23,60'W	531,4	Seismic reflection profile	action
150-1	27.02.10	12:32	72°33,67'S	106°27,01'W	538,6	Seismic reflection profile	action
150-1	27.02.10	18:17	73°3,25'S	106°18,27'W	644,2	Seismic reflection profile	action
150-1	27.02.10	19:46	73°10,50'S	106°17,74'W	696,6	Seismic reflection profile	action
150-1	28.02.10	01:33	73°40,91'S	106°7,55'W	839,1	Seismic reflection profile	profile End
150-1	28.02.10	01:35	73°41,05'S	106°7,25'W	859,1	Seismic reflection	action

ANT-XXVI/3

Station PS75/	Date	Time	Position Lat	Position Lon	Depth [m]	Gear	Action
						profile	
150-1	28.02.10	01:36	73°41,12'S	106°7,09'W	855,1	Seismic reflection profile	hoisting
150-1	28.02.10	02:47	73°45,17'S	105°58,56'W	881,0	Seismic reflection profile	on deck
150-1	28.02.10	02:52	73°45,46'S	105°58,07'W	881,8	Seismic reflection profile	on deck
151-1	28.02.10	05:55	74°10,26'S	106°33,82'W	1309,0	Grab, TV	in the water
151-1	28.02.10	05:56	74°10,24'S	106°33,84'W	1311,0	Grab, TV	lowering
151-1	28.02.10	06:31	74°10,11'S	106°33,48'W	1311,0	Grab, TV	on ground/max depth
151-1	28.02.10	07:07	74°10,27'S	106°34,06'W	1308,0	Grab, TV	hoisting
151-1	28.02.10	07:35	74°10,20'S	106°34,07'W	1298,0	Grab, TV	on deck
152-1	28.02.10	18:46	74°46,82'S	101°31,03'W	660,5	CTD/rosetteWaterSampler	in the water
152-1	28.02.10	18:49	74°46,82'S	101°31,05'W	659,6	CTD/rosetteWaterSampler	lowering
152-1	28.02.10	19:07	74°46,79'S	101°30,99'W	662,7	CTD/rosetteWaterSampler	on ground/max depth
152-1	28.02.10	19:23	74°46,81'S	101°30,81'W	666,5	CTD/rosetteWaterSampler	on deck
153-1	28.02.10	20:45	74°55,52'S	101°38,90'W	951,1	CTD/rosetteWaterSampler	in the water
153-1	28.02.10	21:09	74°55,51'S	101°38,98'W	953,1	CTD/rosetteWaterSampler	on ground/max depth
153-1	28.02.10	21:31	74°55,51'S	101°38,84'W	946,9	CTD/rosetteWaterSampler	on deck
154-1	28.02.10	22:07	74°54,79'S	101°52,86'W	978,4	Mooring	in the water
154-1	28.02.10	22:10	74°54,76'S	101°53,01'W	977,2	Mooring	action
154-1	28.02.10	22:19	74°54,75'S	101°53,48'W	963,9	Mooring	action
154-1	28.02.10	22:41	74°54,87'S	101°52,82'W	974,5	Mooring	in the water
154-1	28.02.10	22:48	74°54,87'S	101°52,93'W	970,7	Mooring	action
154-1	28.02.10	23:12	74°54,91'S	101°52,87'W	965,1	Mooring	action
154-1	28.02.10	23:30	74°54,75'S	101°53,30'W	966,4	Mooring	action
154-1	28.02.10	23:46	74°54,77'S	101°53,37'W	970,7	Mooring	on ground/max depth
155-1	01.03.10	00:26	74°58,43'S	101°43,17'W	1071,0	CTD/rosetteWaterSampler	in the water
155-1	01.03.10	00:51	74°58,36'S	101°42,97'W	1072,0	CTD/rosetteWaterSampler	on ground/max depth
155-1	01.03.10	01:17	74°58,34'S	101°42,62'W	1072,0	CTD/rosetteWaterSampler	on deck
156-1	01.03.10	02:02	75°2,75'S	101°54,06'W	960,4	CTD/rosetteWaterSampler	in the water
156-1	01.03.10	02:25	75°2,80'S	101°53,95'W	966,9	CTD/rosetteWaterSampler	on ground/max depth
156-1	01.03.10	02:43	75°2,85'S	101°53,90'W	970,7	CTD/rosetteWaterS	on deck

Station list PS 75

Station PS75/	Date	Time	Position Lat	Position Lon	Depth [m]	Gear	Action
						ampler	
157-1	01.03.10	03:27	75°4,23'S	102°14,60'W	642,4	CTD/rosetteWaterSa mpler	in the water
157-1	01.03.10	03:28	75°4,22'S	102°14,61'W	642,3	CTD/rosetteWaterSa mpler	lowering
157-1	01.03.10	03:44	75°4,17'S	102°14,33'W	651,8	CTD/rosetteWaterSa mpler	on ground/max depth
157-1	01.03.10	03:45	75°4,17'S	102°14,31'W	652,1	CTD/rosetteWaterSa mpler	hoisting
157-1	01.03.10	03:58	75°4,20'S	102°14,52'W	646,4	CTD/rosetteWaterSa mpler	at surface
157-1	01.03.10	03:59	75°4,21'S	102°14,56'W	645,5	CTD/rosetteWaterSa mpler	on deck
158-1	01.03.10	04:30	75°4,95'S	102°12,70'W	463,7	Seismic reflection profile	action
158-1	01.03.10	04:36	75°4,51'S	102°12,73'W	536,4	Seismic reflection profile	in the water
158-1	01.03.10	04:47	75°3,85'S	102°10,28'W	799,9	Seismic reflection profile	in the water
158-1	01.03.10	05:40	75°1,53'S	101°56,00'W	965,7	Seismic reflection profile	information
158-1	01.03.10	05:47	75°0,99'S	101°55,02'W	967,5	Seismic reflection profile	profile Start
158-1	01.03.10	07:28	74°52,96'S	101°42,93'W	761,0	Seismic reflection profile	profile End
158-1	01.03.10	07:54	74°52,03'S	101°42,13'W	762,8	Seismic reflection profile	alter course
158-1	01.03.10	08:05	74°52,98'S	101°42,96'W	759,7	Seismic reflection profile	profile Start
158-1	01.03.10	09:20	74°58,70'S	101°47,55'W	1058,0	Seismic reflection profile	alter course
158-1	01.03.10	10:04	74°57,01'S	102°0,03'W	1001,0	Seismic reflection profile	profile End
158-1	01.03.10	10:19	74°56,51'S	102°3,88'W	991,1	Seismic reflection profile	action
158-1	01.03.10	10:24	74°56,36'S	102°4,97'W	990,9	Seismic reflection profile	on deck
159-1	01.03.10	13:06	74°47,99'S	102°21,37'W	1045,0	Geothermic corer	in the water
159-1	01.03.10	13:23	74°47,99'S	102°21,31'W	1046,0	Geothermic corer	on ground/max depth
159-1	01.03.10	13:23	74°47,99'S	102°21,31'W	1046,0	Geothermic corer	hoisting
159-1	01.03.10	13:36	74°48,00'S	102°21,26'W	1047,0	Geothermic corer	at surface
159-1	01.03.10	13:42	74°48,04'S	102°21,28'W	1046,0	Geothermic corer	on deck
160-1	02.03.10	01:38	74°33,83'S	102°37,45'W	335,0	Gravity corer	in the water
160-1	02.03.10	01:41	74°33,83'S	102°37,44'W	336,7	Gravity corer	on ground/max depth
160-1	02.03.10	01:43	74°33,83'S	102°37,43'W	336,7	Gravity corer	hoisting
160-1	02.03.10	01:48	74°33,82'S	102°37,43'W	337,7	Gravity corer	at surface
160-1	02.03.10	01:53	74°33,83'S	102°37,46'W	336,2	Gravity corer	on deck
161-1	02.03.10	02:29	74°31,91'S	102°37,36'W	646,6	Gravity corer	in the water

ANT-XXVI/3

Station PS75/	Date	Time	Position Lat	Position Lon	Depth [m]	Gear	Action
161-1	02.03.10	02:39	74°31,90'S	102°37,44'W	645,9	Gravity corer	on ground/max depth
161-1	02.03.10	02:40	74°31,90'S	102°37,45'W	647,0	Gravity corer	hoisting
161-1	02.03.10	02:49	74°31,90'S	102°37,48'W	648,4	Gravity corer	at surface
161-1	02.03.10	02:52	74°31,91'S	102°37,42'W	646,9	Gravity corer	on deck
162-1	02.03.10	05:44	74°50,01'S	103°29,98'W	1064,0	CTD/rosetteWaterSampler	in the water
162-1	02.03.10	05:46	74°50,00'S	103°30,02'W	1060,0	CTD/rosetteWaterSampler	lowering
162-1	02.03.10	06:11	74°49,99'S	103°30,03'W	1060,0	CTD/rosetteWaterSampler	on ground/max depth
162-1	02.03.10	06:12	74°49,99'S	103°30,03'W	1062,0	CTD/rosetteWaterSampler	hoisting
162-1	02.03.10	06:29	74°50,01'S	103°29,95'W	1059,0	CTD/rosetteWaterSampler	at surface
162-1	02.03.10	06:30	74°50,01'S	103°29,94'W	1066,0	CTD/rosetteWaterSampler	on deck
162-2	02.03.10	06:36	74°50,02'S	103°30,00'W	1074,0	Geothermic corer	in the water
162-2	02.03.10	06:38	74°50,02'S	103°30,04'W	1085,0	Geothermic corer	lowering
162-2	02.03.10	06:57	74°49,99'S	103°29,92'W	1045,0	Geothermic corer	on ground/max depth
162-2	02.03.10	07:07	74°50,00'S	103°29,92'W	1052,0	Geothermic corer	hoisting
162-2	02.03.10	07:24	74°50,00'S	103°29,90'W	1054,0	Geothermic corer	at surface
162-2	02.03.10	07:26	74°50,00'S	103°29,90'W	1055,0	Geothermic corer	on deck
163-1	02.03.10	09:04	74°44,50'S	104°23,53'W	1142,0	CTD/rosetteWaterSampler	in the water
163-1	02.03.10	09:32	74°44,52'S	104°23,53'W	1147,0	CTD/rosetteWaterSampler	on ground/max depth
163-1	02.03.10	09:33	74°44,52'S	104°23,54'W	1147,0	CTD/rosetteWaterSampler	hoisting
163-1	02.03.10	09:50	74°44,48'S	104°23,48'W	1137,0	CTD/rosetteWaterSampler	at surface
163-1	02.03.10	09:51	74°44,48'S	104°23,49'W	1138,0	CTD/rosetteWaterSampler	on deck
163-2	02.03.10	09:56	74°44,48'S	104°23,51'W	1138,0	Geothermic corer	in the water
163-2	02.03.10	09:57	74°44,49'S	104°23,51'W	1140,0	Geothermic corer	lowering
163-2	02.03.10	10:18	74°44,48'S	104°23,46'W	1137,0	Geothermic corer	on ground/max depth
163-2	02.03.10	10:28	74°44,48'S	104°23,52'W	1139,0	Geothermic corer	hoisting
163-2	02.03.10	10:47	74°44,47'S	104°23,52'W	1140,0	Geothermic corer	at surface
163-2	02.03.10	10:48	74°44,48'S	104°23,52'W	1138,0	Geothermic corer	on deck
164-1	02.03.10	12:16	74°45,03'S	105°11,72'W	1402,0	CTD/rosetteWaterSampler	in the water
164-1	02.03.10	12:46	74°44,85'S	105°11,67'W	1399,0	CTD/rosetteWaterSampler	on ground/max depth
164-1	02.03.10	12:47	74°44,85'S	105°11,66'W	1401,0	CTD/rosetteWaterSampler	hoisting

Station list PS 75

Station PS75/	Date	Time	Position Lat	Position Lon	Depth [m]	Gear	Action
164-1	02.03.10	13:10	74°44,86'S	105°11,60'W	1405,0	CTD/rosetteWaterSa mpler	at surface
164-1	02.03.10	13:11	74°44,86'S	105°11,60'W	1402,0	CTD/rosetteWaterSa mpler	on deck
164-2	02.03.10	13:17	74°44,86'S	105°12,00'W	1393,0	Geothermic corer	in the water
164-2	02.03.10	13:40	74°44,85'S	105°12,02'W	1392,0	Geothermic corer	on ground/max depth
164-2	02.03.10	13:50	74°44,84'S	105°12,03'W	1391,0	Geothermic corer	hoisting
164-2	02.03.10	14:15	74°44,81'S	105°12,03'W	1390,0	Geothermic corer	at surface
164-2	02.03.10	14:17	74°44,80'S	105°12,02'W	1393,0	Geothermic corer	on deck
165-1	02.03.10	17:28	74°40,22'S	106°36,26'W	1217,0	CTD/rosetteWaterSa mpler	in the water
165-1	02.03.10	17:29	74°40,22'S	106°36,28'W	1216,0	CTD/rosetteWaterSa mpler	lowering
165-1	02.03.10	17:57	74°40,16'S	106°36,45'W	1212,0	CTD/rosetteWaterSa mpler	on ground/max depth
165-1	02.03.10	17:58	74°40,16'S	106°36,46'W	1212,0	CTD/rosetteWaterSa mpler	hoisting
165-1	02.03.10	18:25	74°40,17'S	106°36,51'W	1213,0	CTD/rosetteWaterSa mpler	at surface
165-1	02.03.10	18:26	74°40,17'S	106°36,51'W	1213,0	CTD/rosetteWaterSa mpler	on deck
165-2	02.03.10	18:30	74°40,17'S	106°36,45'W	1213,0	Geothermic corer	in the water
165-2	02.03.10	18:32	74°40,17'S	106°36,41'W	1213,0	Geothermic corer	lowering
165-2	02.03.10	18:54	74°40,17'S	106°36,40'W	1214,0	Geothermic corer	on ground/max depth
165-2	02.03.10	19:05	74°40,17'S	106°36,34'W	1212,0	Geothermic corer	hoisting
165-2	02.03.10	19:24	74°40,10'S	106°36,33'W	1209,0	Geothermic corer	at surface
165-2	02.03.10	19:29	74°40,07'S	106°36,37'W	1210,0	Geothermic corer	on deck
166-1	02.03.10	22:47	74°36,23'S	106°38,56'W	1381,0	CTD/rosetteWaterSa mpler	in the water
166-1	02.03.10	23:18	74°36,18'S	106°38,61'W	1377,0	CTD/rosetteWaterSa mpler	on ground/max depth
166-1	02.03.10	23:18	74°36,18'S	106°38,61'W	1377,0	CTD/rosetteWaterSa mpler	hoisting
166-1	02.03.10	23:38	74°36,16'S	106°38,54'W	1372,0	CTD/rosetteWaterSa mpler	at surface
166-1	02.03.10	23:39	74°36,16'S	106°38,54'W	1369,0	CTD/rosetteWaterSa mpler	on deck
166-2	02.03.10	23:46	74°36,15'S	106°38,53'W	1372,0	Geothermic corer	in the water
166-2	03.03.10	00:12	74°36,10'S	106°38,68'W	1374,0	Geothermic corer	on ground/max depth
166-2	03.03.10	00:23	74°36,10'S	106°38,63'W	1371,0	Geothermic corer	hoisting
166-2	03.03.10	00:44	74°36,15'S	106°38,64'W	1375,0	Geothermic corer	at surface
166-2	03.03.10	00:49	74°36,18'S	106°38,63'W	1375,0	Geothermic corer	on deck
166-3	03.03.10	01:00	74°36,25'S	106°38,68'W	1386,0	Gravity corer	in the water
166-3	03.03.10	01:19	74°36,28'S	106°38,59'W	1385,0	Gravity corer	on ground/max

ANT-XXVI/3

Station PS75/	Date	Time	Position Lat	Position Lon	Depth [m]	Gear	Action
							depth
166-3	03.03.10	01:38	74°36,24'S	106°38,62'W	1384,0	Gravity corer	at surface
166-3	03.03.10	01:43	74°36,23'S	106°38,61'W	1381,0	Gravity corer	on deck
167-1	03.03.10	03:47	74°37,34'S	105°48,00'W	525,9	Gravity corer	in the water
167-1	03.03.10	03:50	74°37,36'S	105°48,07'W	526,5	Gravity corer	lowering
167-1	03.03.10	04:00	74°37,37'S	105°48,11'W	526,3	Gravity corer	on ground/max depth
167-1	03.03.10	04:01	74°37,38'S	105°48,12'W	524,0	Gravity corer	hoisting
167-1	03.03.10	04:09	74°37,37'S	105°47,93'W	524,8	Gravity corer	at surface
167-1	03.03.10	04:13	74°37,38'S	105°47,93'W	524,3	Gravity corer	on deck
168-1	03.03.10	04:48	74°36,65'S	105°51,87'W	651,7	Gravity corer	in the water
168-1	03.03.10	04:50	74°36,68'S	105°51,88'W	651,7	Gravity corer	lowering
168-1	03.03.10	04:59	74°36,71'S	105°51,96'W	652,0	Gravity corer	on ground/max depth
168-1	03.03.10	05:00	74°36,71'S	105°51,96'W	651,3	Gravity corer	hoisting
168-1	03.03.10	05:09	74°36,74'S	105°51,82'W	648,2	Gravity corer	at surface
168-1	03.03.10	05:13	74°36,75'S	105°51,72'W	651,2	Gravity corer	on deck
169-1	03.03.10	08:02	74°20,01'S	106°0,04'W	1406,0	CTD/rosetteWaterSampler	in the water
169-1	03.03.10	08:33	74°19,98'S	106°0,07'W	1408,0	CTD/rosetteWaterSampler	on ground/max depth
169-1	03.03.10	08:34	74°19,98'S	106°0,06'W	1407,0	CTD/rosetteWaterSampler	hoisting
169-1	03.03.10	09:00	74°20,02'S	106°0,05'W	1408,0	CTD/rosetteWaterSampler	at surface
169-1	03.03.10	09:01	74°20,01'S	106°0,05'W	1407,0	CTD/rosetteWaterSampler	on deck
169-2	03.03.10	09:07	74°20,00'S	106°0,06'W	1407,0	Geothermic corer	in the water
169-2	03.03.10	09:29	74°20,00'S	106°0,00'W	1405,0	Geothermic corer	on ground/max depth
169-2	03.03.10	09:40	74°20,00'S	105°59,95'W	1404,0	Geothermic corer	hoisting
169-2	03.03.10	10:01	74°20,00'S	106°0,01'W	1405,0	Geothermic corer	at surface
169-2	03.03.10	10:05	74°20,00'S	106°0,05'W	1407,0	Geothermic corer	on deck
170-1	03.03.10	11:23	74°12,51'S	105°33,15'W	1686,0	CTD/rosetteWaterSampler	in the water
170-1	03.03.10	12:00	74°12,51'S	105°33,07'W	1683,0	CTD/rosetteWaterSampler	on ground/max depth
170-1	03.03.10	12:01	74°12,51'S	105°33,07'W	1684,0	CTD/rosetteWaterSampler	hoisting
170-1	03.03.10	12:28	74°12,50'S	105°32,94'W	1682,0	CTD/rosetteWaterSampler	at surface
170-1	03.03.10	12:29	74°12,50'S	105°32,94'W	1685,0	CTD/rosetteWaterSampler	on deck
170-2	03.03.10	12:35	74°12,50'S	105°32,95'W	1684,0	Geothermic corer	action
170-2	03.03.10	13:01	74°12,53'S	105°32,99'W	1685,0	Geothermic corer	on ground/max depth
170-2	03.03.10	13:11	74°12,54'S	105°33,00'W	1685,0	Geothermic corer	hoisting

Station list PS 75

Station PS75/	Date	Time	Position Lat	Position Lon	Depth [m]	Gear	Action
170-2	03.03.10	13:37	74°12,54'S	105°33,09'W	1684,0	Geothermic corer	at surface
170-2	03.03.10	13:37	74°12,54'S	105°33,09'W	1684,0	Geothermic corer	on deck
171-1	03.03.10	14:46	74°13,50'S	105°0,12'W	1399,0	CTD/rosetteWaterSampler	in the water
171-1	03.03.10	14:47	74°13,51'S	105°0,10'W	1399,0	CTD/rosetteWaterSampler	lowering
171-1	03.03.10	15:19	74°13,53'S	104°59,84'W	1395,0	CTD/rosetteWaterSampler	on ground/max depth
171-1	03.03.10	15:19	74°13,53'S	104°59,84'W	1395,0	CTD/rosetteWaterSampler	hoisting
171-1	03.03.10	15:45	74°13,44'S	105°0,06'W	1392,0	CTD/rosetteWaterSampler	at surface
171-1	03.03.10	15:46	74°13,44'S	105°0,07'W	1391,0	CTD/rosetteWaterSampler	on deck
172-1	03.03.10	16:37	74°14,03'S	104°41,07'W	702,0	CTD/rosetteWaterSampler	in the water
172-1	03.03.10	16:37	74°14,03'S	104°41,07'W	702,0	CTD/rosetteWaterSampler	lowering
172-1	03.03.10	16:55	74°14,02'S	104°40,96'W	699,3	CTD/rosetteWaterSampler	on ground/max depth
172-1	03.03.10	16:56	74°14,01'S	104°40,97'W	697,4	CTD/rosetteWaterSampler	hoisting
172-1	03.03.10	17:05	74°14,00'S	104°41,12'W	691,0	CTD/rosetteWaterSampler	at surface
172-1	03.03.10	17:06	74°13,99'S	104°41,14'W	689,5	CTD/rosetteWaterSampler	on deck
173-1	03.03.10	21:45	74°8,35'S	105°43,79'W	1505,0	Gravity corer	in the water
173-1	03.03.10	21:55	74°8,35'S	105°43,74'W	1507,0	Gravity corer	lowering
173-1	03.03.10	22:15	74°8,34'S	105°43,82'W	1507,0	Gravity corer	on ground/max depth
173-1	03.03.10	22:16	74°8,34'S	105°43,82'W	1507,0	Gravity corer	hoisting
173-1	03.03.10	22:34	74°8,36'S	105°43,76'W	1506,0	Gravity corer	at surface
173-1	03.03.10	22:42	74°8,35'S	105°43,75'W	1508,0	Gravity corer	on deck
173-2	03.03.10	22:59	74°8,35'S	105°43,84'W	1504,0	Geothermic corer	in the water
173-2	03.03.10	23:24	74°8,33'S	105°43,82'W	1508,0	Geothermic corer	on ground/max depth
173-2	03.03.10	23:36	74°8,33'S	105°43,79'W	1508,0	Geothermic corer	hoisting
173-2	04.03.10	00:01	74°8,30'S	105°43,84'W	1507,0	Geothermic corer	at surface
173-2	04.03.10	00:02	74°8,30'S	105°43,84'W	1507,0	Geothermic corer	on deck
174-1	04.03.10	01:27	73°57,94'S	105°30,21'W	692,3	CTD/rosetteWaterSampler	in the water
174-1	04.03.10	01:45	73°57,98'S	105°30,15'W	699,3	CTD/rosetteWaterSampler	on ground/max depth
174-1	04.03.10	01:46	73°57,98'S	105°30,14'W	697,7	CTD/rosetteWaterSampler	hoisting
174-1	04.03.10	02:00	73°57,98'S	105°30,13'W	697,3	CTD/rosetteWaterSampler	at surface
174-1	04.03.10	02:01	73°57,98'S	105°30,13'W	696,5	CTD/rosetteWaterS	on deck

ANT-XXVI/3

Station PS75/	Date	Time	Position Lat	Position Lon	Depth [m]	Gear	Action
						ampler	
175-1	04.03.10	02:39	74°1,00'S	105°40,66'W	1093,0	CTD/rosetteWaterSa mpler	in the water
175-1	04.03.10	03:04	74°0,95'S	105°41,16'W	1094,0	CTD/rosetteWaterSa mpler	on ground/max depth
175-1	04.03.10	03:05	74°0,95'S	105°41,20'W	1096,0	CTD/rosetteWaterSa mpler	hoisting
175-1	04.03.10	03:24	74°0,88'S	105°41,45'W	1067,0	CTD/rosetteWaterSa mpler	at surface
175-1	04.03.10	03:25	74°0,88'S	105°41,44'W	1064,0	CTD/rosetteWaterSa mpler	on deck
175-2	04.03.10	03:30	74°0,97'S	105°41,45'W	1077,0	Geothermic corer	in the water
175-2	04.03.10	03:52	74°0,92'S	105°41,54'W	1068,0	Geothermic corer	on ground/max depth
175-2	04.03.10	04:03	74°0,90'S	105°41,54'W	1065,0	Geothermic corer	hoisting
175-2	04.03.10	04:20	74°0,88'S	105°41,52'W	1062,0	Geothermic corer	at surface
175-2	04.03.10	04:21	74°0,88'S	105°41,51'W	1061,0	Geothermic corer	on deck
176-1	04.03.10	15:58	74°40,40'S	109°54,84'W	950,5	CTD/rosetteWaterSa mpler	in the water
176-1	04.03.10	15:59	74°40,39'S	109°54,84'W	952,8	CTD/rosetteWaterSa mpler	lowering
176-1	04.03.10	16:22	74°40,26'S	109°54,68'W	966,1	CTD/rosetteWaterSa mpler	on ground/max depth
176-1	04.03.10	16:23	74°40,25'S	109°54,68'W	967,8	CTD/rosetteWaterSa mpler	hoisting
176-1	04.03.10	16:40	74°40,22'S	109°54,63'W	969,4	CTD/rosetteWaterSa mpler	on deck
177-1	05.03.10	06:15	73°51,03'S	107°52,91'W	741,2	Gravity corer	in the water
177-1	05.03.10	06:28	73°51,04'S	107°52,97'W	740,1	Gravity corer	on ground/max depth
177-1	05.03.10	06:38	73°51,04'S	107°52,97'W	740,0	Gravity corer	at surface
177-1	05.03.10	06:42	73°51,05'S	107°52,95'W	739,3	Gravity corer	on deck
178-1	05.03.10	09:30	74°5,52'S	106°44,83'W	622,6	CTD/rosetteWaterSa mpler	in the water
178-1	05.03.10	09:46	74°5,48'S	106°44,95'W	619,9	CTD/rosetteWaterSa mpler	on ground/max depth
178-1	05.03.10	10:00	74°5,50'S	106°45,01'W	626,2	CTD/rosetteWaterSa mpler	on deck
178-2	05.03.10	10:06	74°5,49'S	106°45,03'W	626,9	Geothermic corer	in the water
178-2	05.03.10	10:18	74°5,48'S	106°45,02'W	624,8	Geothermic corer	on ground/max depth
178-2	05.03.10	10:29	74°5,49'S	106°45,03'W	628,6	Geothermic corer	hoisting
178-2	05.03.10	10:43	74°5,47'S	106°45,01'W	622,8	Geothermic corer	on deck
179-1	05.03.10	11:58	74°2,60'S	106°11,02'W	1141,0	CTD/rosetteWaterSa mpler	in the water
179-1	05.03.10	12:25	74°2,55'S	106°11,08'W	1149,0	CTD/rosetteWaterSa mpler	on ground/max

Station list PS 75

Station PS75/	Date	Time	Position Lat	Position Lon	Depth [m]	Gear	Action
							depth
179-1	05.03.10	12:44	74°2,51'S	106°11,09'W	1155,0	CTD/rosetteWaterSa mpler	on deck
179-2	05.03.10	12:50	74°2,51'S	106°10,98'W	1148,0	Geothermic corer	in the water
179-2	05.03.10	13:08	74°2,50'S	106°11,06'W	1153,0	Geothermic corer	on ground/max depth
179-2	05.03.10	13:18	74°2,50'S	106°11,09'W	1155,0	Geothermic corer	hoisting
179-2	05.03.10	13:42	74°2,49'S	106°11,08'W	1160,0	Geothermic corer	on deck
180-1	05.03.10	19:30	73°31,48'S	106°12,00'W	830,7	CTD/rosetteWaterSa mpler	in the water
180-1	05.03.10	19:52	73°31,44'S	106°11,99'W	830,4	CTD/rosetteWaterSa mpler	on ground/max depth
180-1	05.03.10	20:17	73°31,45'S	106°12,11'W	827,0	CTD/rosetteWaterSa mpler	on deck
180-2	05.03.10	20:26	73°31,42'S	106°11,88'W	828,5	Large Box Corer	action
180-2	05.03.10	20:39	73°31,43'S	106°11,98'W	831,2	Large Box Corer	on ground/max depth
180-2	05.03.10	20:54	73°31,45'S	106°12,01'W	830,5	Large Box Corer	on deck
180-3	05.03.10	20:58	73°31,43'S	106°11,96'W	829,8	Large Box Corer	in the water
180-3	05.03.10	21:12	73°31,44'S	106°11,92'W	828,5	Large Box Corer	on ground/max depth
180-3	05.03.10	21:27	73°31,39'S	106°11,83'W	824,4	Large Box Corer	on deck
180-4	05.03.10	21:42	73°31,42'S	106°12,03'W	829,2	Geothermic corer	in the water
180-4	05.03.10	21:56	73°31,44'S	106°12,04'W	830,8	Geothermic corer	on ground/max depth
180-4	05.03.10	22:07	73°31,42'S	106°12,04'W	830,4	Geothermic corer	hoisting
180-4	05.03.10	22:22	73°31,41'S	106°12,13'W	827,5	Geothermic corer	on deck
181-1	05.03.10	22:45	73°31,73'S	106°11,83'W	850,5	Geothermic corer	in the water
181-1	05.03.10	23:00	73°31,71'S	106°11,99'W	844,4	Geothermic corer	on ground/max depth
181-1	05.03.10	23:10	73°31,71'S	106°12,03'W	843,2	Geothermic corer	hoisting
181-1	05.03.10	23:26	73°31,72'S	106°12,04'W	840,7	Geothermic corer	on deck
182-1	05.03.10	23:47	73°32,12'S	106°12,09'W	843,8	Geothermic corer	action
182-1	06.03.10	00:03	73°32,13'S	106°12,03'W	844,2	Geothermic corer	on ground/max depth
182-1	06.03.10	00:13	73°32,14'S	106°12,09'W	843,1	Geothermic corer	hoisting
182-1	06.03.10	00:27	73°32,15'S	106°12,02'W	843,0	Geothermic corer	on deck
182-2	06.03.10	00:37	73°32,14'S	106°12,10'W	842,2	CTD/rosetteWaterSa mpler	in the water
182-2	06.03.10	00:59	73°32,15'S	106°12,12'W	842,4	CTD/rosetteWaterSa mpler	on ground/max depth
182-2	06.03.10	01:21	73°32,17'S	106°12,05'W	843,2	CTD/rosetteWaterSa mpler	on deck
183-1	06.03.10	01:36	73°31,45'S	106°12,17'W	825,7	Gravity corer	in the water
183-1	06.03.10	01:46	73°31,44'S	106°12,16'W	826,7	Gravity corer	on

ANT-XXVI/3

Station PS75/	Date	Time	Position Lat	Position Lon	Depth [m]	Gear	Action
							ground/max depth
183-1	06.03.10	02:02	73°31,42'S	106°12,16'W	825,5	Gravity corer	on deck
184-1	06.03.10	02:15	73°31,17'S	106°12,04'W	816,8	CTD/rosetteWaterSa mpler	in the water
184-1	06.03.10	02:36	73°31,14'S	106°12,09'W	816,7	CTD/rosetteWaterSa mpler	on ground/max depth
184-1	06.03.10	02:57	73°31,25'S	106°12,11'W	819,0	CTD/rosetteWaterSa mpler	on deck
184-2	06.03.10	03:02	73°31,29'S	106°12,12'W	821,1	Geothermic corer	in the water
184-2	06.03.10	03:17	73°31,26'S	106°12,09'W	819,8	Geothermic corer	on ground/max depth
185-1	06.03.10	03:41	73°31,17'S	106°12,19'W	818,1	Geothermic corer	in the water
184-2	06.03.10	03:41	73°31,17'S	106°12,19'W	818,1	Geothermic corer	on deck
185-1	06.03.10	03:57	73°31,09'S	106°12,29'W	817,2	Geothermic corer	on ground/max depth
185-1	06.03.10	04:21	73°31,08'S	106°12,51'W	812,0	Geothermic corer	on deck
186-1	06.03.10	05:47	73°20,11'S	106°0,48'W	699,1	CTD/rosetteWaterSa mpler	in the water
186-1	06.03.10	06:06	73°19,99'S	106°0,20'W	690,0	CTD/rosetteWaterSa mpler	on ground/max depth
186-1	06.03.10	06:23	73°20,04'S	106°0,44'W	699,4	CTD/rosetteWaterSa mpler	on deck
187-1	06.03.10	14:10	73°2,06'S	109°9,58'W	477,9	Seismic reflection profile	in the water
187-1	06.03.10	15:26	73°1,23'S	108°49,50'W	498,1	Seismic reflection profile	in the water
187-1	06.03.10	15:29	73°1,30'S	108°48,65'W	507,2	Seismic reflection profile	profile Start
187-1	06.03.10	18:16	72°57,85'S	108°0,62'W	592,2	Seismic reflection profile	action
187-1	06.03.10	18:41	72°56,60'S	107°54,64'W	604,4	Seismic reflection profile	action
187-1	07.03.10	01:55	72°52,41'S	105°45,66'W	547,5	Seismic reflection profile	action
187-1	07.03.10	03:16	72°49,81'S	105°23,16'W	586,9	Seismic reflection profile	action
187-1	07.03.10	09:36	72°27,86'S	104°1,11'W	637,2	Seismic reflection profile	alter course
187-1	07.03.10	13:05	72°12,78'S	103°40,22'W	642,2	Seismic reflection profile	action
187-1	07.03.10	14:30	72°6,14'S	103°42,98'W	593,8	Seismic reflection profile	action
187-1	07.03.10	14:56	72°4,29'S	103°40,25'W	585,9	Seismic reflection profile	action
187-1	07.03.10	15:12	72°3,23'S	103°38,24'W	615,9	Seismic reflection profile	action
187-1	07.03.10	21:39	71°32,37'S	103°7,74'W	674,7	Seismic reflection profile	action

Station list PS 75

Station PS75/	Date	Time	Position Lat	Position Lon	Depth [m]	Gear	Action
187-1	07.03.10	21:53	71°31,20'S	103°6,10'W	670,6	Seismic reflection profile	action
187-1	08.03.10	04:21	70°59,92'S	102°22,10'W	1667,0	Seismic reflection profile	profile End
188-1	08.03.10	05:45	70°54,98'S	102°16,26'W	1972,0	Magnetic Turn Circle	profile Start
188-1	08.03.10	06:50	70°54,45'S	102°19,27'W	1978,0	Magnetic Turn Circle	on ground/max depth
188-1	08.03.10	06:51	70°54,44'S	102°19,60'W	1977,0	Magnetic Turn Circle	profile End
189-1	08.03.10	16:58	71°48,01'S	104°4,95'W	698,0	CTD/rosetteWaterSampler	in the water
189-1	08.03.10	17:18	71°47,99'S	104°5,08'W	692,8	CTD/rosetteWaterSampler	on ground/max depth
189-1	08.03.10	17:36	71°48,07'S	104°5,07'W	693,9	CTD/rosetteWaterSampler	on deck
190-1	08.03.10	21:06	71°52,75'S	103°23,44'W	777,2	CTD/rosetteWaterSampler	in the water
190-1	08.03.10	21:27	71°52,74'S	103°23,24'W	775,1	CTD/rosetteWaterSampler	on ground/max depth
190-1	08.03.10	21:48	71°52,75'S	103°23,19'W	774,7	CTD/rosetteWaterSampler	on deck
190-2	08.03.10	21:53	71°52,75'S	103°23,22'W	776,5	Geothermic corer	in the water
190-2	08.03.10	22:06	71°52,75'S	103°23,13'W	775,0	Geothermic corer	on ground/max depth
190-2	08.03.10	22:16	71°52,76'S	103°23,14'W	775,4	Geothermic corer	hoisting
190-2	08.03.10	22:33	71°52,77'S	103°23,38'W	776,9	Geothermic corer	on deck
190-3	08.03.10	23:01	71°52,72'S	103°23,14'W	776,3	Gravity corer	in the water
190-3	08.03.10	23:10	71°52,72'S	103°23,15'W	774,8	Gravity corer	on ground/max depth
190-3	08.03.10	23:25	71°52,72'S	103°23,15'W	775,0	Gravity corer	on deck
191-1	09.03.10	00:29	71°52,69'S	102°53,81'W	578,0	CTD/rosetteWaterSampler	in the water
191-1	09.03.10	00:46	71°52,65'S	102°54,00'W	582,0	CTD/rosetteWaterSampler	on ground/max depth
191-1	09.03.10	01:02	71°52,64'S	102°54,15'W	584,8	CTD/rosetteWaterSampler	on deck
192-1	09.03.10	03:27	71°44,64'S	103°19,49'W	792,7	Gravity corer	in the water
192-1	09.03.10	03:41	71°44,65'S	103°19,56'W	793,0	Gravity corer	on ground/max depth
192-1	09.03.10	03:54	71°44,65'S	103°19,50'W	792,4	Gravity corer	on deck
192-2	09.03.10	04:08	71°44,69'S	103°19,60'W	792,8	Giant box grab	in the water
192-2	09.03.10	04:21	71°44,65'S	103°19,61'W	793,4	Giant box grab	on ground/max depth
192-2	09.03.10	04:33	71°44,69'S	103°19,63'W	793,5	Giant box grab	on deck
192-3	09.03.10	04:50	71°44,65'S	103°19,54'W	792,4	Geothermic corer	in the water
192-3	09.03.10	05:05	71°44,69'S	103°19,69'W	793,2	Geothermic corer	on

ANT-XXVI/3

Station PS75/	Date	Time	Position Lat	Position Lon	Depth [m]	Gear	Action
							ground/max depth
192-3	09.03.10	05:15	71°44,69'S	103°19,73'W	792,8	Geothermic corer	hoisting
192-3	09.03.10	05:30	71°44,69'S	103°19,79'W	793,4	Geothermic corer	on deck
193-1	09.03.10	07:12	71°32,47'S	103°7,66'W	678,4	Gravity corer	in the water
193-1	09.03.10	07:24	71°32,44'S	103°7,75'W	675,7	Gravity corer	on ground/max depth
193-1	09.03.10	07:35	71°32,43'S	103°7,75'W	675,3	Gravity corer	at surface
193-1	09.03.10	07:40	71°32,46'S	103°7,80'W	676,1	Gravity corer	on deck
194-1	09.03.10	08:42	71°27,22'S	103°0,43'W	646,8	Gravity corer	in the water
194-1	09.03.10	08:51	71°27,25'S	103°0,46'W	652,0	Gravity corer	on ground/max depth
194-1	09.03.10	09:01	71°27,24'S	103°0,46'W	651,1	Gravity corer	at surface
194-1	09.03.10	09:06	71°27,23'S	103°0,43'W	651,1	Gravity corer	on deck
194-2	09.03.10	09:23	71°27,24'S	103°0,46'W	651,7	Geothermic corer	in the water
194-2	09.03.10	09:35	71°27,21'S	103°0,43'W	649,0	Geothermic corer	on ground/max depth
194-2	09.03.10	09:45	71°27,21'S	103°0,46'W	648,1	Geothermic corer	hoisting
194-2	09.03.10	10:00	71°27,26'S	103°0,66'W	655,4	Geothermic corer	on deck
194-3	09.03.10	10:18	71°27,33'S	103°0,71'W	655,0	Gravity corer	in the water
194-3	09.03.10	10:27	71°27,32'S	103°0,73'W	655,8	Gravity corer	on ground/max depth
194-3	09.03.10	10:28	71°27,31'S	103°0,73'W	656,5	Gravity corer	hoisting
194-3	09.03.10	10:42	71°27,30'S	103°0,69'W	655,7	Gravity corer	on deck
195-1	09.03.10	13:47	71°4,01'S	102°22,03'W	1518,0	CTD/rosetteWaterSampler	action
195-1	09.03.10	14:18	71°3,95'S	102°22,00'W	1447,4	CTD/rosetteWaterSampler	on ground/max depth
195-1	09.03.10	14:42	71°4,03'S	102°22,06'W	1447,0	CTD/rosetteWaterSampler	on deck
195-2	09.03.10	14:46	71°4,02'S	102°22,01'W	1448,0	Geothermic corer	in the water
195-2	09.03.10	15:21	71°3,98'S	102°22,28'W	1447,0	Geothermic corer	on ground/max depth
195-2	09.03.10	15:30	71°3,96'S	102°22,34'W	1446,0	Geothermic corer	hoisting
195-2	09.03.10	15:55	71°3,97'S	102°22,01'W	1450,0	Geothermic corer	on deck
195-3	09.03.10	16:07	71°3,98'S	102°22,16'W	1449,0	Multi corer	in the water
195-3	09.03.10	16:30	71°4,02'S	102°22,37'W	1443,0	Multi corer	on ground/max depth
195-3	09.03.10	16:51	71°4,12'S	102°22,62'W	1434,0	Multi corer	on deck
196-1	09.03.10	19:10	71°12,58'S	103°20,09'W	588,5	Seismic reflection profile	in the water
196-1	09.03.10	20:16	71°13,82'S	103°1,37'W	585,2	Seismic reflection profile	in the water
196-1	09.03.10	20:18	71°13,85'S	103°0,83'W	587,8	Seismic reflection profile	profile Start
196-1	10.03.10	01:50	71°20,93'S	101°29,73'W	443,2	Seismic reflection	profile End

Station list PS 75

Station PS75/	Date	Time	Position Lat	Position Lon	Depth [m]	Gear	Action
						profile	
196-1	10.03.10	02:00	71°21,08'S	101°27,07'W	451,3	Seismic reflection profile	alter course
196-1	10.03.10	03:04	71°21,53'S	101°30,97'W	444,2	Seismic reflection profile	profile Start
196-1	10.03.10	07:58	71°0,06'S	102°21,98'W	1659,0	Seismic reflection profile	alter course
196-1	10.03.10	12:12	70°37,83'S	102°23,53'W	2791,0	Seismic reflection profile	action
196-1	10.03.10	12:44	70°34,88'S	102°23,55'W	2921,0	Seismic reflection profile	action
196-1	10.03.10	18:41	70°0,00'S	102°26,02'W	3245,0	Seismic reflection profile	alter course
196-1	11.03.10	20:12	68°33,98'S	107°41,13'W	4163,0	Seismic reflection profile	alter course
196-1	12.03.10	16:08	70°18,96'S	109°2,42'W	3793,0	Seismic reflection profile	action
196-1	12.03.10	16:51	70°22,98'S	109°5,90'W	3700,0	Seismic reflection profile	action
196-1	12.03.10	20:10	70°41,49'S	109°21,11'W	3231,0	Seismic reflection profile	action
196-1	12.03.10	20:25	70°42,81'S	109°22,20'W	3272,0	Seismic reflection profile	action
196-1	12.03.10	20:50	70°45,00'S	109°24,02'W	3192,0	Seismic reflection profile	alter course
196-1	13.03.10	11:12	71°59,99'S	108°30,99'W	571,6	Seismic reflection profile	profile End
196-1	13.03.10	11:14	72°0,17'S	108°30,89'W	573,2	Seismic reflection profile	action
196-1	13.03.10	11:15	72°0,25'S	108°30,84'W	571,6	Seismic reflection profile	hoisting
196-1	13.03.10	12:22	72°4,82'S	108°28,80'W	576,9	Seismic reflection profile	on deck
196-1	13.03.10	12:24	72°4,94'S	108°28,73'W	575,9	Seismic reflection profile	on deck
197-1	13.03.10	12:44	72°4,60'S	108°28,85'W	572,5	Ocean bottomSeismometer	in the water
197-1	13.03.10	12:45	72°4,62'S	108°28,86'W	572,6	Ocean bottomSeismometer	on ground/max depth
197-2	13.03.10	13:58	72°2,55'S	107°54,59'W	600,8	Ocean bottomSeismometer	in the water
197-2	13.03.10	13:59	72°2,54'S	107°54,62'W	584,1	Ocean bottomSeismometer	on ground/max depth
197-3	13.03.10	15:14	72°0,46'S	107°20,75'W	588,7	Ocean bottomSeismometer	in the water
197-3	13.03.10	15:15	72°0,46'S	107°20,77'W	595,1	Ocean bottomSeismometer	on ground/max depth
197-4	13.03.10	17:00	71°57,94'S	106°40,62'W	590,4	Ocean bottomSeismometer	in the water
197-4	13.03.10	17:01	71°57,94'S	106°40,63'W	591,8	Ocean	on

ANT-XXVI/3

Station PS75/	Date	Time	Position Lat	Position Lon	Depth [m]	Gear	Action
						bottomSeismometer	ground/max depth
197-5	13.03.10	18:16	71°55,95'S	106°11,55'W	572,2	Ocean bottomSeismometer	in the water
197-5	13.03.10	18:17	71°55,94'S	106°11,58'W	571,8	Ocean bottomSeismometer	on ground/max depth
197-6	13.03.10	19:33	71°53,83'S	105°36,96'W	506,9	Ocean bottomSeismometer	in the water
197-6	13.03.10	19:34	71°53,83'S	105°37,00'W	506,2	Ocean bottomSeismometer	on ground/max depth
198-1	13.03.10	21:20	71°50,04'S	104°50,33'W	605,2	CTD/rosetteWaterSa mpler	in the water
198-1	13.03.10	21:37	71°50,07'S	104°50,37'W	604,7	CTD/rosetteWaterSa mpler	on ground/max depth
198-1	13.03.10	21:57	71°50,09'S	104°50,17'W	607,2	CTD/rosetteWaterSa mpler	on deck
199-1	13.03.10	22:27	71°52,05'S	105°0,53'W	597,0	Seismic refraction profile	in the water
199-1	13.03.10	23:35	71°52,92'S	105°18,97'W	580,6	Seismic refraction profile	in the water
199-1	13.03.10	23:43	71°53,02'S	105°21,07'W	545,7	Seismic refraction profile	profile Start
199-1	14.03.10	00:37	71°53,78'S	105°36,77'W	507,8	Seismic refraction profile	action
199-1	14.03.10	00:50	71°54,02'S	105°40,45'W	518,3	Seismic refraction profile	action
199-1	14.03.10	01:19	71°54,50'S	105°48,42'W	532,8	Seismic refraction profile	action
199-1	14.03.10	02:41	71°55,83'S	106°11,45'W	573,2	Seismic refraction profile	action
199-1	14.03.10	04:21	71°57,97'S	106°40,66'W	591,9	Seismic refraction profile	action
199-1	14.03.10	06:40	72°0,42'S	107°20,82'W	594,3	Seismic refraction profile	action
199-1	14.03.10	08:42	72°2,55'S	107°54,85'W	597,9	Seismic refraction profile	action
199-1	14.03.10	10:46	72°4,66'S	108°28,62'W	576,5	Seismic refraction profile	action
199-1	14.03.10	11:30	72°5,44'S	108°40,33'W	566,3	Seismic refraction profile	profile End
199-1	14.03.10	11:44	72°5,70'S	108°44,10'W	569,0	Seismic refraction profile	action
199-1	14.03.10	11:46	72°5,73'S	108°44,63'W	562,1	Seismic refraction profile	hoisting
199-1	14.03.10	12:54	72°6,09'S	108°58,83'W	546,7	Seismic refraction profile	on deck
199-1	14.03.10	12:58	72°6,10'S	108°59,77'W	546,1	Seismic refraction profile	on deck
200-1	14.03.10	13:36	72°7,03'S	109°13,72'W	541,3	CTD/rosetteWaterSa mpler	in the water

Station list PS 75

Station PS75/	Date	Time	Position Lat	Position Lon	Depth [m]	Gear	Action
200-1	14.03.10	13:51	72°6,96'S	109°14,15'W	536,3	CTD/rosetteWaterSa mpler	on ground/max depth
200-1	14.03.10	14:09	72°6,92'S	109°14,32'W	536,4	CTD/rosetteWaterSa mpler	on deck
201-1	14.03.10	15:47	72°4,96'S	108°29,52'W	572,2	Ocean bottomSeismometer	action
201-1	14.03.10	16:15	72°4,59'S	108°28,75'W	577,5	Ocean bottomSeismometer	on ground/max depth
201-1	14.03.10	16:17	72°4,60'S	108°28,71'W	577,2	Ocean bottomSeismometer	on deck
202-1	14.03.10	17:25	72°2,88'S	107°59,98'W	606,2	CTD/rosetteWaterSa mpler	in the water
202-1	14.03.10	17:42	72°2,95'S	108°0,10'W	605,1	CTD/rosetteWaterSa mpler	on ground/max depth
202-1	14.03.10	18:01	72°2,94'S	108°0,15'W	604,7	CTD/rosetteWaterSa mpler	on deck
203-1	14.03.10	18:26	72°2,53'S	107°54,74'W	595,0	Ocean bottomSeismometer	action
203-1	14.03.10	18:30	72°2,49'S	107°54,66'W	599,0	Ocean bottomSeismometer	on ground/max depth
203-1	14.03.10	18:37	72°2,45'S	107°54,78'W	593,9	Ocean bottomSeismometer	action
203-1	14.03.10	18:50	72°2,53'S	107°54,59'W	602,3	Ocean bottomSeismometer	on deck
204-1	14.03.10	20:06	72°0,41'S	107°20,89'W	587,1	Ocean bottomSeismometer	action
204-1	14.03.10	20:09	72°0,36'S	107°20,83'W	581,4	Ocean bottomSeismometer	on ground/max depth
204-1	14.03.10	20:17	72°0,26'S	107°20,50'W	589,6	Ocean bottomSeismometer	action
204-1	14.03.10	20:18	72°0,24'S	107°20,47'W	587,7	Ocean bottomSeismometer	action
204-1	14.03.10	20:33	72°0,27'S	107°20,86'W	580,1	Ocean bottomSeismometer	on deck
205-1	14.03.10	21:27	71°59,51'S	106°59,98'W	616,3	CTD/rosetteWaterSa mpler	in the water
205-1	14.03.10	21:43	71°59,46'S	106°59,64'W	616,8	CTD/rosetteWaterSa mpler	on ground/max depth
205-1	14.03.10	21:58	71°59,47'S	106°59,52'W	615,2	CTD/rosetteWaterSa mpler	on deck
206-1	14.03.10	22:37	71°58,21'S	106°41,83'W	590,1	Ocean bottomSeismometer	action
206-1	14.03.10	22:45	71°57,86'S	106°40,82'W	586,0	Ocean bottomSeismometer	action
206-1	14.03.10	22:54	71°57,77'S	106°41,15'W	588,5	Ocean bottomSeismometer	at surface
206-1	14.03.10	22:59	71°57,78'S	106°41,06'W	585,9	Ocean	on

ANT-XXVI/3

Station PS75/	Date	Time	Position Lat	Position Lon	Depth [m]	Gear	Action
						bottomSeismometer	ground/max depth
206-1	14.03.10	23:12	71°57,86'S	106°41,14'W	588,2	Ocean bottomSeismometer	on deck
207-1	15.03.10	00:20	71°55,91'S	106°11,45'W	572,2	Ocean bottomSeismometer	action
207-1	15.03.10	00:23	71°55,88'S	106°11,45'W	576,7	Ocean bottomSeismometer	action
207-1	15.03.10	00:30	71°55,80'S	106°11,51'W	568,6	Ocean bottomSeismometer	action
207-1	15.03.10	00:31	71°55,79'S	106°11,55'W	569,4	Ocean bottomSeismometer	at surface
207-1	15.03.10	00:42	71°55,97'S	106°11,71'W	571,7	Ocean bottomSeismometer	on ground/max depth
207-1	15.03.10	00:45	71°55,98'S	106°11,85'W	571,3	Ocean bottomSeismometer	on deck
208-1	15.03.10	00:52	71°55,97'S	106°11,81'W	571,8	CTD/rosetteWaterSampler	in the water
208-1	15.03.10	01:08	71°55,97'S	106°11,62'W	571,5	CTD/rosetteWaterSampler	on ground/max depth
208-1	15.03.10	01:19	71°55,98'S	106°11,27'W	570,6	CTD/rosetteWaterSampler	on deck
209-1	15.03.10	02:41	71°53,92'S	105°36,99'W	510,3	Ocean bottomSeismometer	action
209-1	15.03.10	03:00	71°53,77'S	105°37,18'W	507,8	Ocean bottomSeismometer	on ground/max depth
209-1	15.03.10	03:02	71°53,76'S	105°37,19'W	509,0	Ocean bottomSeismometer	on deck
210-1	15.03.10	03:05	71°53,77'S	105°37,20'W	507,3	CTD/rosetteWaterSampler	in the water
210-1	15.03.10	03:22	71°53,79'S	105°37,19'W	506,8	CTD/rosetteWaterSampler	on ground/max depth
210-1	15.03.10	03:34	71°53,83'S	105°37,04'W	508,4	CTD/rosetteWaterSampler	on deck
210-2	15.03.10	03:40	71°53,83'S	105°37,06'W	508,3	Geothermic corer	in the water
210-2	15.03.10	03:52	71°53,78'S	105°37,13'W	505,7	Geothermic corer	on ground/max depth
210-2	15.03.10	04:02	71°53,78'S	105°37,11'W	506,0	Geothermic corer	hoisting
210-2	15.03.10	04:12	71°53,81'S	105°37,10'W	506,5	Geothermic corer	on deck
211-1	15.03.10	07:16	71°39,36'S	106°9,22'W	578,2	Gravity corer	in the water
211-1	15.03.10	07:26	71°39,36'S	106°9,21'W	577,6	Gravity corer	on ground/max depth
211-1	15.03.10	07:34	71°39,35'S	106°9,18'W	576,9	Gravity corer	at surface
211-1	15.03.10	07:39	71°39,34'S	106°9,18'W	578,2	Gravity corer	on deck
212-1	15.03.10	08:16	71°42,25'S	106°13,83'W	567,8	Gravity corer	in the water
212-1	15.03.10	08:25	71°42,25'S	106°13,81'W	568,0	Gravity corer	on ground/max

Station list PS 75

Station PS75/	Date	Time	Position Lat	Position Lon	Depth [m]	Gear	Action
							depth
212-1	15.03.10	08:33	71°42,24'S	106°13,86'W	568,3	Gravity corer	at surface
212-1	15.03.10	08:38	71°42,24'S	106°13,91'W	567,0	Gravity corer	on deck
213-1	15.03.10	12:39	71°54,28'S	108°13,89'W	565,4	Seismic reflection profile	in the water
213-1	15.03.10	13:40	71°58,41'S	108°25,92'W	572,2	Seismic reflection profile	on ground/max depth
213-1	15.03.10	13:45	71°58,75'S	108°26,84'W	574,3	Seismic reflection profile	in the water
213-1	15.03.10	14:01	71°59,94'S	108°29,20'W	575,8	Seismic reflection profile	alter course
213-1	15.03.10	15:09	72°6,14'S	108°27,13'W	573,8	Seismic reflection profile	profile Start
213-1	15.03.10	23:00	72°46,57'S	107°52,21'W	595,4	Seismic reflection profile	action
213-1	15.03.10	23:55	72°51,33'S	107°50,31'W	606,7	Seismic reflection profile	action
213-1	16.03.10	00:37	72°54,86'S	107°48,03'W	615,2	Seismic reflection profile	action
213-1	16.03.10	01:09	72°57,62'S	107°46,14'W	626,2	Seismic reflection profile	action
213-1	16.03.10	05:01	73°18,55'S	107°32,91'W	755,2	Seismic reflection profile	profile End
213-1	16.03.10	05:06	73°18,96'S	107°32,60'W	755,4	Seismic reflection profile	hoisting
213-1	16.03.10	06:08	73°22,19'S	107°30,14'W	769,7	Seismic reflection profile	on deck
214-1	16.03.10	16:49	74°31,91'S	102°37,48'W	646,6	Gravity corer	in the water
214-1	16.03.10	16:59	74°31,96'S	102°37,28'W	640,8	Gravity corer	on ground/max depth
214-1	16.03.10	17:13	74°32,01'S	102°37,04'W	636,1	Gravity corer	on deck
214-2	16.03.10	17:25	74°32,06'S	102°36,79'W	631,1	Geothermic corer	in the water
214-2	16.03.10	17:37	74°32,05'S	102°36,70'W	633,7	Geothermic corer	on ground/max depth
214-2	16.03.10	17:48	74°32,04'S	102°36,67'W	636,0	Geothermic corer	hoisting
214-2	16.03.10	18:05	74°32,09'S	102°36,51'W	634,6	Geothermic corer	on deck
215-1	16.03.10	23:59	74°35,51'S	104°2,51'W	555,7	Large Box Corer	in the water
215-1	17.03.10	00:07	74°35,50'S	104°2,52'W	555,6	Large Box Corer	on ground/max depth
215-1	17.03.10	00:18	74°35,52'S	104°2,42'W	553,6	Large Box Corer	on deck
216-1	17.03.10	03:27	74°36,84'S	105°51,29'W	648,6	CTD/rosette Water Sampler	in the water
216-1	17.03.10	03:47	74°36,70'S	105°51,15'W	654,5	CTD/rosette Water Sampler	on ground/max depth
216-1	17.03.10	04:02	74°36,66'S	105°51,24'W	652,6	CTD/rosette Water Sampler	on deck
216-2	17.03.10	04:07	74°36,66'S	105°51,21'W	655,9	Multi corer	in the water
216-2	17.03.10	04:18	74°36,66'S	105°51,25'W	653,5	Multi corer	on

ANT-XXVI/3

Station PS75/	Date	Time	Position Lat	Position Lon	Depth [m]	Gear	Action
							ground/max depth
216-2	17.03.10	04:30	74°36,64'S	105°51,04'W	656,5	Multi corer	on deck
216-3	17.03.10	04:38	74°36,65'S	105°51,08'W	655,9	Geothermic corer	in the water
216-3	17.03.10	04:50	74°36,68'S	105°51,12'W	655,3	Geothermic corer	on ground/max depth
216-3	17.03.10	05:01	74°36,71'S	105°51,17'W	652,0	Geothermic corer	hoisting
216-3	17.03.10	05:17	74°36,79'S	105°51,07'W	654,7	Geothermic corer	on deck
217-1	17.03.10	19:30	73°54,53'S	109°55,50'W	373,2	CTD/rosetteWaterSampler	in the water
217-1	17.03.10	19:45	73°54,55'S	109°55,44'W	373,7	CTD/rosetteWaterSampler	on ground/max depth
217-1	17.03.10	19:58	73°54,58'S	109°55,36'W	372,4	CTD/rosetteWaterSampler	on ground/max depth
217-1	17.03.10	20:00	73°54,59'S	109°55,34'W	372,0	CTD/rosetteWaterSampler	on deck
218-1	17.03.10	21:02	73°50,03'S	109°30,11'W	398,8	CTD/rosetteWaterSampler	in the water
218-1	17.03.10	21:17	73°49,99'S	109°30,06'W	399,5	CTD/rosetteWaterSampler	on ground/max depth
218-1	17.03.10	21:26	73°49,99'S	109°30,06'W	399,1	CTD/rosetteWaterSampler	on deck
219-1	17.03.10	22:59	73°40,02'S	108°59,91'W	459,5	CTD/rosetteWaterSampler	in the water
219-1	17.03.10	23:13	73°39,94'S	109°0,00'W	457,3	CTD/rosetteWaterSampler	on ground/max depth
219-1	17.03.10	23:27	73°39,98'S	108°59,94'W	458,8	CTD/rosetteWaterSampler	on deck
219-2	17.03.10	23:33	73°40,00'S	108°59,96'W	461,1	Large Box Corer	in the water
219-2	17.03.10	23:42	73°39,97'S	108°59,95'W	458,2	Large Box Corer	on ground/max depth
219-2	17.03.10	23:52	73°40,00'S	108°59,91'W	458,6	Large Box Corer	on deck
220-1	18.03.10	01:30	73°30,00'S	108°30,05'W	568,1	CTD/rosetteWaterSampler	in the water
220-1	18.03.10	01:46	73°29,97'S	108°29,98'W	567,9	CTD/rosetteWaterSampler	on ground/max depth
220-1	18.03.10	02:04	73°29,95'S	108°29,94'W	567,5	CTD/rosetteWaterSampler	on deck
221-1	18.03.10	04:06	73°25,01'S	107°30,11'W	765,3	CTD/rosetteWaterSampler	in the water
221-1	18.03.10	04:29	73°24,97'S	107°29,82'W	767,7	CTD/rosetteWaterSampler	on ground/max depth
221-1	18.03.10	04:41	73°24,95'S	107°29,75'W	769,2	CTD/rosetteWaterSampler	on deck
222-1	18.03.10	06:28	73°11,16'S	107°47,80'W	669,6	Seismic reflection	in the water

Station list PS 75

Station PS75/	Date	Time	Position Lat	Position Lon	Depth [m]	Gear	Action
						profile	
222-1	18.03.10	07:35	73°15,63'S	107°32,95'W	762,6	Seismic reflection profile	in the water
222-1	18.03.10	07:37	73°15,76'S	107°32,58'W	762,2	Seismic reflection profile	profile Start
222-1	18.03.10	10:04	73°25,59'S	107°0,22'W	945,4	Seismic reflection profile	action
222-1	18.03.10	11:25	73°25,70'S	106°59,95'W	943,8	Seismic reflection profile	profile Start
222-1	18.03.10	13:18	73°16,07'S	107°4,41'W	872,4	Seismic reflection profile	alter course
222-1	18.03.10	13:48	73°13,36'S	107°2,64'W	865,0	Seismic reflection profile	profile End
222-1	18.03.10	13:49	73°13,29'S	107°2,38'W	855,7	Seismic reflection profile	action
222-1	18.03.10	15:12	73°13,20'S	107°2,41'W	853,8	Seismic reflection profile	profile Start
222-1	18.03.10	17:04	73°19,24'S	106°32,68'W	756,3	Seismic reflection profile	action
222-1	18.03.10	17:19	73°19,94'S	106°28,54'W	763,5	Seismic reflection profile	action
222-1	18.03.10	18:20	73°23,26'S	106°12,65'W	768,3	Seismic reflection profile	action
222-1	18.03.10	18:50	73°24,63'S	106°4,89'W	727,1	Seismic reflection profile	profile End
222-1	18.03.10	18:54	73°24,81'S	106°3,84'W	721,4	Seismic reflection profile	action
222-1	18.03.10	20:02	73°28,09'S	105°47,93'W	613,0	Seismic reflection profile	on deck
222-1	18.03.10	20:06	73°28,30'S	105°47,00'W	599,2	Seismic reflection profile	on deck
223-1	18.03.10	21:17	73°23,28'S	106°12,43'W	772,3	Gravity corer	in the water
223-1	18.03.10	21:28	73°23,29'S	106°12,38'W	772,5	Gravity corer	on ground/max depth
223-1	18.03.10	21:37	73°23,33'S	106°12,27'W	768,2	Gravity corer	at surface
223-1	18.03.10	21:41	73°23,33'S	106°12,28'W	777,9	Gravity corer	on deck
224-1	18.03.10	22:58	73°25,06'S	106°50,00'W	897,7	CTD/rosetteWaterSampler	in the water
224-1	18.03.10	23:21	73°25,07'S	106°50,09'W	932,1	CTD/rosetteWaterSampler	on ground/max depth
224-1	18.03.10	23:43	73°25,10'S	106°50,27'W	933,5	CTD/rosetteWaterSampler	on deck
225-1	19.03.10	00:55	73°16,22'S	107°4,58'W	872,2	Gravity corer	in the water
225-1	19.03.10	01:06	73°16,20'S	107°4,43'W	873,8	Gravity corer	on ground/max depth
225-1	19.03.10	01:20	73°16,15'S	107°4,00'W	872,8	Gravity corer	on deck
226-1	19.03.10	04:15	73°1,00'S	108°29,10'W	550,0	Magnetic Turn Circle	profile Start
226-1	19.03.10	04:45	73°1,28'S	108°27,25'W	548,0	Magnetic Turn Circle	profile Start
226-1	19.03.10	05:12	73°0,82'S	108°28,28'W	548,0	Magnetic Turn Circle	on ground/max

ANT-XXVI/3

Station PS75/	Date	Time	Position Lat	Position Lon	Depth [m]	Gear	Action
							depth
226-1	19.03.10	05:15	73°0,79'S	108°29,38'W	544,7	Magnetic Turn Circle	profile End
227-1	19.03.10	06:40	72°57,05'S	109°9,94'W	507,6	CTD/rosetteWaterSa mpler	in the water
227-1	19.03.10	06:57	72°57,06'S	109°9,89'W	507,6	CTD/rosetteWaterSa mpler	on ground/max depth
227-1	19.03.10	07:13	72°57,04'S	109°9,81'W	507,6	CTD/rosetteWaterSa mpler	on deck
228-1	19.03.10	09:15	72°49,96'S	108°9,94'W	558,5	CTD/rosetteWaterSa mpler	in the water
228-1	19.03.10	09:33	72°49,94'S	108°9,80'W	560,4	CTD/rosetteWaterSa mpler	on ground/max depth
228-1	19.03.10	09:44	72°49,95'S	108°9,72'W	558,9	CTD/rosetteWaterSa mpler	on deck
229-1	19.03.10	11:19	72°50,02'S	107°20,04'W	673,4	CTD/rosetteWaterSa mpler	in the water
229-1	19.03.10	11:38	72°50,01'S	107°19,94'W	675,0	CTD/rosetteWaterSa mpler	on ground/max depth
229-1	19.03.10	11:53	72°49,98'S	107°19,98'W	674,6	CTD/rosetteWaterSa mpler	on deck
230-1	19.03.10	13:29	72°49,94'S	106°30,05'W	597,4	CTD/rosetteWaterSa mpler	in the water
230-1	19.03.10	13:45	72°49,96'S	106°30,12'W	597,9	CTD/rosetteWaterSa mpler	on ground/max depth
230-1	19.03.10	13:55	72°49,96'S	106°30,13'W	598,3	CTD/rosetteWaterSa mpler	on deck
230-2	19.03.10	14:00	72°49,96'S	106°30,13'W	598,2	Geothermic corer	in the water
230-2	19.03.10	14:12	72°49,97'S	106°30,13'W	598,6	Geothermic corer	on ground/max depth
230-2	19.03.10	14:35	72°49,94'S	106°30,54'W	598,8	Geothermic corer	on deck
231-1	19.03.10	16:16	72°50,04'S	105°40,66'W	556,2	CTD/rosetteWaterSa mpler	in the water
231-1	19.03.10	16:32	72°50,10'S	105°40,73'W	555,3	CTD/rosetteWaterSa mpler	on ground/max depth
231-1	19.03.10	16:44	72°50,14'S	105°40,49'W	554,6	CTD/rosetteWaterSa mpler	on deck
232-1	19.03.10	17:06	72°49,99'S	105°29,93'W	561,8	HydroSweep/ParaSo und profile	profile Start
232-1	19.03.10	18:17	72°43,30'S	104°59,05'W	568,4	HydroSweep/ParaSo und profile	alter course
232-1	19.03.10	18:42	72°46,24'S	104°50,77'W	567,6	HydroSweep/ParaSo und profile	alter course
232-1	19.03.10	19:35	72°51,39'S	105°10,06'W	580,1	HydroSweep/ParaSo und profile	alter course
232-1	20.03.10	01:33	72°45,59'S	105°7,76'W	556,2	HydroSweep/ParaSo und profile	on ground/max depth

Station list PS 75

Station PS75/	Date	Time	Position Lat	Position Lon	Depth [m]	Gear	Action
232-1	20.03.10	02:00	72°44,16'S	104°56,63'W	565,0	HydroSweep/ParaSound profile	profile End
233-1	20.03.10	02:37	72°45,19'S	105°1,08'W	559,6	Gravity corer	in the water
233-1	20.03.10	02:50	72°45,25'S	105°0,99'W	555,0	Gravity corer	on ground/max depth
233-1	20.03.10	03:04	72°45,10'S	105°0,91'W	564,4	Gravity corer	on deck
234-1	20.03.10	03:52	72°47,03'S	105°6,56'W	583,5	Gravity corer	in the water
234-1	20.03.10	04:01	72°47,05'S	105°6,29'W	582,8	Gravity corer	on ground/max depth
234-1	20.03.10	04:13	72°47,09'S	105°6,42'W	585,2	Gravity corer	on deck
235-1	20.03.10	08:31	72°39,96'S	107°9,89'W	751,4	Gravity corer	in the water
235-1	20.03.10	08:42	72°39,95'S	107°9,93'W	751,7	Gravity corer	on ground/max depth
235-1	20.03.10	08:42	72°39,95'S	107°9,93'W	751,7	Gravity corer	at surface
235-1	20.03.10	08:57	72°39,92'S	107°9,92'W	751,7	Gravity corer	on deck
235-2	20.03.10	09:08	72°39,95'S	107°10,01'W	751,8	Gravity corer	in the water
235-2	20.03.10	09:19	72°39,94'S	107°10,08'W	751,0	Gravity corer	on ground/max depth
235-2	20.03.10	09:32	72°39,93'S	107°10,11'W	751,5	Gravity corer	at surface
235-2	20.03.10	09:36	72°39,93'S	107°10,13'W	750,8	Gravity corer	on deck
236-1	20.03.10	11:35	72°29,58'S	107°58,76'W	622,3	Piston corer	in the water
236-1	20.03.10	11:44	72°29,60'S	107°58,82'W	621,8	Piston corer	on ground/max depth
236-1	20.03.10	11:53	72°29,62'S	107°58,85'W	622,8	Piston corer	at surface
236-1	20.03.10	11:57	72°29,62'S	107°58,84'W	622,8	Piston corer	on deck
237-1	20.03.10	12:56	72°26,40'S	108°5,95'W	650,0	Gravity corer	on ground/max depth
237-1	20.03.10	13:07	72°26,33'S	108°5,87'W	648,8	Gravity corer	on ground/max depth
237-1	20.03.10	13:25	72°26,57'S	108°6,02'W	650,4	Gravity corer	on deck
238-1	20.03.10	17:11	72°11,96'S	110°0,17'W	510,9	CTD/rosetteWaterSampler	in the water
238-1	20.03.10	17:26	72°11,98'S	110°0,05'W	508,6	CTD/rosetteWaterSampler	on ground/max depth
238-1	20.03.10	17:42	72°11,96'S	110°0,00'W	508,9	CTD/rosetteWaterSampler	on deck
239-1	20.03.10	20:15	72°18,01'S	111°10,12'W	568,2	CTD/rosetteWaterSampler	in the water
239-1	20.03.10	20:32	72°18,01'S	111°9,96'W	569,1	CTD/rosetteWaterSampler	on ground/max depth
239-1	20.03.10	20:46	72°18,00'S	111°9,90'W	568,7	CTD/rosetteWaterSampler	on deck
240-1	20.03.10	21:37	72°16,79'S	110°55,60'W	569,0	Gravity corer	in the water
240-1	20.03.10	21:45	72°16,78'S	110°55,56'W	569,2	Gravity corer	on

ANT-XXVI/3

Station PS75/	Date	Time	Position Lat	Position Lon	Depth [m]	Gear	Action
							ground/max depth
240-1	20.03.10	21:53	72°16,78'S	110°55,54'W	569,3	Gravity corer	on deck
241-1	21.03.10	00:23	72°23,96'S	112°10,04'W	503,2	CTD/rosetteWaterSampler	in the water
241-1	21.03.10	00:39	72°23,97'S	112°9,91'W	505,2	CTD/rosetteWaterSampler	on ground/max depth
241-1	21.03.10	00:53	72°24,11'S	112°9,83'W	502,5	CTD/rosetteWaterSampler	on deck
242-1	21.03.10	03:47	72°8,74'S	112°2,95'W	545,5	Gravity corer	in the water
242-1	21.03.10	03:55	72°8,70'S	112°2,93'W	545,3	Gravity corer	on ground/max depth
242-1	21.03.10	04:03	72°8,69'S	112°2,86'W	544,6	Gravity corer	at surface
242-1	21.03.10	04:09	72°8,70'S	112°2,82'W	544,4	Gravity corer	on deck
243-1	21.03.10	10:52	72°41,30'S	108°49,49'W	511,8	Seismic reflection profile	in the water
243-1	21.03.10	12:01	72°37,53'S	109°8,80'W	508,5	Seismic reflection profile	in the water
243-1	21.03.10	12:07	72°37,24'S	109°10,49'W	505,9	Seismic reflection profile	on ground/max depth
243-1	21.03.10	12:08	72°37,19'S	109°10,77'W	511,9	Seismic reflection profile	profile Start
243-1	21.03.10	14:05	72°32,09'S	109°41,46'W	492,7	Seismic reflection profile	action
243-1	21.03.10	14:40	72°30,55'S	109°50,91'W	491,8	Seismic reflection profile	action
243-1	21.03.10	15:10	72°29,14'S	109°58,56'W	486,8	Seismic reflection profile	action
243-1	22.03.10	00:35	72°5,30'S	112°24,42'W	532,1	Seismic reflection profile	profile End
243-1	22.03.10	01:48	72°3,07'S	112°34,24'W	534,2	Seismic reflection profile	on deck
244-1	23.03.10	02:23	69°7,98'S	123°13,71'W	1391,0	Grab, TV	in the water
244-1	23.03.10	02:58	69°7,87'S	123°13,84'W	1364,0	Grab, TV	on ground/max depth
244-1	23.03.10	03:40	69°7,75'S	123°13,99'W	1312,0	Grab, TV	on deck
245-1	23.03.10	04:30	69°8,29'S	123°13,68'W	1479,0	Grab, TV	in the water
245-1	23.03.10	05:05	69°8,32'S	123°13,58'W	1492,0	Grab, TV	on ground/max depth
245-1	23.03.10	05:27	69°8,30'S	123°13,50'W	1482,0	Grab, TV	at surface
245-1	23.03.10	05:32	69°8,29'S	123°13,51'W	1480,0	Grab, TV	on deck
245-2	23.03.10	05:43	69°8,30'S	123°13,51'W	1483,0	Grab, TV	in the water
245-2	23.03.10	06:08	69°8,28'S	123°13,50'W	1480,0	Grab, TV	hoisting
245-2	23.03.10	06:17	69°8,30'S	123°13,53'W	1484,0	Grab, TV	on ground/max depth
245-2	23.03.10	06:21	69°8,30'S	123°13,55'W	1485,0	Grab, TV	on deck
245-3	23.03.10	06:29	69°8,28'S	123°13,56'W	1472,0	Grab, TV	in the water

Station list PS 75

Station PS75/	Date	Time	Position Lat	Position Lon	Depth [m]	Gear	Action
245-3	23.03.10	07:33	69°8,29'S	123°13,48'W	1484,0	Grab, TV	on ground/max depth
245-3	23.03.10	07:34	69°8,30'S	123°13,49'W	1481,0	Grab, TV	hoisting
245-3	23.03.10	07:55	69°8,30'S	123°13,51'W	1483,0	Grab, TV	at surface
245-3	23.03.10	07:58	69°8,28'S	123°13,51'W	1475,0	Grab, TV	on deck
246-1	23.03.10	08:54	69°8,41'S	123°13,00'W	1603,0	Grab, TV	in the water
246-1	23.03.10	08:58	69°8,42'S	123°12,94'W	1644,0	Grab, TV	on ground/max depth
246-1	23.03.10	08:59	69°8,42'S	123°12,93'W	1640,0	Grab, TV	hoisting
246-1	23.03.10	09:34	69°8,37'S	123°12,92'W	1598,0	Grab, TV	on deck
246-2	23.03.10	09:52	69°8,38'S	123°12,96'W	1597,0	Grab, TV	in the water
246-2	23.03.10	10:04	69°8,37'S	123°12,98'W	1587,0	Grab, TV	on ground/max depth
246-2	23.03.10	10:04	69°8,37'S	123°12,98'W	1587,0	Grab, TV	hoisting
246-2	23.03.10	10:14	69°8,42'S	123°12,85'W	1647,0	Grab, TV	on deck
247-1	23.03.10	10:45	69°9,48'S	123°14,02'W	2284,0	Dredge, chain bag	in the water
247-1	23.03.10	11:38	69°8,48'S	123°13,11'W	1681,0	Dredge, chain bag	on ground/max depth
247-1	23.03.10	11:38	69°8,48'S	123°13,11'W	1681,0	Dredge, chain bag	profile Start
247-1	23.03.10	11:54	69°8,04'S	123°12,60'W	1509,0	Dredge, chain bag	profile End
247-1	23.03.10	11:59	69°7,98'S	123°12,56'W	1507,0	Dredge, chain bag	hoisting
247-1	23.03.10	12:42	69°7,78'S	123°12,19'W	1507,0	Dredge, chain bag	information
247-1	23.03.10	13:15	69°7,49'S	123°11,64'W	1498,0	Dredge, chain bag	on deck
247-2	23.03.10	14:18	69°9,82'S	123°14,23'W	2357,0	Dredge, chain bag	in the water
247-2	23.03.10	15:17	69°8,53'S	123°13,13'W	1734,0	Dredge, chain bag	on ground/max depth
247-2	23.03.10	15:18	69°8,50'S	123°13,09'W	1708,0	Dredge, chain bag	profile Start
247-2	23.03.10	15:30	69°8,14'S	123°12,73'W	1504,0	Dredge, chain bag	profile End
247-2	23.03.10	15:32	69°8,13'S	123°12,76'W	1502,0	Dredge, chain bag	hoisting
247-2	23.03.10	16:45	69°8,16'S	123°12,80'W	1499,0	Dredge, chain bag	at surface
247-2	23.03.10	16:47	69°8,17'S	123°12,79'W	1498,0	Dredge, chain bag	on deck
248-1	23.03.10	17:09	69°8,36'S	123°10,64'W	1894,0	Dredge, chain bag	in the water
248-1	23.03.10	17:47	69°8,34'S	123°10,61'W	1887,0	Dredge, chain bag	on ground/max depth
248-1	23.03.10	17:48	69°8,33'S	123°10,59'W	1878,0	Dredge, chain bag	profile Start
248-1	23.03.10	18:08	69°7,70'S	123°9,85'W	1522,0	Dredge, chain bag	profile End
248-1	23.03.10	18:10	69°7,65'S	123°9,81'W	1517,0	Dredge, chain bag	hoisting
248-1	23.03.10	19:00	69°7,64'S	123°9,78'W	1518,0	Dredge, chain bag	information
248-1	23.03.10	19:25	69°7,63'S	123°9,82'W	1517,0	Dredge, chain bag	on deck
249-1	23.03.10	20:04	69°8,55'S	123°13,48'W	1739,0	Grab, TV	in the water
249-1	23.03.10	21:47	69°8,54'S	123°13,52'W	1724,0	Grab, TV	on ground/max depth
249-1	23.03.10	22:34	69°8,49'S	123°13,59'W	1678,0	Grab, TV	on deck
250-1	23.03.10	23:00	69°8,86'S	123°13,38'W	2025,0	Dredge, chain bag	in the water
250-1	23.03.10	23:40	69°8,86'S	123°13,44'W	2014,0	Dredge, chain bag	on

ANT-XXVI/3

Station PS75/	Date	Time	Position Lat	Position Lon	Depth [m]	Gear	Action
							ground/max depth
250-1	24.03.10	00:03	69°8,32'S	123°13,46'W	1499,0	Dredge, chain bag	hoisting
250-1	24.03.10	00:51	69°8,29'S	123°13,58'W	1479,0	Dredge, chain bag	information
250-1	24.03.10	01:14	69°8,41'S	123°13,70'W	1561,0	Dredge, chain bag	profile Start
250-1	24.03.10	01:16	69°8,42'S	123°13,66'W	1573,0	Dredge, chain bag	profile End
250-1	24.03.10	01:17	69°8,43'S	123°13,57'W	1572,0	Dredge, chain bag	on deck
251-1	24.03.10	02:22	69°10,62'S	122°52,10'W	2254,0	Dredge, chain bag	in the water
251-1	24.03.10	03:06	69°10,58'S	122°51,95'W	2235,0	Dredge, chain bag	on ground/max depth
251-1	24.03.10	03:33	69°9,86'S	122°52,71'W	1500,0	Dredge, chain bag	profile Start
251-1	24.03.10	03:33	69°9,86'S	122°52,71'W	1500,0	Dredge, chain bag	profile End
251-1	24.03.10	03:33	69°9,86'S	122°52,71'W	1500,0	Dredge, chain bag	hoisting
251-1	24.03.10	04:25	69°10,06'S	122°53,86'W	1935,0	Dredge, chain bag	information
251-1	24.03.10	04:54	69°10,25'S	122°54,50'W	2087,0	Dredge, chain bag	at surface
251-1	24.03.10	04:56	69°10,26'S	122°54,56'W	2098,0	Dredge, chain bag	on deck
252-1	24.03.10	05:11	69°10,58'S	122°54,24'W	2158,0	Dredge, chain bag	in the water
252-1	24.03.10	05:54	69°10,61'S	122°54,18'W	2163,0	Dredge, chain bag	on ground/max depth
252-1	24.03.10	05:58	69°10,57'S	122°54,11'W	2154,0	Dredge, chain bag	profile Start
252-1	24.03.10	06:20	69°9,94'S	122°52,87'W	1521,0	Dredge, chain bag	profile End
252-1	24.03.10	06:24	69°9,88'S	122°52,78'W	1502,0	Dredge, chain bag	hoisting
252-1	24.03.10	07:11	69°9,88'S	122°52,76'W	1502,0	Dredge, chain bag	information
252-1	24.03.10	07:33	69°9,91'S	122°52,79'W	1506,0	Dredge, chain bag	at surface
252-1	24.03.10	07:36	69°9,92'S	122°52,78'W	1508,0	Dredge, chain bag	on deck
253-1	24.03.10	08:16	69°13,00'S	122°44,10'W	3712,0	CTD/rosetteWaterSampler	in the water
253-1	24.03.10	09:28	69°13,04'S	122°44,13'W	3715,0	CTD/rosetteWaterSampler	on ground/max depth
253-1	24.03.10	10:32	69°13,09'S	122°43,91'W	3715,0	CTD/rosetteWaterSampler	on deck
254-1	25.03.10	07:09	71°52,57'S	118°50,17'W	1322,0	Multi corer	in the water
254-1	25.03.10	07:32	71°52,59'S	118°50,00'W	1318,0	Multi corer	on ground/max depth
254-1	25.03.10	07:53	71°52,58'S	118°49,97'W	1316,0	Multi corer	on deck
254-2	25.03.10	08:18	71°52,60'S	118°50,06'W	1317,0	Multi corer	in the water
254-2	25.03.10	08:39	71°52,60'S	118°50,03'W	1317,0	Multi corer	on ground/max depth
254-2	25.03.10	09:00	71°52,60'S	118°49,92'W	1315,0	Multi corer	on deck
255-1	25.03.10	10:29	72°0,11'S	118°29,83'W	511,8	Box corer	in the water
255-1	25.03.10	10:36	72°0,11'S	118°29,86'W	511,6	Box corer	on ground/max depth
255-1	25.03.10	10:50	72°0,06'S	118°29,91'W	509,3	Box corer	on deck
256-1	25.03.10	12:48	72°13,99'S	118°0,31'W	518,0	CTD/rosetteWaterSampler	in the water
256-1	25.03.10	13:04	72°13,98'S	118°0,18'W	517,7	CTD/rosetteWaterSampler	on ground/max

Station list PS 75

Station PS75/	Date	Time	Position Lat	Position Lon	Depth [m]	Gear	Action
							depth
256-1	25.03.10	13:18	72°13,95'S	117°59,84'W	521,8	CTD/rosetteWaterSa mpler	on deck
257-1	25.03.10	14:25	72°10,93'S	117°39,80'W	542,2	Gravity corer	in the water
257-1	25.03.10	14:34	72°10,91'S	117°39,90'W	542,4	Gravity corer	on ground/max depth
257-1	25.03.10	14:46	72°10,81'S	117°40,13'W	542,0	Gravity corer	on deck
258-1	25.03.10	16:06	72°5,19'S	117°11,05'W	506,1	CTD/rosetteWaterSa mpler	in the water
258-1	25.03.10	16:22	72°5,11'S	117°11,29'W	504,8	CTD/rosetteWaterSa mpler	on ground/max depth
258-1	25.03.10	16:34	72°5,04'S	117°11,42'W	505,7	CTD/rosetteWaterSa mpler	on deck
259-1	26.03.10	02:20	72°16,12'S	111°59,43'W	531,0	Seismic reflection profile	in the water
259-1	26.03.10	03:27	72°11,00'S	112°11,56'W	535,2	Seismic reflection profile	on ground/max depth
259-1	26.03.10	03:38	72°10,00'S	112°12,96'W	534,2	Seismic reflection profile	information
259-1	26.03.10	03:40	72°9,82'S	112°13,11'W	534,1	Seismic reflection profile	profile Start
259-1	26.03.10	13:54	71°22,67'S	113°44,49'W	1488,0	Seismic reflection profile	action
259-1	26.03.10	14:24	71°20,44'S	113°48,84'W	1757,0	Seismic reflection profile	action
259-1	26.03.10	15:42	71°14,79'S	113°59,76'W	2199,0	Seismic reflection profile	profile End
259-1	26.03.10	15:43	71°14,71'S	113°59,86'W	2201,0	Seismic reflection profile	alter course
259-1	26.03.10	15:44	71°14,63'S	113°59,93'W	2205,0	Seismic reflection profile	profile Start
259-1	26.03.10	16:57	71°8,73'S	113°59,08'W	2416,0	Seismic reflection profile	action
259-1	26.03.10	17:12	71°7,48'S	113°58,66'W	2460,0	Seismic reflection profile	action
259-1	27.03.10	01:10	70°26,05'S	113°59,97'W	3308,0	Seismic reflection profile	profile End
259-1	27.03.10	01:15	70°25,66'S	114°0,00'W	3314,0	Seismic reflection profile	information
259-1	27.03.10	01:22	70°25,10'S	114°0,04'W	3319,0	Seismic reflection profile	hoisting
259-1	27.03.10	02:33	70°21,77'S	113°58,20'W	3480,0	Seismic reflection profile	on deck
260-1	27.03.10	02:40	70°21,75'S	113°57,88'W	3517,0	Geothermic corer	in the water
260-1	27.03.10	03:35	70°21,85'S	113°57,43'W	3540,0	Geothermic corer	on ground/max depth
260-1	27.03.10	03:43	70°21,89'S	113°57,42'W	3537,0	Geothermic corer	hoisting
260-1	27.03.10	04:40	70°22,02'S	113°56,82'W	3536,0	Geothermic corer	at surface
260-1	27.03.10	04:42	70°22,00'S	113°56,82'W	3540,0	Geothermic corer	on deck

ANT-XXVI/3

Station PS75/	Date	Time	Position Lat	Position Lon	Depth [m]	Gear	Action
261-1	28.03.10	14:11	64°33,36'S	107°4,89'W	5002,0	Gravity corer	in the water
261-1	28.03.10	15:05	64°33,39'S	107°4,88'W	5002,0	Gravity corer	on ground/max depth
261-1	28.03.10	16:00	64°33,38'S	107°4,93'W	5001,0	Gravity corer	at surface
261-1	28.03.10	16:06	64°33,40'S	107°4,87'W	5001,0	Gravity corer	on deck
262-1	28.03.10	18:48	64°32,33'S	107°4,75'W	4992,0	Gravity corer	in the water
262-1	28.03.10	19:41	64°32,40'S	107°4,71'W	4999,0	Gravity corer	on ground/max depth
262-1	28.03.10	19:42	64°32,40'S	107°4,74'W	4996,0	Gravity corer	hoisting
262-1	28.03.10	20:47	64°32,39'S	107°5,07'W	4994,0	Gravity corer	on deck
263-1	30.03.10	02:32	60°49,99'S	115°48,79'W	5159,0	Seismic reflection profile	in the water
263-1	30.03.10	02:56	60°51,14'S	115°52,05'W	5161,0	Seismic reflection profile	on ground/max depth
263-1	30.03.10	02:58	60°51,25'S	115°52,31'W	5163,0	Seismic reflection profile	information
263-1	30.03.10	03:27	60°49,61'S	115°51,94'W	5172,0	Seismic reflection profile	profile Start
263-1	30.03.10	04:22	60°46,13'S	115°58,79'W	5144,0	Seismic reflection profile	action
263-1	30.03.10	05:25	60°42,23'S	116°6,55'W	5138,0	Seismic reflection profile	alter course
263-1	30.03.10	06:53	60°49,80'S	116°6,58'W	5459,0	Seismic reflection profile	alter course
263-1	30.03.10	07:52	60°46,15'S	115°58,79'W	5149,0	Seismic reflection profile	action
263-1	30.03.10	08:34	60°43,34'S	115°52,62'W	5163,0	Seismic reflection profile	alter course
263-1	30.03.10	09:55	60°40,61'S	115°37,22'W	5179,0	Seismic reflection profile	profile End
263-1	30.03.10	09:56	60°40,53'S	115°37,12'W	5180,0	Seismic reflection profile	hoisting
263-1	30.03.10	09:57	60°40,46'S	115°37,01'W	5183,0	Seismic reflection profile	action
263-1	30.03.10	10:12	60°39,50'S	115°35,10'W	5078,0	Seismic reflection profile	on deck
263-1	30.03.10	10:16	60°39,16'S	115°34,43'W	5016,0	Seismic reflection profile	on deck

Die "Berichte zur Polar- und Meeresforschung" (ISSN 1866-3192) werden beginnend mit dem Heft Nr. 569 (2008) ausschließlich elektronisch als Open-Access-Publikation herausgegeben. Ein Verzeichnis aller Hefte einschließlich der Druckausgaben (Heft 377-568) sowie der früheren "Berichte zur Polarforschung" (Heft 1-376, von 1982 bis 2000) befindet sich im Internet in der Ablage des electronic Information Center des AWI (**ePIC**) unter der URL <http://epic.awi.de>. Durch Auswahl "Reports on Polar- and Marine Research" auf der rechten Seite des Fensters wird eine Liste der Publikationen in alphabetischer Reihenfolge (nach Autoren) innerhalb der absteigenden chronologischen Reihenfolge der Jahrgänge erzeugt.

To generate a list of all Reports past issues, use the following URL: <http://epic.awi.de> and select the right frame to browse "Reports on Polar and Marine Research". A chronological list in declining order, author names alphabetical, will be produced, and pdf-icons shown for open access download.

Verzeichnis der zuletzt erschienenen Hefte:

Heft-Nr. 604/2010 — "The Expedition of the Research Vessel 'Polarstern' to the Antarctic in 2007/2008 (ANT-XXIV/2)", edited by Ulrich Bathmann

Heft-Nr. 605/2010 — "The Expedition of the Research Vessel 'Polarstern' to the Antarctic in 2003 (ANT-XXI/1)", edited by Otto Schrems

Heft-Nr. 606/2010 — "The Expedition of the Research Vessel 'Polarstern' to the Antarctic in 2008 (ANT-XXIV/3)", edited by Eberhard Fahrbach and Hein de Baar

Heft-Nr. 607/2010 — "The Expedition of the Research Vessel 'Polarstern' to the Arctic in 2009 (ARK-XXIV/2)", edited by Michael Klages

Heft-Nr. 608/2010 — "Airborne lidar observations of tropospheric Arctic clouds", by Astrid Lampert

Heft-Nr. 609/2010 — "Daten statt Sensationen - Der Weg zur internationalen Polarforschung aus einer deutschen Perspektive", by Reinhard A. Krause

Heft-Nr. 610/2010 — "Biology of meso- and bathypelagic chaetognaths in the Southern Ocean", by Svenja Kruse

Heft-Nr. 611/2010 — "Materialparameter zur Beschreibung des zeitabhängigen nichtlinearen Spannungs – Verformungsverhaltens von Firn in Abhängigkeit von seiner Dichte", by Karl-Heinz Bässler

Heft-Nr. 612/2010 — "The Expedition of the Research Vessel 'Polarstern' to the Arctic in 2009 (ARK-XXIV/1)", edited by Gereon Budéus

Heft-Nr. 613/2010 — "The Expedition of the Research Vessel 'Polarstern' to the Antarctic in 2009 (ANT-XXV/3 - LOHAFEX)", edited by Victor Smetacek and Syed Wajih A. Naqvi

Heft-Nr. 614/2010 — "The Expedition of the Research Vessel 'Polarstern' to the Antarctic in 2009 (ANT-XXVI/1)", edited by Saad el Naggar and Andreas Macke

Heft-Nr. 615/2010 — "The Expedition of the Research Vessel 'Polarstern' to the Arctic in 2009 (ARK-XXIV/3)", edited by Wilfried Jokat

Heft-Nr. 616/2010 — "The Expedition of the Research Vessel 'Polarstern' to the Antarctic in 2009 (ANT-XXV/4)", edited by Christine Provost

Heft-Nr. 617/2010 — "The Expedition of the Research Vessel 'Polarstern' to the Amundsen Sea, Antarctica, in 2010 (ANT-XXVI/3)", edited by Karsten Gohl